Supporting climate risk management in tropical agriculture with statistical crop modelling

DISSERTATION

zur Erlangung des akademischen Grades
Doctor of Philosophy
(Ph.D.)

eingereicht an der
Lebenswissenschaftlichen Fakultät der
Humboldt-Universität zu Berlin

von
Rahel Laudien, M. Sc.

Kommissarischer Präsident der Humboldt-Universität zu Berlin:
Prof. Dr. Peter Frensch

Dekan der Lebenswissenschaftlichen Fakultät:
Prof. Dr. Dr. Christian Ulrichs

Gutachter:
Prof. Dr. Christoph Gornott
Prof. Dr. Hermann Lotze-Campen
Prof. Dr. Reimund Paul Rötter

Tag der mündlichen Prüfung: 2. September 2022

Abstract

After a long period of decline and stagnation, the number of undernourished people in the world has been increasing since 2017. Climate change will further exacerbate pressure on agriculture and food security, particularly for smallholder and subsistence-based farming systems in the tropics. These farming systems are vulnerable to climate change as they are strongly affected by climate impacts and lack adaptive capacity. Anticipating and responding to global warming through climate risk management is needed to increase the resilience of food systems and food security. Crop models play an indispensable role in this regard. They allow quantifying crop responses to changes in climatic conditions and thus identify risks. This dissertation demonstrates how statistical crop modelling can inform climate risk management and adaptation in tropical agriculture in the case studies of Peru, Tanzania and Burkina Faso.

The first study assesses weather influences on starchy maize yields on the sub-national and local scale in Peru. Moreover, the influence of higher water availability on maize yields is investigated to inform climate adaptation planning as suggested by the Peruvian *Nationally Determined Contributions*. The second study provides a within-season maize yield forecast six weeks prior to the harvest on the sub-national level in Tanzania. This can support governments to anticipate looming harvest losses. In addition to a yield forecast, the third study provides a crop production forecast for maize, millet and sorghum on the national level in Burkina Faso. By comparing produced calories from these crops with the historic demand, early information on shortages in domestic cereal production can be obtained.

The three publications present novel statistical crop modelling approaches on sub-national scales in Peru, Tanzania and Burkina Faso. The models explain a substantial part of crop yield variability based on weather variables. This indicates strong weather influences on maize yields and high model performance. The studies underline the importance of spatially-distinct variables and model parameters to take account of diverse weather-yield relations within the countries. Especially, weather influences related to extreme events, such as dry spells and erratic precipitation within the growing season influence maize yield variability. Moreover, the three studies found a strong explanatory power of yield trends (study one and two) and harvest area trends (study three). The latter highlights the relevance of obtaining information on sown areas within the growing season for accurate predictions in practice. In contrast to most yield forecasting studies, we applied a rigorous validation, including an out-of-sample variable selection. This validation mimics the operational context in which model formation and variable selection are purely based on information from past years. The statistical crop modelling approach relies on globally available climate data and provides robust results even for limited available yield data - making it potentially transferrable to other regions.

The dissertation aims to deepen the understanding of weather-related influences on crop yields, food production and food availability in the tropics. Moreover, the findings demonstrate how statistical crop modelling can inform climate risk management and adaptation at different spatial levels in the tropics through an assessment of weather influences, the evaluation of adaptation options and within-season crop yield and production forecasting.

Zusammenfassung

Die Anzahl der unterernährten Menschen in der Welt steigt nach einer langen Phase des Rückgangs und der Stagnation seit 2017 wieder an. Der Klimawandel wird den Druck auf die Landwirtschaft und die Ernährungssicherheit weiter erhöhen, insbesondere für kleinbäuerliche und von Subsistenzwirtschaft geprägte Agrarsysteme in den Tropen. Diese sind zum einen stark vom Klimawandel betroffen und zum anderen aufgrund begrenzter Anpassungsfähigkeit besonders vulnerable. Um die Widerstandsfähigkeit der Ernährungssysteme und die Ernährungssicherheit zu stärken, bedarf es eines Klimarisikomanagements und Klimaanpassung, da dies sowohl die Antizipation als auch die Reaktion auf die Auswirkungen der globalen Erwärmung ermöglicht. Eine zentrale Rolle spielen in dieser Hinsicht landwirtschaftliche Modelle. Sie können die Reaktionen von Pflanzen auf Veränderungen in den Klimabedingungen quantifizieren und damit Risiken identifizieren. Diese Dissertation demonstriert anhand dreier in Peru, in Tansania und in Burkina Faso durchgeführten Fallstudien, wie statistische Erntemodelle das Klimarisikomanagement und die Anpassung in der tropischen Landwirtschaft unterstützen können.

In der ersten Studie werden die Wettereinflüsse auf die Maiserträge auf subnationaler und lokaler Ebene in Peru untersucht. Dabei wird auch der Einfluss höherer Wasserverfügbarkeit auf die Maiserträge quantifiziert, um die Klimaanpassungsbestrebungen der peruanischen *Nationally Determined Contributions* zu unterstützen. Die zweite Studie erstellt eine Vorhersage der Maiserträge sechs Wochen vor der Ernte auf subnationaler Ebene in Tansania. Dies kann es Regierungen ermöglichen, vorsorgende Maßnahmen zu treffen, um die Auswirkungen von drohenden Ernteverlusten zu mildern. Die dritte Studie liefert neben einer Ertragsvorhersage eine Produktionsvorhersage für Mais, Sorghumhirse und Millethirse auf nationaler Ebene in Burkina Faso. Der Vergleich der aus diesen Kulturen erzeugten Kalorien mit dem historischen Bedarf, ermöglicht es frühzeitig Informationen über Engpässe in der heimischen Getreideproduktion zu erlangen.

In den drei Veröffentlichungen werden neue Ansätze statistischer Erntemodellierung auf subnationaler Ebene in Peru, Tansania und Burkina Faso vorgestellt. Die Modelle erklären einen beträchtlichen Anteil der Ertragsvariabilität auf Grundlage von Wettervariablen. Das weist sowohl auf einen starken Einfluss des Wetters auf Maiserträge hin als auch auf eine hohe Modellgüte. Die Studien betonen die Notwendigkeit von räumlich differenzierten Variablen und Modellparametern, sodass die unterschiedlichen Wetter-Ertrags-Beziehungen innerhalb der Länder berücksichtigt werden können. Insbesondere Wettereinflüsse in Bezug auf Extremereignisse, wie Trockenperioden oder ungünstig verteilte Niederschläge innerhalb der Wachstumsperiode, beeinflussen die Variabilität der Maiserträge. Darüber hinaus zeigen die drei Studien eine starke Erklärungskraft von Ertragstrends (Studie eins und zwei) und Ernteflächentrends (Studie drei). Letzteres unterstreicht die Relevanz der Ermittlung von Aussaatflächen innerhalb der Wachstumsperiode für präzise Vorhersagen in der Praxis. Im Gegensatz zu den meisten Ertragsvorhersagestudien, haben wir eine strenge Validierung, inklusive der unabhängigen Variablenauswahl, durchgeführt. Diese Validierung spiegelt die Situation in der Praxis wieder, in der lediglich Informationen der vergangenen Jahre die Modellbildung und Variablenauswahl beeinflussen können. Unser Ansatz der statistischen Erntemodellierung stützt sich auf weltweit verfügbare Klimadaten und liefert selbst bei begrenzten Ertragsdaten robuste Ergebnisse, so dass er potenziell auf andere Regionen übertragbar ist.

Acknowledgements

To my Mum.

I want to thank Christoph Gornott, Bernhard Schauberger and Hermann Lotze-Campen who supervised and supported me in the best way. These are big words and I mean them. I enjoyed the many sessions, Christoph, Bernhard and I sat together discussing my research endeavours. I felt motivated after almost every meeting and keen on discovering what the next steps in my research will reveal. They introduced me to the world of science. They inspired me and triggered me to set new goals. They had trust in me from the very first day on - not knowing how I would cope. They supported me in dark times of my life. I will never forget the honest and generous help I received and I feel grateful that I had the luck to have them around in these times.

In contrast to the general opinion that doing a PhD is depressing and frustrating, my PhD time was to a surprisingly large extent a very happy one. This is because I was surrounded by my colleagues Ponraj, Steffi, Claudia, Abel, Roopam, Felicitas, Lisa, Gina, Paula, Steffi, Julia, Sebastian, Haen Chen, Kira, Thiago, Jonas, Hamani, Kanwal, Holger, Jan and Hetty. I enjoyed our discussions at least as much as I enjoyed playing foosball or travelling the tropics with you. I would like to thank the farmers I met in Kenya, Tanzania and France for taking the time to have a chat with me. They deeply impressed me and gave me a glimpse of local realities. Hasse was one of many voices, questioning whether a PhD is needed. After all, it was him and the other folks of *climate adaptation services* who gave me one of the most important ingredients for doing a PhD: motivation to do something useful.

My family is the biggest gift in my life. I wish my research had a little more links to the non-maize world, so that I could have used the knowledge of the greatest philosopher of my world - my father. I would like to thank my father and Anke, my brother Joseph, my sister Sarah, my brother Max and my sister Fanny for always being there for me. I want to thank Daniel. I am grateful every day that we met in Marseille 10 years ago in *Quatre Vents*. Life with you feels good and everything seems possible with you next to me. I would like to thank my friends Lise, Caro, Eva, Andrea, Nicole, Lisa, Grace, Janis, Larissa and Diana. Forgetting time and research is easiest with you. I would like to thank Antje and Tabea for making it possible for me to finalize this dissertation - despite day-care close-downs, a broken leg and corona outbreaks - by taking care of our daughter. Last, I would like to thank our daughter Nora. I smile even more ever since you were born.

A special thanks goes to Joseph, Lilly, Max, Alex, Andrea and Karsten for proofreading this dissertation making it hopefully enjoyable to read.

Table of contents

1 Introduction

For the first time in over a decade of declining and stagnating numbers of undernourished people in the world, there has been an increase since 2017 - reaching 768 million people in 2020. This reversal in the trend can largely be attributed to conflicts, climate extremes and economic downturns, which makes it increasingly difficult to end hunger by 2030 (FAO et al., 2021). In future, global food demand will increase due to a growing world population, which is projected to rise from 7.7 billion in 2019 to 9.7 billion in 2050 (UNDESA, 2019). To feed the world, global food production must grow substantially. At the same time, the expansion of arable land needs to be halted to avoid further environmental damages, biodiversity loss and greenhouse gas emissions (van Ittersum et al., 2016). Thus, sustainable production increases will need to go hand in hand with a decline in per capita food demand. Avoiding food waste (Gustavsson et al., 2011; Mc Carthy et al., 2018) and reducing crop production for non-food uses (Cassidy et al., 2013) will be key to meeting the global food demand. Addressing these challenges seems to be most urgent in the tropics across many parts of Africa and South America. In these regions, the strongest population growth is expected (UNDESA, 2019), while agricultural production remains below its potential (Foley et al., 2011; van Ittersum et al., 2013). Moreover, the largest expansion of agricultural land to biodiversity-rich areas has occurred in these areas (Gibbs et al., 2010).

Climate change exacerbates the pressure on agriculture with the strongest negative impacts projected in the tropics (Hasegawa et al., 2022; Rosenzweig et al., 2014). To increase agricultural production, farming systems need to adapt to changing climatic conditions including slow onset events as well as extreme events, which are increasing in intensity and/or frequency (Seneviratne et al., 2021). The transformation towards a resilient food system that provides sufficient, safe and nutritious food for a growing world population requires information on climate risks in agriculture. This provides the basis for exploring ways to anticipate and respond to them. Crop models play an indispensable role in this regard as they allow quantifying crop responses to changes in climatic conditions. This dissertation demonstrates how statistical crop modelling can support this process, especially climate risk management and adaptation in tropical agriculture to increase the resilience of cropping systems and contribute to improved food security.

The subsequent sections review climate change impacts on tropical agriculture in chapter 1.1 and climate risk management and adaptation options in agriculture in chapter 1.2 with a specific focus on crop production. The role of statistical crop modelling in support of climate risk management and adaptation is discussed in chapter 1.3. Chapter 1.4 introduces the case studies of Peru, Tanzania and Burkina Faso, which share similar characteristics in terms of farming systems and climatic conditions in the tropics. The three publications that form the basis of this dissertation are introduced in chapter 2 and follow in the sub-chapters 2.1, 2.2 and 2.3. The discussion in chapter 3 includes a section on main findings across all publications (chapter 3.1) and an outlook with open research questions (chapter 3.2). The dissertation ends with concluding remarks and personal hopes in chapter 4.

1.1 Climate change impacts on agriculture in the tropics

Climate change impacts agricultural production in various ways through changes in modal conditions, seasonal changes and extreme events. Modal changes, such as the shift in climatic envelopes can alter the crop suitability in certain areas, which can lead to shifts in growing areas (Chemura et al., 2020; Kummu et al., 2021; Travis, 2016). Also, the distribution of pests and pathogens, such as the poleward expansion of many groups of crop pests and pathogens since the 1960s (Bebber, 2015)

changes with increasing warming and can potentially lead to drastic harvest losses. Seasonal changes can affect agriculture as warming trends lead to a shortened life cycle of major crops (Kerr et al., 2022; Wang et al., 2009) and a lengthening of the growing season in extratropical regions (Mueller et al., 2015). Extreme events increasingly cause crop losses (Cottrell et al., 2019), e.g. related to droughts (Kim et al., 2019), heat (Liu et al., 2019; Zampieri et al., 2017) or a combination of multiple hazards (Matiu et al., 2017). Apart from the described temperature and/or precipitation-related impacts, the atmospheric composition related to CO_2, dust, ozone and other short-lived climate pollutants changes. Elevated CO_2 concentrations affect agricultural production through changes in the photosynthesis rate, water use efficiency or nutrient content of crops (Kerr et al., 2022). Taken together, there is a complex interplay of climate drivers on crop production.

These human-induced climate change impacts have had regionally different, but mostly negative effects on global crop production since the pre-industrial era (Kerr et al., 2022). Advancements in plant breeding, irrigation, fertilisation and integrated pest management are associated with a 2.5 to 3-fold increase in major crop yields since the 1960s on the global level. On the contrary, climate change had mostly negative effects on crop yields and acts as a drag on the growth of agricultural production (Kerr et al., 2022). In a counterfactual analysis that attributes observed yield trends to anthropogenic warming, Moore (2022) showed a negative effect of global warming on maize and wheat yield trends and a positive effect for rice in cooler regions with an average reduction in the annual calorie production from these crops by 5.3 % from 2008 to 2017 (Moore, 2022). The overall negative impact of climate change on crop yields is projected to continue in the 21st century. Without adaptation, yields are projected to decrease by 2.3 % for maize, 3.3 % for soybean, 0.7 % for rice and 1.3 % for wheat per decade (Hasegawa et al., 2022).

Both observed and projected climate change impacts vary by region. Whereas yields for some crops benefitted from climate change impacts in the mid and high-latitudes (e.g. wheat in Northern Europe, rice and wheat in Eastern Asia, maize and soybean in North America), mostly negative impacts could be found in Sub-Saharan Africa, South America and the Caribbean (Ortiz-Bobea et al., 2021). The strongest negative climate impacts are projected in the tropics (Rosenzweig et al., 2014), particularly for Africa, Central and South America at the end of this century (Aggarwal et al., 2019; Hasegawa et al., 2022; Porter et al., 2019) due to the current temperature level and degree of warming. Regions with current average temperatures above approx. 15 °C are projected to face negative effects of climate change on agricultural production. When current average temperatures exceed approx. 20 °C, even small degrees of warming result in negative effects (Hasegawa et al., 2022). Higher temperatures lead to increasing atmospheric vapour-pressure deficits which in turn increase evapotranspiration and thus reduce soil moisture, with negative impacts on yields (Levis et al., 2018; Lobell et al., 2013, 2014). Moreover, temperatures in many tropical regions are already today closer to the optimum temperatures for plant growth (Hatfield et al., 2011) so that further temperature increases will exceed the optimal range.

Smallholder farming systems are most prevalent in tropical agriculture, particularly in Latin America, Sub-Saharan Africa, and South and East Asia (Samberg et al., 2016) and are disproportionally vulnerable to climate change (Donatti et al., 2019; Kerr et al., 2022; Morton, 2007). The livelihoods of smallholder farmers often primarily depend on agriculture so that changes in rainfall, temperature and the occurrence of extreme events directly affect their income, food security situation and well-being (Harvey et al., 2014; Morton, 2007; Vignola et al., 2015). Moreover, smallholder farmers have limited capacities to adapt to climate change for various reasons, such as lacking policy,

infrastructure and institutional support as well as limited access to credits and viable markets (Kerr et al., 2022; Mbow et al., 2019). Also, insecure land tenure rights can constrain farmers' ability to adapt to climate change (Murken & Gornott, 2022). The negative impacts of global warming on tropical agriculture and the high vulnerability of smallholder farmers further jeopardize their food and nutrition security (Wheeler & von Braun, 2013), which underlines the need for strong adaptation efforts.

1.2 Climate risk management and adaptation in agriculture

Negative climate impacts on agriculture require strong responses through climate risk management and adaptation to increase the resilience of farming systems. Climate risks result from "dynamic interactions between climate-related hazards with the exposure and vulnerability of the affected human or ecological system" (Begum et al., 2022). Risks of unmitigated climate impacts can be addressed through risk reduction by either preventing or preparing for them. For this purpose, integrating climate change adaptation and disaster risk reduction is needed (Begum et al., 2022; Lavell et al., 2012; UNDRR, 2019) to anticipate and respond to slow onset events as well as extreme events, which are increasing in intensity and/or frequency due to climate change (Seneviratne et al., 2021). However, not all of the risks can be prevented, so that the residual risks will have to be addressed through either risk finance and transfer or loss and damage when limits to adaptation are reached (Begum et al., 2022).

Adaptation options that reduce risks to agricultural crop production include the sustainable intensification of production, e.g. through the use of fertilizer and improved cultivars, or infrastructural and technological measures, such as investments in irrigation facilities. Nature-based adaptation solutions entail the adjustment of planting dates or agricultural diversification to spread risks in case of harvest losses. Moreover, water and soil management practices as well as agroecological approaches, including intercropping, cover crops, crop rotations, mixed systems or agroforestry, belong to nature-based solutions (Berrang-Ford et al., 2021; Kerr et al., 2022). Apart from these field-level adaptation options, several institutional measures can contribute to risk reduction. By providing tailored climate information such as early warnings (Tall et al., 2018), climate services can facilitate the implementation of adaptation options. Spreading risks through livelihood diversification or migration (Loison, 2015), increasing adaptive capacity through community-based adaptation (Ensor et al., 2018) or integrated approaches addressing climate adaptation and mitigating simultaneously (Harvey et al., 2014) are also possibilities to reduce climate-related risks in agriculture.

1.3 Statistical crop modelling in support of climate risk management

Crop models are indispensable tools to inform decision-making in climate risk management and adaptation as they allow quantifying crop responses to weather and climatic conditions. Three main approaches of crop models can be distinguished – process-based models, statistical crop models and integrated approaches. Process-based or crop simulation models attempt to represent key processes of crop growth and yield formation and can quantify the interaction of genotype, environment and management on various outputs, such as crop production, yield, carbon sequestration or greenhouse gas emissions. Statistical or empirical crop models assess the relationship between climatic variables and yield empirically. Last, integrated approaches combine biophysical and socio-economic considerations – thereby attempting to inform complex, multi-targeted policy decisions across different scales, e.g. related to food security (Rötter et al., 2018).

This dissertation focuses on the use of statistical models, including machine learning, to inform climate risk management. Statistical crop models have a long history with early examples by Runge (1968) and Thompson (1975). They estimate climate-yield relationships based on empirical observations. With increasingly available weather and crop yield data (derived from official statistics, field measurements or farmer surveys), statistical models became a common tool in climate impact assessments (Lobell & Asseng 2017). Compared to process-based models, they require fewer input data and can use spatially and temporally aggregated data as input (Holzkämper, 2017; Rötter et al., 2018), which facilitates their application and transfer to data scare contexts often found in countries in the Global South. Especially in the tropics where yield loss related biotic stressors are a common issue (Aggarwal et al., 2006; van Ittersum et al., 2016), statistical models offer an advantage as they inherently cover indirect yield-limiting factors linked to climatic variables. This allows to better capture pests and diseases in statistical crop models (Rötter et al., 2018).

For the purpose of supporting climate-related risk reduction in the agricultural sector, crop models can provide support in various ways. Crop models can improve the understanding of physical and socio-economic systems and be used to identify major climatic drivers. They can predict and thus help to anticipate future climate risks to crop production. Moreover, crop models can be applied to test and prioritize climate adaptation options based on their environmental and socio-economic impacts (Holzkämper, 2017). Statistical crop models have mostly been applied for agricultural climate impact assessments (e.g. Brás et al., 2021; Lobell, David. B et al., 2011; Lobell et al., 2006, 2008; Ray et al., 2015; Schlenker & Lobell, 2010). By identifying main climatic drivers on yield, they are able to prioritize regions in which climate adaptation will be particularly needed. Statistical crop models usually do not explicitly account for adaptation processes, unless management-related variables are included, such as in Jiang & Koo (2014). However, these models implicitly take autonomous adaptation into account, which continuously progresses over time and is therefore represented in observational data (Gornott & Wechsung, 2016; Holzkämper, 2017). Statistical models have a high potential for short-term, i.e. seasonal yield predictions (Liu & Basso, 2019; Schauberger et al., 2017, 2020), for which machine learning is increasingly being used (Meroni et al., 2021). These forecasts can inform early warning systems on food insecurity (Choularton & Krishnamurthy, 2019) to support governments in taking actions to alleviate looming food crises (Liu & Basso, 2019). Independently of the modelling approach, any model requires thorough validation before it can inform real-world applications.

1.4 Case studies

The three case studies of this dissertation - Peru, Tanzania and Burkina Faso - are located in the tropics and share similar characteristics in the farming systems. Agriculture in these countries is dominated by smallholder and subsistence farming systems with mostly low input agronomic management. Because most people's livelihoods in these countries directly depend on agriculture – either as a source of food or income, the food security situation of the population is directly impacted by unfavourable weather conditions and climate change. The following sub-chapters highlight some characteristics concerning the climatic conditions and the farming systems in Peru, Tanzania and Burkina Faso.

Figure 1: Map of case studies

1.4.1 Peru

Peru's geography is characterised by the Andes, which run north-south and divide the country into three prominent landforms with distinct climatic and growing conditions resulting in a high level of biodiversity. The coastal region (costa) along the Pacific Ocean is characterised by semi-arid subtropical desert climate. Mean temperatures vary from 13 ° to 26 °C and annual rainfall is on average 150 mm. Agriculture in the coastal region is dominated by intensively grown export crops (USAID, 2017), which mostly rely on irrigation based on water coming from glacial melt of the Andes (Liersch & Gornott, 2015). With ongoing climate change and continuous melting of the glaciers (Ortiz, 2012), water scarcity will further hamper agricultural production in this region. The Andean highlands (sierra) have lower temperatures (11 ° to 18 °C on average) due to their higher elevations. Annual rainfall shows substantial variations (50 to 1000 mm per year), depending on the location within the Andes (eastern or western slope). The rainy season is from September to March (USAID, 2017). Particularly in the dry season from May to August, irrigation stemming from glacier melt is needed (Liersch & Gornott, 2015). Most farmers live in the Andean region, practising subsistence and rainfed agriculture to grow traditional crops, such as potatoes, quinoa and maize. A shift of agricultural production to higher elevations occurs in response to increasing temperatures, which increases the risk of being impacted by snowstorms, drought and floods (USAID, 2017). The amazon rainforest (selva) is a high-precipitation region (1000 to 3000 mm per year) with high temperatures (22 ° to 31 °C) throughout the whole year. Pastoralism mainly takes place in the mountainous and high-elevated jungle areas, where it provides food and income, especially for rural communities (USAID, 2017).

Median yields for the most grown crops in Peru are 3.4 t/ha for maize, 0.8 t/ha for coffee, 7.7 t/ha for rice, 15.9 t/ha for potatoes and 12.9 t/ha for bananas (from 2016-2020 based on FAO, 2020). The high level of input use (INEI, 2013) and irrigation coverage (75 % of agricultural area is equipped with irrigation schemes on the national level (FAO, 2018)) primarily reflects the export-orientated agro-industry in the coastal region. However, 80 % of farmers in Peru are subsistence farmers (USAID, 2017) in the highlands, where traditional farming practices on small parcels of land prevail (Sietz et al., 2012). Approximately 19 % of the population in Peru is threatened by severe food insecurity (2016-2018; FAO, 2018).

1.4.2 Tanzania

The climate in Tanzania is largely influenced by its topography and its differences in altitude. It ranges from tropical climate in the lowlands at the coast with annual mean temperatures of 26 °C to temperate climate found in the highlands in the north and south-west of the country with annual mean temperatures of 18 °C. Whereas rainfall on the central plateau, which covers most of the country, ranges from 500 to 1000 mm per year, precipitation in the lowlands and highlands exceeds 1300 mm (Tomalka et al., 2020). In Northeast Tanzania and the coastal areas, there is a bimodal rainfall pattern resulting from the seasonal migration of the Intertropical Convergence Zone (Zorita & Tilya, 2002). The short rains are called Vuli and occur from October to December, whereas the longer rain period is called Masika and occurs from March to May. The rest of the country has a unimodal rainfall pattern called Musumi with rainfall occurring from December to April (Arce & Caballero, 2015).

Agriculture in Tanzania is characterised by small-scale farming with low-input agronomic management. The average farm size per household is 2 ha and 91 % of total farmland is occupied by small-scale farms (Yoshino et al., 2017). Most crop production is based on rain-fed agriculture (only approx. 2.7 % of crop land is equipped with irrigation; FAO, 2018), making crop production particularly susceptible to shortages in rain. Maize is the most grown crop in Tanzania (median yield from 2016-2020 = 1.6 t/ha), followed by rice (2.9 t/ha), cassava (7.3 t/ha), groundnuts (0.7 t/ha), sunflower (1 t/ha) and beans (1.3 t/ha). The main cash crops are rice, nuts (sesame, cashew, coconut), cotton, coffee and tobacco (FAO, 2020). Even though agriculture accounts for 50 % of Tanzania's total exports, it has little impact on job creation and technological development as most exporting goods are unprocessed (Yoshino et al., 2017). With 94.3 % of households having an income from agriculture (National Bureau of Statistics Tanzania, 2014), the livelihood of the vast majority of people in Tanzania is directly impacted by adverse climate impacts on agriculture.

1.4.3 Burkina Faso

Large parts of Burkina Faso are located on the central Savannah plateau with slight elevations and an average altitude of 400 m. The climate is predominantly Sahelian tropical climate with increasing precipitation amounts and duration of the rainy season towards the South. Three climate zones can be distinguished. The Sahelian zone in the north of the country receives the lowest amounts of rain (300 to 600 mm per year; FAO, 2015). Moreover, annual mean temperatures of up to 29 ° (Tomalka et al., 2021) and the hot and dry winds from the Sahara (harmattans) that prevail from March to May lead to high evapotranspiration rates and thus dry conditions. The dry season can last up to nine months (October to June; FAO, 2015). As only 0.9 % of arable land is irrigated in Burkina Faso (FAO, 2018), the growing season is mainly aligned with the rainy season, resulting in a short growing season of fewer than 100 days (FAO, 2015). Therefore, agriculture in this zone is dominated by livestock rather than crop production (Tomalka et al., 2021). Whereas the Sudano-Sahelian zone in the centre of Burkina Faso receives 600 to 900 mm of rainfall per year, rainfall in the southern Sudanian zone amounts to up to 1200 mm in the rainy season, which lasts up to seven months from May to October (FAO, 2015). Average annual temperatures are around 27 °C (Tomalka et al., 2021). This zone is due to the growing season length of about 160 days and fertile soils the most suited for agricultural crop production, which translates into higher yields compared to the rest of the country (FAO, 2015). On national level, median yields from 2016 to 2020 for the most grown crops are 1 t/ha for sorghum, 0.5 t/ha for cow peas, 0.8 t/ha for millet, 1.7 t/ha for maize and 1.2 t/ha for cotton (FAO, 2020).

Burkina Faso is one of the poorest countries in the world and belongs to the group of least developed countries. The high population growth rate of 2.8 % per year (World Bank, 2022) and the high level of

violence and unrests in the country contribute to the severe food security situation (USAID, 2020), with almost half of the Burkinabe population being affected by either moderate or severe food insecurity (FAO, 2018).

2 Publications

This dissertation presents three publications, which are shortly introduced in this section and follow in the subsequent sub-chapters (2.1, 2.2 and 2.3). Rights of use are specified within the respective sub-chapter of the publication.

(1) Laudien, R., Schauberger, B., Gleixner, S., & Gornott, C. (2020). Assessment of weather-yield relations of starchy maize at different scales in Peru to support the NDC implementation. *Agricultural and Forest Meteorology*, *295*, 108154. https://doi.org/10.1016/j.agrformet.2020.108154

The first study assesses weather influences on starchy maize yields on the sub-national and local scale in Peru based on different yield data sources (official agricultural statistics and survey data) and different statistical approaches (a linear regression model, a linear panel data model and a machine learning algorithm). Moreover, the influence of higher water availability on maize yields on the sub-national level is assessed in support of the Peruvian *Nationally Determined Contributions* and the herein suggested adaptation options to climate change.

(2) Laudien, R., Schauberger, B., Makowski, D., & Gornott, C. (2020). Robustly forecasting maize yields in Tanzania based on climatic predictors. *Scientific Reports*, *10*(1), 1–12. https://doi.org/10.1038/s41598-020-76315-8

The second study provides a within-season maize yield forecast six weeks before the harvest on the sub-national level in Tanzania, which can support governments in preparing for looming food crises. The study utilizes a rigorous and transparent validation that mimics the operational context in which the model has to be trained purely on past data. Furthermore, we tested the robustness by providing a completely independent forecast for the harvest year 2019.

(3) Laudien, R., Schauberger, B., Waid, J., & Gornott, C. (2022). A forecast of staple crop production in Burkina Faso to enable early warnings of shortages in domestic food availability. *Scientific Reports*, *12*(1), 1638. https://doi.org/10.1038/s41598-022-05561-9

By combining a yield forecast with information on harvest areas, the third study provides a crop production forecast one month before the harvest for maize, millet and sorghum on the national level in Burkina Faso. Moreover, the produced calories from these crops are compared with the historic demand. This allows us to provide early information on shortages in domestic cereal production, which can inform early warning systems of food security.

2.1 Assessment of weather-yield relations of starchy maize at different scales in Peru to support the NDC implementation

This chapter is a reproduction of the article published as:

Laudien, R., Schauberger, B., Gleixner, S., & Gornott, C. (2020). Assessment of weather-yield relations of starchy maize at different scales in Peru to support the NDC implementation. *Agricultural and Forest Meteorology*, *295*, 108154. https://doi.org/10.1016/j.agrformet.2020.108154

Agricultural and Forest Meteorology 295 (2020) 108154

Contents lists available at ScienceDirect

Agricultural and Forest Meteorology

journal homepage: www.elsevier.com/locate/agrformet

Assessment of weather-yield relations of starchy maize at different scales in Peru to support the NDC implementation

Rahel Laudien*, Bernhard Schauberger, Stephanie Gleixner, Christoph Gornott

Potsdam Institute for Climate Impact Research (PIK), Member of the Leibniz Association, P.O. Box 60 12 03, D-14412 Potsdam, Germany

ARTICLE INFO

Keywords:
Starchy maize
Yield
Peru
NDCs
Climate adaptation
Statistical crop model

ABSTRACT

Climate change poses a substantial risk to agricultural production in Peru. Nationally Determined Contributions (NDCs) are currently developed and outline Peru's mitigation actions and adaptation plans to climate change in various sectors. To support the implementation of adaptation measures in the agricultural sector, information on weather-related risks for crop production and the effectiveness of adaptation options on the local scale are needed. We assess weather influences on starchy maize yields on different scales in Peru based on statistical crop models and a machine learning algorithm. The models explain 91% of yield variability (55% based on the cross-validation) on the regional scale. On the local scale, weather-related yield variation can be explained in some areas, but to a lower extent. Based on these models, we assess the effectiveness of adaptation measures which increase water availability to protect against negative impacts from dry weather conditions. The results show that a higher water availability of 77mm in the growing season would have regionally different effects, ranging from an increase of 20% to a decrease of 17% in maize yields. This large range underlines the importance of a local assessment of adaptation options. With this example, we illustrate how a statistical approach can support a risk-informed selection of adaptation measures at the local scale as suggested in Peru's NDC implementation plan.

1. Introduction

The Nationally Determined Contributions (NDCs) implementation plan is currently developed in Peru, as a follow-up to the COP21 in Paris in 2015. It provides the basis for Peru's contributions to reducing greenhouse gas emissions and outlines how Peru plans to adapt to climate change impacts in various sectors. Climate change projections show that the agricultural sector in Peru is expected to be confronted with higher temperatures and fewer rainy days but more intense rainfall events (Christensen et al., 2013; Giorgi et al., 2014). In addition to changes in precipitation patterns, the melting of Peru's glaciers (Rabatel et al., 2013) diminishes an important water source for agriculture.

To support the development of the NDCs in Peru, information on the expected impacts of climate change and altered weather conditions on agriculture is required to formulate effective adaptation measures. In addition to information on long-term climatic changes, information on production risks for the near future is needed to provide guidance on how to reduce weather risks by short-term adaptation planning and how to deal with already altered climate conditions.

To test if an adaptation measure is appropriate to reduce risks in crop production, process-based and statistical crop models are important tools to resolve the impact of weather on crop yields (Challinor et al., 2014), and the particular effect of adaptation measures under different environmental conditions. A statistical model, which is trained on past weather and yield data, can provide valuable empirical support for informing adaptation measures in the near future (Iglesias et al., 2010; Lobell et al., 2008; Lobell and Burke, 2010; Mu et al., 2013).

As outlined in the NDCs of Peru, the local scale is of particular

Abbreviations: NDCs, Nationally Determined Contributions; COP21, 21st session of the Conference of the Parties; RRM, regional regression model; PDM, panel data model, DT, decision tree; ENSO, El Niño–Southern Oscillation; GDD, growing degree days; AIC, Akaike Information Criterion; MSE, mean squared error; NSEe (NSEv), Nash–Sutcliffe efficiency coefficient of the estimation (validation) result; CART, Classification and Regression Tree; SENAMHI, Servicio Nacional de Meteorología e Hidrología del Perú; PISCO, Peruvian Interpolation Data of the SENAMHI's Climatological and Hydrological Observations; JRA-55, Japanese 55-year Reanalysis; MODIS, Moderate Resolution Imaging Spectroradiometer, cloud fraction

* Corresponding author.
E-mail addresses: laudien@pik-potsdam.de (R. Laudien), schauber@pik-potsdam.de (B. Schauberger), gleixner@pik-potsdam.de (S. Gleixner), gornott@pik-potsdam.de (C. Gornott).

https://doi.org/10.1016/j.agrformet.2020.108154
Received 2 December 2019; Received in revised form 11 August 2020; Accepted 20 August 2020

importance when it comes to developing and implementing adaptation measures as often ways to anticipate and protect against climate change impacts need to be found on the local scale (Gobierno del Perú, 2018). To support an effective selection of appropriate adaptation measures at this level, a model assessment needs to be able to provide information about yield impacts and effects of adaptation at this scale. Apart from a global assessment by Ray et al. (2015) that describes weather-related yield variation on the regional level in Peru, there is – to our best knowledge – no local or regional assessment of the complex weather influences on crop production covering the whole country of Peru. Moreover, there is no assessment of suitable adaptation measures informed by risk assessments of current or future weather conditions.

In this study, we assess the influence of weather on starchy maize yields. Together with potato (*Solanum tuberosum L.*), starchy maize (*Zea mays L ssp. amiláceo*) belongs to the main food crops in Peru. It is mostly produced for self-consumption, which makes its production particularly important for the food security of 42% of the rural population who live in poverty in Peru (INEI, 2019).

We assess weather influences on starchy maize yields on different scales in Peru with a regional regression model, a panel data model and the machine learning algorithm decision tree. Based on these models, we evaluate the effectiveness of adaption measures which increase water availability (e.g. irrigation, water storage and harvesting or soil management, as named in Peru's NDCs) as action options under unfavourable weather conditions. With this example, we illustrate how a statistical approach can support a risk-informed selection of adaptation measures suggested in Peru's NDCs. This can support the implementation process of the NDCs and the design of effective adaptation measures for current and future periods at the local scale.

1.1. Weather variability and climate change in Peru

Already today, Peru is affected by high weather variability – both spatially and temporally. Peru has 15 Köppen-Geiger climate zones (Fig. A.1 of the supplementary information, SI), which range from hot and cold desert climate at the coast to subtropical highland climate in the Andes and tropical rainforest climate in the Amazon (Peel et al., 2007). This spatial climatic diversity results in different growing conditions across the country. Even within the same climate zones, the inter-annual weather variability is high because of periodically recurring El Niño–Southern Oscillation (ENSO) events. El Niño particularly impacts the coastal region of the Andes in Peru (Bourrel et al., 2015). The recent Coastal El Niño event in 2016/17 led to severe floods and landslides along the northern and central coastal region (Rodríguez-Morata et al., 2019). The El Niño in 2015/16 was associated with exceptionally dry conditions in the south of Peru. Agriculture in Peru needs to be able to adapt to these varying weather conditions for which early warnings are still difficult to obtain, despite progress in the prediction lead time (Ludescher et al., 2014).

In addition to these already prevalent weather risks on agriculture, climate change will amplify risks for Peru's agricultural sector. In the last four decades, the strongest warming within Peru occurred in the southern Andes of Peru (warming rates reached up to 0.3°C per decade since 1981; SI Fig. A.2). This warming trend is projected to continue to an additional increase of 1° to 2°C until mid-century depending on the emission scenario (Collins et al., 2013; Marengo et al., 2009). Apart from the direct impact of increased temperatures on agriculture, higher temperatures also increase the atmospheric water demand and consequently evapotranspiration rates (Allen et al., 1998). This in turn reduces the amount of water available to agriculture (Lobell et al., 2013).

With regards to future precipitation projections, a general tendency towards fewer rainy days, but more intense rainfall events, is expected (Christensen et al., 2013; Giorgi et al., 2014). Whereas the northern Coast and the Amazon region are expected to experience fewer consecutive dry days throughout the 21st century, the number of dry days and consequently dry spells are projected to increase over southern Peru (Giorgi et al., 2014; Sörensson et al., 2010) where the main starchy maize producing regions can be found.

Many glaciers have already lost up to 30% of their surface area since the 1960s (Rabatel et al., 2013) such that an important water source for agriculture is diminishing. Melting glaciers, dryer conditions in southern Peru and more erratic rainfall suggest that adaptation options (e.g. irrigation, water storage and harvesting or soil management) that address water scarcity and precipitation vagaries will be important to maintain and increase agricultural productivity in Peru.

2. Material and methods

In this study, we used two yield data sources and three different statistical models to assess the influence of weather on starchy maize yields in Peru. Based on the models, we evaluated the effectiveness of artificially increased water availability to increase yields.

2.1. Input data

2.1.1. Yield data

The first source of crop yield data is obtained from official statistics from the Ministry of Agriculture of Peru (MINAGRI, 2018). The time series covers 13 years (from 2005 to 2017) and is available on region level. The dataset comprises 19 out of the 25 regions in Peru.

The second yield data source is a household survey on plot level carried out by the Peruvian national statistical institute “Instituto Nacional de Estadística e Informática” (INEI, 2017). The first survey wave started in 2014. However, the size assessment of the agricultural plots changed in 2016 (source: personal communication with INEI), so that the first two and the last two waves are not comparable. Therefore, we only considered the last two waves (2016 and 2017) of the survey to have a consistent measurement of the plot sizes in the data set. This is important as yield is calculated as production over area. The data set of waves 2016 and 2017 comprises 19,704 yield observations in total (SI Fig. A.3). We aggregated the plot level data to cluster level. The clusters were derived from the IV national census from 2012 and are the primary sampling unit of the survey. Clusters are below districts, i.e. the lowest administrative unit in Peru (SI Fig. A.4 shows a map of regions and clusters in Peru). The aggregation to cluster level was necessary to limit a potential sampling bias or reporting error on plot level and because the GPS locations of the plots are not publically available, thus precluding a correlation with weather data. We averaged the yields per cluster with weights based on harvest area.

2.1.2. Weather data

We used the following climate data for our analysis. For precipitation, we used a data set provided by the Peruvian meteorological service SENAMHI (Servicio Nacional de Meteorología e Hidrología del Perú) called PISCO (the Peruvian Interpolation Data of the SENAMHI's Climatological and Hydrological Observations, Aybar et al., 2019). The data set provides daily precipitation sums at a spatial resolution of 0.1° and has a robust performance in particular in the coastal regions and the western flank of the Andes (Aybar et al., 2019), which are particularly used for maize production. While PISCO also includes temperature data, this was not available for the whole study period. Therefore, we used surface temperature data from JRA-55 (Japanese 55-year Reanalysis; Kobayashi et al., 2015). JRA-55 provides 6-hourly temperature at a resolution of ca. 0.6°. To represent the influence of solar radiation on plant growth, we used cloud fraction derived from MODIS (Moderate Resolution Imaging Spectroradiometer; Platnick et al., 2015) due to its high spatial and temporal resolution for a long time series. MODIS provides daily raster imageries at a resolution of 5km. We used cloud fraction instead of solar radiation due to reliability issues in the data quality of solar radiation over the Amazon (Dutra et al., 2015) and because cloud fraction can be regarded as tantamount to solar radiation (Muneer and Gul, 2000). Even though the

combination of different climate data sources bears the risk of incorporating physical inconsistencies, the different sources were considered the best available choices for Peru in particular in regard of spatial resolution, which is crucial in complex terrain. Moreover, physical correlations are less relevant when aggregating climate data temporally and spatially to administrative levels. For the regional assessment, we calculated the mean over all grid points per region. For the local assessment, we aggregated the weather data to cluster scale. Due to the small size of the clusters, we used the weather grid point that has the shortest distance to the cluster center calculated by the Euclidean distance.

2.1.3. Crop calendar

To represent the weather conditions during the growing season, we followed the crop calendar provided by MINAGRI (MINAGRI, 2017). Even though the survey also contains information about the growing season, we preferred the MINAGRI crop calendar to allow for a better comparison between the two yield data sources and to avoid possible errors in the survey-based seasons (Section 2.1.1). Per region the most frequent sowing and harvesting month were selected. If the previous (next) sowing month (harvesting month) had a share higher than 25%, it was also included in the growing season. For the regions Lambayeque and Ica no clear growing season could be found, because several months have a similarly high share. Therefore, we used the dates of the provinces within these regions with the highest production of starchy maize.

2.2. Modelling approaches

We used three modelling approaches (Fig. 1). To assess weather-yield relations on the regional level, we used a regional regression model (RRM). The data set on region level covering 2005 to 2017 was used as input yield data. For each of the 19 regions, a RRM (Eq. (1)) with different variables and parameters was constructed to account for the diverse climatic conditions within the country.

Due to the short time series of the household survey (covering the harvesting years 2015 to 2017), we used a panel data model (PDM) to analyse weather influences on maize yields at the local level. The PDM uses one parameter set for all the considered spatial units (Eq. (2)). Both the RRM and PDM follow the approach of Gornott and Wechsung (2016).

$$y_{it} = \sum_{k=1}^{K} \beta_{ki} X_{kit} + \alpha_i + \varepsilon_{it} \quad (1)$$

$$y_{it} = \sum_{k=1}^{K} \beta_{k} X_{kit} + \alpha_i + \varepsilon_{it} \quad (2)$$

with β as parameters, X as explanatory input variable, α as unobserved time-invariant individual effects, ε as error term for K variables ($k = 1, ..., K$), N spatial units ($i = 1, ..., N$) and T years ($t = 1, ..., T$)

In addition to these two regression models, we used a decision tree (DT) to cross-check the results obtained from the PDM. The PDM is based on fewer input data, which bears the risk of generating less robust results. We therefore apply a machine learning algorithm as an additional validation. The DT is a non-parametric machine learning algorithm which does not require distributional assumptions and is robust to outliers (Song and Lu, 2015). For our analysis, we used the CART (Classification and Regression Tree) algorithm (Breiman et al., 1984). To avoid overfitting, we pruned the tree by defining the minimum amount of observations required to perform a split to 50 and the minimum amount of observations for an end node to 25. This is referred to as pre-pruning and stops the tree from growing completely until it

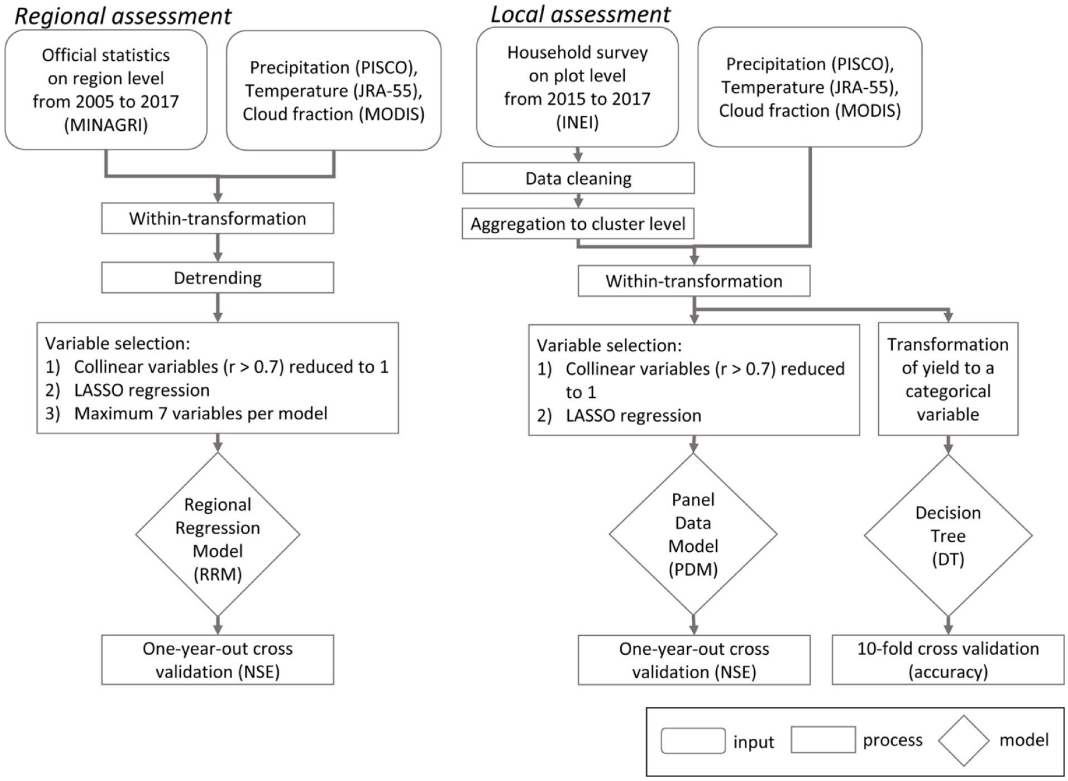

Fig. 1. Work flow of the analysis for regional (left) and local assessment (right).

perfectly classifies the training set (Patel and Upadhyay, 2012).

For our analysis, we used R (R Core Team, 2014) with the package glmnet (Friedman et al., 2008) to perform LASSO regression, the package rpart (Therneau et al., 2019) to perform the decision tree and the package ggplot2 (Wickham, 2009) to produce the figures.

2.2.1. Pre-processing

The household survey contained obvious inconsistencies that required data cleaning. Some observations in the survey have higher harvest areas than planted areas or unrealistically high production on small plots (e.g. > 300kg production on < 0.03ha harvest area). The sowing and harvesting dates show questionable entries for many observations, i.e. either strong deviations from the median dates per region or a growing season longer than a year. These inconsistencies could originate from differing techniques applied by enumerators or wrong statements made by the interviewees. Different units used for production (kg, arroba, bag, quintal and other units), and plot sizes (m^2, ha, acre and other units) make the data set prone to errors and inaccuracies, because the conversion factors used to standardize production and plot size might be inaccurate. To ensure a proper data base, we deemed it essential to clean the data before modelling. First, we removed observations with missing values for yield. Second, we omitted yields outside the 1^{st} and 99^{th} percentiles to guard against outliers, leaving only yields between 0.24 and 3.75 t/ha. Third, we only kept clusters that have yield data for at least three harvesting years (the survey in 2016 also asked for harvests in 2015, with equal plot size calculations as in 2016 and 2017). Fourth, we removed those clusters that show very little yield variability (standard deviation < 0.01 percentile), as constant yields are unlikely and probably reporting errors. In sum, after data cleaning (remaining n = 19,253), aggregating to cluster level (n = 1,994), only considering clusters with three harvesting years (n = 324) and sufficient variability, we used 291 aggregated yield observations (SI Fig. A.3).

In addition, we applied the following transformations: For all three models, we applied a within-transformation to remove time-constant effects from the variables (Wooldridge, 2014). For the RRM that is based on a time series of 13 years, we removed the trend in the yield data by testing different de-trending methods (none, linear, quadratic) and then applying the one that resulted in the lowest Akaike Information Criterion (AIC; Bozdogan, 1987). For the DT, we transformed quantitative maize yields into a categorical variable by splitting it into five groups (using the 0th, 20th, 40th, 60th, 80th, 100th percentiles as group limits).

2.2.2. Variable creation and selection

Following the climatic envelope for maize growth (SI Text A.1), we generated the following variables (formulas are provided in SI Text A.2): To represent temperature conditions, we included mean temperature (T.mean), the mean and maximum of daily maximum temperatures (T.max and maxOfmax, respectively) and the mean and minimum of daily minimum temperatures (T.min and minOfmin, respectively). The two extreme values were included to account for single high and low temperature events that could already induce crop damages. To represent cumulative extreme temperature influences, we included Freezing Degree Days (FDD) to account for the harmful influence of cold temperatures below 0°C and Heat Degree Days above 30°C (HDD) to cover too high temperatures. Variations in temperature within the season are represented by the coefficient of variation (CV, defined as standard deviation over mean). We calculated the CV of T.mean, T.max and T.min.

We included the precipitation sum in the growing season (P.sum) to represent the overall water availability for maize. We also included the number of days with precipitation above a threshold of 5 (PA5), 10 (PA10), 15 (PA15) and 20mm (PA20) per day as well as the maximum daily precipitation (P.max) to cover the influence of single precipitation events. The number of days without precipitation (DWP) accounts for dry conditions. Because the distribution of rainfall within the growing season is of particular importance for plant growth, we included dry spells of more than 5 (cdd5) and 10 consecutrive dry days (cdd10) and wet spells of more than 5 (cwd5) and 10 consecutive wet days (cwd10). The coefficient of variation of the precipitation sum (P.cv) represents the variability of rainfall within the growing season.

To cover the influence of solar radiation, we included the mean cloud fraction (C.mean), the minimum cloud fraction (C.min) and the coefficient of variation of the mean cloud fraction (C.cv).

The variables were separately calculated for the vegetative and reproductive phase of the growing season. The separation between vegetative and reproductive phase was based on the sum of growing degree days (GDD; SI Text A.2 Eq. (22)). The days in the growing season until 50% of the full-season GDD sum was reached were allocated to the vegetative phase and the remainder to the reproductive phase, following Schauberger et al. (2017).

Since there is a large number of potentially relevant variables, a selection process was applied for the RRM and the PDM to elucidate important influences. 1) To avoid multicollinearity, only those variables were selected that are not strongly collinear (i.e. Pearson's r > 0.7) with another explanatory variable. For the RRM: if a set of variables was strongly collinear, then from this set only one variable was included, choosing the one with the highest correlation with yield. For the PDM: variables were selected for which more clusters have a high correlation with yield. 2) Least Absolute Shrinkage and Selection Operator (LASSO) regression was performed for the final feature selection. Through regularization, LASSO performs a co-variate selection, which improves both the prediction accuracy and the interpretability (Tibshirani, 1996). For the RRM: to select the optimum lambda (the regularization penalty for the LASSO regression), we used the lowest cross-validation (years were omitted subsequently) mean squared error (MSE). For the PDM: because of a higher amount of input data, we used the lowest cross-validation MSE of a 10-fold cross-validation to select the optimal lambda. Because in this case the folds were selected across time and space, we used the mean minimum lambda value of 30 model runs. 3) As an extra safeguard against overfitting in the RRM, we included one further restriction, allowing only half as many variables as there are observations. For the DT, the described variable selection process was not applied as the algorithm explicitly selects the variables that achieve the highest information gain and pre-pruning avoids overfitting.

2.2.3. Validation

To validate the RRM and the PDM results, we performed a one-year-out cross-validation. For each year subsequently, all observations in that year are removed from the dataset and the remaining observations from the other years are used to estimate the model and predict yield changes for the removed year. The goodness of fit was then evaluated based on the Nash–Sutcliffe efficiency coefficient (NSE; Nash and Sutcliffe, 1970), for the combined out-of-sample predictions. In contrast to R^2, NSE does not only evaluate similarities in variability, but also the mean model bias, which makes it a robust quality measure. In addition, we tested the significance of the models based on the F-statistics and the performance of the models compared to a constant model that only takes the mean yield per region as a predictor. With the Breusch–Godfrey test we assessed autocorrelation and with the Breusch–Pagan test we tested for heteroscedasticity. As highly co-linear variables were removed in the variable selection process, a test for multicollinearity was not necessary.

The DT is validated based on a 10-fold cross-validation and the model fit is assed based on accuracy, which is defined as the share of correctly predicted values of all predicted values.

We compare the model fit of the different modelling approaches on region level. Therefore, the observed and modelled yields of the PDM and the DT were aggregated to region level.

2.3. Assessment of adaptation options

We assessed the effect of increased water availability on crop yields. To get an estimate of how much more water is going to be needed in future with ongoing climate change, we focused in our analysis on changes in the atmospheric water demand. A warming climate increases the atmospheric water demand (Allen et al., 1998). This in turn reduces the amount of water available to agriculture (Konings et al., 2017; Konings and Gentine, 2017; Lobell et al., 2013; Novick et al., 2016). The actual water availability depends also on other factors, most importantly on precipitation and soil water holding capacity. However, as climate models do not agree on a sign of the change in precipitation in the future in Peru (SI Fig. A.5), we concentrated on the change in atmospheric moisture demand.

For an estimate of future changes in the atmospheric water demand, we focused on potential evaporation in the ISIMIP2b simulations from the global hydrological model WaterGAP2 (Müller Schmied et al., 2016). The model was driven with climate data from four global climate models (namely GFDL-ESM2M, HadGEM2-ES, IPSL-CM5A-LR, MIROC5), which were bias-adjusted and provided within ISIMIP2b (Warszawski et al., 2014). We focused on the RCP8.5 scenario, which is the RCP emission scenarios without climate policy interventions, to take into account the range from conditions similar to today to unmitigated climate change. The spatial variation of current potential evapotranspiration over Peru and expected changes by mid-century are shown in Fig. 2. The ensemble mean change of potential evaporation under RCP8.5 in Peru is an increase of ca. 77mm for the growing season in the middle of this century. This amount of water is estimated to feed the atmospheric water demand and as such is not available to crops. Therefore, we assume this amount to be the minimum necessary additional water in the near future to compensate for the negative temperature effects on water availability. We used this estimated change in potential evapotranspiration and assessed the effect of 77mm more water per growing season on starchy maize yields.

To distribute the additional water evenly over the growing season, we assumed that the farmer would irrigate twice per month (on day 1 and 15 of each month) by an amount of 77mm divided by the number of months times two. As most growing seasons are around nine months, this means ca. 9mm of irrigation per month. We compared the original model output (the estimation with currently available water) with the adaptation scenario outputs and evaluated the changes in simulated maize yields.

3. Results

3.1. Starchy maize yields in Peru

In Peru, 273,868 tons of starchy maize were produced in 2017. The main producing regions were Cusco, Apurimac, Huancavelica, La Libertad, Ayacucho and Cajamarca (Fig. 3). These six regions accounted for 70% of the total national production in 2017.

Between 2005 and 2017, yields for starchy maize in Peru were 1.7t/ha on average. In 2017, the highest yields could be found in the southern coastal regions in Peru (Ica, Arequipa and Tacna) with the highest yields in Ica (4.5t/ha). The lowest yields were obtained in Piura, Amazonas and Cajamarca (0.8 to 1t/ha). Apart from Cusco, which had relatively high yields (2.5t/ha), most regions with high total production only showed medium yield levels (Apurimac = 1.9t/ha, Huancavelica = 1.6t/ha, La Libertad = 1.6t/ha, Ayacucho = 1.3t/ha). An exception is Cajamarca, which had the lowest yield level (0.8t/ha) compared to the other regions even though it was one of the most producing regions. Accordingly the harvest area was one of the highest compared to the other regions, whereas the high-yield regions had lower harvest areas (Ica, Lima, Tacna and Moquegua; MINAGRI, 2018). The vast majority of starchy maize production was based on smallholder agriculture with an average harvest areas of 0.13ha. Even in Piura and Lambayeque, which were the regions with the highest harvest area for starchy maize in Peru, the harvest areas was only 0.28ha on average (INEI, 2017).

As there is no spatially explicit information in the data set when maize is planted or harvested, we chose the entire official growing period (Fig. 4) as reported by the Ministry of Agriculture

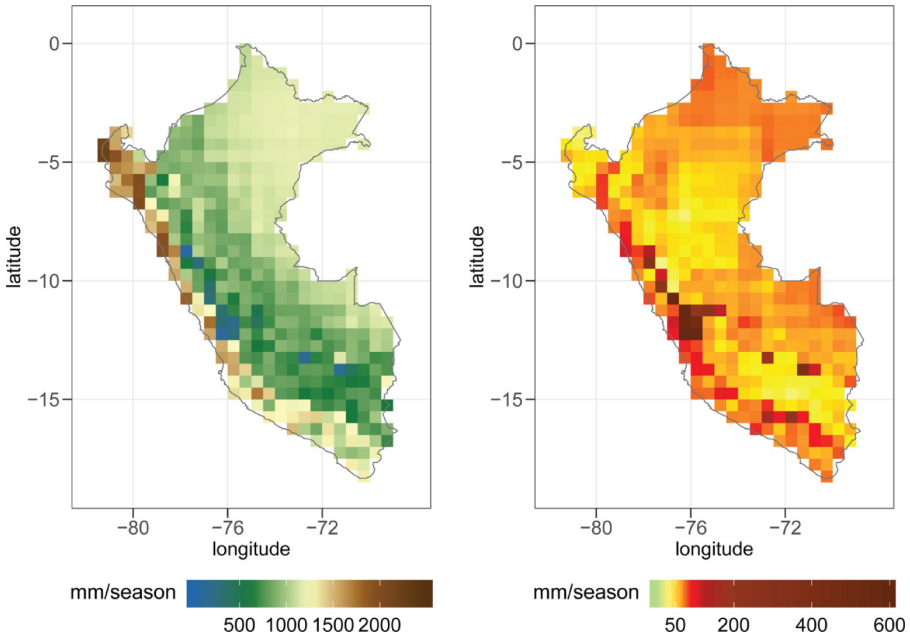

Fig. 2. Mean potential evapotranspiration from 2000 to 2020 (left) and the change in mean evapotranspiration in the period from 2040 to 2060 compared to the period from 2000 to 2020 (right), both figures show modelled data for consistency.

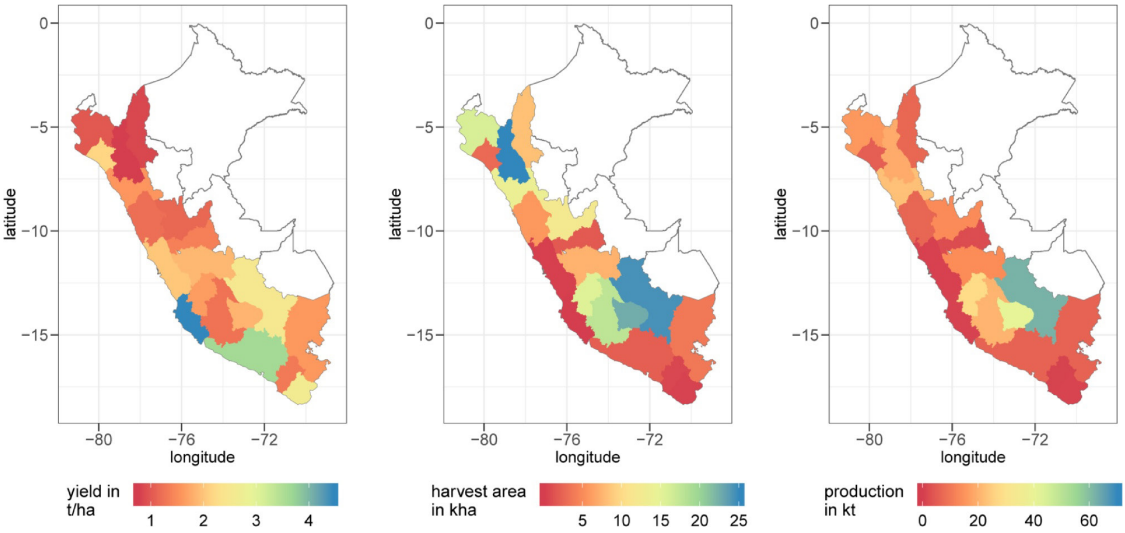

Fig. 3. Yield, harvest area and production of starchy maize in Peru in 2017.

(MINAGRI, 2017). The length of the growing season ranged from 204 (5th Percentile) to 306 (95th Percentile) days and the main growing season is from September to June. Exemptions were Piura and Lima with relatively late sowing in January/February and late harvest in August. Lambayeque and Ica have a high amount of larger farms with irrigation facilities available, which is why the growing season in these two regions is less dependent on the start of the rainy season. In these two regions, starchy maize is produced almost all year long and a clear growing season cannot be found. The sowing and harvesting months in these two regions do not represent most of farmers, but represent the month with the highest share of farmers who planted/harvested.

3.2. The influence of weather on starchy maize yields

3.2.1. Regional assessment

We used a RRM to assess weather influences on yield variability from 2005 to 2017 on region level. The model shows a good performance for almost the whole country (Fig. 6). The median NSE for the estimation with all data (coined 'NSEe' hereinafter) is 0.91, which corresponds to an explained variability of 91%. The exhaustive one-year-out cross-validation produces a median NSE (coined 'NSEv' for 'validation') of 0.55 (i.e. an explained variability of 55%). The model is also able to reproduce most of the extreme years as can be seen with the high harvests in Amazonas in 2014 and in Lambayeque in 2011 or the low harvests in 2016 in Huánuco and in Tacna (Fig. 5). The yield variability in Lima cannot be reproduced by the model (NSE of -0.75; SI Fig. A.6), which can be explained by the diverging agricultural conditions and the high degree of urbanization in this region. Also the models for Apurimac (NSE of -0.24) and Huancavelica (NSE of -0.45) show an overall weak performance, even if some years can be reproduced well by the models.

We tested whether the assumptions in linear regression are fulfilled. Whereas heteroscedasticity does not occur in any of the RRMs, a few models show autocorrelation, which is why we used robust standard errors in these cases (Zeileis, 2004). The significance of the models on the 0.05 significance level and the lower RMSE of the RRMs compared to a constant model (SI Table A.1) suggest that the model results are useful (apart from the models for Lima, Apurimac and Huancavelica)

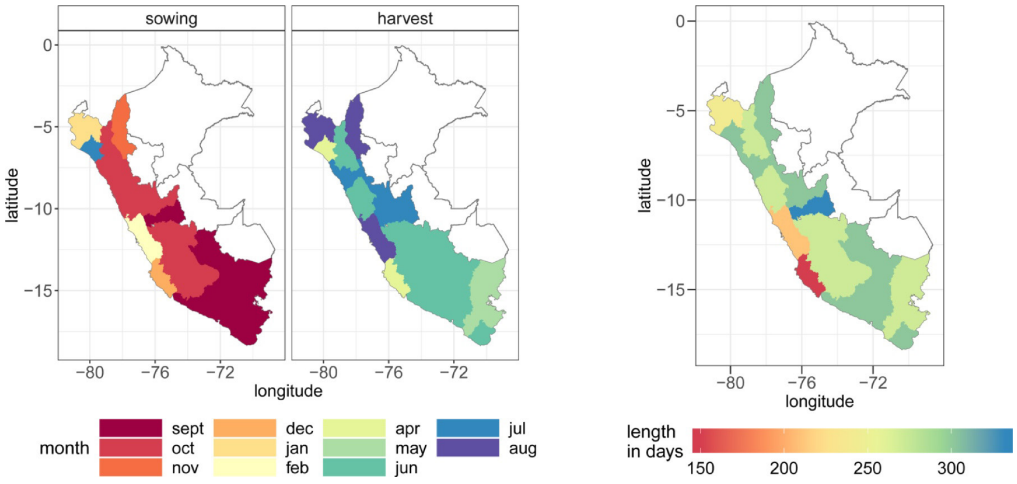

Fig. 4. Sowing and harvesting month (left) and the length of the growing season (right) for starchy maize yields on region level in Peru.

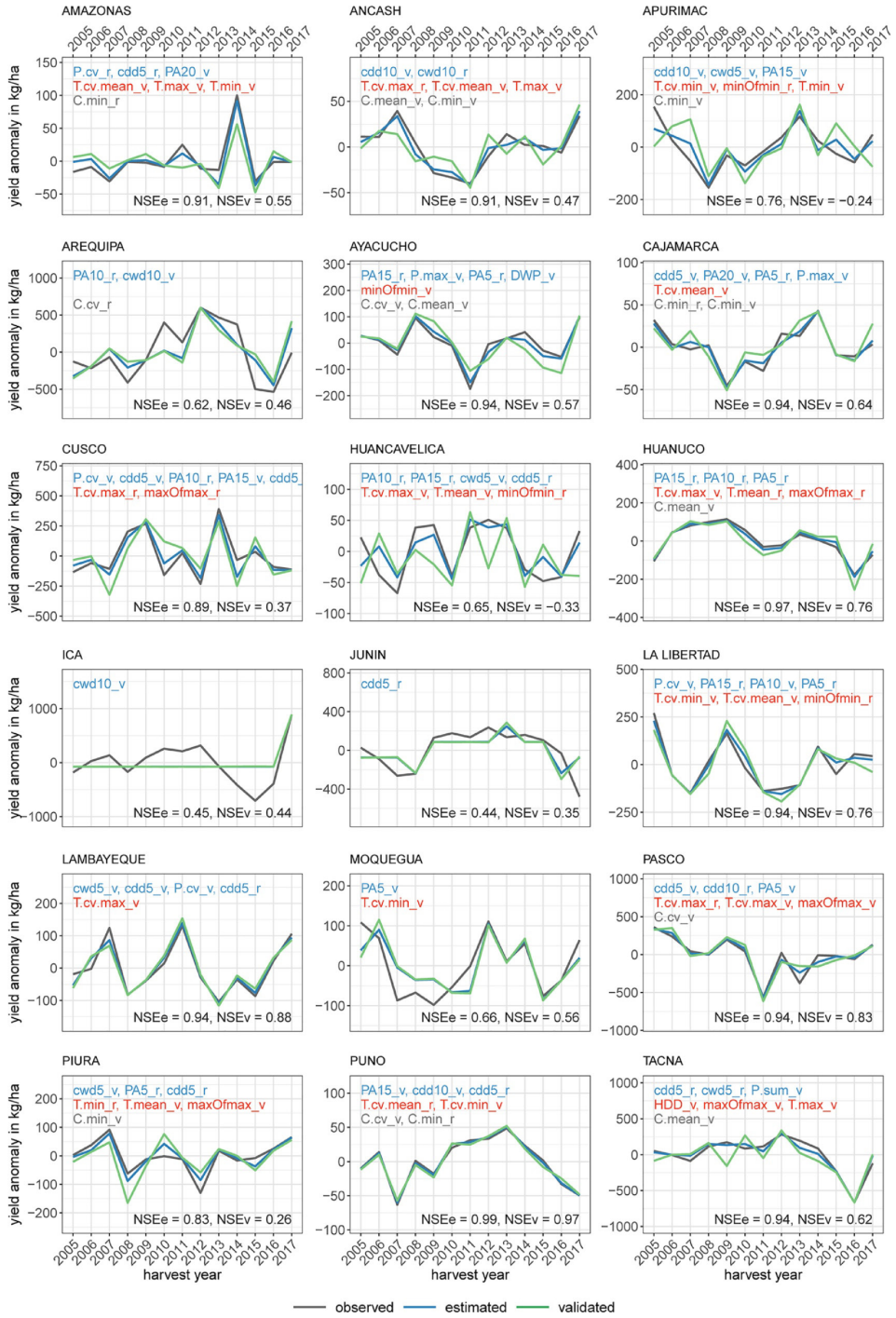

Fig. 5. Observed and simulated maize yield anomalies in Peruvian regions. Black lines show observed yield anomalies, blue lines show anomalies estimated with the full model and green lines those estimated out-of-sample. Region-specific selected variables are shown in blue for precipitation, red for temperature and grey for cloud fraction. The abbreviations of the variable names are explained in Table 1. Lima is not shown here for space reasons and because it is not used for further applications, but it can be seen in SI Fig. A.6. (For interpretation of the references to colour in this figure legend, the reader is referred to the web version of this article.)

Table 1
Abbreviations of selected variables. The column "count" denotes the frequency of selected variables over all RRMs (excluding the model for Lima). The variables are generated for the vegetative (indicated by the suffix "_v") and the reproductive phase (indicated by "_r") of the growing season.

Precipitation-related variables			Temperature-related variables			Cloud-related variables		
Name	Explanation	Count	Name	Explanation	Count	Name	Explanation	Count
cdd5 (cdd10)	Consecutive dry days of more than 5 (10) days	11 (3)	*T.cv.max*	Coefficient of variation of maximum temperature	6	*C.min*	Mean minumum cloud fraction [%]	6
PA5, PA10, PA15, PA20	Precipitation events above 5, 10, 15 or 20[mm]	7, 4, 5,2	*T.cv.mean*	Coefficient of variation of mean temperature	5	*C.cv*	Coefficient of variation of mean cloud fraction	4
P.cv	Coefficient of variation of daily precipitation sum	4	*maxOfmax*	Maximum of the maximum temperature [°C]	5	*C.mean*	Mean cloud fraction [%]	4
cwd5 (cwd10)	Consecutive wet days of more than 5 (10) days	3 (3)	*T.cv.min*	Coefficient of variation of minimum temperature	3			
P.max	Maximum precipitation [mm]	2	*T.max*	Mean maximum temperature [°C]	3			
DWP	Days without precipitation	1	*T.min*	Mean minimum temperature [°C]	2			
P.sum	Precipitation sum [mm]	1	*T.mean*	Mean temperature [°C]	2			
			minOfmin	Minimum of the minimum temperature [°C]	2			
			HDD	Heat degree days	1			

and that weather explains a substantial share of observed maize yield variation.

The variable selection reflects the high climatic variability within Peru. Precipitation seems to determine yields most evidenced by the most frequent selection of precipitation-based variables when compared to others. The variable cdd5 is selected most often. Strong variations in both maximum and mean temperatures influence maize yields in most regions (mostly negatively). Selected variables related to cloud fraction are most often minimum cloud fraction and the coefficient is usually positive, which may be due to a higher cloud fraction often being synonymic with more precipitation. A comparative description of the variable selection in different regions in Peru can be found in SI Text A.3 and SI Table A.1 provides the region-specific coefficients of selected variables.

3.2.2. Local assessment

As stated by the Peruvian NDCs, the local scale is of particular importance in adaptation planning (Gobierno del Perú, 2018). Therefore, we also analysed the weather influence on starchy maize yields on the local level. For this assessment, we used a PDM that takes a survey covering the harvesting years 2015 to 2017 as input data. Over all observations (n = 291), the model has an NSE of 0.20 in the estimation. Autocorrelation and heteroscedasticity do not impair the model. The non-exhaustive one-year-out cross-validation produces an NSE of 0.11, which is a lower model performance compared to the RRM. However, in 33% of the clusters the NSE in the validation is higher than 0.25 and the model is significant and has a higher performance compared to a constant model, indicating a detectable impact of weather on crop yields beyond random influence (SI Table A.2). The following descriptions only relate to these clusters (Fig. 6).

The variable selection process revealed an influence of 16 weather variables on starchy maize yields for the harvesting years 2015 to 2017 and the considered observations. Like in the RRM, precipitation seems to have a stronger influence on maize yields than temperature and cloud fraction. Overall, the model suggests a positive influence of moderately wet conditions on starchy maize yields. Consecutive dry spells of more than 5 and 10 days influenced yields negatively in the reproductive phase, whereas consecutive wet days of more than 5 days showed a positive impact in the whole growing season. Maximum precipitation showed a positive impact, but precipitation above 20mm had a negative impact. Mean cloud fraction, which is often related with rainy weather conditions, showed a positive impact. The negative influence of variations in cloud fraction can be explained by the deviation from high cloud fractions, which are related with dryer weather conditions. Temperature-related influences were most pronounced for variations in temperature (mean, maximum and minimum). Heat degree days and minimum temperature proved to be detrimental for starchy maize yields. For the considered observations, the model suggests that too dry conditions had a stronger negative impact on yields than too wet weather conditions.

To compare the results with the RRM, we aggregated the results to region level. Whereas the RRM is able to explain yield variability in almost all regions in Peru, the PDM captures yield variability in nine out of 16 regions (Moquegua, Huancavelica, Lambayeque, Cajamarca, Ayacucho, Junín, Tacna, Arequipa and La Libertad), evidenced by an NSEv higher than 0.25. The model seems to be particularly suitable to capture the weather influences on starchy maize yields in the cold and hot desert climate that is found in the coastal region of Peru. Wet conditions, on the other hand, like those in the tropical wet and dry or savanna climate, the tropical rainforest and monsoon climate like in Ancash, Amazonas and Pasco are not well captured by the model. The regional differences in the model performances indicate that the PDM is better in representing dry weather influences on maize yields than too wet weather conditions.

Because the PDM on the local level can explain yield variability for fewer regions compared to the RRM, we used another modelling

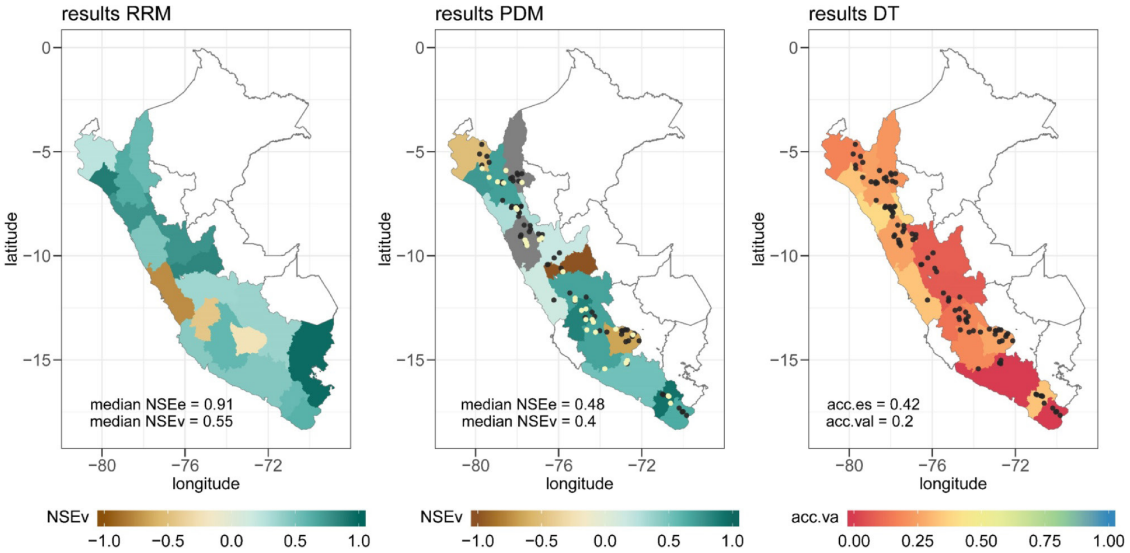

Fig. 6. Model performance in the out-of-sample validation for the RRM (left), the PDM (middle) and the DT (right). Points show the location of the considered cluster centroids (points in yellow in the PDM show clusters with a higher model performance than an NSEv of 0.25, black points show all other clusters). Grey color in the PDM panel indicates NSEv values < -1. Regions in white have no observations in our data base. (For interpretation of the references to colour in this figure legend, the reader is referred to the web version of this article.)

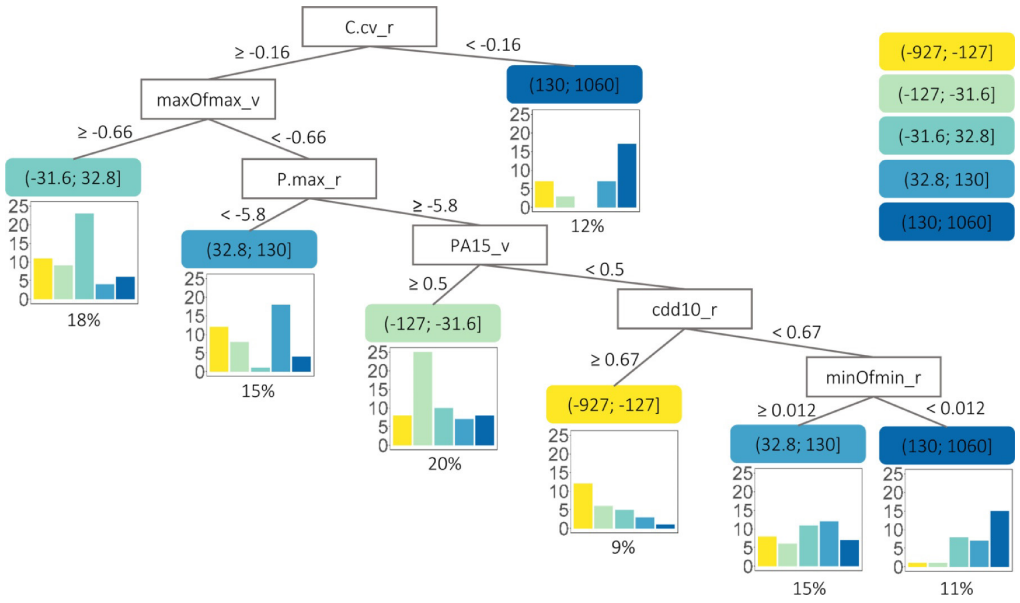

Fig. 7. A decision tree for starchy maize yield anomalies on the local scale in Peru. Yield anomalies in kg/ha are split into five categories (each comprising ca. 58 observations, with 291 observations in total), denoted by different colors. For each end node, the majority category is indicated by color, while the number of observations in each category are displayed in the histogram below the nodes. Percentages show the fractions of all observations contained in the node. Variable explanations are provided in Table 1.

approach to corroborate our results. We therefore applied a decision tree to the same input data as for the PDM (Fig. 7). The accuracy of the DT is 42% in the training set and 20% in the test set (Fig. 6).

In both the PDM and the DT, the variables C.cv, P.max, cdd10 and minOfmin were selected. In the DT, the first split variable on the top node was cloud fraction, which shows that major yield differences can be explained by deviations from high cloud fractions that are usually related with dryer weather conditions. 12% of observations had high yield levels when cloud variation is smaller. Whereas 18% of the observations showed a positive relation with high maximum temperatures, in most cases (the remaining 70%) there was a negative impact of maximum temperatures. The influence of precipitation depends on the yield range and suggests non-linear influences. Whereas low maximum precipitation was related to higher yields in 15% of the observations and precipitation above 15mm with lower yields in 20% of the observations, more dry spells of 10 days were connected with low yields

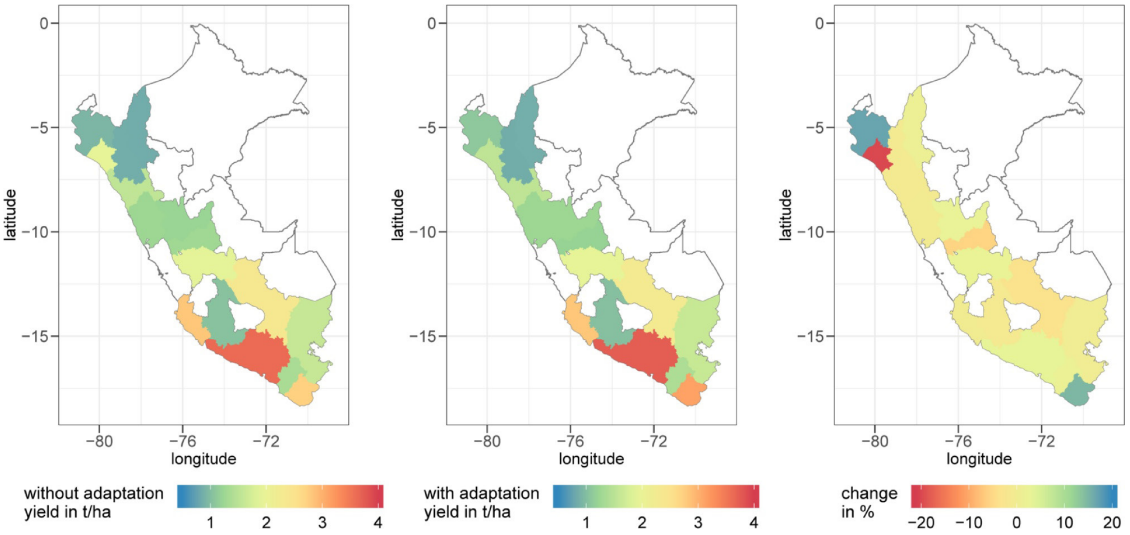

Fig. 8. The effect of 77mm more available water during the growing season on starchy maize yields.

for 9% of observations and with higher yields for the remaining 26% of the observations.

3.3. Assessing an adaptation option

Due to the high performance of the RRM for large parts of the country, we used the RRM to assess the effect of higher water availability on starchy maize yields. This is relevant to gauge expectations on adaptation measures that aim to compensate the water loss due to increased potential evapotranspiration under climate change in the middle of this century (Section 2.3).

Our analysis shows that 77mm more water availability in the growing season would have regionally different effects (Fig. 8). The model suggests an increase of 17% (i.e. 160kg/ha) in Piura and an increase of 15% (i.e. 405kg/ha) in Tacna. In contrast, the model result for Lambayeque shows a drop in yields by 21% (i.e. 380kg/ha). Even though Lambayeque is a neighbouring region of Tacna, yields are influenced more strongly by the negative influence of excessive rain, such that a higher water availability in the growing season would have a negative influence on yields. Half of the regions show only a slight change (-2% to +2%), and partly an insignificant change in yields (SI Table A.3).

4. Discussion

We have shown that three different statistical crop models can explain a substantial fraction of starchy maize yield variation in Peru by variations in weather. Model performances diverge, with a regional regression model showing the highest skill in yield estimation while local-scale panel data and decision tree models account for less of the observed variation. The effect of more plant-available water – to counterbalance possibly higher atmospheric demands under climate change – was assessed, resulting in mostly limited, regionally distinct yield effects.

Whereas the RRMs on the regional scale showed a high performance, the PDM on the local scale could capture yield variability only to a limited extent. There are also divergences in the importance of climatic variables between the two scales. We cannot exactly decipher the underlying reasons for the difference in the model performances and the variable selections due to different input data and different modelling approaches used. Differences between the RRM and the PDM could be related to issues in data quality, the modelling approach or a lacking influence of weather on crop yields at the local scale caused by higher importance of management factors.

The yield input data for the local assessment is a survey and we identified inconsistencies in the data set (detailed in Section 2.2.1). Despite the applied filters, some uncertainties remain such as those stemming from the normalization of different units for production and plot sizes or the high inner-regional differences in the growing season length. The PDM performs better on an aggregated (region) level, which also indicates that the survey might contain reporting errors that are averaged by the spatial aggregation and that other influences on crop yields may also play an important role at local level.

Due to the short time series of the survey data, we had to apply a different modelling approach for the local assessment, i.e. a pooled PDM instead of an RRM. The PDM uses one parameter set to explain weather-yield relations for entire Peru. Because of the highly diverse climatic conditions within Peru, one parameter set may only be able to capture the complex yield-weather relations in Peru to a limited extent.

Moreover, existing adaptation efforts, e.g. irrigation possibilities, or individual farmers' decision on sowing dates or cultivar choices could contribute to a low model performance in some regions. The high inter-regional differences in weather-responses underline the need for a spatially distinct assessment of adaptation options to climate change.

In addition to regression analysis (RRM and PDM), we used a machine learning algorithm. The regression models conform to the assumptions of linear regression, apart from a few RRMs that showed autocorrelation. In this case, we used robust standard errors. To explicitly address autocorrelation in those regions, a multi-variate time series model could be applied in future research. To avoid overfitting, we restricted the maximum number of selected variables per RRM to half of the amount of available observations. This is a conservative approach, because in LASSO regression the number of nonzero coefficients is an unbiased estimate for the degrees of freedom (Zou et al., 2007). Though it could still be argued that the number of variables is high with respect to the number of observations (13 years), the comparable performance of the model in the cross-validation clearly points to a robust measurement of the influence of weather on maize yields that can be transferred to unknown data sets. The F-statistics and the lower RMSE values compared to a constant model suggest that the models are robust. Due to the lower model performance of the PDM, we applied a machine learning algorithm as an additional validation for the

variable selection. The decision tree has the advantage of being less dependent on rigid model assumptions as found in regression analysis (e.g. it is also able to capture non-linear weather influences). Despite the limited amount of observations, the DT revealed largely similar weather-yield relations, underlining that there are large-scale patterns of weather impacts on maize yields in Peru and that the variable selection can be considered robust.

Given the higher performance of the RRM, we assessed the effect of more plant-available water on starchy maize yields on the regional scale. Higher plant-available water could be realised by several adaptation measures, but these need to be implemented with diligence as irrigation has already led to unsustainable water withdrawal rates (Drenkhan et al., 2015). Water consumption from the agricultural sector accounts for 89% of total fresh water use in Peru (ANA, 2013). In addition, with on-going climate change the water sources coming from the Andes are diminishing (Rabatel et al., 2013). Therefore, a focus should be on improving irrigation efficiency and other adaptation measures, such as improved water storage, water harvesting and better soil management practices, as proposed by the NDCs (Gobierno del Perú, 2018).

The result suggests that in some regions more water availability would neither decrease nor increase yields substantially (Section 3.3 and SI Table A.3). Apart from possible uncertainties stemming from the model coefficients or the model structure, this can be related to the presence of favourable rain conditions or sufficient adaptation practices already in place that regulate water availability, such as irrigation. In this case, other adaptation measures need to be tested to enable an increase in yields. The NDCs emphasize the need for good soil fertilization practices, erosion and flood control, salinity management, diversification of the production system, pest and disease control, improved seed varieties and the implementation of early warning and agricultural risk transfer systems. Also the necessity to provide information services in the agricultural sector, better access to markets and adding value to agricultural products are emphasised. Based on this list of possible adaptation options, local adaptation strategies need to be developed together with relevant stakeholders that take account of the interconnectedness of adaptation options in various sectors (Goosen et al., 2014). Our study provides an example of how a statistical modelling approach can inform this process.

As the results show, there are strong regional differences within Peru. Despite the high societal relevance of local weather-yield relations (Gobierno del Perú, 2018), a quantitative assessment of weather impacts on maize yield at the local level has not yet been done for Peru, to our best knowledge. To increase the pertinence of such modelling efforts, in particular for adaptation planning, comprehensive and consistent local yield data are required. The currently available data base seems limiting for this high-resolution modelling. Thus, once longer time series of high-quality yield and weather data become available on the local scale, future research should be directed towards supporting local adaptation planning by quantitative analyses of weather influences on crops.

Particularly in regions that show a low model performance, a further evaluation is needed and results should be tested on the ground. Despite the discussed uncertainties, we consider the assessment of more plant-available water useful as it provides a first indication of the effectiveness of adaptation measures suggested by the NDCs. Our results can be used to prioritize regions in which more water availability would potentially increase or decrease maize yields through the implementation of appropriate adaptation measures.

5. Conclusion

In this study, we assessed the influence of weather on starchy maize yields on the regional and the local scale in Peru based on a regional regression model, a panel data model and a machine learning algorithm. Based on these models, we assessed the effect of higher water availability on starchy maize yields, which is suggested by the Peruvian NDCs to adapt to climate change.

To our best knowledge, this is the first paper assessing weather-yield relations in Peru in such temporal and spatial detail and our study underlines the importance of a spatially-distinct assessment of adaptation options. Under such diverse climatic conditions as can be found in Peru, a local assessment is needed to account for the complex weather-yield relations. This study shows how a statistical approach can support the implementation of NDCs by providing quantitative information about the effectiveness of adaptation measures that can be used to identify priority areas for adaptation efforts.

Declaration of Competing Interest

The authors declare that they have no known competing financial interests or personal relationships that could have appeared to influence the work reported in this paper.

Acknowledgements

The research was supported by the projects AgRATI, funded by Climate-KIC, and by the project EPICC. EPICC is part of the International Climate Initiative (IKI). The Federal Ministry for the Environment, Nature Conservation and Nuclear Safety (BMU) supports this initiative on the basis of a decision adopted by the German Bundestag.

Supplementary materials

Supplementary material associated with this article can be found, in the online version, at doi:10.1016/j.agrformet.2020.108154.

References

Allen, R.G., Pereira, L.S., Raes, D., Smith, M., 1998. Crop evapotranspiration - Guidelines for computing crop water requirements - FAO Irrigation and drainage paper 56. Rom.

ANA, 2013. Plan Nacional De Recursos Hídricos Del Perú[WWW Document]. URLhttps://www.onemi.gov.cl/wp-content/themes/onemi-bootstrap-master/library/doc/plan_nacional_0_0.pdf (accessed 7.11.19).

Aybar, C., Fernández, C., Huerta, A., Lavado, W., Vega, F., Felipe-Obando, O., 2019. Construction of a high-resolution gridded rainfall dataset for Peru from 1981 to the present day. Hydrol. Sci. J. 00, 1–16. https://doi.org/10.1080/02626667.2019.1649411.

Bourrel, L., Rau, P., Dewitte, B., Labat, D., Lavado, W., Coutaud, A., Vera, A., Alvarado, A., Ordoñez, J., 2015. Low-frequency modulation and trend of the relationship between ENSO and precipitation along the northern to centre Peruvian Pacific coast. Hydrol. Process. 29, 1252–1266. https://doi.org/10.1002/hyp.10247.

Bozdogan, H., 1987. Model selection and Akaike's Information Criterion (AIC): the general theory and its analytical extensions. Psychometrika 52, 345–370.

Breiman, L., Friedman, J., Stone, C.J., Olshen, R.A., 1984. Classification and Regression Trees. Taylor & Francis Ltd.

Challinor, A.J., Watson, J., Lobell, D.B., Howden, S.M., Smith, D.R., Chhetri, N., 2014. A meta-analysis of crop yield under climate change and adaptation. Nat. Clim. Chang. 4, 287–291. https://doi.org/10.1038/nclimate2153.

Christensen, J.H., Kumar, K.K., Aldria, E., An, S.-I., Cavalcanti, I.F.a., Castro, M.De, Dong, W., Goswami, P., Hall, A., Kanyanga, J.K., Kitoh, A., Kossin, J., Lau, N.-C., Renwick, J., Stephenson, D.B., Xie, S.-P., Zhou, T., 2013. Climate Phenomena and their Relevance for Future Regional Climate Change. In: Stocker, T.F., Qin, D., Plattner, G.-K., Tignor, M., Allen, S.K., Boschung, J., Nauels, A., Xia, Y., Bex, V., Midgley, P.M. (Eds.), Climate Change 2013: The Physical Science Basis. Contribution of Working Group I to the Fifth Assessment Report of the Intergovernmental Panel on Climate Change. Cambridge University Press, Cambridge, United Kingdom and New York, NY, USA, pp. 1217–1308. https://doi.org/10.1017/CBO9781107415324.028.

Collins, M., Knutti, R., Arblaster, J., Dufresne, J.-L., Fichefet, T., Friedlingstein, P., Gao, X., Gutowski, W.J., Johns, T., Krinner, G., Shongwe, M., Tebaldi, C., Weaver, A.J., Wehner, M., 2013. Long-term climate change: projections, commitments and irreversibility. In: Stocker, T.F., Qin, D., Plattner, G.-K., Tignor, M., Allen, S.K., Boschung, J., Nauels, A., Xia, Y., Bex, V., Midgley, P.M. (Eds.), Climate Change 2013: The Physical Science Basis. Contribution of Working Group I to the Fifth Assessment Report of the Intergovernmental Panel on Climate Change. Cambridge University Press, Cambridge, United Kingdom and New York, NY, USA, pp. 1029–1136. https://doi.org/10.1017/CBO9781107415324.024.

Drenkhan, F., Carey, M., Huggel, C., Seidel, J., Oré, M.T., 2015. The changing water cycle: climatic and socioeconomic drivers of water-related changes in the Andes of Peru. Wiley Interdiscip. Rev. Water 2, 715–733. https://doi.org/10.1002/wat2.1105.

Dutra, E., Balsamo, G., Calvet, J.-C., 2015. Report on the current state-of-the-art Water Resources Reanalysis [WWW Document]. URLhttp://earth2observe.eu/files/PublicDeliverables/D5.1_Report on the WRR1 tier1.pdf (accessed 7.1.19).

Friedman, J., Hastie, T., Rob Tibshirani, B.N., Tay, K., Simon, N., Qian, J., 2008. Regularization Paths for Generalized Linear Models via Coordinate Descent [WWW Document]. URLhttps://web.stanford.edu/~hastie/Papers/glmnet.pdf.

Giorgi, F., Coppola, E., Raffaele, F., Diro, G.T., Fuentes-Franco, R., Giuliani, G., Mamgain, A., Llopart, M.P., Mariotti, L., Torma, C., 2014. Changes in extremes and hydroclimatic regimes in the CREMA ensemble projections. Clim. Change 125, 39–51. https://doi.org/10.1007/s10584-014-1117-0.

Gobierno del Perú, 2018. Grupo de Trabajo Multisectorial de naturaleza temporal encargado de generar información técnica para orientar la implementación de las Contribuciones Nacionalmente Determinadas (GTM-NDC)[WWW Document]. URLhttp://www.minam.gob.pe/cambioclimatico/wp-content/uploads/sites/127/2019/01/190107_Informe-final-GTM-NDC_v17dic18.pdfPAÑOL.pdf (accessed 3.5.19).

Goosen, H., de Groot-Reichwein, M.A.M., Masselink, L., Koekoek, A., Swart, R., Bessembinder, J., Witte, J.M.P., Stuyt, L., Blom-Zandstra, G., Immerzeel, W., 2014. Climate adaptation services for the Netherlands: an operational approach to support spatial adaptation planning. Reg. Environ. Chang. 14, 1035–1048. https://doi.org/10.1007/s10113-013-0513-8.

Gornott, C., Wechsung, F., 2016. Statistical regression models for assessing climate impacts on crop yields: a validation study for winter wheat and silage maize in Germany. Agric. For. Meteorol. 217, 89–100. https://doi.org/10.1016/j.agrformet.2015.10.005.

Iglesias, A., Quiroga, S., Schlickenrieder, J., 2010. Climate change and agricultural adaptation: assessing management uncertainty for four crop types in Spain. Clim. Res. 44, 83–94. https://doi.org/10.3354/cr00921.

INEI, 2019. Evoluacion de la Pobreza Monetaria - 2007-2018 - Informe Técnico[WWW Document]. URLhttps://www.inei.gob.pe/media/MenuRecursivo/publicaciones_digitales/Est/Lib1646/libro.pdf (accessed 6.22.19).

INEI, 2017. Perú - Encuesta Nacional Agropecuaria [WWW Document]. URLhttps://webinei.inei.gob.pe/anda_inei/index.php/catalog/654/ (accessed 11.30.18).

Kobayashi, S., Ota, Y., Harada, Y., Ebita, A., Moriya, M., Onoda, H., Onogi, K., Kamahori, H., Kobayashi, C., Endo, H., Miyaoka, K., Kiyotoshi, T., 2015. The JRA-55 reanalysis: General specifications and basic characteristics. J. Meteorol. Soc. Jpn. 93, 5–48. https://doi.org/10.2151/jmsj.2015-001.

Konings, A.G., Gentine, P., 2017. Global variations in ecosystem-scale isohydricity. Glob. Chang. Biol. 23, 891–905. https://doi.org/10.1111/gcb.13389.

Konings, A.G., Williams, A.P., Gentine, P., 2017. Sensitivity of grassland productivity to aridity controlled by stomatal and xylem regulation. Nat. Geosci. 10, 284–288. https://doi.org/10.1038/ngeo2903.

Lobell, D.B., Burke, M.B., 2010. On the use of statistical models to predict crop yield responses to climate change. Agric. For. Meteorol. 150, 1443–1452. https://doi.org/10.1016/j.agrformet.2010.07.008.

Lobell, D.B., Burke, M.B., Tebaldi, C., Mastrandrea, M.D., Falcon, W.P., Naylor, R.L., 2008. Prioritizing climate change adaptation needs for food security in 2030. Science 319 (80-.), 607–610. https://doi.org/10.1126/science.1152339.

Lobell, D.B., Hammer, G.L., McLean, G., Messina, C., Roberts, M.J., Schlenker, W., 2013. The critical role of extreme heat for maize production in the United States. Nat. Clim. Chang. 3, 497–501. https://doi.org/10.1038/nclimate1832.

Ludescher, J., Gozolchiani, A., Bogachev, M.I., Bunde, A., Havlin, S., Schellnhuber, H.J., 2014. Very early warning of next El Niño. Proc. Natl. Acad. Sci. 111, 2064–2066. https://doi.org/10.1073/pnas.1323058111.

Marengo, J.A., Jones, R., Alves, L.M., Valverde, M.C., 2009. Future change of temperature and precipitation extremes in South America as derived from the PRECIS regional climate modeling system. Int. J. Climatol. 29, 2241–2255. https://doi.org/10.1002/joc.1863.

MINAGRI, 2018. Anuario Estadístico de Producción Agrícola[WWW Document]. URLhttp://siea.minagri.gob.pe/siea/?q=publicaciones/anuario-de-produccion-agricola (accessed 12.19.18).

MINAGRI, 2017. Calendario de Siembras y Cosechas[WWW Document]. URLhttp://siea.minagri.gob.pe/calendario/ (accessed 10.3.18).

Mu, J.E., McCarl, B.A., Wein, A.M., 2013. Adaptation to climate change: changes in farmland use and stocking rate in the U.S. Mitig. Adapt. Strateg. Glob. Chang. 18, 713–730. https://doi.org/10.1007/s11027-012-9384-4.

Müller Schmied, H., Adam, L., Eisner, S., Fink, G., Florke, M., Kim, H., Oki, T., Portmann, Theodor, F., Reinecke, R., Riedel, C., Song, Q., Zhang, J., Doll, 2016. Variations of global and continental water balance components as impacted by climate forcing uncertainty and human water use. Hydrol. Earth Syst. Sci. 20, 2877–2898. https://doi.org/10.5194/hess-20-2877-2016.

Muneer, T., Gul, M.S., 2000. Evaluation of sunshine and cloud cover based models for generating solar radiation data. Energy Convers. Manag. 41, 461–482. https://doi.org/10.1016/S0196-8904(99)00108-9.

Nash, J.E., Sutcliffe, J.V., 1970. River flow forecasting through conceptual models part I - a discussion of principles. J. Hydrol. 10, 282–290. https://doi.org/10.1016/0022-1694(70)90255-6.

Novick, K.A., Ficklin, D.L., Stoy, P.C., Williams, C.A., Bohrer, G., Oishi, A.C., Papuga, S.A., Blanken, P.D., Noormets, A., Sulman, B.N., Scott, R.L., Wang, L., Phillips, R.P., 2016. The increasing importance of atmospheric demand for ecosystem water and carbon fluxes. Nat. Clim. Chang. 6, 1023–1027. https://doi.org/10.1038/nclimate3114.

Patel, N., Upadhyay, S., 2012. Study of various decision tree pruning methods with their empirical comparison in WEKA. Int. J. Comput. Appl. 60, 20–25. https://doi.org/10.5120/9744-4304.

Peel, M.C., Finlayson, B.L., McMahon, T.A., 2007. Updated world map of the Köppen-Geiger climate classification. Hydrol. Earth Syst. Sci. 11, 1633–1644. https://doi.org/10.5194/hess-11-1633-2007.

Platnick, S., Ackerman, S., King, M., Wind, G., Menzel, P., Frey, R., 2015. MODIS Atmosphere L2 Cloud Product (06_L2). NASA MODIS Adaptive Processing System. Goddard Space Flight Center, USA.

R Core Team, 2014. R: a language and environment for statistical computing[WWW Document]. URLhttp://www.r-project.org/.

Rabatel, A., Francou, B., Soruco, A., Gomez, J., Cáceres, B., Ceballos, J.L., Basantes, R., Vuille, M., Sicart, J., Huggel, C., Scheel, M., Lejeune, Y., Arnaud, Y., Collet, M., Condom, T., Consoli, G., Favier, V., Jomelli, V., Galarraga, R., Ginot, P., Maisincho, L., Mendoza, J., Ménégoz, M., Ramirez, E., Ribstein, P., Suarez, W., Villacis, M., Wagnon, P., Palmas, L., 2013. Current state of glaciers in the tropical Andes: a multi-century perspective on glacier evolution and climate change. Cryosph 7, 81–102. https://doi.org/10.5194/tc-7-81-2013.

Ray, D.K., Gerber, J.S., Macdonald, G.K., West, P.C., 2015. Climate variation explains a third of global crop yield variability. Nat. Commun. 6, 1–9. https://doi.org/10.1038/ncomms6989.

Rodríguez-Morata, C., Díaz, H.F., Ballesteros-Canovas, J.A., Rohrer, M., Stoffel, M., 2019. The anomalous 2017 coastal El Niño event in Peru. Clim. Dyn. 52, 5605–5622. https://doi.org/10.1007/s00382-018-4466-y.

Schauberger, B., Gornott, C., Wechsung, F., 2017. Global evaluation of a semiempirical model for yield anomalies and application to within-season yield forecasting. Glob. Chang. Biol. 23, 4750–4764. https://doi.org/10.1111/gcb.13738.

Song, Y., Lu, Y., 2015. Decision tree methods: applications for classification and prediction. Shanghai Arch. Psychiatry 27, 130–135.

Sörensson, A.A., Menéndez, C.G., Ruscica, R., Alexander, P., Samuelsson, P., Willén, U., 2010. Projected precipitation changes in South America: A dynamical downscaling within CLARIS. Meteorol. Zeitschrift 19, 347–355. https://doi.org/10.1127/0941-2948/2010/0467.

Therneau, T., Atkinson, B., Ripley, B., 2019. rpart: Recursive Partitioning and Regression Trees[WWW Document]. URLhttps://github.com/bethatkinson/rpart.

Tibshirani, R., 1996. Regression Shrinkage and Selection Via the Lasso. J. R. Stat. Soc. Ser. B 58, 267–288. https://doi.org/10.1111/j.2517-6161.1996.tb02080.x.

Warszawski, L., Frieler, K., Huber, V., Piontek, F., Serdeczny, O., Schewe, J., 2014. The inter-sectoral impact model intercomparison project (ISI-MIP): Project framework. Proc. Natl. Acad. Sci. U. S. A. 111, 3228–3232. https://doi.org/10.1073/pnas.1312330110.

Wickham, H., 2009. ggplot2: elegant graphics for data analysis. Springer, New York.

Wooldridge, J.M., 2014. Introductory Econometrics a Modern Approach, fifth ed. Cenage Learning.

Zeileis, A., 2004. Econometric computing with HC and HAC covariance matrix estimators. J. Stat. Softw. 11, 128–129. https://doi.org/10.18637/jss.v011.i10.

Zou, H., Hastie, T., Tibshirani, R., 2007. On the "degrees of freedom" of the lasso. Ann. Stat. 35, 2173–2192. https://doi.org/10.1214/009053607000000127.

2.2 Robustly forecasting maize yields in Tanzania based on climatic predictors

This chapter is a reproduction of the article published as:

Laudien, R., Schauberger, B., Makowski, D., & Gornott, C. (2020). Robustly forecasting maize yields in Tanzania based on climatic predictors. *Scientific Reports*, *10*(1), 1–12. https://doi.org/10.1038/s41598-020-76315-8

www.nature.com/scientificreports

scientific reports

Check for updates

OPEN

Robustly forecasting maize yields in Tanzania based on climatic predictors

Rahel Laudien[1]✉, Bernhard Schauberger[1], David Makowski[2] & Christoph Gornott[1,3]

Seasonal yield forecasts are important to support agricultural development programs and can contribute to improved food security in developing countries. Despite their importance, no operational forecasting system on sub-national level is yet in place in Tanzania. We develop a statistical maize yield forecast based on regional yield statistics in Tanzania and climatic predictors, covering the period 2009–2019. We forecast both yield anomalies and absolute yields at the sub-national scale about 6 weeks before the harvest. The forecasted yield anomalies (absolute yields) have a median Nash–Sutcliffe efficiency coefficient of 0.72 (0.79) in the out-of-sample cross validation, which corresponds to a median root mean squared error of 0.13 t/ha for absolute yields. In addition, we perform an out-of-sample variable selection and produce completely independent yield forecasts for the harvest year 2019. Our study is potentially applicable to other countries with short time series of yield data and inaccessible or low quality weather data due to the usage of only global climate data and a strict and transparent assessment of the forecasting skill.

To support food security planning in face of unfavourable weather conditions, accurate yield forecasts at sub-seasonal to seasonal timescales, i.e. from weeks to months ahead, are important. Such yield forecasts can be used for early warning so that actions can be taken before the disaster occurred. On a regional and national scale, a seasonal yield forecast allows to adjust food imports so that food shortages in case of harvest losses or failures can be alleviated. If available on a high spatial resolution, a yield forecast can also inform farm management practices, such as fertilizer use, and decisions on sale prices and grain storage[1,2].

Despite the importance of yield forecasts, as expressed by the Division of National Food Security of the Ministry of Agriculture in Tanzania (personal communications), no operational yield forecasting system on sub-national level exists up to now. The Famine Early Warning Systems Network (FEWS-net), which provides regular food insecurity reports for East Africa, stopped providing yield forecasts for Tanzania since December 2017. Ogutu et al. (2018)[3] proposed a yield forecasting system for East Africa but this system relies on model simulations that were not validated with observational data at a subnational scale so that the accuracy of the forecast is unknown. Liu and Basso (2020)[2] provide a yield forecast for three case studies in Tanzania based on a process-based model with a lead time of 14–77 days. They calibrate and validate the forecast using survey data at field scale. However, the practical application of this forecast for an operational forecasting system is hampered due to the limited spatial (three regions) and temporal scale (year 2017) and the high potential implementation costs (necessity to collect survey data for every new forecast).

In this study, we provide a statistical yield forecast for the whole country covering the time period from 2009 to 2019, which can be operationalized in a technical and cost-efficient way. We provide a within-season forecast of maize yields at the subnational level about 6 weeks before harvest and relate the yields to weather and sea surface temperature data. We focus on maize (*Zea mays* L.), as this is the main staple crop in Tanzania[4]. We conduct a strict model validation—not only comprising of an out-of-sample validation, but also an out-of-sample variable selection—to assess the forecasting skill.

any. ✉email: laudien@pik-potsdam.de

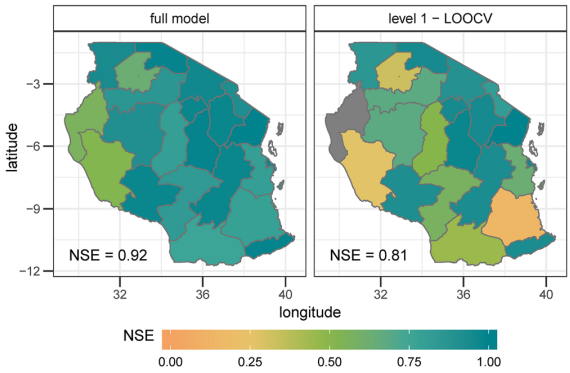

Figure 1. Model performance for yield anomalies from 2009 to 2018 based on selected region-specific weather variables measured in the Nash–Sutcliffe efficiency coefficient (NSE). The NSE can range from 1 (100% agreement between observed and modelled data) to $-\infty$; a value of zero can be interpreted in a way that nothing of the observed variability can be explained by the model. The left panel shows the model performance when the complete time series for each region is included. The right hand panel shows the performance for the leave-one-out cross validation. The colour grey indicates an NSE lower than 0. The median NSE over all regions of Tanzania is shown in the left corner of the panels.

Results

The influence of weather on maize yield variability. In the first step, we assessed how weather influenced maize variability from 2009 to 2018. The median Nash–Sutcliffe efficiency coefficient[5] (NSE) of all models for the estimation results is 0.92 (coined 'NSEe' hereinafter). The NSE of the level 1 validation (coined 'NSEv1') is 0.81. The models show a high performance for almost the whole country (18 out of 21 regions have an NSEv1 of higher than 0.3; Fig. 1). Extreme years, like e.g. the high yields in 2010 in Dar es Salaam and Manyara or low yields in 2016 in Kagera, as well as average yields can be reproduced by the models (Fig. 2).

The variable selection reveals the strong influence of extreme weather events on maize yields in Tanzania. In general, maize yields seem to benefit from higher minimum temperatures, more precipitation and the absence of more than 5 consecutive dry days (Fig. 3).

In the vegetative phase, high rainfall events (precip.p99_v, i.e. precipitation events with more rain than the 99% percentile) are related with higher yields, whereas the occurrence of consecutive dry days of more than 5 days (cdd5) are mostly negatively correlated with yield. Consecutive dry days play an important role in explaining maize variability. In total, cdd5, cdd10 and cdd15 have been selected 17 times. They are mostly negatively correlated with yields, in particular in the vegetative phase. Temperature events below the 1% percentile of the minimum temperature in the reproductive phase (tas.min.p01_r) are related with lower yields—indicating that too low minimum temperatures are detrimental for maize yields.

The influence of sea surface temperatures on maize yield variability. The usage of sea surface temperature (SST) indicators in a separate, alternative model formulation led to a median model performance of an NSE of 0.29 (level 1-LOOCV), which shows that SST variables can explain a substantial part of yield variability, but that the influence of weather is stronger.

The SST of the West Pacific (WP) with a lead time of 120 days has the strongest influence on maize variability from 2009 to 2018. Maize variability shows a positive correlation with the number of times the SST falls below the 1% percentile of the WP SST (Fig. 4). The SST of the Indian Ocean Dipole (IOD) with a lead time of 30 days influences mostly the bimodal rainfall regions in Tanzania. The number of times the SST of the IOD falls below the 1% percentile is mostly positively correlated with yield, whereas the median IOD shows a mostly negative correlation with yield.

Forecasting yield anomalies. We performed a within-season forecast by including the weather and SST variables related to the vegetative phase of the growing season. This allows us to provide a yield forecast around 6 weeks before the calculated harvest date. To assess the hindcast-based operational performance of the forecast, we include the level 1 (i.e. the out-of-sample validation) and level 2 validation (i.e. the out-of-sample variable selection validation).

The forecast shows a high accuracy for the full model (NSE = 0.91) and the level 1 validation (NSE = 0.72). The results of the level 2 validation suggest that the variable selection has a high year-to-year variability so that the performance of this validation is lower. The level 2 validation has a high skill (NSE > 0.3) for 5 regions in Tanzania (Fig. 5). The middle panel of Fig. 8 shows the yearly performance of the forecast of anomalies.

We tested the performance of the forecast compared to a constant model that only takes the mean yield excluding the year that is forecasted as a predictor. The lower RMSE of the forecast compared to a constant model (SI Table 4) underlines the robustness of the forecasting results. A strong correlation between SST and weather

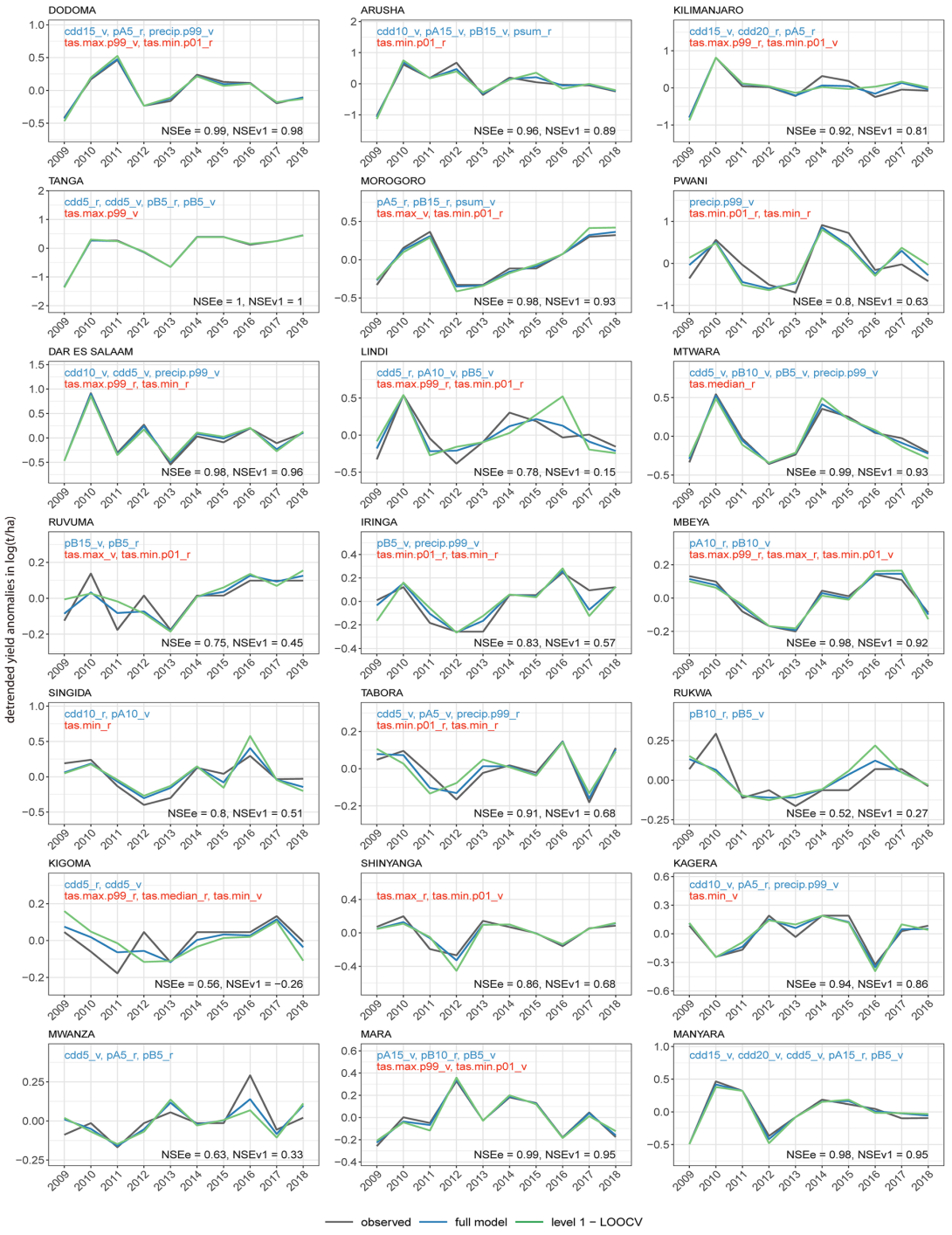

Figure 2. Observed and modelled maize yield anomalies in Tanzanian regions based on region-specific selected weather inputs. Grey lines show observed yield anomalies, blue lines show modelled anomalies using the full time series for model development, green lines indicate out-of-sample (level 1-LOOCV) estimates. The y-axis shows detrended yield anomalies in logarithmic form. The names of the inputs are shown in blue for precipitation and red for temperature-related variables. Explanations of abbreviations for input names are provided in supplemental information (SI) Tables 1, 2 and 3.

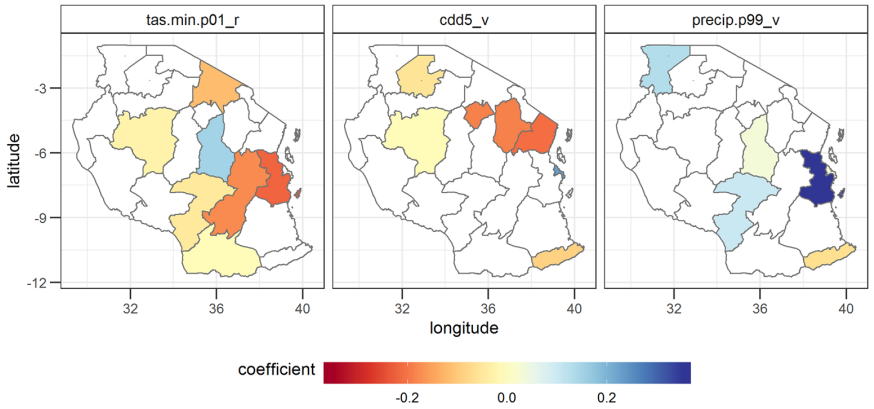

Figure 3. Estimated regression coefficients for the three most often selected variables. The three most often selected variables are temperature events below the 1% minimum temperature percentile in the reproductive phase (tas.min.p01_r), consecutive dry days of more than 5 days in the vegetative phase (cdd5_v) and precipitation events above the 99th precipitation percentile in the vegetative phase (precip.p99_v). Note that this analysis excludes the model coefficients with a performance lower than an NSE of 0.3 in the level 1 validation, because we assumed these models as not robust enough for further analysis. Negative (positive) values indicate that yields tend to decrease (increase) as a function of the values of the variables. The coefficients show standardized values, i.e. they show the change in yield per standard deviation of the input variable. Regions, in which the variable was not selected, are shown in white. The statistical significance of the estimated regression coefficients is shown in SI Fig. 1.

variables exists only in few, non-systematic cases (SI Fig. 4) and is eliminated due to the applied filter during the variable selection. Thus a collinearity between SST and weather variables is not existent.

The variable selection of the forecast reveals similar variables compared to the model based on variables of the vegetative and the reproductive phase. The three most often selected variables are shown in Fig. 6. Precipita-

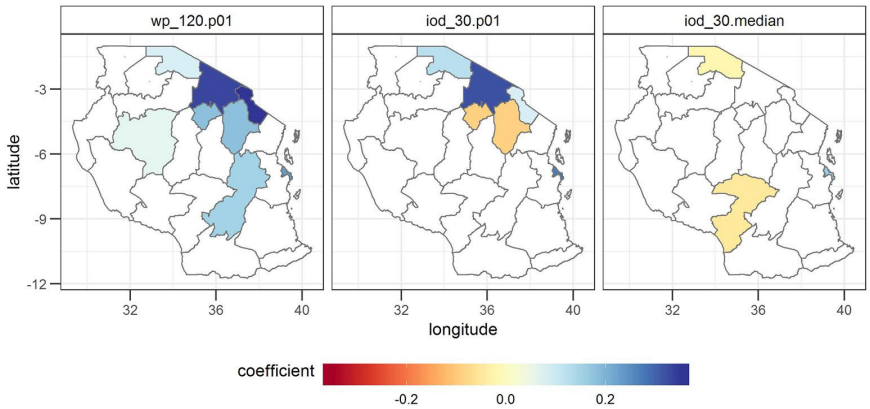

Figure 4. Coefficients of the most often selected sea surface temperature (SST) variables. The three most often selected variables are the number of times the SST falls below the 1% percentile of the West Pacific considering a lead time of 120 days (wp_120.p01), the number of times the SST falls below the 1% percentile of the Indian Ocean Dipole considering a lead time of 30 days (iod_30.p01) and the median SST of the IOD considering a lead time of 30 days (iod_30.median). Further explanations can be found under Fig. 3. The statistical significance of the estimated regression coefficients is shown in SI Fig. 2.

tion events below 5 mm (pB5) are positively correlated with maize yields in the North, but negatively correlated with yields in the rest of the country. Whereas the negative correlation could indicate a negative influence of low precipitation events on yields due to insufficient total rainfall amounts in the vegetative phase, the positive

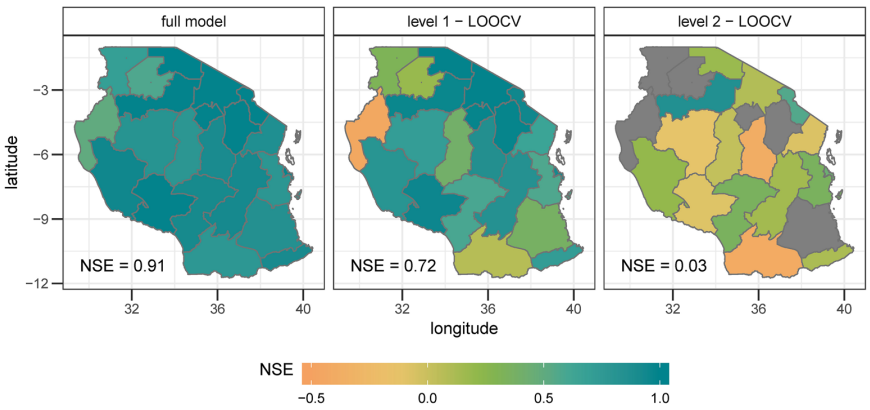

Figure 5. Performance of the forecast of anomalies based on selected region-specific weather and SST variables. Areas in grey show an NSE of lower than -0.5. Further explanation can be found under Fig. 2.

correlation could indicate a positive influence of moderate and well distributed rainfall. The number of times the SST in WP falls below the 1% percentile with a lead time of 120 days (wp_120.p01) is positively correlated with yields, which could be explained by above average rainfall amounts in case of negative SST anomalies in

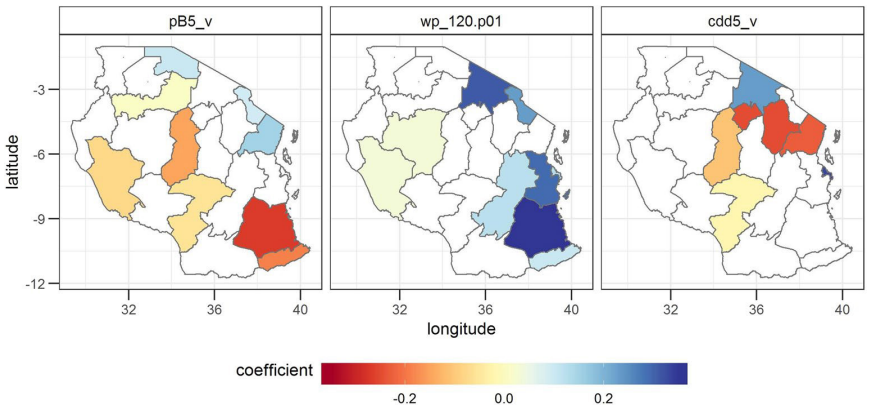

Figure 6. Coefficients of the three most often selected variables in the forecast based on weather and SST variables. Further explanations can be found under Fig. 3. The statistical significance of the estimated regression coefficients is shown in SI Fig. 3.

the West Pacific. Dry conditions represented by the number of consecutive dry days of more than 5 days (cdd5) are mostly negatively correlated with yields.

Forecasting absolute yields. As required for operational forecasting systems, we also provide a forecast of absolute yields. To obtain absolute yields, we added the previously subtracted trend and the mean yield to the forecasted yield anomalies.

The full model evaluation and the level 1 validation indicate a high skill (median NSE of 0.93 and 0.79) of the within-season forecast of absolute yields for the whole country (Fig. 7). The level 2 validation has a median NSE of 0.26 and shows a high performance for 10 of 21 regions, which have an NSE higher than 0.3. The median RMSE is 0.07 t/ha for the estimation, 0.13 t/ha for the level 1 validation and 0.3 t/ha for the level 2 validation.

The reason for the improved forecasting performance is, in most regions, due to the inclusion of the trend, in particular for the level 2 validation (Fig. 8).

Application of the forecast for year 2019. We used the model trained on yield data from 2009 to 2018 to provide a completely independent forecast for the harvest year 2019. The forecast of absolute yields for 2019 shows an overall high performance of the forecast in regions with a unimodal rainfall regime (NSE of 0.89 in the

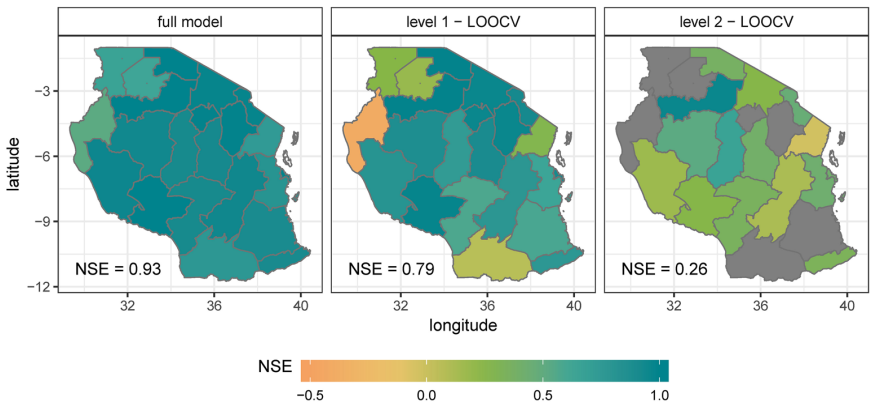

Figure 7. Assessment of the forecasted absolute yields. Areas in grey show an NSE of lower than −0.5.

level 2—LOOCV) and a weak performance in bimodal rainfall regions (NSE of −7.73 in the level 2—LOOCV; Fig. 9).

Discussion

Our study provides a within-season maize yield forecast for entire Tanzania and is, to our best knowledge, the first of its kind. In contrast to existing forecasting studies in East Africa[2,3], we provide an out-of-sample validation and an out-of-sample variable selection. Furthermore, we test the robustness by providing a completely independent forecast for the harvest year 2019. This strict and transparent assessment of uncertainties of the forecast is particularly important in practice, when e.g. policy makers use a yield forecast to inform food security planning.

Over all regions, the forecast of anomalies produces a median NSE of 0.91 in the model estimation and a median NSE of 0.72 in the level 1 validation, which indicates an accurate and robust forecast for large parts of the country. The forecast reproduces both extreme years as well as average yields with high accuracy at a lead time of on average 6 weeks.

Weather influences explain a substantial share of observed maize yield variability in Tanzania as shown by the national median NSE of 0.92 in the estimation and 0.81 in the level 1 validation of the yield model based on weather inputs. Precipitation as well as higher minimum temperatures positively influence maize yields. The variable *consecutive dry days* is the most often selected variable across the regions, which underlines the detrimental effect of dry weather conditions on maize yields. This is in line with Cairns et al. (2013)[6] and Rowhani et al. (2011)[7] who found drought stress to be one of the main weather-related reasons for low maize yields in Sub-Saharan Africa. Apart from weather inputs, the SST of the West Pacific (WP) provides most explained yield variability in the forecast. This can be explained by a strong correlation between the SST in the WP and East African rain[8]. Low SST in the WP, which are related with higher rainfall amounts during the long rains in East Africa[8–10], are positively correlated with maize yields. The variable selection shows that maize yield variability in Tanzania is strongly influenced by extreme events. Also the study of Rowhani et al. (2011)[7] focusing on climate variability and crop production in Tanzania seems to be in line with our finding. They found a strong relationship between the coefficient of variation (cv) of weather variables and cereal yields. In contrast to the cv, the percentile variables can explicitly represent lower or upper extremes and are therefore easier to interpret. The importance of extreme events for explaining maize yield variability in Tanzania implies that there is an upper quality bound for yield forecasts in case of extreme events that are out of the considered range of the training data. The variables selected in the estimation and the forecast show strong similarities for most regions, which suggests that the variable selection is robust.

In contrast to the high estimation and level 1 validation performance, the level 2 validation, which additionally integrates an out-of-sample variable selection, only shows good skills for a limited number of regions in Tanzania. This rigorous level 2 validation is most relevant in practice, as at the moment of forecasting (1–2 month before the harvest), the variable selection can only be done based on yield information from previous years. Despite its importance, this validation is rarely applied by forecasting studies and more than half of the studies even lack a level 1 validation[11]. The study of Ogutu et al. (2018)[3] who provide a forecast for East Africa does not even assess the model results based on observational data. To guarantee that the weaker level 2 performance is not due to model overfitting for the short time series at our disposal, we used a precautionary approach of only allowing a maximum of 5 variables to be selected for a time series of 10 years. This leaves sufficient degrees of freedom (5 DF in the full model and 4 DF for the validation) so that we assume model overfitting to the training as not the main reason for lower performance. Instead, the weaker level 2 performance could be related to the following reasons. First, the short length of the time series of only 10 years may not be sufficient to provide a stable out-of-sample variable selection. In our study period, several ENSO events (e.g. El Niño in 2015/2016 or 2009/2010 and La Nina in 2010/2011 or 2011/2012[12]) and Indian Ocean Dipole phases (e.g. positive phases in 2019 and 2015 and negative phases in 2016 and 2010[13]) occurred, which bring high year-to-year variation in weather

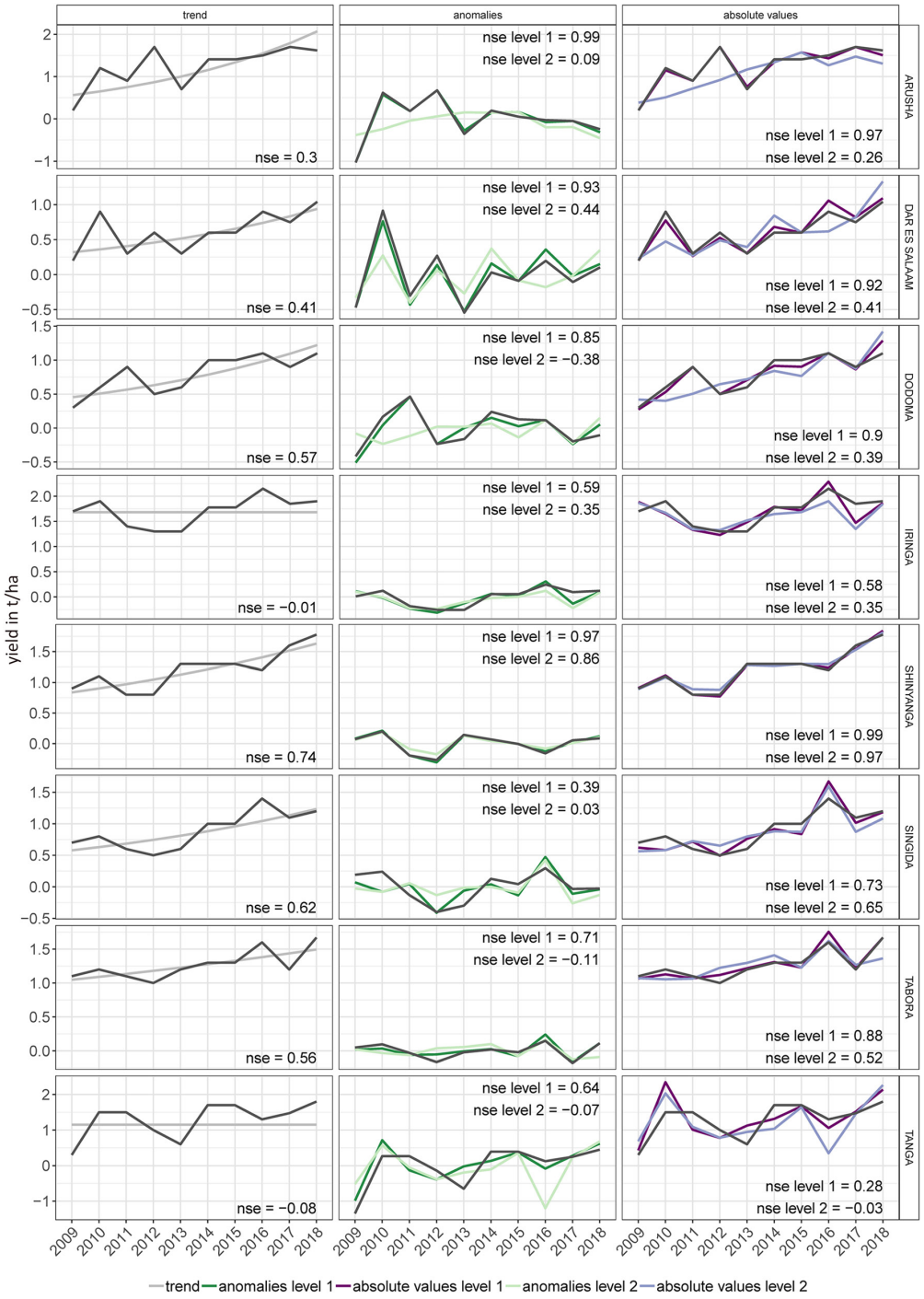

Figure 8. Regional performance of the forecasts derived from the model combining SST and weather inputs. Model assessment was done separately for the trend (left panel), the variability (middle panel) and absolute yields, which is a combination of trend and variability (right panel) for 8 of 21 regions in Tanzania. Plots for all 21 regions can be found in SI Fig. 5. The dark colour (dark green and dark purple) shows the forecast when the level 1 validation is applied. The corresponding NSE value is shown as 'nse.l1'. The light colour (light green and light purple) and the 'nse.l2' show the results of the level 2 validation. Because the trend was fitted based on logarithmic values, the transformation back to linear values results in a slightly curved shape.

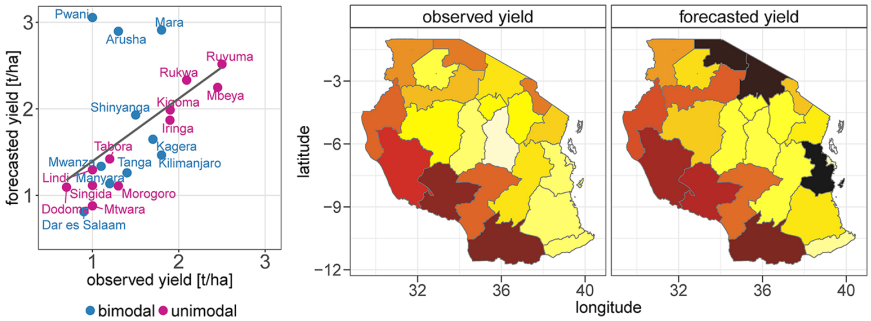

Figure 9. Assessments of the forecasted absolute yields for 2019 in regions with unimodal and bimodal rainfall regimes.

influences and consequently in the variable selection. The time series may not be long enough to train the model for this highly variable weather. The forecast should be repeated and tested on a longer time series when more data becomes available. Also the prediction of ENSO Events[14,15] can be used to inform the yield forecast. Second, uncertainties in the calculated start and end of the growing season, as well as the calculated separation between the vegetative and the reproductive phase can lead to a lower performance of the forecast or inaccuracies in the lead time. The calculated dates may not reflect the real phenological phases and the static dates do not account for the inner-seasonal variability due to differing weather conditions. Third, the forecast relies on reported yield data, which is prone to reporting errors and data quality issues, which may change the forecasting performance.

Because of its relevance in practice, we also provide a forecast of absolute yields, which in addition to the yield variability also includes information about the trend. The results of the absolute yield forecasts are slightly better (median NSE of 0.79 in the level 1 validation) due to the explanatory power of the trend. The disentangling of trend and variability provides transparency about the reasons for the forecasting skills so that in case of a weak weather signal, the trend can be used as the best available information about the expected yields. The forecast is only valid when assuming that the trend of the previous years is going to continue for the following years. For grounding such an assumption, a causal analysis of trends taking into account national policies[16] and international market conditions, as it has been examined for East African countries[17] and the Usangu plain in Tanzania[18], would be mandatory.

The completely independent forecast of yields for the harvest year 2019 shows a high performance for the unimodal rainfall areas and a poor performance in bimodal rainfall regions. The poor performance in the bimodal regions could be related to the outbreak of the fall armyworms, which particularly hit the bimodal rainfall areas in northern, north-eastern and the coastal areas. The below average rainfall during the long rains in these areas fostered the outbreak of the fall armyworms so that an infestation level of 50% was reached in some regions[19]. This result underlines the importance of incorporating local expert knowledge in the evaluation of an operational forecast. Yields in some regions may be strongly influenced by factors that the model does not account for, such as pests and diseases or political, economic or social changes. Therefore, the forecast—as a tool that provides quantitative information about the expected weather-related yields—should be embedded in a forecasting system that integrates several sources of information for the evaluation of the food security situation.

In this study, we constructed an empirical model to decipher climatic influences on maize yield variation in Tanzania. We applied this model to forecast maize yield anomalies and absolute yields at a lead time of about 6 weeks before the harvest on region level in Tanzania. The model provides accurate and robust yield forecasts for large parts of the country. The strict and transparent assessment of the forecasting skill and the low requirements of input data make the forecast potentially suitable to inform operational yield forecasting systems in other countries with inaccessible or low quality weather data and short time series yield data. The proposed model can contribute to better informed local agronomic management strategies and support the implementation of regional agricultural development programs so that food shortages caused by unfavourable weather conditions can be mitigated. This has the potential to accelerate investments in these programs and thus, reduce food insecurity.

Methods

Yield data. We used official maize yield data from 2009 to 2019 obtained from the National Food Security Division of the Ministry of Agriculture of Tanzania. Maize is the most important staple crop in Tanzania[4] and had a total harvest area of 3,428,630 ha in 2019, which represents ca. 25% of the total crop land in Tanzania[20] (statistics from 2017). Maize yields in Tanzania show a high variability and were on average at 1.6 t/ha from 2016 to 2018 (SI Fig. 6). The official statistics report yearly yield data covering all 21 regions of Mainland Tanzania (excluding the island Zanzibar). The administrative boundaries of some regions changed in 2012. To obtain a consistent time series, we used the administrative boundaries from before 2012 by applying a weighted average based on area.

Weather data. We created weather variables based on two climate data sources. For precipitation, we used observed daily rainfall totals from CHIRPS (Climate Hazards group Infrared Precipitation with Stations) at a

resolution of 0.25° × 0.25°[21]. CHIRPS provides reliable precipitation information for East Africa and outperforms previous products, like ARC2 and TAMSAT[22,23]. For daily mean, maximum and minimum temperature, we used ERA5 data[24] provided at a spatial resolution of 0.25° × 0.25°. ERA5 is the most recent reanalyses product and outperforms ERA-Interim for East Africa[25]. The weather variables were created for the time period of available yield statistics (2009–2019), including weather data for the year 2008 in case of growing seasons starting already at the end of 2008.

SST data. In addition to weather data, we included monthly sea surface temperature (SST) anomalies[26] of (1) the El Niño 3.4 zone (170°W–120°W, 5°S–5°N), (2) the West Pacific Box (WP) (130°E–160°E, 10°S–10°N) and (3) the Indian Ocean Dipole (IOD), which is the non-normalized difference between the West Indian Ocean (50°E–70°E, 10°S–10°N) and the Eastern Indian Ocean (90°E–110°E, 10°S–0°N). We included these SST indicators due to their documented influence on East African rainfall. SST anomalies in the El Niño 3.4 zone and the IOD have shown to be positively correlated with rainfall over East Africa during the short rains, whereas SST anomalies in the WP show a negative correlation with East African rainfall during the long rains[8–10]. The influence of these indicators on East African precipitation has a lag of some weeks to months offering the potential to provide yield forecasts at longer lead times. We tested different lead times and included those that showed the highest correlation with yield (SI Fig. 7), i.e. a lead time of 120 days for El Niño 3.4 and WP; and a lead time of 30 days for IOD.

Growing season. The North, North-East and the coastal areas of Tanzania are characterized by a bimodal rainfall pattern. The so-called 'short rains' (or Vuli) occur from October to December and the 'long rains' (Masika) last from March to May. The rest of the country has a unimodal rainfall pattern called Musumi with rainfall occurring from December to April[9]. Because of the low availability of irrigation facilities in Tanzania[20], we did not distinguish irrigated from non-irrigated agriculture and considered the growing seasons to be aligned with the onset of the rain.

We defined the start of the growing season following the approach of Dodd and Jolliffe (2001)[27], which was tested for tropical and subtropical conditions. They define the onset of the growing season when the following three criteria are fulfilled:

1. at least 25 mm rainfall within 6 days
2. starting day and at least 2 other days in this 6-day period are wet (> 0.1 mm)
3. no dry period of 10 or more consecutive days within next 40 days

Because of the bimodal rainfall pattern in North and North-East Tanzania, two onsets of the growing season are found for some grid points. In this case, we considered the onset of the long rains (Masika), which is the main growing season. We used a static crop calendar at region level by first calculating the onset and the end of the growing season per grid point for each harvest year and then calculating the median over all grid points within a region and then a median over all years. We also tested other approaches (SI Section 8) to test the robustness of the results.

We defined the end of the growing season as 110 days after the start, which corresponds to the average time from sowing to maturity of 4 typical maize cultivars in Tanzania (i.e. Stuka, Staha, TMV1 and Pioneer HB3253). This is a reasonable choice since individual growing season lengths vary in a small range from 105 to 114 days[28].

Model inputs. Based on temperature and precipitation data, we created variables that account for the climate drivers that influence maize development and yields (SI Tables 1, 2, 3 show a list of model inputs).

In addition to the median daily mean, maximum and minimum temperature over the growing season (*tas.median, tas.max, tas.min*), we included variables related to extreme temperatures. Above the optimum temperature range, photosynthesis is reduced, whereas respiration rates rise, such that net photosynthesis rates decline[29]. Particularly during flowering, maize is sensitive to heat stress, as it can lead to the desiccation of pollen or a reduction in grain numbers. High temperatures accelerate the development rate and result in a shortened growing season and thus a reduction in light perception. Particularly if the time for grain filling is reduced, grain size and consequently yields decline[30]. To account for the damaging impacts of too high temperatures, we included the number of days where the daily maximum temperature exceeds the region-specific long term 99% percentile of the maximum temperature in the growing season (*tas.max99;* SI Section 9 Eq. 1). Also temperatures below the optimum temperature range, i.e. any temperature below 25 °C according to Rötter and Van De Geijn (1999)[31], are detrimental for maize growth. Therefore, we include the number of times the daily minimum temperature falls below the region-specific long-term 1% percentile of the minimum temperature (*tas.min01*).

The optimal rainfall required in the growing season for maize is around 500–800 mm[32]. We included the precipitation sum (*Psum*) in the growing season to represent the overall water availability for maize. For optimal plant development, the timing and duration of water supply are equally critical. During flowering, maize requires sufficient water supply. Before pollination water stress leads to kernel abortion, even if at the time of pollination sufficient water is available. Excessive rain, in contrast, can lead to soil water saturation and oxygen deficiency, which limits root respiration and the growth of roots. Rainfall that exceeds the water holding capacity of the soil can lead to the leaching of nutrients and nutrient deficiencies of the plant[33]. To represent different precipitation ranges, we included the number of days with precipitation above a threshold of 5, 10 and 15 mm (*pA5, pA10, pA15*, respectively) and below a threshold of 5, 10 and 15 mm (*pB5, pB10, pB15*, respectively). Because the distribution of rainfall within the growing season is of particular importance for plant growth, we included

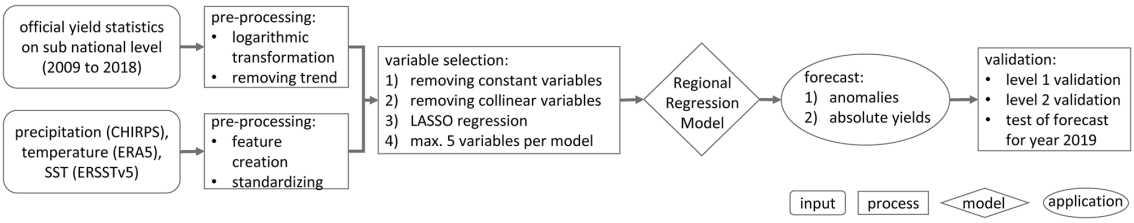

Figure 10. Modelling flow chart.

consecutive dry days of more than 5, 10, 15 and 20 days (*cdd5, cdd10, cdd15*, *cdd20*, respectively). Extremely high precipitation events are covered by the number of times the daily precipitation sum exceeds the region-specific long-term 99% percentile of the daily precipitation sum.

The variables were separately calculated for the vegetative and reproductive phase of the growing season. The separation between both phases was based on the sum of growing degree days (GDD; SI Section 9 Eq. 2). The days in the growing season until 50% of the full-season GDD sum was reached were allocated to the vegetative phase and the remainder to the reproductive phase, following Schauberger et al. (2017)[34].

The SST temperatures were aggregated by taking the median over the growing season. We also included the number of times the 99% percentile of the whole time series is exceeded and the number of times the indicator is below the 1% percentile as an additional variable. The SST indices are only created for the vegetative phase (including the lead time) based on the same approach as for the weather variables.

Model development and assessment. For each of the 21 regions, we applied the work flow as shown in Fig. 10, i.e. we provide the forecast separately for each region comprising of region-specific variables and parameters to account for the diverse climatic conditions within the country.

For our analysis, we used *R*[35] (version 3.5.0) with the packages *tidyr*[36] and *plyr*[37] for data pre-processing, the packages *sp*[38] and *rgdal*[39] for spatial data processing, the package *glmnet*[40] to perform LASSO regression and the package *ggplot2* [41] to generate the figures and maps.

Pre-processing. We standardized all weather and SST input data to allow for a better comparability of the beta coefficients[42]. We transformed the yield input data to logarithmic values and removed the trend by first testing different de-trending methods (mean, linear, quadratic) and then applying the one that resulted in the lowest Akaike Information Criterion (AIC).

Variable selection. We applied the following variable selection process to elucidate important variables for explaining yield variability in the different regions:

- We removed variables that do not show year-to-year variations (i.e. zero variance).
- To avoid multicollinearity, only those variables were selected that are not strongly collinear (i.e. Pearson's $r > 0.7$) with another explanatory variable. If a pair of variables was strongly collinear, then the variable with the higher correlation with yield anomalies was selected.
- Input selection was done using LASSO regression. Through regularization, LASSO performs a co-variate selection, which improves both the prediction accuracy and the interpretability[43]. To select the optimum lambda (the regularization penalty for the LASSO regression), we used the lowest cross-validation (years were omitted subsequently) mean squared error (MSE).
- At last, we removed all variables except for those 5 variables showing the highest correlation with yields. This step was conducted to reduce overfitting of the model based on the rule-of-thumb to include a maximum of half as many independent variables (climate variables) as there are dependent variables (yields).

Model for estimating and forecasting yields before harvest. For each region, we applied a separate regional regression model (Eq. 1) following the approach of Gornott and Wechsung (2016)[44] and Schauberger et al. (2017)[34].

$$\log(y_{it}) = \sum_{k=1}^{K} \beta_{ki} x_{kit} + \varepsilon_{it} \tag{1}$$

with β as parameters, y as the demeaned and detrended response variable, x as the standardized explanatory input variable, ε as error term for K variables ($k = 1, \ldots, K$), N spatial units ($i = 1, \ldots, N$) and T years ($t = 1, \ldots, T$).

With the Breusch–Godfrey and the Breusch–Pagan tests we tested autocorrelation and heteroscedasticity of model residuals. We use the Variance Inflation Factor to test for multicolinearity.

For the within-season forecast, we only included variables during the vegetative phase. This provides a lead time of around 55 days, i.e. around 6 weeks before the harvest in a growing season totalling 110 days. The exact lead time differs per region—depending on the start of the reproductive phase in each region (SI Table 5). We provided the forecast for yield anomalies (i.e. variation around a trend) and for absolute values. For the latter, we added the trend and retransformed the values back to the linear form.

Cross validation. We applied a two level leave-one-out cross validation (LOOCV).

Level 1—LOOCV: we selected the variables based on all observations with LASSO. Then we subsequently removed observations for 1 year from the data set and used the remaining observations from the other years to fit the model and predict yield changes for the removed year, using the pre-selected set of variables.

Level 2—LOOCV: we subsequently removed observations for 1 year from the data set, then selected variables with LASSO and estimated the model based on the remaining data set. We used this model to predict yield changes for the removed year. This level 2—LOOCV guarantees that no information from the removed year is used for the variable selection or the model estimation. For this validation we allow a maximum of only 4 variables per model (allowing one less than half as many variables as there are observations). This validation simulates the operational context, where no yield information from the year to be forecasted is available for model building.

In addition, we used the model we developed based on the yield data from 2009 to 2018 to provide a completely independent forecast for the harvest year 2019. The yield data for 2019 was not known to us during the model development.

The goodness of fit between the observed data and the predicted data was then evaluated based on the Nash–Sutcliffe efficiency coefficient[5] (NSE). In contrast to the explained variance (r^2), NSE does not only evaluate similarities in variability, but also integrates the mean model bias, which makes it a robust measure of the prediction quality. We also calculated the root mean squared error (RMSE) to estimate the average error between observed and predicted yields.

Data availability

All data supporting the findings of this study are either public data sets, are available within the article and its Supplementary Information files or are available from the corresponding author upon reasonable request.

Received: 26 June 2020; Accepted: 27 October 2020
Published online: 12 November 2020

References

1. Liu, L. & Basso, B. *Seasonal Crop Yield Forecast: Methods, Applications, and Accuracies. Advances in Agronomy* Vol. 154 (Elsevier Inc., Amsterdam, 2019).
2. Liu, L. & Basso, B. Linking field survey with crop modeling to forecast maize yield in smallholder farmers' fields in Tanzania. *Food Secur.* **12**, 537–548 (2020).
3. Ogutu, G. E. O., Franssen, W. H. P., Supit, I., Omondi, P. & Hutjes, R. W. A. Probabilistic maize yield prediction over East Africa using dynamic ensemble seasonal climate forecasts. *Agric. For. Meteorol.* **250–251**, 243–261 (2018).
4. National Bureau of Statistics. Basic Demographic and Socio-Economic Profile (2014) https://tanzania.countrystat.org/fileadmin/user_upload/countrystat_fenix/congo/docs/2012 Tanzania Population and Housing Census-Basic Demographic and Socio-Economic Profile.pdf (Accessed 11th July 2020).
5. Nash, J. E. & Sutcliffe, J. V. River flow forecasting through conceptual models part I—a discussion of principles. *J. Hydrol.* **10**, 282–290 (1970).
6. Cairns, J. E. *et al.* Adapting maize production to climate change in sub-Saharan Africa. *Food Secur.* **5**, 345–360 (2013).
7. Rowhani, P., Lobell, D. B., Linderman, M. & Ramankutty, N. Climate variability and crop production in Tanzania. *Agric. For. Meteorol.* **151**, 449–460 (2011).
8. Davenport, F., Funk, C. & Galu, G. How will East African maize yields respond to climate change and can agricultural development mitigate this response?. *Clim. Change* **147**, 491–506 (2018).
9. Hoell, A. & Funk, C. Indo-Pacific sea surface temperature influences on failed consecutive rainy seasons over eastern Africa. *Clim. Dyn.* **43**, 1645–1660 (2014).
10. Funk, C. *et al.* Predicting East African spring droughts using Pacific and Indian Ocean sea surface temperature indices. *Hydrol. Earth Syst. Sci.* **18**, 4965–4978 (2014).
11. Schauberger, B., Jägermeyr, J. & Gornott, C. A systematic review of local to regional yield forecasting approaches and frequently used data resources. *Eur. J. Agron.* **120**, 126153 (2020).
12. NOAA. Cold and Warm Episodes by Season (2020) https://origin.cpc.ncep.noaa.gov/products/analysis_monitoring/ensostuff/ONI_v5.php (Accessed 24th April 2020).
13. NOAA/ESRL. Dipole Mode Index (DMI) (2020) https://stateoftheocean.osmc.noaa.gov/sur/ind/dmi.php (Accessed 24 April 2020).
14. Ludescher, J. *et al.* Very early warning of next El Niño. *Proc. Natl. Acad. Sci.* **111**, 2064–2066 (2014).
15. Meng, J. *et al.* Complexity-based approach for El Niño magnitude forecasting before the spring predictability barrier. *Proc. Natl. Acad. Sci. U.S.A.* **117**, 177–183 (2020).
16. FAO. Review of Food and Agricultural Policies in the United Republic of Tanzania 2005–2011—Country Report (2013) https://www.fao.org/3/a-at476e.pdf (Accessed 5 June 2020).
17. Aylward, C. *et al.* Maize Yield Trends and Agricultural Policy in East Africa. *Evans School of Public Policy and Gonvernance* (2015) https://evans.uw.edu/sites/default/files/EPAR_UW_310_National-Level_MaizeYieldTrends_5.31.16.pdf (Accessed 4 June 2020).
18. Malley, Z. J. U., Taeb, M. & Matsumoto, T. Agricultural productivity and environmental insecurity in the Usangu plain, Tanzania: Policy implications for sustainability of agriculture. *Environ. Dev. Sustain.* **11**, 175–195 (2009).
19. FAO. GIEWS Country Brief United Republic of Tanzania (2019) https://www.fao.org/giews/countrybrief/country/TZA/pdf/TZA.pdf (Accessed 4 May 2020).
20. FAO. FAOSTAT—Food and agriculture data (2019) https://www.fao.org/faostat/ (Accessed 10 April 2019).
21. Funk, C. *et al.* The climate hazards infrared precipitation with stations—a new environmental record for monitoring extremes. *Sci. Data* **2**, 1–21 (2015).
22. Muthoni, F. K. *et al.* Long-term spatial-temporal trends and variability of rainfall over Eastern and Southern Africa. *Theor. Appl. Climatol.* **137**, 1869–1882 (2019).
23. Dinku, T. *et al.* Validation of the CHIRPS satellite rainfall estimates over eastern Africa. *Q. J. R. Meteorol. Soc.* **144**, 292–312 (2018).
24. Copernicus Climate Change Service (C3S). ERA5: Fifth generation of ECMWF atmospheric reanalyses of the global climate (2017) https://cds.climate.copernicus.eu/cdsapp#!/home (Accessed 19 December 2019).
25. Gleixner, S., Demissie, T. & Diro, G. T. Did ERA5 Improve Temperature and Precipitation Reanalysis over East Africa? *Atmosphere.* **11**, 1–19 (2020).
26. Huang, B. *et al.* Extended reconstructed Sea surface temperature, Version 5 (ERSSTv5): upgrades, validations, and intercomparisons. *J. Clim.* **30**, 8179–8205 (2017).

27. Dodd, D. E. S. & Jolliffe, I. T. Early detection of the start of the wet season in semiarid tropical climates of Western Africa. *Int. J. Climatol.* **21**, 1251–1262 (2001).
28. Mourice, S. K., Rweyemamu, C. L., Tumbo, S. D. & Amuri, N. Maize cultivar specific parameters for Decision Support System for Agrotechnology Transfer (DSSAT) application in Tanzania. *Am. J. Plant Sci.* **05**, 821–833 (2014).
29. Barnabás, B., Jäger, K. & Fehér, A. The effect of drought and heat stress on reproductive processes in cereals. *Plant Cell Environ.* **31**, 11–38 (2008).
30. Carter, P. R. & Hestermann, O. B. Handling corn damaged by autumn frost. *National Corn Handbook—Climate and Weather* (1990) https://www.baycounty-mi.gov/Docs/CitizenCorps/HandlingCornDamageByAutumnFrost.pdf (Accessed 1 May 2019).
31. Rötter, R. & Van De Geijn, S. C. Climate change effects on plant growth, crop yield and livestock. *Clim. Change* **43**, 651–681 (1999).
32. Critchley, W. & Siegert, K. Water harvesting (1991) https://www.fao.org/3/U3160E/u3160e04.htm (Accessed 1 May 2019).
33. Rötter, R. P. *et al.* Linking modelling and experimentation to better capture crop impacts of agroclimatic extremes—a review. *Food Crop. Res.* **221**, 142–156 (2018).
34. Schauberger, B., Gornott, C. & Wechsung, F. Global evaluation of a semiempirical model for yield anomalies and application to within-season yield forecasting. *Glob. Change Biol.* **23**, 4750–4764 (2017).
35. R Core Team. R: a language and environment for statistical computing (2018) https://www.r-project.org/.
36. Wickham, H. & Henry, L. tidyr: Easily Tidy Data with 'spread()' and 'gather()' functions (2019) https://cran.r-project.org/package=tidyr.
37. Wickham, H. The split-apply-combine strategy for data analysis. *J. Stat. Softw.* https://doi.org/10.18637/jss.v040.i01 (2011).
38. Pebesma, E. J. & Bivand, R. S. Classes and methods for spatial data in R (2005) https://cran.r-project.org/doc/Rnews/.
39. Bivand, R., Keitt, T. & Rowlingson, B. rgdal: bindings for the 'Geospatial' Data Abstraction Library. R package version 1.3-2 (2018) https://cran.r-project.org/package=rgdal.
40. Friedman, J. *et al.* Regularization paths for generalized linear models via coordinate descent (2008) https://web.stanford.edu/~hastie/Papers/glmnet.pdf.
41. Wickham, H. ggplot2: elegant graphics for data analysis (2009) https://ggplot2-book.org/.
42. Wooldridge, J. M. *Introductory Econometrics A Modern Approach*. (Cenage Learning, 2014).
43. Tibshirani, R. Regression shrinkage and selection via the Lasso. *J. R. Stat. Soc. Ser. B* **58**, 267–288 (1996).
44. Gornott, C. & Wechsung, F. Statistical regression models for assessing climate impacts on crop yields: a validation study for winter wheat and silage maize in Germany. *Agric. For. Meteorol.* **217**, 89–100 (2016).

Acknowledgements
This work has been funded by the EPICC and the ClimSec project. EPICC is part of the International Climate Initiative (IKI). The Federal Ministry for the Environment, Nature Conservation and Nuclear Safety (BMU) supports this initiative on the basis of a decision adopted by the German Bundestag. ClimSec is financed by the German Federal Foreign Office. The work of David Makowski was partly funded by the project CLAND (16-CONV-0003).
We thank Stephanie Gleixner for her contributions to the climate data pre-processing.

Author contributions
R.L., C.G., B.S. and D.M. designed the research. R.L. performed the research and wrote the manuscript with contributions from C.G. and B.S. C.G. initiated the research. D.M. reviewed the statistical modelling approach and contributed to the interpretation of the results. All authors revised the manuscript.

Funding
Open Access funding enabled and organized by Projekt DEAL.

Competing interests
The authors declare no competing interests.

Additional information
Supplementary information is available for this paper at https://doi.org/10.1038/s41598-020-76315-8.

Correspondence and requests for materials should be addressed to R.L.

Reprints and permissions information is available at www.nature.com/reprints.

Publisher's note Springer Nature remains neutral with regard to jurisdictional claims in published maps and institutional affiliations.

2.3 A forecast of staple crop production in Burkina Faso to enable early warnings of shortages in domestic food availability

This chapter is a reproduction of the article published as:

Laudien, R., Schauberger, B., Waid, J., & Gornott, C. (2022). A forecast of staple crop production in Burkina Faso to enable early warnings of shortages in domestic food availability. *Scientific Reports*, *12*(1), 1- 10. https://doi.org/10.1038/s41598-022-05561-9

www.nature.com/scientificreports

scientific reports

Check for updates

OPEN

A forecast of staple crop production in Burkina Faso to enable early warnings of shortages in domestic food availability

Rahel Laudien[1]✉, Bernhard Schauberger[1,2], Jillian Waid[1] & Christoph Gornott[1,3]

Almost half of the Burkinabe population is moderately or severely affected by food insecurity. With climate change, domestic food production may become more under pressure, further jeopardizing food security. In this study, we focus on the production of maize, sorghum and millet as staple cereal crops in Burkina Faso to assess food availability as one component of food security. Based on a statistical weather-driven crop model, we provide a within-season forecast of crop production 1 month before the harvest. Hindcast results from 1984 to 2018 produce an r^2 of 0.95 in case of known harvest areas and an r^2 of 0.88 when harvest areas are modelled instead. We compare actually supplied calories with those usually consumed from staple crops, allowing us to provide early information on shortages in domestic cereal production on the national level. Despite the—on average—sufficient domestic cereal production from maize, sorghum and millet, a considerable level of food insecurity prevails for large parts of the population. We suggest to consider such forecasts as an early warning signal for shortages in domestic staple crop production and encourage a comprehensive assessment of all dimensions of food security to rapidly develop counteractions for looming food crises.

Agriculture in Burkina Faso is primarily subsistence-based and rainfed. The dependence on favourable weather conditions, such as sufficient and well-distributed rainfall and a reliable onset and length of the rainy season[1], make agricultural production in Burkina Faso particularly vulnerable to climate change and altered weather variability. Cereal yields are expected to decrease by 18% in the Northern Sudano-Sahelian countries due to the impact of higher temperatures, which lead to a reduced crop cycle duration and increased evaporation rates and thus water stress[2–4].

From 2017 to 2019, nearly half of the Burkinabe population was moderately or severely affected by food insecurity[5]. Due to ongoing armed conflicts and the outbreak of COVID-19 in 2020, which negatively affected households' income and access to markets, the number of food insecure people is even expected to increase[6]. This underlines the need to study the reasons and devise tools for increasing or stabilizing food supply.

A within-season yield forecast provides information about the expected harvest. This early warning can allow governments to adjust food imports in case of expected harvest losses[7–10] and ask for external food assistance to alleviate food shortages. Yield forecasts can therefore support food security planning in face of unfavourable weather conditions.

Whereas existing yield forecasting studies in Burkina Faso focus on single crops, have a limited geographic coverage or time horizon[11–14], our study covers the whole country and provides a within-season yield forecast for the most important cereal crops of maize, sorghum and millet. In addition to a statistical weather-driven crop yield model tested for the time period from 1984 to 2018, we use information about harvest areas to derive a crop production forecast 1 month before the harvest. We rigorously validate our forecasts in two levels of out-of-sample modelling.

Moreover, we complement existing studies on food security in Burkina Faso—e.g. focusing on food access[15,16], off-farm income[17,18] or dietary diversity[19]—by comparing the supplied calories from staple crops with the historic demand on national level. This allows us to provide early information on shortages in domestic cereal production

ermany. ✉email: laudien@pik-potsdam.de

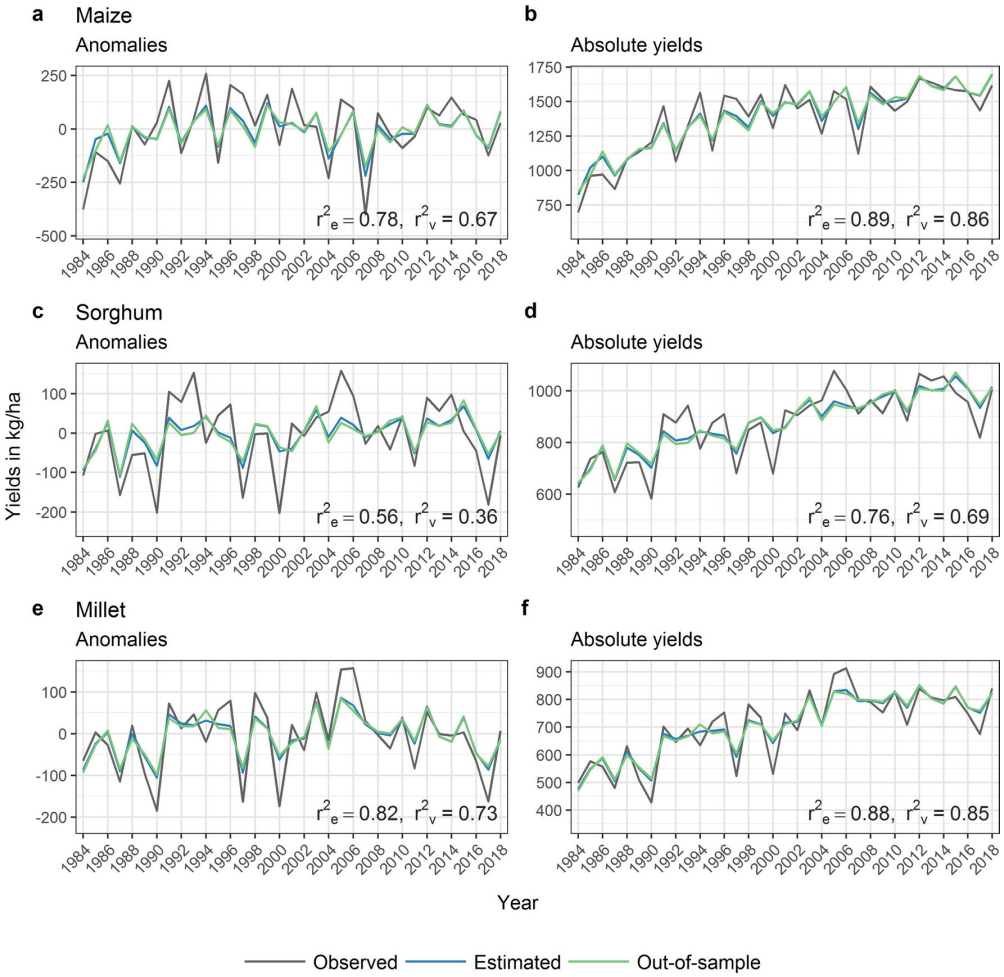

Figure 1. Crop model performance for yield anomalies (left column) and absolute yields (right column) for maize, sorghum and millet from 1984 to 2018. The plot shows the observed yields in grey, the estimation results in blue and the out-of-sample validation results in green. The r^2_e and r^2_v values indicate the explained variance by each model, respectively. The province-specific model performances are shown in SI Fig. 1, a map with province names is shown in SI Fig. 2.

on the national level. Following this approach, our study aims to contribute to a better understanding of food production as one component of food availability in Burkina Faso.

Results

First, we present models to estimate crop yields for maize, sorghum and millet in Burkina Faso at the end of the growing season, i.e. assuming all relevant weather information is known. Combining crop yields with harvest area estimations, we model crop production as yield times harvest area. Second, the estimation models are turned into forecasting models of cereal-based calories by withholding weather information from the last month of the growing season. The produced calories from maize, sorghum and millet are then compared to the calories usually consumed from those crops.

Performance in estimating yields, area and production. The yield model shows that variation in crop yield anomalies, i.e. fluctuations around an underlying trend, is highly influenced by variations in weather (Fig. 1). This is particularly evident for maize and millet. The out-of-sample results (i.e. the validation based on independent test data) indicate a share of 73% of yield variation for maize and 67% of yield variation for millet, explained by variations in weather. For sorghum, the weather-driven variation in yield is lower with 36%. If absolute yields are considered instead of anomalies, the out-of-sample validated explanatory power of our models increases to 86%, 85% and 69% for maize, millet and sorghum, respectively (Fig. 1). The weather-driven

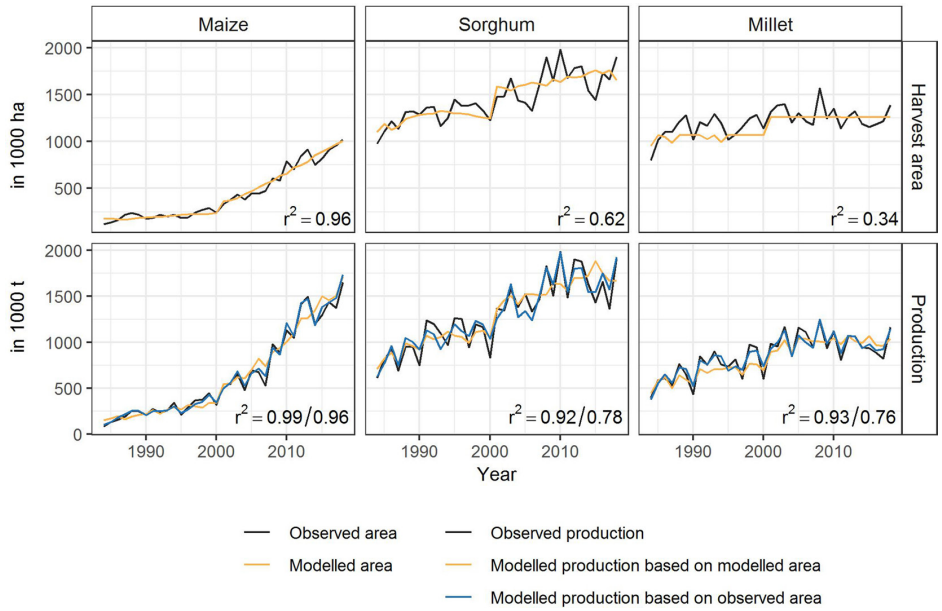

Figure 2. Harvest area and production for maize, sorghum and millet between 1984 and 2018. The black lines show the observed harvest area and production. For area, the best out-of-sample model was chosen. The modelled production is shown for two cases: (1) harvest area is known through e.g. farmer survey or satellite imageries (blue, first r^2 value); (2) harvest area is unknown and was modelled (yellow, second r^2 value).

yield models perform better than a constant model that estimates the mean yield excluding the current year (SI Table 1). Together with the high out-of-sample explained variances, this suggests that the weather influences on crop yields are robustly detected, allowing for assessing yield forecasts based on weather observations.

To model crop production, information about harvest areas is required. As this might not be available in practice, we devised empirical models for harvest areas. The best out-of-sample fit to observed harvest areas can be achieved with the LOESS-based trend for maize and sorghum and the median harvest area for millet, resulting in explained variations of 96% for maize, 62% for sorghum and 34% for millet, respectively (Fig. 2, top row).

Combining yield and area estimations, we modelled crop production as yield times harvest area. We compared two versions: one where the harvest area is assumed as known and one where the harvest area is modelled. For yields, we used the model results of the out-of-sample variable selection. In the case of modelled harvest areas, 96% of observed production variability can be explained for maize, 78% for sorghum and 76% for millet. In case of known harvest areas, the explained variability of production increases to 99% for maize, 92% for sorghum and 93% for millet (Fig. 2).

Hindcast performance of the forecast of supplied calories compared to the usually consumed calories from staple crops. We turned the production models into forecasting models by withholding weather information from the last month of the growing season. Furthermore, production amounts of maize, sorghum and millet were converted into calories and added up to get the calories production of staple crops on national level. This allows us to compare produced calories with the historic demand for calories from staple crops in Burkina Faso.

Assuming unknown, i.e. modelled, harvest areas, the production forecast for maize, sorghum and millet agrees strongly with observed production ($r^2 = 0.88$). With known harvest areas, the r^2 increases to 0.95 and the forecast more accurately represents the amplitude of the peaks (Fig. 3). Notably, this high agreement was achieved with a rigorous validation (level 2: out-of-sample variable selection), where no yield information from the year to be forecasted was used in model construction and estimation—which is similar to an operational context. Crop-specific production forecasts are shown in SI Fig. 3.

From 1984 to 2018 the domestic demand for calories from maize, sorghum and millet has increased in Burkina Faso due to a growing population (SI Fig. 4). Supplied calories from maize, sorghum and millet have increased by enhancing yields and expanding harvest areas (SI Fig. 5). The produced calories (excluding post-harvest losses and the bran) exceeded or fell within the range of usually consumed calories from those crops in the past on nationally aggregated level (Fig. 3). On average, there were 23% more calories produced than consumed.

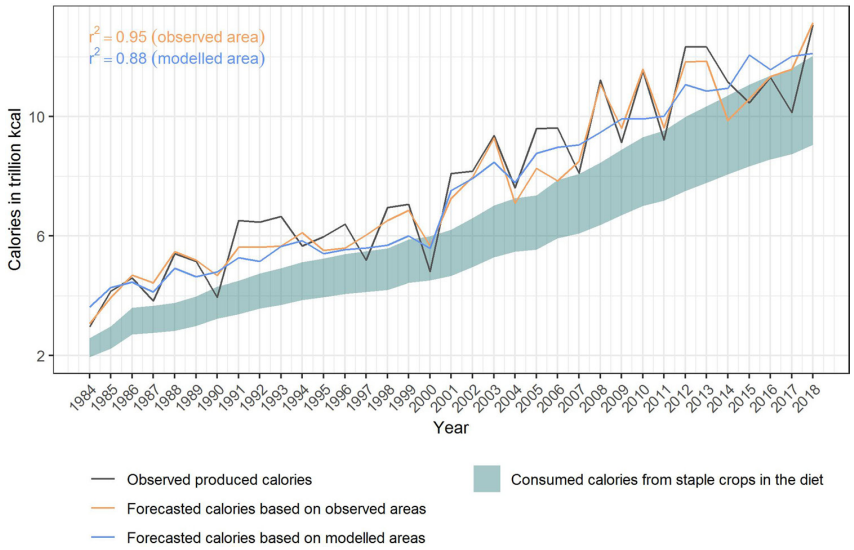

Figure 3. Hindcast performance of aggregated nationally produced calories from staple crops (maize, sorghum and millet) compared to the usually consumed calories from those crops in Burkina Faso. The black line shows the observed produced calories minus post-harvest losses and the bran. The forecast is provided for two cases: (1) harvest areas are known (yellow line), (2) harvest areas are not known and modelled instead (blue line). The band shows the range between the lowest and the highest share of calories from maize, sorghum and millet from 1984 to 2018 in the total supplied calories (i.e. between ca. 47% and 61% of total supplied calories stemmed from maize, sorghum and millet in the past in Burkina Faso).

Discussion

Our study presents models to estimate staple crop yields (maize, sorghum and millet) and harvest areas in Burkina Faso, and combines these into within-season crop production forecasts. Our rigorously validated production forecasts show very high agreement with actually observed production. Thus, the forecast could support near-term planning endeavours to adjust food trade balances, mobilize disaster reliefs and food aid in case of expected harvest losses by anticipating deficiencies in calories supply.

Weather influences can explain a substantial part of crop yield variations in Burkina Faso as indicated by the high performance of the crop yield model in the out-of-sample validation (r^2 between 0.73 (0.86) and 0.36 (0.69) for yield anomalies (or absolute yields, respectively)). Our linear regression models provide robust and interpretable results, which is important in an operational context. As the increasing trend in absolute yields acts as a major driver of explanatory power, the model performance is greater for absolute yields compared to yield anomalies. As the yield estimation quality thus relies on a persisting trend, at least for the next year, a causal analysis of the recent increases (management, fertilizer, improved seeds, irrigation expansion etc.) is recommended, but beyond the scope of this study.

The yield forecast (SI Fig. 6) shows similarly good results compared to the yield model, which suggests that the vegetative and first part of the reproductive phase of the growing season sufficiently cover important weather influences. This is in line with findings of Schauberger et al.[20], who also found a high and sometimes even higher model performance for a reduced growing season, omitting the last part of the reproductive phase. The weather-based yield forecast performed better than a model based on trends only, indicating the relevance of weather for yield formation (SI Fig. 7).

To our best knowledge, there is no previous study covering the same regional scope and time period of crop estimation in Burkina Faso. Yet, our results are partly comparable to two local studies. Our model skill is higher for maize and millet and lower for sorghum compared to the weather-based yield model of Belesova et al.[21] for the province Kossi and the NDVI-based yield forecast of Karst et al.[14] for the department Nouna within Kossi. The lower performance for sorghum could be related to reliability issues in the sorghum data applied here (SI Text 1).

To forecast crop production in Burkina Faso, information about crop yields and harvest areas is required, as production is a function of both. For hindcasting past production, the actual area is available. But this is not necessarily the case during the growing season, although early area information would be crucial for early production estimation. While, in principle, farm surveys or satellite observations could detect sown areas during the season, handling frictions and temporal latencies might obfuscate their reliability in practice. Therefore, we estimated this year's harvest areas based on information from preceding years—assuming persistent trends as for yields. Using this approach, harvest areas can be represented to a large extent for maize and sorghum due to ongoing upward trends in area. Trends in millet areas are less pronounced and thus less indicative for areas in the target year. Calculated crop production shows a high agreement in case of known harvest areas ($r^2 > 0.9$) as well as modelled harvest areas ($r^2 > 0.75$).

Our study provides the first production forecast covering the whole country and the main staple cereal crops in Burkina Faso. The lead time of the crop-specific forecast (SI Fig. 6) is 1 month for each crop (SI Fig. 8). Due to possible delays in the provision of climate data, different harvest dates of the crops (at the forecasting time of sorghum and millet, maize is already harvested) and possible dissemination issues, the lead time of the aggregated production forecast is lower in practice. Nonetheless, we assume that forecasts for the single crops and also real-time estimates of aggregated available production around harvest time can convey valuable information for policy makers. To provide transparency about the forecasting skill, we use two validations. In addition to a classic ('jack-knife') out-of-sample validation, we use a more rigorous out-of-sample variable selection that mimics the operational setting. This validation is rarely used in forecasting[22] and has also not been applied in existing yield forecasting studies in Burkina Faso[11–14]. Production forecasts for maize, sorghum and millet together, derived under this mock-operational setting, agree strongly with observed production ($r^2 = 0.88$ for modelled areas). Thus, we believe that our production forecast could contribute to existing operational food security platforms, such as the Famine Early Warning Systems Network (FEWS NET) which provides food security updates for Burkina Faso incorporating information on crop production, climate, markets, conflicts and nutrition[23].

In addition to the production forecast, we compare produced and usually consumed calories from staple cereals in the past and assume that a similar share in total food supply will also be needed in the current season. To account for uncertainties in this estimate, we considered a wide range between the highest and the lowest proportion of supplied calories within the last 35 years. Nonetheless, the study methodology should be updated regularly to account for changes in dietary preferences and production choices in Burkina Faso—like e.g. the recent increase in domestic production and consumption of rice.

Our results—both from reported and modelled data—suggest that for most years, there were more produced calories from staple crops than the usual amount of consumed calories from these crops on national level. Despite this surplus in the production of staple crops, there is a prevailing high level of food insecurity in Burkina Faso. According to a FAO-led household survey from 2014 to 2019, 48% of the population (ca. 9 Million people) were moderately or severely food insecure and undernourishment affected about 19% of the population from 2017 to 2019[5] (SI Fig. 9). The discrepancy between the potentially available and consumed calories could have several causes: First, our assumptions made to derive consumed calories might be too rigorous. Post-harvest losses might be higher in reality. Also apart from food and feed, we did not include other uses of staple crops, such as sorghum beer production. Even though beer production consumes a practically relevant amount of sorghum in Burkina Faso (on average 27% of total supplied calories from sorghum from 2014 to 2018[24]), limited data availability did not allow for a quantification of this impact over the whole time period and was therefore neglected (SI Fig. 10). Second, our national level results do not provide insights about the seasonal, spatial and group-specific distribution of food within the country. Food shortages in specific regions (e.g. the Sahel region in Northern Burkina Faso), times during the year (e.g. the dry season) and/or in specific population groups (e.g. subsistence framers)[6] are therefore not necessarily reflected in annual and national statistics. Future research should therefore take into account the seasonal and spatial dimension of food availability in Burkina Faso. Third, our study does not account for population-specific demand of food. In particular, the rural population and subsistence farmers with labour intense lifestyles[25] are characterised by a greater dependence on calorie-rich foods such as cereals, tubers and coarse grains and have fewer capacities to diversify the composition of their diets[25]. Therefore, the share of consumed calories from staple crops is likely higher for those vulnerable groups. Our results should therefore be interpreted as representing a lower bound estimate of the actual required calories from staple crops. Fourth, our study focuses on production from staple crops, which is one important component of food availability and thus food security. Deficiencies in the other three components, namely food access, utilization and stability[26], contribute to the high level of food insecurity even when, on paper, there are more produced calories than consumed. Local increases in food prices, political instability, ongoing conflicts as well as terrorist threats and attacks in Burkina Faso negatively impact food security in Burkina Faso[6].

In the past, the increase in production was in line with the strong population growth in Burkina Faso (SI Fig. 4). This increase was achieved by enhanced yields and simultaneously expanded agricultural land (SI Fig. 5). The implementation of improved soil and water conservations practices in the first half of the 1980s, and the shift to early maturing varieties led to yield increases[27]. At the same time, the share of arable land increased from ca. 30% in the beginning of the 1980s to ca. 50% in 2018[28] (SI Fig. 11). Apart from the negative environmental consequences related to this land use change[27], the increase in arable land is limited because of finite land resources and has already been stagnating for the last 10 years (SI Fig. 11). Also increasing crop yields through agricultural intensification is constrained by limited access to agricultural inputs (improved seeds, fertilizer, plant protection and machinery), environmental boundaries[29] and challenges in adopting good agricultural practices[30,31]. Both components—yields and acreage—taken together suggest that domestically produced calories might not be sufficient to meet the increasing demand of a growing population in the long term[32,33]. This looming future deficiency may become more pronounced when adverse effects of climate change materialize in crop production. At this point, other dimensions of food security, namely food access, utilization and stability, will become crucial to guarantee sufficient food supply.

Methods

To forecast crop production in Burkina Faso, information about crop yields (harvested amount per area) and harvest areas is required, as production is a function of both. In the following, we describe a yield model (*yield module*) and a harvest area model (*harvest area module*) on province level to calculate both types of information. Both models can be run in an ex-post (estimation of production after the harvest) and an ex-ante (estimation of production before the harvest) mode. In the forecast (ex-ante) mode, the yield model was only supplied with reduced climate information, omitting weather influences of the last month before the harvest. Then, the results

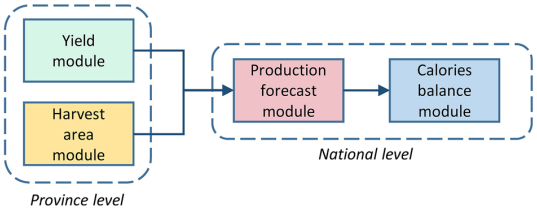

Figure 4. Work flow.

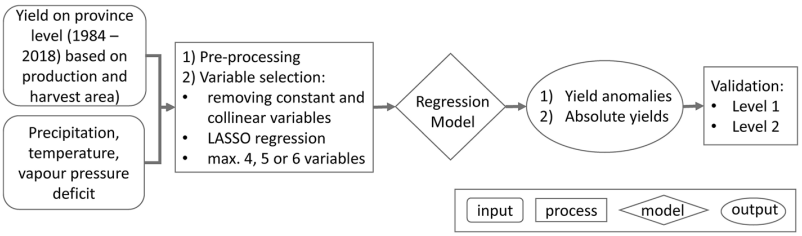

Figure 5. Yield module flow chart.

of the yield and harvest area model were aggregated to the national level (*production forecast module*). Finally, we compared the produced calories from maize, sorghum and millet with the usually consumed calories from those crops (*calories balance module*; Fig. 4).

For our analysis, we used the statistical software *R*—version 4.0.5[34]. A list of used packages can be found in SI Text 2.

Yield module. For each of the 45 provinces, we applied the work flow as shown in Fig. 5, i.e. we set up a separate yield model for each crop and each province. The empirical model comprises crop and province-specific exogenous variables to account for the different growth requirements of each crop type and the diverse climatic conditions within the country.

Input data. We used annual harvest area and production statistics for maize, sorghum and millet on province level from 1984 to 2018 from the Burkinabe Ministère de l'Agriculture et des Aménagements Hydroagricoles/ Direction Générale des Etudes et des Statistiques Sectorielles[35]. Maize, sorghum and millet are the main cereal crops in Burkina Faso and accounted for 53% of total supplied calories from 1984 to 2016 (median value; SI Fig. 12). Climate data from 1984 to 2018 were extracted from two sources. For precipitation, we used observed daily rainfall totals from CHIRPS (Climate Hazards Group Infrared Precipitation with Stations) at a resolution of 0.25×0.25 degrees[36], which provides reliable precipitation information[37]. For daily mean, maximum and minimum temperature, we used ERA5 data[38] provided at a resolution of 0.25×0.25 degrees. ERA5 is a recent re-analysis product and outperforms ERA-Interim over Africa[39]. Based on the ERA5 temperature data, we calculated vapour pressure deficit[40] (VPD, SI Eq. 1) to account for water stress caused by high atmospheric water demand, which leads to a reduction in plant carbon uptake[41] and thus yields. All weather data were mapped to province boundaries, considering only intersecting cells for each province.

Exogenous variables. Based on precipitation, temperature and vapour pressure deficit, we created variables that represent yield influencing climate drivers. We included variables that represent the median state of the weather during the growing season, as well as variables accounting for variation and extremes in weather. For precipitation, we took into account the occurrence of consecutive dry and wet days, respectively, and different thresholds for light and heavy precipitation events. SI Table 2 shows a list of all possible model inputs and SI Text 3 further expands on the reasons for the included variables.

The weather variables were calculated for the growing season in Burkina Faso following the FAO crop calendar[42]. All sowing and harvesting activities happen between May and November. As the yield statistics do not provide variety-specific information, we used the median sowing and harvest dates of all reported varieties (SI Fig. 13 for maize and SI Fig. 14 for sorghum and millet). For sorghum and millet the same crop calendar was used because the FAO does not provide a specific calendar for sorghum and due to the similarity in sowing and harvest dates[6].

The variables were separately calculated for the vegetative (veg), the first (repro1) and the last part of the reproductive phase (repro2) of the growing season. The days in the growing season until 50% of the full-season growing degree days sum (GDD, SI Eq. 2) was reached were allocated to the vegetative phase and the remainder

to the reproductive phase, following Schauberger et al.[20]. The reproductive phase was then split into two separate phases (repro1 and repro2) with repro2 covering the last month before the harvest and repro1 covering the time between veg and repro2. The separation between repro1 and repro2 accounts for different weather influences on crop growth during the reproductive phase (grain filling and maturity phase)[43] and enables a forecast with a lead time of 1 month if weather information from repro2 is withheld from model construction.

Pre-processing. Due to unreasonable values in the yield data, we applied data cleaning steps detailed in SI Text 1. Moreover, possible trends in the yield time series were removed on province level, by choosing the polynomial trend (mean, linear or quadratic) with the lowest Akaike Information Criterion (AIC). The weather variables were standardized to a mean of 0 and a standard deviation of 1 to allow for a better comparability of the beta coefficients[44].

Variable selection. We applied the following variable selection process to elucidate important variables for explaining yield variability in the different provinces:

- We removed variables that do not show year-to-year variations (i.e. zero variance).
- To avoid multicollinearity, only those variables were selected that are not strongly collinear (i.e. Pearson's $r > 0.7$) with another explanatory variable. If a pair of variables was strongly collinear, then the variable with the higher correlation with yield anomalies was retained and the other removed.
- Input selection was done using LASSO regression. Through regularization, LASSO performs a co-variate selection, which improves both the prediction accuracy and the interpretability[45]. To select the optimum lambda, i.e. the regularization penalty for the LASSO regression, we used the lowest cross-validation (years were omitted subsequently) mean squared error (MSE).
- As a last step, we restricted the maximum number of variables to be included in the model to avoid overfitting. Per crop, we tested a maximum of four, five and six variables and selected the set of variables that showed the highest correlation with yields in the out-of-sample validation.

Regression model. For each province, we applied a separate regression model (Eq. 1) following the approach of Gornott and Wechsung[46] and Schauberger et al.[20].

$$y_{it} = \sum_{k=1}^{K} \beta_{ki} x_{kit} + \varepsilon_{it} \tag{1}$$

with β as parameters, y as the demeaned and detrended response variable, x as the standardized explanatory input variable, and ε as error term, for K variables ($k = 1, \ldots, K$), N spatial units ($i = 1, \ldots, N$) and T years ($t = 1, \ldots, T$). Exogenous variables $\boldsymbol{x}$ are specific to each province and crop; all candidate variables are listed in SI Table 1.

In case of autocorrelation and heteroscedasticity of model residuals, which we tested based on the Breusch–Godfrey and the Breusch–Pagan test respectively, we used robust standard errors[47].

Validation. To test the adequacy of our empirical models, we applied two validations:

- Out-of-sample validation: We selected the variables (x in Eq. 1) with the three steps described above based on all observations. Then we subsequently removed observations for 1 year and used the remaining observations to fit the model coefficients for all selected variables (β in Eq. 1) and predict yield anomalies for the removed year.
- Out-of-sample variable selection: We subsequently removed observations for 1 year, then selected variables as described above and estimated the model coefficients based on the remaining data. We used this model to predict yield changes for the removed year. This guarantees that no information from the removed year is used for the variable selection or the model estimation. This validation simulates the operational forecasting context, where no yield information from the year to be forecasted is available for model building.

The goodness of fit between the observed yields and the predicted yields was evaluated based on r^2, which represents the share of explained variance.

Yield forecasting. For the within-season forecast of crop yields, we applied the same pipeline of variable selection, model estimation and model validation as described above, but omitted weather information from the last month before harvest (repro2). The resulting lead time is thus 1 month before the harvest (SI Fig. 8).

Harvest area module. In our study, we compared two types of data availability for harvest areas: fully known and estimated. Data about the harvest areas could be obtained within the season from farmer surveys or satellite imageries. Yet even though this is possible in principle, it might not be available in practice. To still be able to provide a production forecast in an operational context, we tested different options to represent harvest areas based on information from previous years. We tested the following four options: the median harvest area, the median harvest area of the previous 3 (5) years and the trend of the harvest area calculated by a non-

	Maize	Sorghum	Millet
Calories per 100 g in kcal	360	343	340
Median post-harvest loss in %	17	13	11
Bran in %	6	13	14

Table 1. Calories[48], median post-harvest losses per crop[49] and share of bran[48].

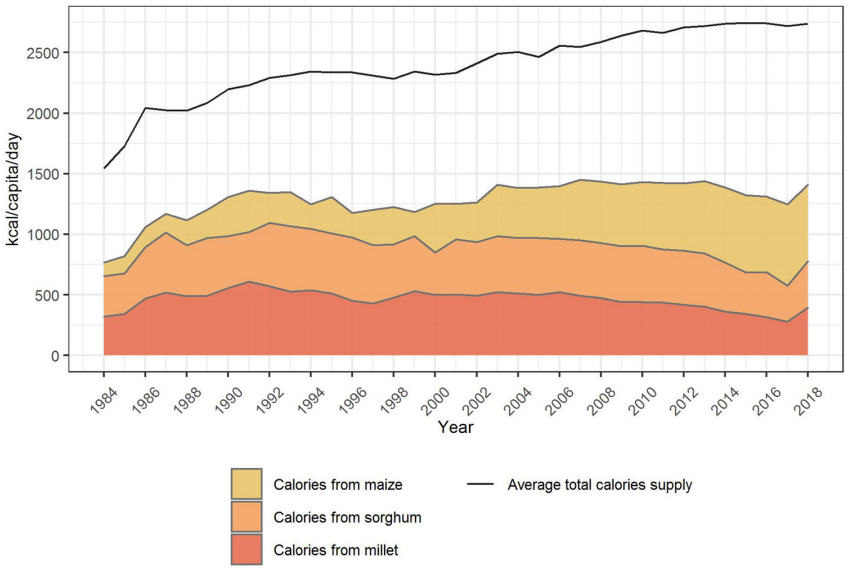

Figure 6. Supplied calories from maize, sorghum and millet and total supplied calories per capita and day in Burkina Faso from 1984 to 2018 in Burkina Faso. The calories supply refers to the total amount of calories available for human food including any commodity derived therefrom as a result of further processing[51]. (source: authors' illustration based on FAO[51] and Roser and Ritchie[52]).

parametric LOESS function with a span of 0.9. We chose the option for calculated harvest area that resulted in the highest correlation (Pearson's *r*) between the observed and the modelled area.

Production forecast module. Production is calculated as yield times harvest area for each crop and province. To obtain total national production of staple crops, province-level production data for maize, sorghum and millet were added up. In the forecasting case, the lead time of the production forecast of all crops together is 1 month before the sorghum and millet harvest (which happens around end of October/begin of November). The maize harvest (end of September/October) has already happened by then; the implications of this are discussed below.

Calories balance module. In the calories balance module, we compare the produced calories with the usually consumed calories from staple crops in Burkina Faso. First, production amounts of maize, sorghum and millet were converted into calories and added up to get the calories production of staple crops on national level, using nutrient information[48] shown in Table 1. Second, we subtracted the share of the bran[48] (Table 1) from the produced calories, which is used for feed in Burkina Faso[24]. Due to post-harvest losses (PHL), not all produced calories are available for food energy uptake. In the last step we therefore subtracted the PHL fraction from the produced calories. We considered the median PHL per crop (Table 1), as annual information about PHL was not sufficiently available. Information about PHL were obtained from Aphlis[49] who account for losses incurring during harvesting, drying, handling operations, household and market level storage and transport.

The total national consumed calories from staple crops in Burkina Faso were obtained by multiplying the calories from staple crops in the diet per day (Fig. 6) with the number of days per year and the total population in Burkina Faso[50] (SI Fig. 4). To account for uncertainties in this estimate, we consider the range between the minimum and the maximum share of calories from maize, sorghum and millet in total supplied calories in the time period from 1984 to 2018 and assume that all seasons fall within this long-term average range.

We only took into account domestically produced calories, deliberately disregarding imports and exports. Given the very low amount of cross-border trade for maize, sorghum and millet in Burkina Faso[5] (SI Fig. 15), we consider domestic production as a good proxy for overall availability.

Received: 20 August 2021; Accepted: 13 January 2022
Published online: 31 January 2022

References

1. Boansi, D., Tambo, J. A. & Müller, M. Intra-seasonal risk of agriculturally-relevant weather extremes in West African Sudan Savanna. *Theor. Appl. Climatol.* **135**, 355–373 (2019).
2. Roudier, P., Sultan, B., Quirion, P. & Berg, A. The impact of future climate change on West African crop yields: What does the recent literature say?. *Glob. Environ. Chang.* **21**, 1073–1083 (2011).
3. Tomalka, J., Lange, S., Röhrig, F. & Gornott, C. Climate Risk Profile: Burkina Faso (2020). https://www.pik-potsdam.de/en/institute/departments/climate-resilience/projects/project-pages/agrica/giz_climate-risk-profile_burkina-faso_en (Accessed 20 Aug 2020).
4. Sultan, B. & Gaetani, M. Agriculture in West Africa in the twenty-first century: Climate change and impacts scenarios, and potential for adaptation. *Front. Plant Sci.* **7**, 1–20 (2016).
5. FAO. FAOSTAT—Suite of Food Security Indicators (2021). http://www.fao.org/faostat/en/#data/FS (Accessed 16 Oct 2020).
6. FAO. GIEWS Country Brief Burkina Faso (FAO, 2020). http://www.fao.org/giews/countrybrief/country/BFA/pdf_archive/BFA_Archive.pdf (Accessed 20 Sept 2020).
7. Liu, L. & Basso, B. Seasonal crop yield forecast: Methods, applications, and accuracies. *Adv. Agron.* **154**, 201–255 (2019).
8. Liu, L. & Basso, B. Linking field survey with crop modeling to forecast maize yield in smallholder farmers' fields in Tanzania. *Food Secur.* **12**, 537–548 (2020).
9. Stone, R. C. & Meinke, H. Operational seasonal forecasting of crop performance. *Philos. Trans.R. Soc. B Biol. Sci.* **360**, 2109–2124 (2005).
10. Jayne, T. S. & Rashid, S. The value of accurate crop production forecasts. https://ageconsearch.umn.edu/record/97032/files/idwp108.pdf (2010). (Accessed 18 Oct 2020)
11. Mishra, A. *et al.* Sorghum yield prediction from seasonal rainfall forecasts in Burkina Faso. *Agric. For. Meteorol.* **148**, 1798–1814 (2008).
12. Zhang, L. *et al.* Using boosted tree regression and artificial neural networks to forecast upland rice yield under climate change in Sahel. *Comput. Electron. Agric.* **166**, 105031 (2019).
13. Leroux, L. *et al.* Maize yield estimation in West Africa from crop process-induced combinations of multi-domain remote sensing indices. *Eur. J. Agron.* **108**, 11–26 (2019).
14. Karst, I. G. *et al.* Estimating yields of household fields in rural subsistence farming systems to study food security in Burkina Faso. *Remote Sens.* **12**, 1–20 (2020).
15. Gross, J., Guirkinger, C. & Platteau, J. P. Buy as you need: Nutrition and food storage imperfections. *J. Dev. Econ.* **144**, 102444 (2020).
16. Morgan, J. D. & Moseley, W. G. The secret is in the sauce: Foraged food and dietary diversity among female farmers in southwestern Burkina Faso. *Can. J. Dev. Stud./Rev. Can. d'études du développement* **41**, 296–313 (2020).
17. Fraval, S. *et al.* Food security in rural Burkina Faso: The importance of consumption of own-farm sourced food versus purchased food. *Agric. Food Secur.* **9**, 1–17 (2020).
18. Tankari, M. R. Rainfall variability and farm households' food insecurity in Burkina Faso: Nonfarm activities as a coping strategy. *Food Secur.* **12**, 567–578 (2020).
19. Somé, J. W. & Jones, A. D. The influence of crop production and socioeconomic factors on seasonal household dietary diversity in Burkina Faso. *PLoS ONE* **13**, 1–16 (2018).
20. Schauberger, B., Gornott, C. & Wechsung, F. Global evaluation of a semiempirical model for yield anomalies and application to within-season yield forecasting. *Glob. Chang. Biol.* **23**, 4750–4764 (2017).
21. Belesova, K. *et al.* Mortality impact of low annual crop yields in a subsistence farming population of Burkina Faso under the current and a 1.5 °C warmer climate in 2100. *Sci. Total Environ.* **691**, 538–548 (2019).
22. Schauberger, B., Jägermeyr, J. & Gornott, C. A systematic review of local to regional yield forecasting approaches and frequently used data resources. *Eur. J. Agron.* **120**, 126153 (2020).
23. FEWS NET. About Us (2020). https://fews.net/about-us (Accessed 16 Oct 2020).
24. FAO. FAOSTAT—Supply Utilization Accounts (2021). http://www.fao.org/faostat/en/#data/SCL. (Accessed 11 Aug 2021)
25. Colen, L. *et al.* Income elasticities for food, calories and nutrients across Africa: A meta-analysis. *Food Policy* **77**, 116–132 (2018).
26. Schmidhuber, J. & Tubiello, F. N. Global food security under climate change. *Proc. Natl. Acad. Sci. USA.* **104**, 19703–19708 (2007).
27. Reij, C., Tappan, G. & Belemvire, A. Changing land management practices and vegetation on the Central Plateau of Burkina Faso (1968–2002). *J. Arid Environ.* **63**, 642–659 (2005).
28. FAO. FAOSTAT - Land Use Indicators (2020). http://www.fao.org/faostat/en/#data/EL. (Accessed 16 Oct 2020).
29. Foley, J. A. *et al.* Solutions for a cultivated planet. *Nature* **478**, 337–342 (2011).
30. Riesgo, P. A. & Gomez, L. *Sustainable Agricultural Practices and Their Adoption in Sub-Saharan Africa—A Selected Review* (2020).https://doi.org/10.2760/360761.
31. Piñeiro, V. *et al.* A scoping review on incentives for adoption of sustainable agricultural practices and their outcomes. *Nat. Sustain.* **3**, 809–820 (2020).
32. Van Ittersum, M. K. *et al.* Yield gap analysis with local to global relevance—A review. *Food Crop. Res.* **143**, 4–17 (2013).
33. Ray, D. K., Mueller, N. D., West, P. C. & Foley, J. A. Yield trends are insufficient to double global crop production by 2050. *PLoS ONE* **8**, e66428 (2013).
34. R Core Team. R: A language and environment for statistical computing. http://www.r-project.org/ (2021).
35. Ministère de l'Agriculture et des Aménagements Hydroagricoles/Direction Générale des Etudes et des Statistiques Sectorielles. *Données officielles de l'Enquête Permanente Agricole (EPA).* (2020).
36. Funk, C. *et al.* The climate hazards infrared precipitation with stations—A new environmental record for monitoring extremes. *Sci. Data* **2**, 1–21 (2015).
37. Beck, H. E. *et al.* Global-scale evaluation of 22 precipitation datasets using gauge observations and hydrological modeling. In *Satellite Precipitation Measurement Advances in Global Change Researc* (eds Levizzani, V. *et al.*) 625–653 (Springer, 2020). https://doi.org/10.1007/978-3-030-35798-6_9.
38. Copernicus Climate Change Service. ERA5: Fifth generation of ECMWF atmospheric reanalyses of the global climate (2017). https://cds.climate.copernicus.eu/cdsapp#!/home (Accessed 19 Dec 2019).
39. Gleixner, S., Demissie, T. & Diro, G. T. Did ERA5 improve temperature and precipitation reanalysis over East Africa?. *Atmosphere* **11**, 996 (2020).

40. Allen, R. G., Pereira, L. S., Raes, D. & Smith, M. *Crop evapotranspiration—Guidelines for computing crop water requirements—FAO Irrigation and drainage paper 56*. (1998).
41. Yuan, W. *et al.* Increased atmospheric vapor pressure deficit reduces global vegetation growth. *Sci. Adv.* **5**, 1–12 (2019).
42. FAO. Crop calendar—An information tool for seed security (2010). http://www.fao.org/agriculture/seed/cropcalendar/welcome.do;jsessionid=5FD03BC73666DEC13FB1C963D67932C9 (Accessed 3 July 2020).
43. Barnabás, B., Jäger, K. & Fehér, A. The effect of drought and heat stress on reproductive processes in cereals. *Plant Cell Environ.* **31**, 11–38 (2008).
44. Wooldridge, J. M. *Introductory Econometrics A Modern Approach* (Cenage Learning, 2014).
45. Tibshirani, R. Regression shrinkage and selection via the lasso. *J. R. Stat. Soc. Ser. B* **58**, 267–288 (1996).
46. Gornott, C. & Wechsung, F. Statistical regression models for assessing climate impacts on crop yields: A validation study for winter wheat and silage maize in Germany. *Agric. For. Meteorol.* **217**, 89–100 (2016).
47. Zeileis, A. Econometric computing with HC and HAC covariance matrix estimators. *J. Stat. Softw.* **11**, 128–129 (2004).
48. FAO. *Food Composition Tables for International Use* (1953).
49. Aphlis. Dry weight loss: Burkina Faso—All crops—All years (2020). https://www.aphlis.net/en/page/20/data-tables#/datatables?tab=dry_weight_losses&metric=prc&country=93&province=0 (Accessed 3 July 2020).
50. World Bank. Population, total (2020). https://data.worldbank.org/indicator/SP.POP.TOTL?locations=BF (Accessed 3 July 2020).
51. FAO. FAOSTAT—Food Supply—Crops Primary Equivalent (2021). http://www.fao.org/faostat/en/#data/CC. (Accessed 11 Aug 2021)
52. Roser, M. & Ritchie, H. Food Supply (2013). https://ourworldindata.org/food-supply (Accessed 3 July 2020).

Author contributions

R.L., C.G. and B.S. designed the research. R.L. performed the analysis and wrote the manuscript with contributions from C.G. and B.S. C.G. initiated the research. J.W. reviewed the dietary energy balance approach and contributed to the interpretation of the results. All authors reviewed the manuscript.

Funding

Open Access funding enabled and organized by Projekt DEAL. This work has been funded by the Agrica, the CC&H PI3 and the ClimSec project. Agrica is financed by the Deutsche Gesellschaft für Internationale Zusammenarbeit (GIZ) GmbH on behalf of the German Federal Foreign Office and Federal Ministry for Economic Cooperation and Development (BMZ). CC&H PI3 is financed by the German Research Foundation (DFG). ClimSec is financed by the German Federal Foreign Office.

Competing interests

The authors declare no competing interests.

Additional information

Supplementary Information The online version contains supplementary material available at https://doi.org/10.1038/s41598-022-05561-9.

Correspondence and requests for materials should be addressed to R.L.

Reprints and permissions information is available at www.nature.com/reprints.

Publisher's note Springer Nature remains neutral with regard to jurisdictional claims in published maps and institutional affiliations.

3 Discussion

In the first study, we assessed the influence of weather on starchy maize yields on the regional and the local scale in Peru. Three different statistical approaches were used: a linear regression model, a linear panel data model and the machine learning algorithm decision tree. Weather-yield relations for starchy maize on the regional level reflect the complex Peruvian climate as shown by the selected weather variables of the linear regression model in different regions on the coast (costa), the Andean highlands (sierra) and the Amazon rainforest (selva). The analysis on the local level was based on a panel data model and a decision tree and revealed similar weather-influences on maize yields, which validates the robustness of the obtained results. As suggested by the Peruvian *Nationally Determined Contributions* to adapt to climate change, we assessed the effect of higher water availability on starchy maize yields based on the linear regression model. The analysis showed regionally different effects on starchy maize yields, which highlights the importance to develop adaptation options at the sub-national scale.

The second study provides a within-season forecast for maize yields on the sub-national scale six weeks before the harvest for Tanzania. Despite the limited availability of only ten years of yield data, the forecast shows a high and robust performance (i.e. median NSE of 0.72 in the out-of-sample validation). We found that particularly extreme weather conditions, i.e. consecutive dry days, high precipitation events and minimum temperatures, have a strong impact on maize yields in Tanzania. The inclusion of the sea surface temperature in the West Pacific as an additional predictor improves the performance and could be used to extend the lead time of the forecast. We utilize a rigorous and transparent two-level validation to mimic the situation in operational practice when the model has to be trained purely on past data. Furthermore, we tested the robustness by providing a completely independent forecast for the harvest year 2019.

The third study provides a within-season forecast of crop production for the staples maize, sorghum and millet one month before the harvest in Burkina Faso based on a rigorous validation. The persistent trend in harvest areas in Burkina Faso contributes to the high skill of the production forecast (i.e. $r^2 > 0.76$). This underlines the high potential this information would have for production forecasts – if detected within the season, e.g. through farmer surveys or remote sensing. Moreover, we compared the produced calories from maize, sorghum and millet with the historic demand allowing us to provide early information on shortages in domestic cereal production. Results show that despite the surplus of produced calories on the national level, a high level of food insecurity prevails for large parts of the Burkinabe population. We recommend a comprehensive assessment of all dimensions of food security considering the seasonal, spatial and group-specific distribution of food within the country.

The following sub-chapters provide a synthesis of the main findings across all three publications (chapter 3.1) and open research questions (3.2).

3.1 Main findings across publications

The three publications present novel statistical crop modelling approaches for maize on the sub-national scale in Peru, Tanzania and Burkina Faso covering the whole country. Previous assessments focused either on single regions within these countries, i.e. Liu & Basso (2020) in Tanzania and Karst et al. (2020) in Burkina Faso, or on the wider region, e.g. Ogutu et al. (2018) for East Africa or Leroux et al. (2019) for West Africa. The statistical crop modelling approach applied in the three studies for Peru, Tanzania and Burkina Faso is potentially transferrable to other countries for two reasons. First,

it relies on globally available climate data and second, it provides robust results even in case of limited yield data availability which can often be found in data-scare regions in the Global South.

The crop yield models can explain a substantial part of crop yield variability based on weather influences. The median performance of the sub-national maize yield models measured in NSE (Nash-Sutcliffe model efficiency coefficient) is 0.55 in Peru, 0.81 in Tanzania and 0.58 in Burkina Faso based on the out-of-sample validation. This indicates a strong sensitivity of maize yield anomalies to weather influences in these countries. In addition to maize, the study for Burkina Faso also included a crop model for sorghum (NSE = 0.34) and millet (NSE = 0.64). The lower performance of the sorghum crop model in Burkina Faso could be related to reliability issues in the sorghum data. The studies underline the importance of spatially-distinct crop models with distinct variables and model parameters to take account of the diverse and complex yield influencing weather characteristics within the countries.

Apart from weather-yield relations, the three studies discussed other influences on the crop model performance. In paper two and three, we found that the persistent trend in yields had high explanatory power for the prediction of absolute yields – leading to a higher forecasting skill for absolute yields than for yield anomalies. In paper three, we found that having information about acreage within the season resulted in a highly accurate within-season production forecast (i.e. $r^2 > 0.92$). This information could be obtained through farmer surveys or remote sensing and has – as our results suggest – high practical relevance for accurate production forecasts in practice.

In contrast to most statistical crop forecasts that rely on either estimation and/or out-of-sample validation results (Schauberger et al., 2020), our second and third publications applied an out-of-sample variable selection. This rigorous validation technique mimics the operational context in which no information from the current year influences model formation or variable selection. We are not aware of previous statistical crop modelling studies that used this validation technique. Recently, Meroni et al. (2021) and Dinh & Aires (2021) presented examples of validation approaches based on the same principle, which they refer to as the nested leave-one-year-out cross-validation and the nested leave-two-out cross-validation respectively. In the first paper, we also focused on rigorous validation by applying two independent models - a machine learning algorithm and a linear panel data model - to test the validity of the variable selection. A rigorous validation is particularly important when the model results are potentially being used to inform adaptation planning (in case of the first publication) or early warning systems on food security (in case of publications two and three). Prediction inaccuracies in these cases could potentially have severe consequences for the livelihoods and food security of people.

The three studies emphasize the importance of integrating crop model results with other sources of information to comprehensively inform climate risk management and adaptation. Our first study illustrates how a statistical crop model can assess the effect of an adaptation option on yields. However, the development and design of adaptation strategies that take account of inter-sectoral aspects (Pardoe et al., 2018) as well as synergies and trade-offs between different options (Palm et al., 2010) need to be done jointly with local stakeholders (Goosen et al., 2014). Similarly, the forecasts provided in study two and three should be embedded in a forecasting system that integrates other sources of information, such as local knowledge. Factors that the model does not explicitly account for, such as changes in the occurrence of pests and diseases, need to be identified by local experts as they can negatively influence the reliability of the model. An example is the

outbreak of the fall armyworm in 2019 in East Africa with detrimental consequences for agricultural production, particularly in the Northern regions and coastal areas in Tanzania, for which the models show weak performances. Additionally, changes in the economic, social or political environment need to be identified to safeguard against inaccurate predictions.

3.2 Outlook

The following sub-chapters discuss open research questions concerning model improvements (3.2.1 to 3.2.3) and integration with other information for comprehensive assessments of food security (3.2.4) and climate adaptation (3.2.5).

3.2.1 Comparing observed planting and harvest dates with calculated ones to improve the accuracy of growing season data

In tropical and rainfed agricultural systems, the planting date is aligned with the onset of the rains. Therefore, farmers need information on the onset of the rains to decide about the optimal planting date. Both early planting (reduced germination of seeds) and late planting (lower water availability at the end of the growing season) could negatively affect yields (Krell et al., 2022) and thus the food availability of subsistence farmers. Having accurate growing season data is also crucial for crop modelling to better capture growing season-specific weather influences and key phenological phases (Schauberger et al., 2020). In contrast to static crop calendars, e.g. provided by the FAO (FAO, 2010), a dynamic crop calendar takes account of year-to-year variations at the beginning and the end of the growing season. Using a dynamic crop calendar has the potential to improve the model performance because yield-influencing weather conditions of the growing season can be more accurately represented. This is particularly relevant in regions with strong year-to-year variations in the onset of the rains, like in our study areas in East Africa (Wenhaji Ndomeni et al., 2018) and West Africa (Paeth & Hense, 2004).

Different approaches exist to calculate the onset of the growing season based on rainfall characteristics (e.g. Dodd & Jolliffe, 2001; Laux et al., 2008; Stern et al., 1981) to obtain a dynamic crop calendar. These approaches define the onset of the growing season as the time when a sufficient amount of rain occurred over a defined period without the interruption by a dry spell. Even though the approach of Dodd & Jolliffe (2001) is considered suitable for semi-arid tropical conditions, we could not verify whether the specific criteria (i.e. precipitation amount, number of wet days, length of dry spell) match the local conditions and take account of the diverse climatic conditions within the study areas. For this purpose, observational data derived from survey data or satellite imageries should be used to compare the observed planting dates with the calculated ones. This way, thresholds of the criteria that define the beginning of the growing season could be optimised for specific climate zones. Additionally, the length of the growing season could be determined based on crop-specific observed harvest dates. The comparison could also provide insights on how closely the time of planting is aligned with the onset of the rains. A strong discrepancy could indicate that apart from rain, other factors might influence the decision on the planting time.

3.2.2 Analysing the implications of different spatial scales on model performance

Statistical crop modelling is often done at the spatial level of political boundaries due to input data availability and possible applications of crop model results. Official yield statistics, which are often used as input data for crop models, are reported on administrative levels and thus determine the spatial scale of the crop model. Moreover, for the purpose of informing decision-making, model outputs should be provided at the level at which decision-making takes place. For example, production forecasts at a national scale can contribute to increased food security by supporting

governments in adjusting imports, exports and trading prices (Delincé, 2017), whereas yield forecasts at the local level can inform management decisions, e.g. concerning cultivar selection or planting date (Zinyengere et al., 2011). However, administrative boundaries do not necessarily follow climatic and/or growing conditions with potentially negative implications for statistical inference. Diverging crop-weather influences within one administrative unit, e.g. due to differences in soil or management practices, can lead to biased parameter estimates and/or lower precision, and thus lower predictive model skill. Despite statistical remedies for clustered data, such as using fixed-effects models (Wooldridge, 2014), the problem arises if clusters are unknown.

This dissertation used statistical crop models at different spatial levels - from local to sub-national to national scales. We found that spatially distinct variables and parameters could better represent the diverse climatic conditions within the countries, particularly in Peru and Tanzania. The question is whether setting up the model on higher resolutions (if data was available) would have improved model performance. On the other hand, the aggregation of input data to lower resolutions can also be beneficial in contexts where data quality is suspected to be low, as independent errors are levelled out (Gornott & Wechsung, 2016). Future research should therefore systematically analyse how setting up the model on different spatial scales influences model performance. For this purpose, different administrative levels and nature-based boundaries, such as agro-ecological or agro-climatic zones, should be tested alongside different aggregation methods (Ewert et al., 2011). Moreover, clusters of similar management characteristics and growing conditions should be identified via statistical clustering techniques to derive the context-specific optimal spatial scale for statistical crop modelling. This analysis can make the trade-off between resolution and model accuracy transparent, which can direct potential applications of statistical crop models.

3.2.3 Using interpretable and causal machine learning to improve the accuracy and usability of predictions in an operational context

Machine learning has proven high predictive power in many applications, including yield forecasting (e.g. Cai et al., 2019; Meroni et al., 2021; Wolanin et al., 2020) and has the advantage of capturing complex and non-linear interactions. Although machine learning algorithms do not necessarily outperform regression models (Johnson et al., 2016), they should be used in addition to such models to provide a suite of different modelling approaches. Deriving ensemble means or medians from multiple crop models often outperform single models (Fleisher et al., 2017; Iizumi et al., 2018; B. Liu et al., 2016) if errors in different models are independent (Lobell & Asseng, 2017). Algorithms, such as random forest, neural networks, gradient boosting and support vector machines, should be tested for their suitability to accurately forecast yield within the growing season. While yield statistics are often only available for a short time period, particularly in the Global South, Meroni et al. (2021) show that machine learning algorithms can still be applied if validation is performed rigorously as proven in our second and third publications.

Special focus should be placed on increasing the interpretability of predictions by explaining either general or causal relationships of the model. In the second publication of this dissertation, the interpretability of forecasts was facilitated by comparing and interpreting standardized model coefficients of linear regression models. Especially in complex linear models with several predictors, the interpretation of results becomes increasingly difficult. Further research should therefore expand on facilitating the interpretability of yield forecasts obtained by complex linear regression models and/or machine learning. Model-agnostic methods, such as visualization techniques of feature importance or the use of Shapley Values are independent of the applied model, which facilitates the comparability of different modelling approaches. Additionally, ad hoc methods should be used for

specific models, such as tools to uncover features learned in hidden layers in neural networks (Molnar, 2022). Detecting causal relations in machine learning helps to understand cause-effect connections and offers explanations for the reasons behind predictions. This can be realised through different tools, such as causal modelling tools and causal diagrams, which go beyond the identification of associations between variables and provide answers to counterfactual questions (Pearl, 2019). Improving the interpretability and explaining causal relationships can, in practice, enhance the uptake of a yield forecast as it builds trust in the model performance based on domain expertise. Moreover, it helps to identify possible errors and biases in the prediction and thus can improve the model performance, e.g. a model that is accurate for wrong reasons can be identified (Murdoch et al., 2019).

3.2.4 Analysing all dimensions of food security by integrating weather-driven crop yield models with survey data

The literature on the impacts of climate change on food security predominantly focuses on food availability and particularly food production (Davis et al., 2021; Wheeler & von Braun, 2013). However, our third study suggests that the other dimensions of food security - namely food access, utilization and stability – strongly influence the food security situation in Burkina Faso so that despite a surplus of produced calories from staples, a high degree of food insecurity prevails for large parts of the population. Similar results were found by Lewis (2017) for Ethiopia where high crop production on the national level also did not lead to a reduction in food insecurity. These findings align with Schmidhuber & Tubiello (2007) who conclude that the socio-economic environment in which climate change evolves is more relevant to food security than the expected biophysical changes due to climate change. Myers et al. (2017) highlight that next to immediate biological effects (such as crop yield losses), socio-economic factors, such as price increases and income effects, are also related to sharp declines in access to food and thus food security, especially for the global poor. Integrating all dimensions of food security is therefore needed to comprehensively understand the complex underlying causes of food insecurity and to potentially make predictions for the food security status of a population.

For this purpose, the weather-driven statistical crop modelling approaches should be linked with household survey data to better understand the complex interplay of climatic and socio-economic factors that influence food and nutrition security. Therefore, variables related to food availability (e.g. quantify of produced food), food access (e.g. price of agricultural commodities and access to markets), food utilization (e.g. dietary diversity, availability of safe drinking water, state of health) and food stability (e.g. political conflicts, unrest) should be included to represent all pillars of food security (FAO et al., 2021). In addition, nutrition security should be integrated, which goes beyond food security by considering not only the amount of calories produced, accessed and consumed but also the nutrients it contains (Ingram, 2020). Particularly, the provision of micronutrients, such as iodine, vitamin A and iron should be considered as they have high relevance for global health and development in low-income countries (Han et al., 2022). The integration of different data sources could be achieved by setting up a Bayesian Belief Network (BBN). This machine learning technique provides a graphical representation of the probabilistic dependencies and independencies in a system, where each variable has the potential to have a direct (probabilistic) relationship with any other variable in the network (Eyre et al., 2021). Based on the BBN, interactions between weather and socio-economic factors that contribute to food and nutrition (in)security and different scenarios for future developments can be analysed. Additionally, sensitivity tests allow the identification of

factors with the highest probabilistic impacts on food and nutrition security and possible interventions can be simulated. The latter can inform adaptation policies and direct interventions where they are most needed.

3.2.5 Comprehensively assessing adaptation options by integrating local knowledge

Existing crop modelling efforts that assess climate adaptation strongly focus on the impacts of on-farm management practices on agricultural outcomes. Especially, changes in planting dates, irrigation, crop cultivar and fertilizer have been studied extensively with crop models as agricultural adaptation strategies (Challinor et al., 2018). The adaptation potential of existing on-farm management practices to reduce yield losses was found to be on average 8 % in mid-century and 11 % in end-century. This is insufficient to compensate for the projected yield losses from climate change, particularly in currently warmer regions (Hasegawa et al., 2022), such as the tropics. However, these studies usually do not account for technological developments and agricultural intensification, which happen regardless of adaptation. This leads to a systematic underestimation of projected yields (Lobell, 2014). Furthermore, the adaptation options currently reflected in crop modelling studies do not reflect the breadth of available options found in practice, which range from on-farm management practices to transformational changes, including the shift to other cropping areas, crops or production systems (Vermeulen et al., 2018). This is particularly problematic in smallholder farming systems in the tropics where crop diversification and intercropping are common but remain underrepresented in model-based adaptation research (Claessens et al., 2012).

Alongside crop model improvements (e.g. focusing on other crops than wheat, maize, soybean and rice; integrating mixed farming systems and agro-forestry), integrated assessment models (Ewert et al., 2015) should be further developed. Moreover, crop modelling efforts should be integrated with bottom-up adaptation approaches, i.e. qualitative research including focus group discussions and interviews. These approaches can provide local information to support adaptation planning, such as context or site-specific information on livelihoods, culture, constraints and opportunities of adaptation (Beveridge et al., 2018). Whereas crop models can quantify yield changes related to specific adaptation options, they can neither assess impacts on the farming or food system nor on other potentially influenced sectors. Therefore, adaptation strategies need to be designed together with local stakeholders and experts. This is crucial to consider inter-sectoral aspects (Rosenzweig et al., 2017), e.g. related to food, water and energy (Pardoe et al., 2018), as well as synergies and trade-offs between different adaptation options (Palm et al., 2010) and adaptation and mitigation (Thornton & Comberti, 2017).

4 Concluding remarks and personal hopes

This dissertation aims to contribute to a deeper understanding of weather-yield relations in the tropics and how these findings can inform climate risk management and adaptation in one of the most vulnerable regions to climate change. Whereas adaptation efforts will inevitably be necessary to protect us from negative impacts of global warming, the primary goal is to mitigate climate change. This requires quick action, as the newest IPCC Assessment Report 6 concludes. Global greenhouse gas emissions need to go down from 2025 onwards so that limiting warming to 1.5 °C remains possible (IPCC, 2022). With every ton of CO_2 avoided, fewer people will face the negative consequences of global warming on food and nutrition security. However, climate change is just one of many drivers behind recent setbacks in global food security as recent developments demonstrate. The war in Ukraine increases food prices, particularly for wheat with detrimental consequences for food availability in the Global South (FAO, 2022). The corona pandemic provides another example, showing how the disruption of food supply chains affects the accessibility of food worldwide (Béné et al., 2021). Given the complex nature of food insecurity, solutions will have to be manifold and require vast transformational efforts, including insights from science. This dissertation is an attempt towards improving the predictability of food and nutrition security based on scientific approaches.

At the end of this dissertation, I would like to quote my father: “The relevant question is not whether something is good, as this question is impossible to answer. The question is whether it contributes to something better.” (inspired by Kelson, 2016 and Rawls, 1979). With this dissertation, I hope I have contributed to something better. Maybe these results and my future research endeavours can add one more piece of the puzzle towards improving early warning systems on food insecurity. Using these and similar research approaches to support real-world solutions will require more steps that go beyond the sphere of science. Reaching the last mile will require making the results useable for local stakeholders and integrating them with other relevant information (Goosen et al., 2014) so that it can enable better decisions.

5 References

Aggarwal, P. K., Kalra, N., Chander, S., & Pathak, H. (2006). InfoCrop: A dynamic simulation model for the assessment of crop yields, losses due to pests, and environmental impact of agro-ecosystems in tropical environments. I. Model description. *Agricultural Systems*, *89*(1), 1–25. https://doi.org/10.1016/j.agsy.2005.08.001

Aggarwal, P. K., Vyas, S., Thornton, P., & Campbell, B. (2019). How much does climate change add to the challenge of feeding the planet this century? *Environmental Research Letters*, *14*(4), 1–10. https://doi.org/10.1088/1748-9326/aafa3e

Arce, C. E., & Caballero, J. (2015). *Tanzania - Agricultural Sector Risk Assessment*. https://openknowledge.worldbank.org/bitstream/handle/10986/22277/Tanzania000Agr0ctor0risk0assessment.pdf?sequence=5&isAllowed=y

Bebber, D. P. (2015). Range-Expanding Pests and Pathogens in a Warming World. *Annual Review of Phytopathology*, *53*(1), 335–356. https://doi.org/10.1146/annurev-phyto-080614-120207

Begum, R. A., Lemper, R., Ali, E., Benjaminsen, T. A., Bernauer, T., Cramer, W., Cui, X., Mach, K., Nagy, G., Stenseth, N. C., Sukumar, R., & Wester, P. (2022). Point of Departure and Key Concepts. In H.-O. Pörtner, D. C. Roberts, M. Tignor, E. S. Poloczanska, K. Mintenbeck, A. Alegría, M. Craig, S. Langsdorf, S. Löschke, V. Möller, A. Okem, & B. Rama (Eds.), *Climate Change 2022: Impacts, Adaptation, and Vulnerability. Contribution of Working Group II to the Sixth Assessment Report of the Intergovernmental Panel on Climate Change*. Cambridge University Press. In Press.

Béné, C., Bakker, D., Chavarro, M. J., Even, B., Melo, J., & Sonneveld, A. (2021). Global assessment of the impacts of COVID-19 on food security. *Global Food Security*, *31*, 2–9. https://doi.org/10.1016/j.gfs.2021.100575

Berrang-Ford, L., Siders, A. R., Lesnikowski, A., Fischer, A. P., Callaghan, M. W., Haddaway, N. R., Mach, K. J., Araos, M., Shah, M. A. R., Wannewitz, M., Doshi, D., Leiter, T., Matavel, C., Musah-Surugu, J. I., Wong-Parodi, G., Antwi-Agyei, P., Ajibade, I., Chauhan, N., Kakenmaster, W., … Abu, T. Z. (2021). A systematic global stocktake of evidence on human adaptation to climate change. *Nature Climate Change*, *11*(11), 989–1000. https://doi.org/10.1038/s41558-021-01170-y

Beveridge, L., Whitfield, S., & Challinor, A. (2018). Crop modelling: towards locally relevant and climate-informed adaptation. *Climatic Change*, *147*(3–4), 475–489. https://doi.org/10.1007/s10584-018-2160-z

Brás, T. A., Seixas, J., Carvalhais, N., & Jägermeyr, J. (2021). Severity of drought and heatwave crop losses tripled over the last five decades in Europe. *Environmental Research Letters*, *16*(6), 1–13. https://doi.org/10.1088/1748-9326/abf004

Cai, Y., Guan, K., Lobell, D., Potgieter, A. B., Wang, S., Peng, J., Xu, T., Asseng, S., Zhang, Y., You, L., & Peng, B. (2019). Integrating satellite and climate data to predict wheat yield in Australia using machine learning approaches. *Agricultural and Forest Meteorology*, *274*, 144–159. https://doi.org/10.1016/j.agrformet.2019.03.010

Cassidy, E. S., West, P. C., Gerber, J. S., & Foley, J. A. (2013). Redefining agricultural yields: From tonnes to people nourished per hectare. *Environmental Research Letters*, *8*(3), 1–8. https://doi.org/10.1088/1748-9326/8/3/034015

Challinor, A. J., Müller, C., Asseng, S., Deva, C., Nicklin, K. J., Wallach, D., Vanuytrecht, E., Whitfield, S., Ramirez-Villegas, J., & Koehler, A. K. (2018). Improving the use of crop models for risk assessment and climate change adaptation. *Agricultural Systems*, *159*, 296–306. https://doi.org/10.1016/j.agsy.2017.07.010

Chemura, A., Schauberger, B., & Gornott, C. (2020). Impacts of climate change on agro-climatic suitability of major food crops in Ghana. *PLoS ONE*, *15*(6), 1–21. https://doi.org/10.1371/journal.pone.0229881

Choularton, R. J., & Krishnamurthy, P. K. (2019). How accurate is food security early warning? Evaluation of FEWS net accuracy in Ethiopia. *Food Security*, *11*(2), 333–344. https://doi.org/10.1007/s12571-019-00909-y

Claessens, L., Antle, J. M., Stoorvogel, J. J., Valdivia, R. O., Thornton, P. K., & Herrero, M. (2012). A method for evaluating climate change adaptation strategies for small-scale farmers using survey, experimental and modeled data. *Agricultural Systems*, *111*, 85–95. https://doi.org/10.1016/j.agsy.2012.05.003

Cottrell, R. S., Nash, K. L., Halpern, B. S., Remenyi, T. A., Corney, S. P., Fleming, A., Fulton, E. A., Hornborg, S., Johne, A., Watson, R. A., & Blanchard, J. L. (2019). Food production shocks across land and sea. *Nature Sustainability*, *2*(2), 130–137. https://doi.org/10.1038/s41893-018-0210-1

Davis, K. F., Downs, S., & Gephart, J. A. (2021). Towards food supply chain resilience to environmental shocks. *Nature Food*, *2*(1), 54–65. https://doi.org/10.1038/s43016-020-00196-3

Delincé, J. (2017). *Recent practices and advances for AMIS crop yield forecasting at farm/parcel level: A review*. https://www.fao.org/3/i7339e/i7339e.pdf

Dinh, T. L. A., & Aires, F. (2021). Using the leave-two-out method to determine the optimal statistical crop model. *Geoscientific Model Development Discussions*, 1–23. https://doi.org/10.5194/gmd-2021-218

Dodd, D. E. S., & Jolliffe, I. T. (2001). Early detection of the start of the wet season in semiarid tropical climates of Western Africa. *International Journal of Climatology*, *21*(10), 1251–1262. https://doi.org/10.1002/joc.640

Donatti, C. I., Harvey, C. A., Martinez-Rodriguez, M. R., Vignola, R., & Rodriguez, C. M. (2019). Vulnerability of smallholder farmers to climate change in Central America and Mexico: current knowledge and research gaps. *Climate and Development*, *11*(3), 264–286. https://doi.org/10.1080/17565529.2018.1442796

Ensor, J. E., Park, S. E., Attwood, S. J., Kaminski, A. M., & Johnson, J. E. (2018). Can community-based adaptation increase resilience? *Climate and Development*, *10*(2), 134–151. https://doi.org/10.1080/17565529.2016.1223595

Ewert, F., Rötter, R. P., Bindi, M., Webber, H., Trnka, M., Kersebaum, K. C., Olesen, J. E., van Ittersum, M. K., Janssen, S., Rivington, M., Semenov, M. A., Wallach, D., Porter, J. R., Stewart, D., Verhagen, J., Gaiser, T., Palosuo, T., Tao, F., Nendel, C., … Asseng, S. (2015). Crop modelling for integrated assessment of risk to food production from climate change. *Environmental Modelling and Software*, *72*, 287–303. https://doi.org/10.1016/j.envsoft.2014.12.003

Ewert, F., van Ittersum, M. K., Heckelei, T., Therond, O., Bezlepkina, I., & Andersen, E. (2011). Scale changes and model linking methods for integrated assessment of agri-environmental systems.

Agriculture, Ecosystems and Environment, *142*(1–2), 6–17. https://doi.org/10.1016/j.agee.2011.05.016

Eyre, R. W., House, T., Xavier Gómez-Olivé, F., & Griffiths, F. E. (2021). Bayesian belief network modelling of household food security in rural South Africa. *BMC Public Health*, *21*(1), 1–16. https://doi.org/10.1186/s12889-021-10938-y

FAO. (2010). *Crop Calendar - An Information Tool for Crop Production*. https://cropcalendar.apps.fao.org/#/home

FAO. (2015). *AQUASTAT Profil de Pays – Burkina Faso*. https://www.fao.org/3/I9864FR/i9864fr.pdf

FAO. (2018). *Suite of Food Security Indicators*. https://www.fao.org/faostat/en/#data/FS

FAO. (2020). *Crops and livestock products*. https://www.fao.org/faostat/en/#data/QCL

FAO. (2022). *Information Note: The importance of Ukraine and the Russian Federation for global agricultural markets and the risks associated with the current conflict - 25 March 2022 Update*. https://www.fao.org/3/cb9236en/cb9236en.pdf

FAO, IFAD, UNICEF, WFP, & WHO. (2021). *The State of Food Security and Nutrition in the World 2021*. https://doi.org/10.4060/cb4474en

Fleisher, D. H., Condori, B., Quiroz, R., Alva, A., Asseng, S., Barreda, C., Bindi, M., Boote, K. J., Ferrise, R., Franke, A. C., Govindakrishnan, P. M., Harahagazwe, D., Hoogenboom, G., Naresh Kumar, S., Merante, P., Nendel, C., Olesen, J. E., Parker, P. S., Raes, D., … Woli, P. (2017). A potato model intercomparison across varying climates and productivity levels. *Global Change Biology*, *23*(3), 1258–1281. https://doi.org/10.1111/gcb.13411

Foley, J. A., Ramankutty, N., Brauman, K. A., Cassidy, E. S., Gerber, J. S., Johnston, M., Mueller, N. D., O'Connell, C., Ray, D. K., West, P. C., Balzer, C., Bennett, E. M., Carpenter, S. R., Hill, J., Monfreda, C., Polasky, S., Rockström, J., Sheehan, J., Siebert, S., … Zaks, D. P. M. (2011). Solutions for a cultivated planet. *Nature*, *478*(7369), 337–342. https://doi.org/10.1038/nature10452

Gibbs, H. K., Ruesch, A. S., Achard, F., Clayton, M. K., Holmgren, P., Ramankutty, N., & Foley, J. A. (2010). Tropical forests were the primary sources of new agricultural land in the 1980s and 1990s. *Proceedings of the National Academy of Sciences of the United States of America*, *107*(38), 16732–16737. https://doi.org/10.1073/pnas.0910275107

Goosen, H., de Groot-Reichwein, M. A. M., Masselink, L., Koekoek, A., Swart, R., Bessembinder, J., Witte, J. M. P., Stuyt, L., Blom-Zandstra, G., & Immerzeel, W. (2014). Climate Adaptation Services for the Netherlands: An operational approach to support spatial adaptation planning. *Regional Environmental Change*, *14*(3), 1035–1048. https://doi.org/10.1007/s10113-013-0513-8

Gornott, C., & Wechsung, F. (2016). Statistical regression models for assessing climate impacts on crop yields: A validation study for winter wheat and silage maize in Germany. *Agricultural and Forest Meteorology*, *217*, 89–100. https://doi.org/10.1016/j.agrformet.2015.10.005

Gustavsson, J., Cederberg, C., & Sonesson, U. (2011). *Global food losses and food waste - Extent, causes and prevention*. https://www.fao.org/3/mb060e/mb060e.pdf

Han, X., Ding, S., Lu, J., & Li, Y. (2022). Global, regional, and national burdens of common micronutrient deficiencies from 1990 to 2019: A secondary trend analysis based on the Global

Burden of Disease 2019 study. *EClinicalMedicine*, *44*, 1–12. https://doi.org/https://doi.org/10.1016/j.eclinm.2022.101299

Harvey, C. A., Chacón, M., Donatti, C. I., Garen, E., Hannah, L., Andrade, A., Bede, L., Brown, D., Calle, A., Chará, J., Clement, C., Gray, E., Hoang, M. H., Minang, P., Rodríguez, A. M., Seeberg-Elverfeldt, C., Semroc, B., Shames, S., Smukler, S., … Wollenberg, E. (2014). Climate-Smart Landscapes: Opportunities and Challenges for Integrating Adaptation and Mitigation in Tropical Agriculture. *Conservation Letters*, *7*(2), 77–90. https://doi.org/10.1111/conl.12066

Hasegawa, T., Wakatsuki, H., Ju, H., Vyas, S., Nelson, G. C., Farrell, A., Deryng, D., Meza, F., & Makowski, D. (2022). A global dataset for the projected impacts of climate change on four major crops. *Scientific Data*, *9*(58), 1–11. https://doi.org/10.1038/s41597-022-01150-7

Hatfield, J. L., Boote, K. J., Kimball, B. A., Ziska, L. H., Izaurralde, R. C., Ort, D., Thomson, A. M., & Wolfe, D. (2011). Climate impacts on agriculture: Implications for crop production. *Agronomy Journal*, *103*(2), 351–370. https://doi.org/10.2134/agronj2010.0303

Holzkämper, A. (2017). Adapting Agricultural Production Systems to Climate Change—What's the Use of Models? *Agriculture*, *7*(86), 1–15. https://doi.org/10.3390/agriculture7100086

Iizumi, T., Shin, Y., Kim, W., Kim, M., & Choi, J. (2018). Global crop yield forecasting using seasonal climate information from a multi-model ensemble. *Climate Services*, *11*, 13–23. https://doi.org/10.1016/j.cliser.2018.06.003

INEI. (2013). *Resultados Definitivos: IV Censo Nacional Agropecuario 2012*. https://sinia.minam.gob.pe/download/file/fid/39753

Ingram, J. (2020). Nutrition security is more than food security. *Nature Food*, *1*(2), 2–2. https://doi.org/10.1038/s43016-019-0002-4

IPCC. (2022). *Climate Change 2022: Mitigation of Climate Change. Contribution of Working Group III to the Sixth Assessment Report of the Intergovernmental Panel on Climate Change* (P. R. Shukla, J. Skea, R. Slade, A. al Khourdajie, R. van Diemen, D. McCollum, M. Pathak, S. Some, P. Vyas, R. Fradera, M. Belkacemi, A. Hasija, G. Lisboa, S. Luz, & J. Malley, Eds.). https://doi.org/doi: 10.1017/9781009157926

Jiang, Y., & Koo, W. W. (2014). Estimating the local effect of weather on field crop production with unobserved producer behavior: A bioeconomic modeling framework. *Environmental Economics and Policy Studies*, *16*(3), 279–302. https://doi.org/10.1007/s10018-014-0079-9

Johnson, M. D., Hsieh, W. W., Cannon, A. J., Davidson, A., & Bédard, F. (2016). Crop yield forecasting on the Canadian Prairies by remotely sensed vegetation indices and machine learning methods. *Agricultural and Forest Meteorology*, *218–219*, 74–84. https://doi.org/10.1016/j.agrformet.2015.11.003

Karst, I. G., Mank, I., Traoré, I., Sorgho, R., Stückemann, K. J., Simboro, S., Sié, A., Franke, J., & Sauerborn, R. (2020). Estimating yields of household fields in rural subsistence farming systems to study food security in Burkina Faso. *Remote Sensing*, *12*(11), 1–20. https://doi.org/10.3390/rs12111717

Kelson, H. (2016). *Was ist Gerechtigkeit*. Reclam, Philipp, jun. GmbH, Verlag.

Kerr, R. B., Hasegawa, T., Lasco, R., Bhatt, I., Deryng, D., Farrell, A., Gurney-Smith, H., Ju, H., Lluch-Cota, S., Meza, F., Nelson, G., Neufeldt, H., & Thornton, P. (2022). Food, Fibre, and other

Ecosystem Products. In H.-O. Pörtner, D.C. Roberts, M. Tignor, E.S. Poloczanska, K. Mintenbeck, A. Alegría, M. Craig, S. Langsdorf, S. Löschke, v. Möller, A. Okem, & B. Rama (Eds.), *Climate Change 2022: Impacts, Adaptation and Vulnerability. Working Group II Contribution to the IPCC Sixth Assessment Report*. Cambridge University Press. In Press.

Kim, W., Iizumi, T., & Nishimori, M. (2019). Global patterns of crop production losses associated with droughts from 1983 to 2009. *Journal of Applied Meteorology and Climatology*, *58*(6), 1233–1244. https://doi.org/10.1175/JAMC-D-18-0174.1

Krell, N., Davenport, F., Harrison, L., Turner, W., Peterson, S., Shukla, S., Marter-Kenyon, J., Husak, G., Evans, T., & Caylor, K. (2022). Using real-time mobile phone data to characterize the relationships between small-scale farmers' planting dates and socio-environmental factors. *Climate Risk Management*, *35*, 100396. https://doi.org/10.1016/j.crm.2022.100396

Kummu, M., Heino, M., Taka, M., Varis, O., & Viviroli, D. (2021). Climate change risks pushing one-third of global food production outside the safe climatic space. *One Earth*, *4*(5), 720–729. https://doi.org/10.1016/j.oneear.2021.04.017

Laux, P., Kunstmann, H., & Bárdossy, A. (2008). Predicting the regional onset of the rainy season in West Africa. *International Journal of Climatology*, *28*(3), 329–342. https://doi.org/10.1002/joc.1542

Lavell, A., Oppenheimer, M., Diop, C., Hess, J., Lempert, R., Li, J., Muir-Wood, R., & Myeong, S. (2012). *Managing the Risks of Extreme Events and Disasters to Advance Climate Change Adaptation. A Special Report of Working Groups I and II of the Intergovernmental Panel on Climate Change* (C. B. Field, v. Barros, T.F. Stocker, D. Qin, D.J. Dokken, K.L. Ebi, M.D. Mastrandrea, K.J. Mach, G.-K. Plattner, S.K. Allen, M. Tignor, & P.M. Midgley, Eds.). Cambridge University Press. In Press.

Leroux, L., Castets, M., Baron, C., Escorihuela, M. J., Bégué, A., & lo Seen, D. (2019). Maize yield estimation in West Africa from crop process-induced combinations of multi-domain remote sensing indices. *European Journal of Agronomy*, *108*, 11–26. https://doi.org/10.1016/j.eja.2019.04.007

Levis, S., Badger, A., Drewniak, B., Nevison, C., & Ren, X. (2018). CLMcrop yields and water requirements: avoided impacts by choosing RCP 4.5 over 8.5. *Climatic Change*, *146*, 501–515. https://doi.org/10.1007/s10584-016-1654-9

Lewis, K. (2017). Understanding climate as a driver of food insecurity in Ethiopia. *Climatic Change*, *144*(2), 317–328. https://doi.org/10.1007/s10584-017-2036-7

Liersch, S., & Gornott, C. (2015). *Effects of climate change on sustainable food and nutrition security - with case studies in Kenya, Pakistan and Peru*. https://www.welthungerhilfe.org/fileadmin/pictures/publications/en/project_and_professional_papers/2015_effects_of_climate_change.pdf

Liu, B., Asseng, S., Müller, C., Ewert, F., Elliott, J., Lobell, D. B., Martre, P., Ruane, A. C., Wallach, D., Jones, J. W., Rosenzweig, C., Aggarwal, P. K., Alderman, P. D., Anothai, J., Basso, B., Biernath, C., Cammarano, D., Challinor, A., Deryng, D., … Zhu, Y. (2016). Similar estimates of temperature impacts on global wheat yield by three independent methods. *Nature Climate Change*, *6*(12), 1130–1136. https://doi.org/10.1038/nclimate3115

Liu, L., & Basso, B. (2019). Seasonal crop yield forecast: Methods, applications, and accuracies. *Advances in Agronomy*, *154*, 201–255. https://doi.org/10.1016/bs.agron.2018.11.002

Liu, L., & Basso, B. (2020). Linking field survey with crop modeling to forecast maize yield in smallholder farmers' fields in Tanzania. *Food Security*, *12*(3), 537–548. https://doi.org/10.1007/s12571-020-01020-3

Liu, S. L., Wang, X., Ma, S. T., Zhao, X., Chen, F., Xiao, X. P., Lal, R., & Zhang, H. L. (2019). Extreme stress threatened double rice production in Southern China during 1981–2010. *Theoretical and Applied Climatology*, *137*(3–4), 1987–1996. https://doi.org/10.1007/s00704-018-2719-7

Lobell, David. B., Schlenker, W., & Costa-Roberts, J. (2011). Climate Trends and Global Crop Production Since 1980. *Science*, *333*, 616–620. https://doi.org/10.1126/science.1206034

Lobell, D. B. (2014). Climate change adaptation in crop production: Beware of illusions. *Global Food Security*, *3*(2), 72–76. https://doi.org/10.1016/j.gfs.2014.05.002

Lobell, D. B., & Asseng, S. (2017). Comparing estimates of climate change impacts from process-based and statistical crop models. *Environmental Reserach Letters*, *12*, 1–12. https://doi.org/10.1088/1748-9326/015001

Lobell, D. B., Burke, M. B., Tebaldi, C., Mastrandrea, M. D., Falcon, W. P., & Naylor, R. L. (2008). Prioritizing Climate Change Adaptation Needs for Food Security in 2030. *Science*, *319*, 607–610. https://doi.org/10.1126/science.1152339

Lobell, D. B., Field, C. B., Cahill, K. N., & Bonfils, C. (2006). Impacts of future climate change on California perennial crop yields: Model projections with climate and crop uncertainties. *Agricultural and Forest Meteorology*, *141*(2–4), 208–218. https://doi.org/10.1016/j.agrformet.2006.10.006

Lobell, D. B., Hammer, G. L., McLean, G., Messina, C., Roberts, M. J., & Schlenker, W. (2013). The critical role of extreme heat for maize production in the United States. *Nature Climate Change*, *3*(5), 497–501. https://doi.org/10.1038/nclimate1832

Lobell, D. B., Roberts, M. J., Schlenker, W., Braun, N., Little, B. B., Rejesus, R. M., & Hammer, G. L. (2014). Greater Sensitivity to Drought Accompanies Maize Yield Increase in the U.S. Midwest. *Science*, *344*, 516–519. https://doi.org/10.1126/science.1251423

Loison, S. A. (2015). Rural Livelihood Diversification in Sub-Saharan Africa: A Literature Review. *Journal of Development Studies*, *51*(9), 1125–1138. https://doi.org/10.1080/00220388.2015.1046445

Matiu, M., Ankerst, D. P., & Menzel, A. (2017). Interactions between temperature and drought in global and regional crop yield variability during 1961-2014. *PLoS ONE*, *12*(5), 1–23. https://doi.org/10.1371/journal.pone.0178339

Mbow, C., Rosenzweig, C., Barioni, L. G., Benton, T. G., Herrero, M., Krishnapillai, M., Liwenga, E., Pradhan, P., Rivera-Ferre, M. G., Sapkota, T., Tubiello, F. N., & Xu, Y. (2019). Food security. In P. R. Shukla, J. Skea, E. Calvo Buendia, V. Masson-Delmotte, H.-O. Pörtner, D. C. Roberts, P. Zhai, R. Slade, S. Connors, S. R. van Diemen, M. Ferrat, E. Haughey, S. Luz, S. Neogi, M. Pathak, J. Petzold, J. Portugal Pereira, P. Vyas, E. Huntley, … J. Malley (Eds.), *Climate Change and Land: an IPCC special report on climate change, desertification, land degradation, sustainable land management, food security, and greenhouse gas fluxes in terrestrial ecosystems*. In press.

Mc Carthy, U., Uysal, I., Badia-Melis, R., Mercier, S., O'Donnell, C., & Ktenioudaki, A. (2018). Global food security – Issues, challenges and technological solutions. *Trends in Food Science and Technology*, *77*, 11–20. https://doi.org/10.1016/j.tifs.2018.05.002

Meroni, M., Waldner, F., Seguini, L., Kerdiles, H., & Rembold, F. (2021). Yield forecasting with machine learning and small data: What gains for grains? *Agricultural and Forest Meteorology*, *308–309*, 1–13. https://doi.org/10.1016/j.agrformet.2021.108555

Molnar, C. (2022). *Interpretable Machine Learning: A Guide for Making Black Box Models Explainable* (2nd ed.). https://christophm.github.io/interpretable-ml-book/

Moore, F. C. (2022). *The Fingerprint of Anthropogenic Warming on Global Agriculture*. *EarthArXiv*, https://doi.org/https://doi.org/10.31223/X5Q30Z

Morton, J. F. (2007). The impact of climate change on smallholder and subsistence agriculture. *Proceedings of the National Academy of Sciences*, *104*(50), 19680–19685. https://doi.org/10.1073/pnas.0701855104

Mueller, B., Hauser, M., Iles, C., Rimi, R. H., Zwiers, F. W., & Wan, H. (2015). Lengthening of the growing season in wheat and maize producing regions. *Weather and Climate Extremes*, *9*, 47–56. https://doi.org/10.1016/j.wace.2015.04.001

Murdoch, W. J., Singh, C., Kumbier, K., Abbasi-Asl, R., & Yu, B. (2019). Definitions, methods, and applications in interpretable machine learning. *Proceedings of the National Academy of Sciences of the United States of America*, *116*(44), 22071–22080. https://doi.org/10.1073/pnas.1900654116

Murken, L., & Gornott, C. (2022). The importance of different land tenure systems for farmers' response to climate change: A systematic review. *Climate Risk Management*, *35*, 1–18. https://doi.org/10.1016/j.crm.2022.100419

Myers, S. S., Smith, M. R., Guth, S., Golden, C. D., Vaitla, B., Mueller, N. D., Dangour, A. D., & Huybers, P. (2017). Climate Change and Global Food Systems: Potential Impacts on Food Security and Undernutrition. *Annu. Rev. Public Health*, *38*, 259–277. https://doi.org/10.1146/annurev

National Bureau of Statistics Tanzania. (2014). *Tanzania Integrated Labour Force Survey 2014*. https://s3-eu-west-1.amazonaws.com/s3.sourceafrica.net/documents/118113/Tanzania-Integrated-Labour-Force-Survey-2014.pdf

Ogutu, G. E. O., Franssen, W. H. P., Supit, I., Omondi, P., & Hutjes, R. W. A. (2018). Probabilistic maize yield prediction over East Africa using dynamic ensemble seasonal climate forecasts. *Agricultural and Forest Meteorology*, *250–251*, 243–261. https://doi.org/10.1016/j.agrformet.2017.12.256

Ortiz-Bobea, A., Ault, T. R., Carrillo, C. M., Chambers, R. G., & Lobell, D. B. (2021). Anthropogenic climate change has slowed global agricultural productivity growth. *Nature Climate Change*, *11*(4), 306–312. https://doi.org/10.1038/s41558-021-01000-1

Ortiz, R. (2012). *Climate Change and Agricultural Production*. https://www.climate-expert.org/fileadmin/user_upload/PDF/Costa_Rica/getdocument.pdf

Paeth, H., & Hense, A. (2004). SST versus Climate Change Signals in West African Rainfall: 20th-Century Variations and Future Projections. *Climatic Change*, *65*(1/2), 179–208. https://doi.org/10.1023/B:CLIM.0000037508.88115.8a

Palm, C. A., Smukler, S. M., Sullivan, C. C., Mutuo, P. K., Nyadzi, G. I., & Walsh, M. G. (2010). Identifying potential synergies and trade-offs for meeting food security and climate change

objectives in sub-Saharan Africa. *Proceedings of the National Academy of Sciences*, *107*(46), 19661–19666. https://doi.org/10.1073/pnas.0912248107

Pardoe, J., Conway, D., Namaganda, E., Vincent, K., Dougill, A. J., & Kashaigili, J. J. (2018). Climate change and the water–energy–food nexus: insights from policy and practice in Tanzania. *Climate Policy*, *18*(7), 863–877. https://doi.org/10.1080/14693062.2017.1386082

Pearl, J. (2019). The seven tools of causal inference, with reflections on machine learning. *Communications of the ACM*, *62*(3), 54–60. https://doi.org/10.1145/3241036

Porter, J. R., Challinor, A. J., Henriksen, C. B., Howden, S. M., Martre, P., & Smith, P. (2019). Invited review: Intergovernmental Panel on Climate Change, agriculture, and food—A case of shifting cultivation and history. *Global Change Biology*, *25*(8), 2518–2529. https://doi.org/10.1111/gcb.14700

Rawls, J. (1979). *Eine Theorie der Gerechtigkeit*. Suhrkamp Verlag.

Ray, D. K., Gerber, J. S., Macdonald, G. K., & West, P. C. (2015). Climate variation explains a third of global crop yield variability. *Nature Communications*, *6*, 1–9. https://doi.org/10.1038/ncomms6989

Rosenzweig, C., Arnell, N. W., Ebi, K. L., Lotze-Campen, H., Raes, F., Rapley, C., Smith, M. S., Cramer, W., Frieler, K., Reyer, C. P. O., Schewe, J., van Vuuren, D., & Warszawski, L. (2017). Assessing inter-sectoral climate change risks: The role of ISIMIP. *Environmental Research Letters*, *12*(1), 1–16. https://doi.org/10.1088/1748-9326/12/1/010301

Rosenzweig, C., Elliott, J., Deryng, D., Ruane, A. C., Müller, C., Arneth, A., Boote, K. J., Folberth, C., Glotter, M., Khabarov, N., Neumann, K., Piontek, F., Pugh, T. A. M., Schmid, E., Stehfest, E., Yang, H., & Jones, J. W. (2014). Assessing agricultural risks of climate change in the 21st century in a global gridded crop model intercomparison. *Proceedings of the National Academy of Sciences of the United States of America*, *111*(9), 3268–3273. https://doi.org/10.1073/pnas.1222463110

Rötter, R., Hoffmann, M., Koch, M., & Müller, C. (2018). Progress in modelling agricultural impacts of and adaptations to climate change. *Current Opinion in Plant Biology*, *45*, 255–261. https://doi.org/10.1016/j.pbi.2018.05.009

Runge, E. C. A. (1968). Effects of Rainfall and Temperature Interactions During the Growing Season on Corn Yield. *Agronomy Journal*, *60*(5), 503–507. https://doi.org/10.2134/agronj1968.00021962006000050018x

Samberg, L. H., Gerber, J. S., Ramankutty, N., Herrero, M., & West, P. C. (2016). Subnational distribution of average farm size and smallholder contributions to global food production. *Environmental Research Letters*, *11*(12). https://doi.org/10.1088/1748-9326/11/12/124010

Schauberger, B., Gornott, C., & Wechsung, F. (2017). Global evaluation of a semiempirical model for yield anomalies and application to within-season yield forecasting. *Global Change Biol.*, *23*, 4750–4764. https://doi.org/10.1111/gcb.13738

Schauberger, B., Jägermeyr, J., & Gornott, C. (2020). A systematic review of local to regional yield forecasting approaches and frequently used data resources. *European Journal of Agronomy*, *120*, 1–15. https://doi.org/10.1016/j.eja.2020.126153

Schlenker, W., & Lobell, D. B. (2010). Robust negative impacts of climate change on African agriculture. *Environmental Research Letters*, *5*(1). https://doi.org/10.1088/1748-9326/5/1/014010

Schmidhuber, J., & Tubiello, F. N. (2007). Global food security under climate change. *Proceedings of the National Academy of Sciences of the United States of America*, *104*(50), 19703–19708. https://doi.org/10.1073/pnas.0701976104

Seneviratne, S. I., Zhang, X., M. Adnan, W. Badi, C. Dereczynski, A. Di Luca, Ghosh, S., Iskandar, I., Kossin, J., Lewis, S., Otto, F., Pinto, I., Satoh, M., Vicente-Serrano, S. M., Wehner, M., & Zhou, B. (2021). Weather and Climate Extreme Events in a Changing Climate. In V. Masson- Delmotte, P. Zhai, A. Pirani, S.L. Connors, C. Péan, S. Berger, N. Caud, Y. Chen, L. Goldfarb, M.I. Gomis, M. Huang, K. Leitzell, E. Lonnoy, J.B.R. Matthews, T.K. Maycock, T. Waterfield, O. Yelekçi, R. Yu, & B. Zhou (Eds.), *Climate Change 2021: The Physical Science Basis. Contribution of Working Group I to the Sixth Assessment Report of the Intergovernmental Panel on Climate Change*. Cambridge University Press. In Press.

Sietz, D., Choque, S. E. M., & Lüdeke, M. K. B. (2012). Typical patterns of smallholder vulnerability to weather extremes with regard to food security in the Peruvian Altiplano. *Regional Environmental Change*, *12*(3), 489–505. https://doi.org/10.1007/s10113-011-0246-5

Stern, R. D., Dennett, M. D., & Garbutt, D. J. (1981). The Start of the Rains in West Africa. *Journal of Climatology*, *1*, 59–68.

Tall, A., Coulibaly, J. Y., & Diop, M. (2018). Do climate services make a difference? A review of evaluation methodologies and practices to assess the value of climate information services for farmers: Implications for Africa. *Climate Services*, *11*, 1–12. https://doi.org/10.1016/j.cliser.2018.06.001

Thompson, L. M. (1975). Weather Variability, Climatic Change, and Grain Production. *Science*, *188*(4188), 535–541. https://doi.org/10.1126/science.188.4188.535

Thornton, T. F., & Comberti, C. (2017). Synergies and trade-offs between adaptation, mitigation and development. *Climatic Change*, *140*(1), 5–18. https://doi.org/10.1007/s10584-013-0884-3

Tomalka, J., Lange, S., Röhrig, F., & Gornott, C. (2020). *Climate Risk Profile: Tanzania (Climate Risk Profiles for Sub-Saharan Africa Series)*. https://agrica.de/wp-content/uploads/2021/01/GIZ_Climate-Risk-Profile-Tanzania_EN_final.pdf

Tomalka, J., Lange, S., Röhrig, F., & Gornott, C. (2021). *Climate Risk Profile: Burkina Faso*. https://agrica.de/wp-content/uploads/2021/02/CRP_Burkina-Faso_EN_20210208.pdf

Travis, W. R. (2016). Agricultural impacts: Mapping future crop geographies. *Nature Climate Change*, *6*, 544–545. https://doi.org/10.1038/nclimate2965

UNDESA. (2019). *World Population Prospects 2019 Highlights*. United Nations Department of Economic and Social Affairs - Population Division (UNDESA). https://population.un.org/wpp/Publications/Files/WPP2019_Highlights.pdf

UNDRR. (2019). *Global Assessment Report on Disaster Risk Reduction 2019*. United Nations Office for Disaster Risk Reduction (UNDRR). https://www.undrr.org/media/73965/download

USAID. (2017). *Climate change risk in Peru: Country risk profile* (Issue February). https://www.climatelinks.org/sites/default/files/asset/document/2017_Climate%20Change%20Risk%20Profile_Peru.pdf

USAID. (2020). *Food Assistance Fact Sheet Burkina Faso*. https://www.usaid.gov/sites/default/files/documents/1866/FFP_Fact_Sheet_Burkina_Faso.pdf

van Ittersum, M. K., Cassman, K. G., Grassini, P., Wolf, J., Tittonell, P., & Hochman, Z. (2013). Yield gap analysis with local to global relevance-A review. *Field Crops Research*, *143*, 4–17. https://doi.org/10.1016/j.fcr.2012.09.009

van Ittersum, M. K., van Bussel, L. G. J., Wolf, J., Grassini, P., van Wart, J., Guilpart, N., Claessens, L., de Groot, H., Wiebe, K., Mason-D'Croz, D., Yang, H., Boogaard, H., van Oort, P. A. J., van Loon, M. P., Saito, K., Adimo, O., Adjei-Nsiah, S., Agali, A., Bala, A., … Cassman, K. G. (2016). Can sub-Saharan Africa feed itself? *Proceedings of the National Academy of Sciences of the United States of America*, *113*(52), 14964–14969. https://doi.org/10.1073/pnas.1610359113

Vermeulen, S. J., Dinesh, D., Howden, S. M., Cramer, L., & Thornton, P. K. (2018). Transformation in Practice: A Review of Empirical Cases of Transformational Adaptation in Agriculture Under Climate Change. *Frontiers in Sustainable Food Systems*, *2*, 1–17. https://doi.org/10.3389/fsufs.2018.00065

Vignola, R., Harvey, C. A., Bautista-Solis, P., Avelino, J., Rapidel, B., Donatti, C., & Martinez, R. (2015). Ecosystem-based adaptation for smallholder farmers: Definitions, opportunities and constraints. *Agriculture, Ecosystems and Environment*, *211*, 126–132. https://doi.org/10.1016/j.agee.2015.05.013

Wang, J., Wang, E., Luo, Q., & Kirby, M. (2009). Modelling the sensitivity of wheat growth and water balance to climate change in Southeast Australia. *Climatic Change*, *96*(1), 79–96. https://doi.org/10.1007/s10584-009-9599-x

Wenhaji Ndomeni, C., Cattani, E., Merino, A., & Levizzani, V. (2018). An observational study of the variability of East African rainfall with respect to sea surface temperature and soil moisture. *Quarterly Journal of the Royal Meteorological Society*, *144*, 384–404. https://doi.org/10.1002/qj.3255

Wheeler, T., & von Braun, J. (2013). Climate change impacts on global food security. *Science*, *341*, 508–513. https://doi.org/10.1126/science.1239402

Wolanin, A., Mateo-Garciá, G., Camps-Valls, G., Gómez-Chova, L., Meroni, M., Duveiller, G., Liangzhi, Y., & Guanter, L. (2020). Estimating and understanding crop yields with explainable deep learning in the Indian Wheat Belt. *Environmental Research Letters*, *15*(2). https://doi.org/10.1088/1748-9326/ab68ac

Wooldridge, J. M. (2014). *Introductory Econometrics A Modern Approach* (5th ed.). Cenage Learning.

World Bank. (2022). *World Bank Open Data*. https://data.worldbank.org/country/burkina-faso?

Yoshino, Y., Belghith, N. B. H., Kasirye, D., Chatzinikolaou, A., Mdluli, S., & Dreyhaupt, S. (2017). *United Republic of Tanzania Systematic Country Diagnostic: To the Next Level of Development*. https://openknowledge.worldbank.org/bitstream/handle/10986/26236/TZ-SCD-Final-Approved-by-AFRVP-03012017.pdf?sequence=1&isAllowed=y

Zampieri, M., Ceglar, A., Dentener, F., & Toreti, A. (2017). Wheat yield loss attributable to heat waves, drought and water excess at the global, national and subnational scales. *Environmental Research Letters*, *12*, 1–11. https://doi.org/10.1088/1748-9326/aa723b

Zinyengere, N., Mhizha, T., Mashonjowa, E., Chipindu, B., Geerts, S., & Raes, D. (2011). Using seasonal climate forecasts to improve maize production decision support in Zimbabwe. *Agricultural and Forest Meteorology*, *151*, 1792–1799. https://doi.org/10.1016/j.agrformet.2011.07.015

Zorita, E., & Tilya, F. F. (2002). Rainfall variability in Northern Tanzania in the March – May season (long rains) and its links tolarge-scale climate forcing. *Climate Research*, *20*, 31–40. https://www.jstor.org/stable/24866791

6 Supplementary Information

6.1 Supplementary Information to: "Assessment of weather-yield relations of starchy maize at different scales in Peru to support the NDCs implementation"

Author names and affiliations:
Rahel Laudien[a], Bernhard Schauberger[a], Stephanie Gleixner[a], Christoph Gornott[a]

[a]Potsdam Institute for Climate Impact Research (PIK)
Member of the Leibniz Association
P.O. Box 60 12 03
D-14412 Potsdam
Germany

Corresponding author:

Rahel Laudien (laudien@pik-potsdam.de)

Supplementary figures

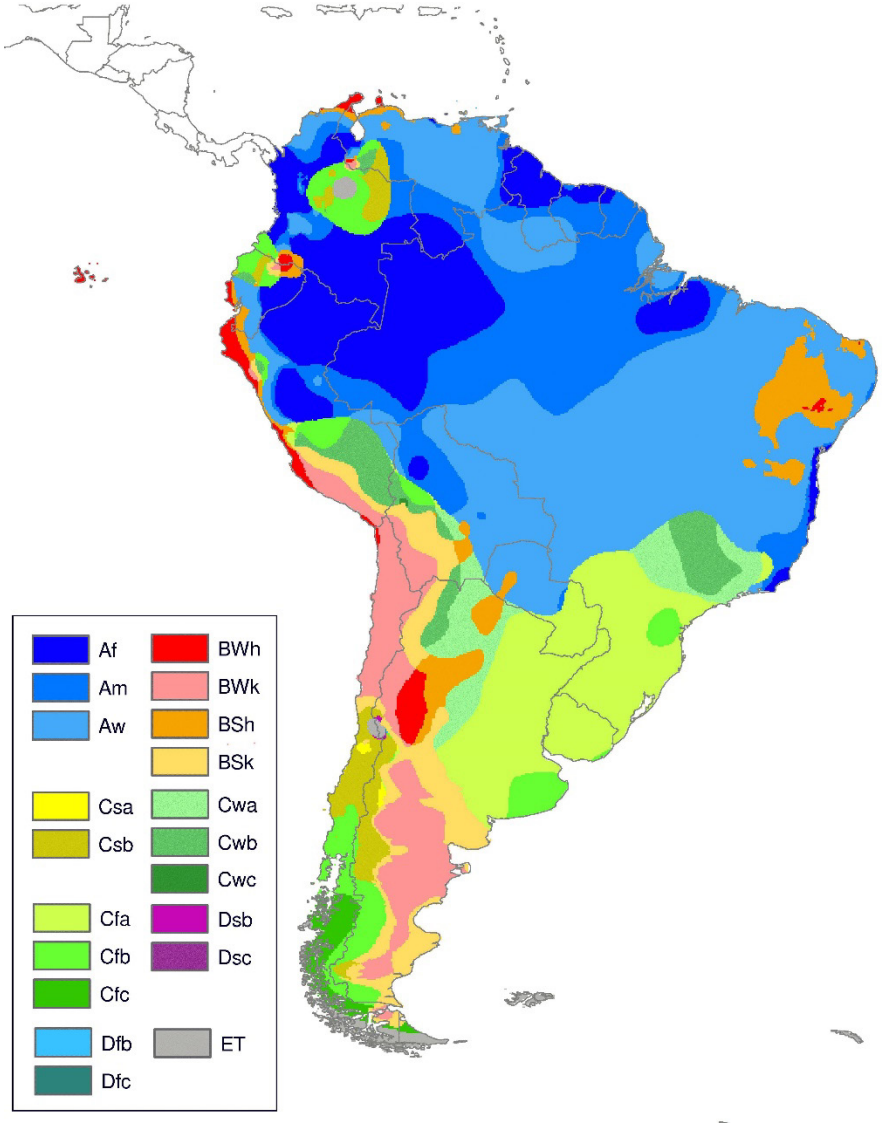

Fig. A.1. Köppen-Geiger climate classification of South America (Peel et al., 2007);

A = Tropical, B = Arid, C = Temperate, D = Cold, ET = Polar Tundra, f = Rainforest, m = Monsoon, w = Savannah, s = Dry Summer, W = Desert, S = Steppe, a = Hot Summer, b = Warm Summer, c = Cold Summer, h = Hot, k = Cold

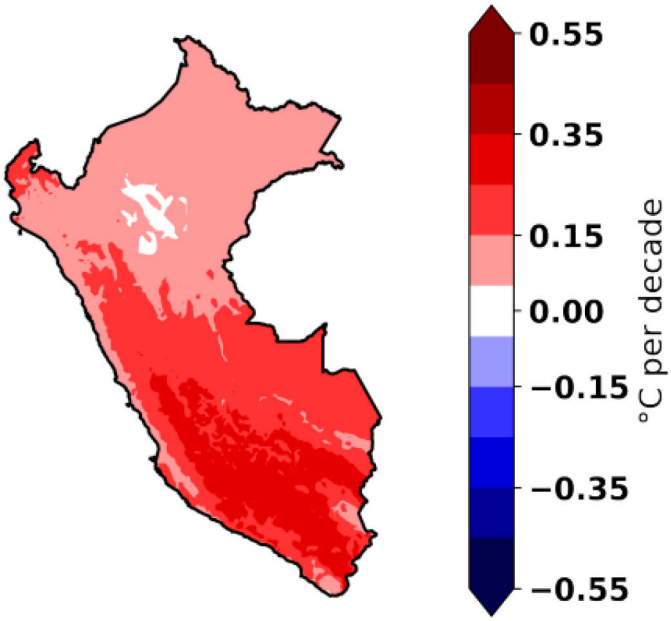

Fig. A.2. Historic warming in Peru; linear trend in mean surface air temperature from 1981 to 2016 based on PISCO data (Aybar et al., 2019)

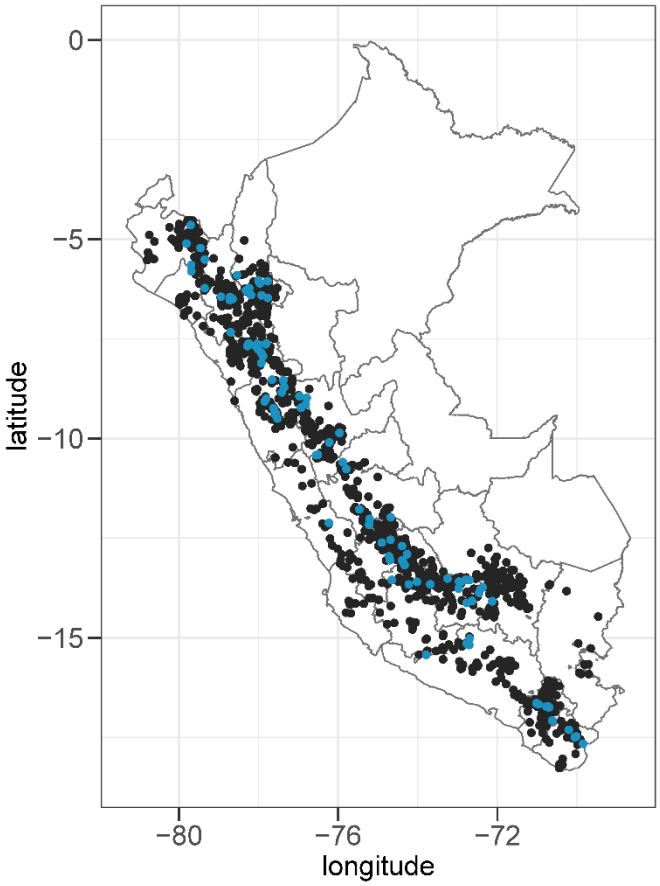

Fig. A.3. Location of starchy maize producing households interviewed in the survey waves 2016 and 2017 of the agricultural survey carried out by the Peruvian national statistical institute "Instituto Nacional de Estadística e Informática" (INEI, 2017); the points show the centre of the primary sampling unit of the survey, called clusters (in Spanish: *Conglomerados*); black points show all clusters

of the survey waves 2016 and 2017 (i.e. 19,704 observations coming from 1,213 unique clusters), blue points show the clusters that we used in the study after data cleaning techniques were applied (i.e. 291 observations coming from 97 unique clusters)

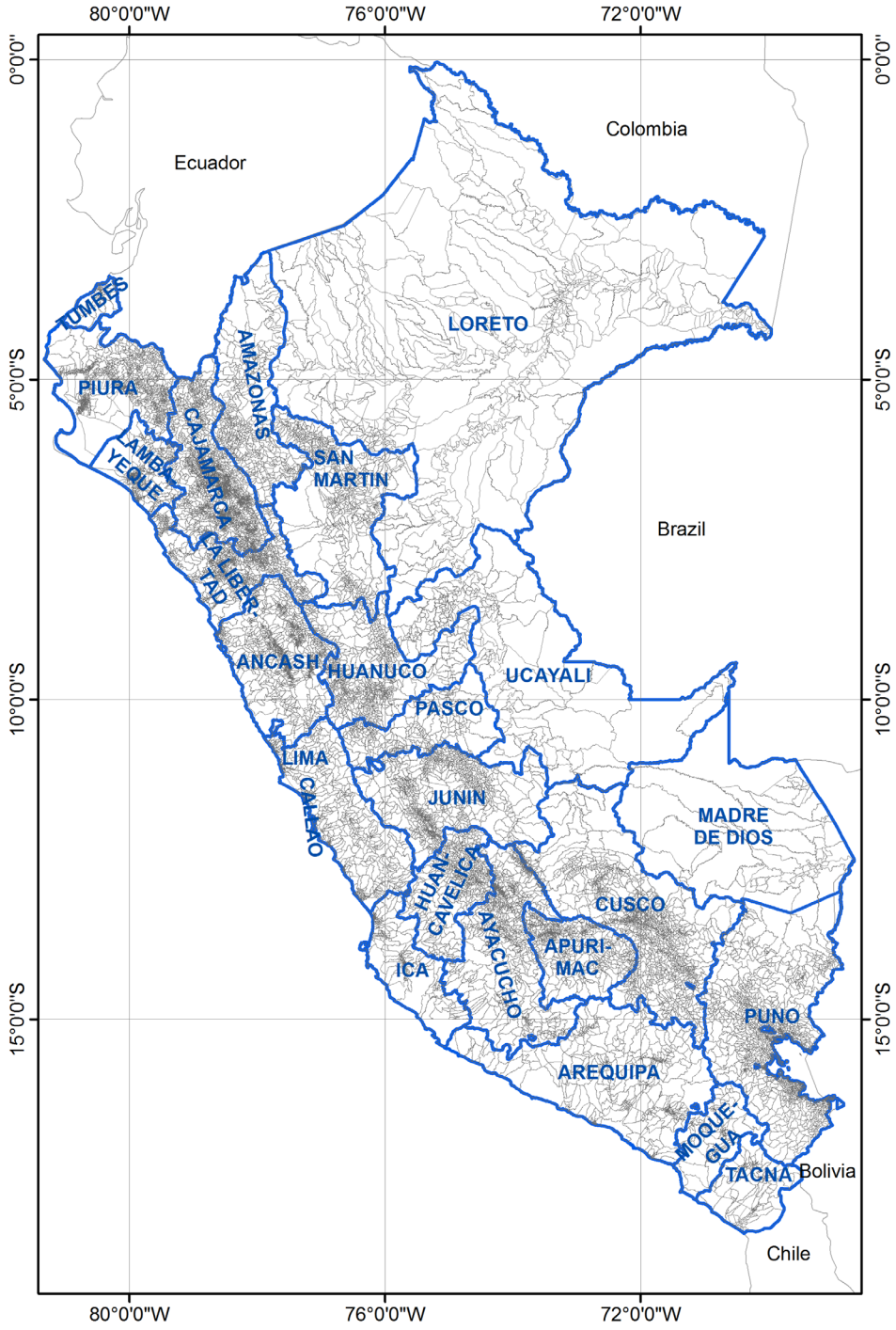

Fig. A.4. Administrative map of Peru showing regions (in Spanish: *departamentos*) in blue and clusters (in Spanish: *conglomerados*) in light grey; clusters are the primary sampling unit of the agricultural household survey carried out by the Peruvian national statistical institute "Instituto Nacional de Estadística e Informática" (INEI, 2017).

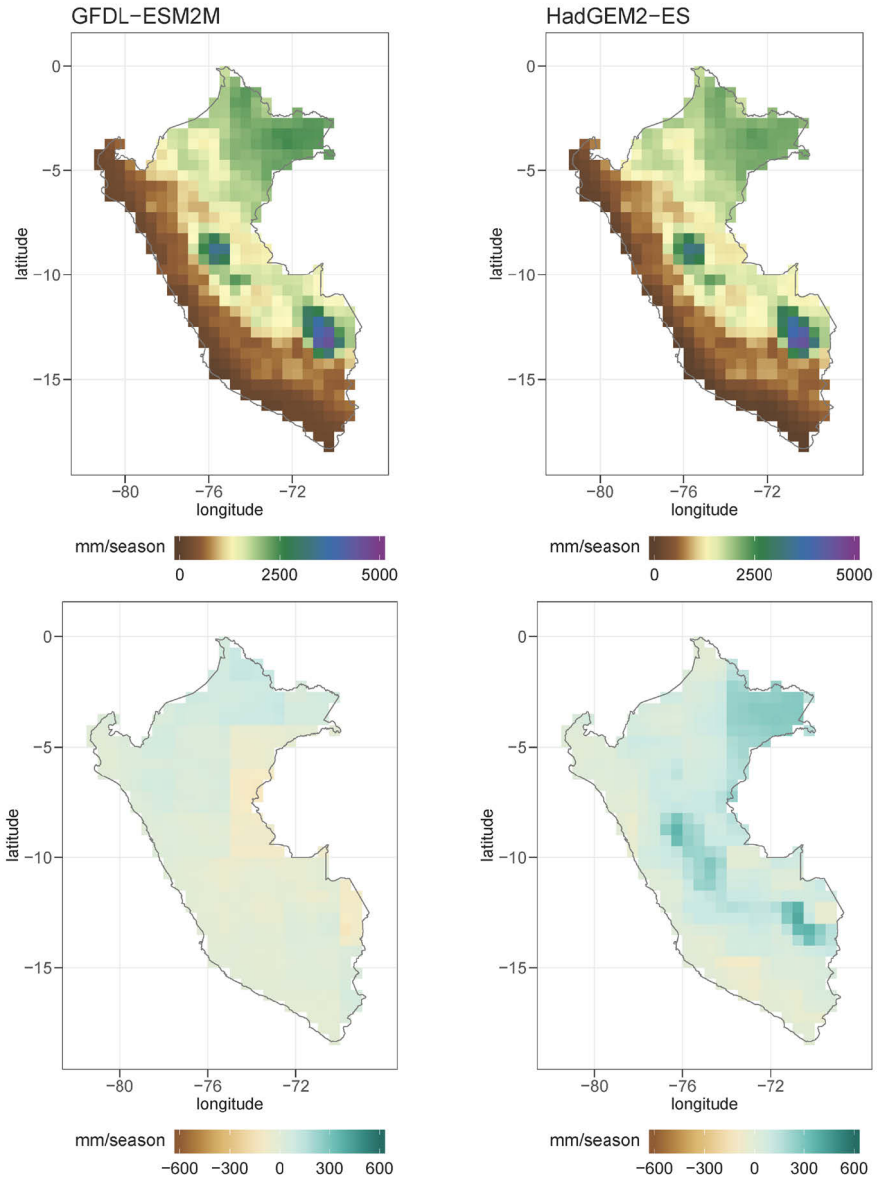

Fig. A.5. Projected precipitation changes in Peru in 2040 to 2060 (compared to 2000-2020) during the main growing season (from September to June) based on the global climate models GFDL-ESM2M, HadGEM2-ES, IPSL-CM5A-LR and MIROC5, which were bias-adjusted and provided within ISIMIP2b (Warszawski et al., 2014); the panels on top show the modelled mean precipitation in the growing season from 2000 to 2020; the panels below show the differences in mean precipitation in the growing season from 2000-2020 and 2040-2060

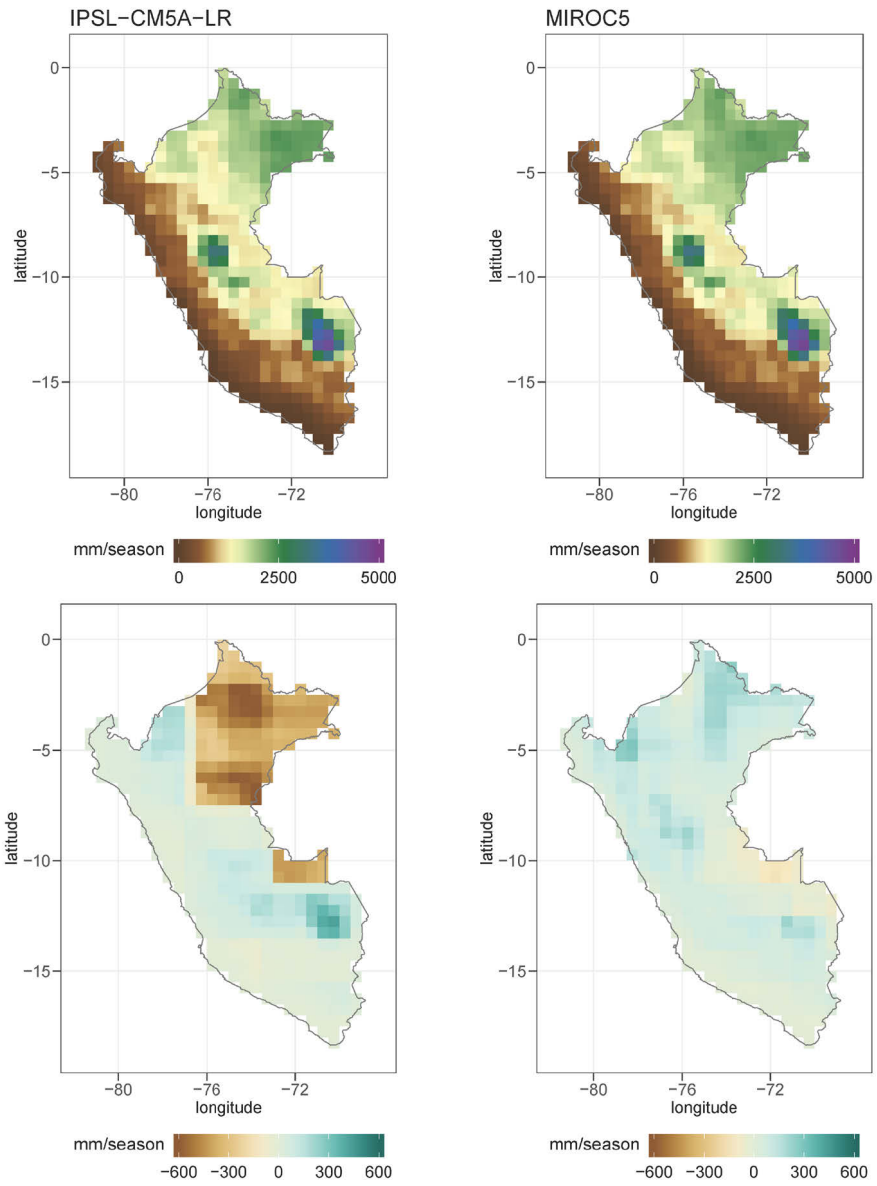

Fig. A.5. (continued)

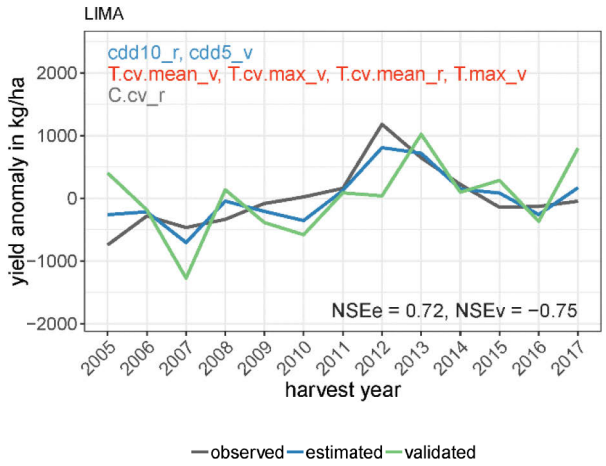

Fig. A.6. Observed and simulated maize yield anomalies in the region Lima. Black lines show observed yield anomalies, blue lines show anomalies estimated with the full model and green lines those estimated out-of-sample. Selected variables are shown in blue for precipitation, red for temperature and grey for cloud fraction (Abbreviations: *cdd10 = Consecutive dry days of more than 10 days*, *cdd5 = Consecutive dry days of more than 5 days*, *T.cv.mean = Coefficient of variation of mean temperature*; *T.cv.max = Coefficient of variation of maximum temperature*, *T.max = Mean maximum temperature [°C]*, *C.cv = Coefficient of variation of mean cloud fraction*; "_v" stands for vegetative phase and "_r" stands for reproductive phase)

Supplementary Tables

AMAZONAS

term	estimate	std.error	t.stat	p.value
T.cv.mean_v	-2501.79	962.16	-2.60	0.04
P.cv_r	-94.87	73.47	-1.29	0.24
T.max_v	62.25	19.62	3.17	0.02
T.min_v	-43.52	16.54	-2.63	0.04
cdd5_r	-9.76	4.65	-2.10	0.08
C.min_r	2.79	1.05	2.66	0.04
PA20_v	-3.90	2.03	-1.92	0.10
NSEe	0.91			
NSEv	0.55			
RMSE	9.81			
RMSE.const	34.52			
p.value of f.stat	< 0.05			

ANCASH

term	estimate	std.error	t.stat	p.value
T.cv.max_r	-450.07	407.70	-1.10	0.31
T.cv.mean_v	-564.05	464.49	-1.21	0.27
cdd10_v	17.24	7.33	2.35	0.06
T.max_v	14.14	9.10	1.55	0.17
cwd10_r	1.02	0.30	3.40	0.01
C.mean_v	0.53	1.23	0.43	0.68
C.min_v	-0.59	0.72	-0.83	0.44
NSEe	0.91			
NSEv	0.47			
RMSE	6.98			
RMSE.const	24.9			
p.value of f.stat	< 0.01			

APURIMAC

term	estimate	std.error	t.stat	p.value
cdd10_v	-86.86	42.35	-2.05	0.09
C.min_v	10.83	20.91	0.52	0.62
T.cv.min_v	150.81	790.53	0.19	0.86
cwd5_v	0.77	1.42	0.54	0.61
minOfmin_r	-16.97	17.40	-0.98	0.37
T.min_v	69.11	58.82	1.18	0.28
PA15_v	7.06	12.24	0.58	0.59
NSEe	0.76			
NSEv	-0.24			
RMSE	38.55			
RMSE.const	84.63			
p.value of f.stat	0.13			

AREQUIPA

term	estimate	std.error	t.stat	p.value
C.cv_r	-1109.00	682.57	-1.62	0.14
PA10_r	426.53	271.94	1.57	0.15
cwd10_v	27.20	12.93	2.10	0.06
NSEe	0.62			
NSEv	0.46			
RMSE	221.09			
RMSE.const	389.21			
p.value of f.stat	< 0.05			

AYACUCHO

term	estimate	std.error	t.stat	p.value
C.cv_v	-458.61	301.06	-1.52	0.18
minOfmin_v	-17.63	12.68	-1.39	0.21
PA15_r	25.06	10.89	2.30	0.06
P.max_v	7.52	2.75	2.73	0.03
C.mean_v	1.73	3.86	0.45	0.67
PA5_r	-2.69	1.25	-2.15	0.08
DWP_v	2.67	1.14	2.35	0.06
NSEe	0.94			
NSEv	0.57			
RMSE	16.87			
RMSE.const	72.31			
p.value of f.stat	< 0.01			

CAJAMARCA

term	estimate	std.error	t.stat	p.value
T.cv.mean_v	-365.88	352.50	-1.04	0.34
cdd5_v	19.51	3.37	5.79	0.00
C.min_r	-2.93	0.61	-4.77	0.00
PA20_v	-3.41	2.69	-1.27	0.25
C.min_v	2.07	0.39	5.30	0.00
PA5_r	1.09	0.33	3.34	0.02
P.max_v	-0.32	0.41	-0.78	0.47
NSEe	0.94			
NSEv	0.64			
RMSE	5.48			
RMSE.const	24.58			
p.value of f.stat	< 0.01			

CUSCO

term	estimate	std.error	t.stat	p.value
P.cv_v	-1557.50	605.18	-2.57	0.04
T.cv.max_r	3531.93	4706.80	0.75	0.48
maxOfmax_r	-108.17	27.13	-3.99	0.01
cdd5_v	64.35	48.65	1.32	0.23
PA10_r	-33.48	7.59	-4.41	0.00
PA15_v	-39.64	12.01	-3.30	0.02
cdd5_r	-50.94	41.60	-1.22	0.27
NSEe	0.89			
NSEv	0.37			
RMSE	59.46			
RMSE.const	190.35			
p.value of f.stat	< 0.05			

HUANCAVELICA

term	estimate	std.error	t.stat	p.value
PA10_r	2.18	5.08	0.43	0.68
T.cv.max_v	2173.78	2183.72	1.00	0.36
T.mean_v	-18.07	39.98	-0.45	0.67
PA15_r	17.42	15.07	1.16	0.29
cwd5_v	1.68	1.10	1.53	0.18
cdd5_r	2.50	8.16	0.31	0.77
minOfmin_r	2.13	15.26	0.14	0.89
NSEe	0.65			
NSEv	-0.33			
RMSE	24.77			
RMSE.const	45.23			
p.value of f.stat	0.3			

HUANUCO

term	estimate	std.error	t.stat	p.value
T.cv.max_v	-9348.19	1170.05	-7.99	0.00
T.mean_r	-80.72	39.39	-2.05	0.09
maxOfmax_r	-33.51	15.43	-2.17	0.07
PA15_r	11.53	2.63	4.38	0.00
C.mean_v	6.19	4.47	1.39	0.21
PA10_r	3.64	3.07	1.18	0.28
PA5_r	5.70	1.12	5.08	0.00
NSEe	0.97			
NSEv	0.76			
RMSE	13.66			
RMSE.const	88.11			
p.value of f.stat	< 0.001			

ICA

term	estimate	std.error	t.stat	p.value
cwd10_v	107.44	34.40	3.12	0.01
NSEe	0.45			
NSEv	0.44			
RMSE	285.8			
RMSE.const	416.87			
p.value of f.stat	< 0.01			

JUNIN

term	estimate	std.error	t.stat	p.value
cdd5_r	-161.11	52.40	-3.07	0.01
NSEe	0.44			
NSEv	0.35			
RMSE	152.96			
RMSE.const	221.56			
p.value of f.stat	< 0.01			

LA LIBERTAD

term	estimate	std.error	t.stat	p.value
T.cv.min_v	4678.72	2475.00	1.89	0.11
T.cv.mean_v	-12219.59	3334.53	-3.66	0.01
P.cv_v	245.85	137.71	1.79	0.12
minOfmin_r	38.09	15.39	2.47	0.05
PA15_r	92.39	35.04	2.64	0.04
PA10_v	46.63	15.53	3.00	0.02
PA5_r	-18.16	4.58	-3.97	0.01
NSEe	0.94			
NSEv	0.76			
RMSE	29.71			
RMSE.const	130.76			
p.value of f.stat	< 0.01			

LAMBAYEQUE

term	estimate	std.error	t.stat	p.value
T.cv.max_v	-1919.11	1302.52	-1.47	0.18
cwd5_v	-96.15	23.44	-4.10	0.00
cdd5_v	-54.39	9.14	-5.95	0.00
P.cv_v	29.57	9.75	3.03	0.02
cdd5_r	-6.40	5.16	-1.24	0.25

NSEe	0.94
NSEv	0.88
RMSE	18.48
RMSE.const	81.38
p.value of f.stat	< 0.001

LIMA

term	estimate	std.error	t.stat	p.value
T.cv.mean_v	57083.12	28027.33	2.04	0.09
T.cv.max_v	-44441.64	28803.12	-1.54	0.17
C.cv_r	-5664.20	2939.05	-1.93	0.10
T.cv.mean_r	25795.98	22889.98	1.13	0.30
cdd10_r	152.04	231.20	0.66	0.54
T.max_v	-140.65	218.66	-0.64	0.54
cdd5_v	-498.79	254.23	-1.96	0.10

NSEe	0.72
NSEv	-0.75
RMSE	248.41
RMSE.const	511.3
p.value of f.stat	0.17

MOQUEGUA

term	estimate	std.error	t.stat	p.value
T.cv.min_v	1415.05	399.55	3.54	0.00
PA5_v	36.22	13.75	2.63	0.02

NSEe	0.66
NSEv	0.56
RMSE	42.26
RMSE.const	78.06
p.value of f.stat	< 0.01

PASCO

term	estimate	std.error	t.stat	p.value
T.cv.max_r	-18242.99	7083.80	-2.58	0.04
T.cv.max_v	-6568.94	4018.42	-1.63	0.15
C.cv_v	-2937.66	1672.40	-1.76	0.13
cdd5_v	-78.95	60.37	-1.31	0.24
cdd10_r	70.10	35.23	1.99	0.09
maxOfmax_v	-70.20	51.45	-1.36	0.22
PA5_v	-14.10	4.80	-2.94	0.03

NSEe	0.94
NSEv	0.83
RMSE	56.18
RMSE.const	252.78
p.value of f.stat	< 0.01

PIURA

term	estimate	std.error	t.stat	p.value
T.min_r	-32.37	13.92	-2.32	0.06
cwd5_v	-4.17	1.43	-2.93	0.03
PA5_r	37.33	12.63	2.96	0.03
C.min_v	9.91	4.96	2.00	0.09
T.mean_v	82.92	28.61	2.90	0.03
maxOfmax_v	-31.52	20.22	-1.56	0.17
cdd5_r	-27.66	12.48	-2.22	0.07

NSEe	0.83
NSEv	0.26
RMSE	21.67
RMSE.const	57.37
p.value of f.stat	< 0.05

PUNO

term	estimate	std.error	t.stat	p.value
T.cv.mean_r	-1161.05	126.91	-9.15	0.00
T.cv.min_v	-490.71	53.34	-9.20	0.00
C.cv_v	169.10	40.21	4.21	0.01
PA15_v	10.96	0.82	13.28	0.00
cdd10_v	-5.24	3.06	-1.71	0.14
C.min_r	-2.90	0.30	-9.56	0.00
cdd5_r	5.18	1.84	2.82	0.03

NSEe	0.99
NSEv	0.97
RMSE	2.68
RMSE.const	35
p.value of f.stat	< 0.001

TACNA

term	estimate	std.error	t.stat	p.value
HDD_v	-250.99	83.30	-3.01	0.02
maxOfmax_v	-50.39	30.08	-1.68	0.14
T.max_v	-14.90	57.47	-0.26	0.80
cdd5_r	39.37	29.35	1.34	0.23
cwd5_r	-6.92	4.60	-1.51	0.18
P.sum_v	5.53	1.76	3.15	0.02
C.mean_v	-13.23	9.68	-1.37	0.22
NSEe	0.94			
NSEv	0.62			
RMSE	58.62			
RMSE.const	253.02			
p.value of f.stat	< 0.01			

Table A.1. Table of coefficients of the RRM per region; the *estimate* shows the estimated value of the regression term; *std. error* shows the standard error of the regression term; *t.stat* shows the t-statistic; *p.value* shows the two-sided p-value of the observed t-statistic; *NSEe* (*NSEv*) shows the Nash–Sutcliffe efficiency coefficient of the estimation (validation) result; *RMSE* shows the root mean squared error between the observed yields and the estimated yields, *RMSE.const* shows the RMSE between observed yields and a constant model that takes the mean yield per region as a predictor; *p.value of f.stat* shows the one-sided p-value of the observed F-statistic

term	estimate	std.error	t.stat	p.value
T.cv.max_r	806.19	1717.16	0.47	0.64
T.cv.mean_v	-1104.83	2074.09	-0.53	0.59
T.cv.mean_r	1914.65	1066.26	1.80	0.07
C.cv_v	-209.20	79.86	-2.62	0.01
cdd10_r	-73.19	19.26	-3.80	0.00
P.cv_r	70.79	29.43	2.40	0.02
T.cv.min_r	45.34	14.18	3.20	0.00
minOfmin_v	-32.97	23.61	-1.40	0.16
minOfmin_r	-31.14	19.93	-1.56	0.12
P.cv_v	22.02	23.85	0.92	0.36
PA20_r	-10.30	9.10	-1.13	0.26
cwd5_r	6.02	1.76	3.42	0.00
C.mean_v	3.52	4.22	0.83	0.40
cdd5_v	12.08	13.24	0.91	0.36
cdd5_r	-5.60	12.79	-0.44	0.66
cwd5_v	3.41	1.95	1.75	0.08
P.max_r	1.80	1.57	1.14	0.25
C.mean_r	2.90	2.80	1.03	0.30
HDD_v	-0.25	0.85	-0.29	0.77
NSEe	0.2			
NSEv	0.11			
RMSE	197.81			
RMSE.const	222.12			
p.value of f.stat	< 0.001			

Table A.2. Table of coefficients of the PDM; the *estimate* shows the estimated value of the regression term; *std. error* shows the standard error of the regression term; *t.stat* shows the t-statistic; *p.value* shows the two-sided p-value of the observed t-statistic; *NSEe* (*NSEv*) shows the Nash–Sutcliffe efficiency coefficient of the estimation (validation) result; *RMSE* shows the root mean squared error between the observed yields and the estimated yields, *RMSE.const* shows the RMSE between

observed yields and a constant model that takes the mean yield per region as a predictor; *p.value of f.stat* shows the one-sided p-value of the observed F-statistic

Region	Mean yield in kg/ha	Mean yield in kg/ha with 77mm more water	Difference in kg/ha	Difference in %	p.value
AMAZONAS	849.3	861.4	12.0	1.4	0.00
ANCASH	1241.5	1239.0	-2.5	-0.2	0.20
AREQUIPA	3618.7	3740.1	121.4	3.4	0.06
AYACUCHO	1031.4	1018.6	-12.8	-1.2	0.01
CAJAMARCA	858.2	850.8	-7.3	-0.9	0.06
CUSCO	2342.3	2264.7	-77.7	-3.3	0.00
HUANUCO	1206.0	1239.2	33.2	2.8	0.00
ICA	2815.3	2815.3	0.0	0.0	NaN
JUNIN	1885.9	1935.4	49.6	2.6	0.17
LA LIBERTAD	1547.7	1533.1	-14.7	-0.9	0.34
LAMBAYEQUE	1917.4	1533.3	-384.1	-20.0	0.00
MOQUEGUA	1345.5	1373.3	27.9	2.1	0.02
PASCO	1256.6	1184.1	-72.5	-5.8	0.00
PIURA	932.3	1088.7	156.4	16.8	0.00
PUNO	1603.1	1608.9	5.9	0.4	0.00
TACNA	2729.9	3133.3	403.4	14.8	0.00

Table A.3. The effect of 77mm more water in growing season on starchy maize yields. The additional amount is the minimum necessary additional water in 2040-2060 to compensate for an increased potential evapotranspiration due to increased temperatures in Peru; the results are based on the RRMs, the p.value shows the two-sided p-value of the observed t-statistic

Supplementary Text

Text A.1. Climatic conditions for maize

Depending on the cultivar and the phenological stage, the optimal climatic conditions for maize vary. Over the entire growing season, the optimal temperature range is between 25°C and 30°C (Rötter and Van De Geijn, 1999). Above the optimum temperature range, photosynthesis is reduced, whereas respiration rates rise, such that net photosynthesis rates decline (Barnabás et al., 2008). If temperatures exceed 42°C, maize growth stops (Yin et al., 1995). Particularly during flowering, maize is sensitive to heat stress, as it can lead to the desiccation of pollen or a reduction in grain numbers (Sánchez et al., 2014). If the time for grain filling is reduced, grain size and consequently yields decline (Rötter et al., 2018). Maize is also susceptible to frost with lethal damages of the stem, leaf and ear occurring already after a couple of hours below 0°C (Carter and Hestermann, 1990).

The optimal rainfall required in the growing season is around 500 to 800mm (Critchley and Siegert, 1991). For optimal plant development, the timing and duration of water supply are equally critical. During flowering, maize requires sufficient water supply. Before pollination water stress leads to kernel abortion, even if at the time of pollination sufficient water is available (Westgate and Boyer, 1985). Excessive rain, in contrast, can lead to soil water saturation and oxygen deficiency, which limits root respiration and the growth of roots. Also root water uptake is reduced in water-logged soils (Rötter et al., 2018). Rainfall that exceeds the water holding capacity of the soil can lead to the leaching of nutrients and nutrient deficiencies of the plant. Soil loss and mechanic damages of the plant can occur in case of flooding and soil erosion (Rötter et al., 2018).

Compound abiotic stresses may be particularly damaging, beyond the sum of the damages caused by individual stressors (Barnabás et al., 2008). Higher temperatures are often accompanied with dryer conditions, which leads to a higher vapour pressure deficit and drives faster transpiration rates. As a response, plants can reduce the stomatal conductance and save water, but at the price of less carbon assimilation and lower nutrient uptake, which in turn leads to lower growth rates (Lobell et al., 2013; Long, 2006).

Text A.2. Equations for the calculation of weather variables; the variables are calculated for the vegetative and the reproductive phase of the growing season; *d* denotes the number of days within the vegetative or the reproductive phase; *Days* denotes the total number of days within the vegetative or the reproductive phase

$$T.mean = \frac{1}{Days}\sum_{d=1}^{Days} T_d \quad (1)$$

With T as daily mean temperature

$$T.max = \frac{1}{Days}\sum_{d=1}^{Days} \max(T_d) \quad (2)$$

With T as daily mean temperature

$$maxOfmax = \max(T_d) \quad (3)$$

With T as daily maximum temperature

$$T.min = \frac{1}{Days}\sum_{d=1}^{Days} \min(T_d) \quad (4)$$

With T as daily mean temperature

$$minOfmin = \min(T_d) \quad (5)$$

With T as daily minimum temperature

$$T.cv.mean = \frac{\sqrt{\frac{1}{Days}\sum_{d=1}^{Days}(T_d - T.mean)^2}}{T.mean} \quad (6)$$

With T as daily mean temperature and $T.mean$ as defined in Eq. 1

$$T.cv.min = \frac{\sqrt{\frac{1}{Days}\sum_{d=1}^{Days}(T_d - T.min)^2}}{T.min} \quad (7)$$

With T as daily minimum temperature and $T.min$ as defined in Eq. 4

$$T.cv.max = \frac{\sqrt{\frac{1}{Days}\sum_{d=1}^{Days}(T_d - T.max)^2}}{T.max} \quad (8)$$

With T as daily maximum temperature and $T.max$ as defined in Eq. 2

$$HDD = \sum_{d=1}^{Days}(T_d - T^{HDD}) \quad T_d^{HDD} = \begin{cases} 0, & T_d < 30 \\ T_d, & T_d \geq 30 \end{cases} \quad (9)$$

With T as daily maximum temperature and T^{HDD} as the temperature ≥ 30°C

$$FDD = \sum_{d=1}^{Days} T_d^{FDD} \quad T_d^{FDD} = \begin{cases} 0, & T_d > 0 \\ T_d, & T_d \leq 0 \end{cases} \quad (10)$$

With T as daily minimum temperature

$$P.sum = \sum_{d=1}^{Days} P_d \quad (11)$$

With P as daily precipitation

$$P.mean = \frac{1}{Days}\sum_{d=1}^{Days} P_d \quad (12)$$

With P as daily precipitation

$$P.max = \max(P_d) \quad (13)$$

With P as daily precipitation

$$P.cv = \frac{\sqrt{\frac{1}{Days}\sum_{d=1}^{Days}(P_d - P.mean)^2}}{P.mean} \quad (14)$$

With P as daily precipitation and $P.mean$ as defined in Eq. 12

$$DWP = \sum_{d=1}^{Days} P_d^{DWP} \qquad P_d^{DWP} = \begin{cases} 0, & P_d > 0 \\ 1, & P_d = 0 \end{cases} \tag{15}$$

With P as daily precipitation

$$PA5 = \sum_{d=1}^{Days} P_d^{A5} \qquad P_d^{A5} = \begin{cases} 0, & P_d \leq 5 \\ 1, & P_d > 5 \end{cases} \tag{16}$$

With P as daily precipitation; the equation is also used for the thresholds 10mm, 15mm and 20mm

$$cdd5 = \sum_{d=5}^{Days} P_d^{cdd5} \qquad P_d^{cdd5} = \begin{cases} 1, & P_d < 0.5 \vee P_{d-1} < 0.5 \vee P_{d-2} < 0.5 \vee P_{d-3} < 0.5 \vee P_{d-4} < 0.5 \\ 0, & otherwise \end{cases} \tag{17}$$

With P as daily precipitation; the equation is also used for the calculation of consecutive dry days of more than 10 days (cdd10)

$$cwd5 = \sum_{d=5}^{Days} P_d^{cwd5} \qquad P_d^{cwd5} = \begin{cases} 1, & P_d > 0.5 \vee P_{d-1} > 0.5 \vee P_{d-2} > 0.5 \vee P_{d-3} > 0.5 \vee P_{d-4} > 0.5 \\ 0, & otherwise \end{cases} \tag{18}$$

With P as daily precipitation; the equation is also used for the calculation of consecutive wet days of more than 10 days (cwd10)

$$C.mean = \frac{1}{Days} \sum_{d=1}^{Days} C_d \tag{19}$$

With C as cloud fraction

$$C.min = \frac{1}{Days} \sum_{d=1}^{Days} \min(C_d) \tag{20}$$

With C as cloud fraction

$$C.cv = \frac{\sqrt{\frac{1}{Days} \sum_{d=1}^{Days} (C_d - C.mean)^2}}{C.mean} \tag{21}$$

With C as cloud fraction and $C.mean$ as defined in Eq. 19

$$GDD = \sum_{d=1}^{Days} T_d^{GDD} \qquad T_d^{GDD} = \begin{cases} 0, & T_d < T^{Base} \\ T_d - T^{Base}, & x \geq T^{Base} \leq T_d \leq T^{Opt} \\ T^{Opt} - T^{Base}, & x \geq T_d > T^{Opt} \end{cases} \tag{22}$$

With T as daily mean temperature; T^{Base} as base temperature of 10°C; T^{Opt} as optimal temperature of 30°C (Gilmore and Rogers, 1958)

Text A.3. Description of variable selection per RRM

Even though the selected variables differ per region, some patterns can be observed. Lambayeque and Piura are in the low elevated northern coastal region. Whereas precipitation in these two regions generally has a positive impact on yields, the distribution of rain matters a lot in the hot desert climate. Both too many consecutive dry or wet days are detrimental for yields. Also too high temperatures have a negative impact. The southern coast of Peru, which is mostly in the cold desert climate (Ica, Arequipa and Moquegua) is determined by a positive impact of precipitation on maize production. Tacna is south of these regions and also has some areas that are in the hot desert climate. Here, high temperatures (HDD, maxOfmax and T.max) in the vegetative phase depress yields. Also rain distribution seems to be important – as both cwd and cdd have a negative impact, whereas precipitation sum positively influences maize yields.

In the Highlands, most regions encompass several climatic zones. Cusco, Ayacucho and Huancavelica, for example, are within the subtropical highland climate and cold semi-arid climate, which is why even within one region high variations in terms of weather occurs. Yields in Cusco are negatively impacted by too high precipitation and too high temperatures. In contrast, the model for Ayacucho even suggests that particularly high precipitation levels (above 15mm and maximum precipitation) are beneficial, whereas moderate precipitation levels (above 5mm) were negative for starchy maize yields. The negative coefficient of minimum temperature – suggesting that lower minimum temperatures are beneficial – is unexpected in mountainous areas and requires further investigation. For the model in Junín only consecutive dry spells longer than 5 days in the reproductive phase were relevant. It correlates negatively with yields and can explain 35% of yield variability. Huánuco and Pasco are both in the tropical rainforest climate. Whereas in both regions too high temperatures are detrimental for maize production, Huánuco shows a positive correlation with precipitation whereas in Pasco too high precipitation in the vegetative phase were harmful. Yields in Cajamarca in the northern Highlands are negatively influenced by too wet conditions in particular in the vegetative phase (precipitation above 20mm and maximum precipitation show negative correlations, whereas consecutive dry days have a positive impact). Also high variations in the mean temperature have a negative impact. A similar pattern can be seen in Amazonas, where also variations in the mean temperature and in precipitation are negatively influencing starchy maize yields. Moreover, too wet weather (precipitation above 20mm) and too long dry spells proved to be detrimental.

References

Aybar, C., Fernández, C., Huerta, A., Lavado, W., Vega, F., Felipe-Obando, O., 2019. Construction of a high-resolution gridded rainfall dataset for Peru from 1981 to the present day. Hydrological Sciences Journal 00, 1–16. https://doi.org/10.1080/02626667.2019.1649411

Barnabás, B., Jäger, K., Fehér, A., 2008. The effect of drought and heat stress on reproductive processes in cereals. Plant, Cell and Environment 31, 11–38. https://doi.org/10.1111/j.1365-3040.2007.01727.x

Carter, P.R., Hestermann, O.B., 1990. Handling Corn Damaged By Autumn Frost [WWW Document]. National Corn Handbook - Climate & Weather. URL https://www.baycounty-mi.gov/Docs/CitizenCorps/HandlingCornDamageByAutumnFrost.pdf (accessed 5.1.19).

Critchley, W., Siegert, K., 1991. Water harvesting [WWW Document]. URL http://www.fao.org/3/U3160E/u3160e04.htm (accessed 5.1.19).

Gilmore, E.C., Rogers, J.S., 1958. Heat Units as a Method of Measuring Maturity in Corn. Agronomy Journal 50, 611–315. https://doi.org/10.2134/agronj1958.00021962005000100014x

INEI, 2017. Perú - Encuesta Nacional Agropecuaria [WWW Document]. URL https://webinei.inei.gob.pe/anda_inei/index.php/catalog/654/ (accessed 11.30.18).

Lobell, D.B., Hammer, G.L., McLean, G., Messina, C., Roberts, M.J., Schlenker, W., 2013. The critical role of extreme heat for maize production in the United States. Nature Climate Change 3, 497–501. https://doi.org/10.1038/nclimate1832

Long, S.P., 2006. Food for Thought: Lower-Than-Expected Crop Yield Stimulation with Rising CO2 Concentrations. Science (1979) 312, 1918–1921. https://doi.org/10.1126/science.1114722

Peel, M.C., Finlayson, B.L., McMahon, T.A., 2007. Updated world map of the Köppen-Geiger climate classification. Hydrology and Earth System Sciences 11, 1633–1644. https://doi.org/10.5194/hess-11-1633-2007

Rötter, R.P., Appiah, M., Fichtler, E., Kersebaum, K.C., Trnka, M., Hoffmann, M.P., 2018. Linking modelling and experimentation to better capture crop impacts of agroclimatic extremes—A review. Field Crops Research 221, 142–156. https://doi.org/10.1016/j.fcr.2018.02.023

Rötter, R., Van De Geijn, S.C., 1999. Climate Change Effects on Plant Growth, Crop Yield and Livestock. Climatic Change 43, 651–681.

Sánchez, B., Rasmussen, A., Porter, J.R., 2014. Temperatures and the growth and development of maize and rice: A review. Global Change Biology 20, 408–417. https://doi.org/10.1111/gcb.12389

Westgate, M.E., Boyer, J.S., 1985. Osmotic adjustment and the inhibition of leaf, root, stem and silk growth at low water potentials in maize. Planta 164, 540–549.

Yin, X., Kropff, M.J., McLaren, G., Visperas, R.M., 1995. A nonlinear model for crop development as a function of temperature. Agricultural and Forest Meteorology 77, 1–16. https://doi.org/10.1016/0168-1923(95)02236-Q

6.2 Supplementary Information to: "Robustly forecasting maize yields in Tanzania based on climatic predictors"

Author names and affiliations:
Rahel Laudien[a*], Bernhard Schauberger[a], David Makowski[b], Christoph Gornott[ac]

[a]Potsdam Institute for Climate Impact Research (PIK)
Member of the Leibniz Association
P.O. Box 60 12 03
D-14412 Potsdam
Germany

[b]National Research Institute for Agriculture, Food and Environment (INRAE)
UMR 518 AgroParisTech Université Paris-Saclay
16 rue Claude Bernard
F-75231 Paris Cedex 05
France

[c]Agroecosystem Analysis and Modelling
Faculty of Organic Agricultural Sciences
University of Kassel
Mönchebergstraße 19
34109 Kassel
Germany

Corresponding author:
Rahel Laudien (laudien@pik-potsdam.de, +49 331 28820771)

Co-authors:
Christoph Gornott (gornott@pik-potsdam.de, +49 331 2882655)
Bernhard Schauberger (schauber@pik-potsdam.de, +49 331 28820890)
David Makowski (david.makowski@inrae.fr, +33 698883675)

1. Input variables for the Regional Regression Model

input name	Definition	unit	Vegetative phase			Reproductive phase		
			median	min	max	median	min	max
psum	Precipitation sum	mm	303.97	85.50	1080.59	200.86	3.65	689.90
cdd5	Consecutive dry days of equal or more than 5 days		1.00	0.00	4.00	2.00	0.00	6.00
cdd10	Consecutive dry days of equal or more than 10 days		0.00	0.00	2.00	0.00	0.00	3.00
cdd15	Consecutive dry days of equal or more than 15 days		0.00	0.00	1.00	0.00	0.00	2.00
cdd20	Consecutive dry days of equal or more than 20 days		0.00	0.00	1.00	0.00	0.00	1.00
pB5	Number of precipitation events below 5mm per day		9.00	3.00	19.00	8.00	2.00	25.00
pB10	Number of precipitation events below 10mm per day		18.00	6.00	35.00	13.00	2.00	34.00
pB15	Number of precipitation events below 15mm per day		23.50	8.00	40.00	17.00	2.00	38.00
pA5	Number of precipitation events equal or above 5mm per day		20.00	6.00	39.00	14.00	0.00	33.00
pA10	Number of precipitation events equal or above 10mm per day		11.00	2.00	26.00	7.00	0.00	25.00
pA15	Number of precipitation events equal or above 15mm per day		6.00	0.00	18.00	3.00	0.00	18.00
precip.p99	Number of times the daily precipitation sum exceeds the 99% percentile of the daily precipitation sum		0.00	0.00	4.00	0.00	0.00	3.00

SI Table 1. *Variables related to precipitation*

input name	Definition	unit	Vegetative phase			Reproductive phase		
			median	min	max	median	min	max
tas.median	Median of the daily mean temperature	°C	23.93	21.51	28.18	23.87	19.81	27.42
tas.max	Median of the daily maximum temperature	°C	28.00	24.97	33.36	27.90	24.61	31.47
tas.min	Median of the daily minimum temperature	°C	19.29	17.58	26.28	19.21	14.34	25.22
tas.max.p99	Number of times the daily maximum temperature exceeds the 99% percentile of the daily maximum temperature		0.00	0.00	9.00	0.00	0.00	7.00
tas.min.p01	Number of times the daily minimum temperature falls below the 1% percentile of the daily minimum temperature		0.00	0.00	5.50	0.00	0.00	5.50

SI Table 2. *Variables related to temperature*

input name	Definition	median	min	max
iod_30.median	Median Indian Ocean Dipole over the last 30 days before the start of the growing season	-0.04	-0.57	0.52
iod_30.p01	Number of times the Indian Ocean Dipole falls below the 1% Percentile of the Indian Ocean Dipole over the last 30 days before the start of the growing season	0.00	0.00	2.00
iod_30.p99	Number of times the Indian Ocean Dipole exceeds the 99% Percentile of the Indian Ocean Dipole over the last 30 days before the start of the growing season	3.00	1.00	3.00
nino34_90.median	Median SST anomaly in the El Nino 3.4. zone over the last 90 days before the start of the growing season	-0.26	-1.61	2.58

nino34_90.p01	Number of times the SST anomaly in the El Nino 3.4 falls below the 1% Percentile of the SST anomaly in the El Nino 3.4 zone over the last 90 days before the start of the growing season	0.00	0.00	4.00
nino34_90.p99	Number of times the SST anomaly in the El Nino 3.4 zone exceeds the 99% Percentile of the SST anomaly in the El Nino 3.4 zone over the last 90 days before the start of the growing season	5.00	0.00	5.00
wp_90.median	Median SST anomaly in the West Pacific over that last 90 days before the start of the growing season	0.42	0.08	0.85
wp_90.p01	Number of times the SST anomaly in the West Pacific falls below the 1% Percentile of the SST anomaly in the West Pacific over the last 90 days before the start of the growing season	0.00	0.00	2.00
wp_90.p99	Number of times the SST anomaly in the West Pacific exceeds the 99% Percentile of the SST anomaly in the West Pacific over the last 90 days before the start of the growing season	3.00	0.00	5.00

SI Table 3. *Variables related to sea surface temperatures (SST)*

2. Significance of estimated regression coefficients

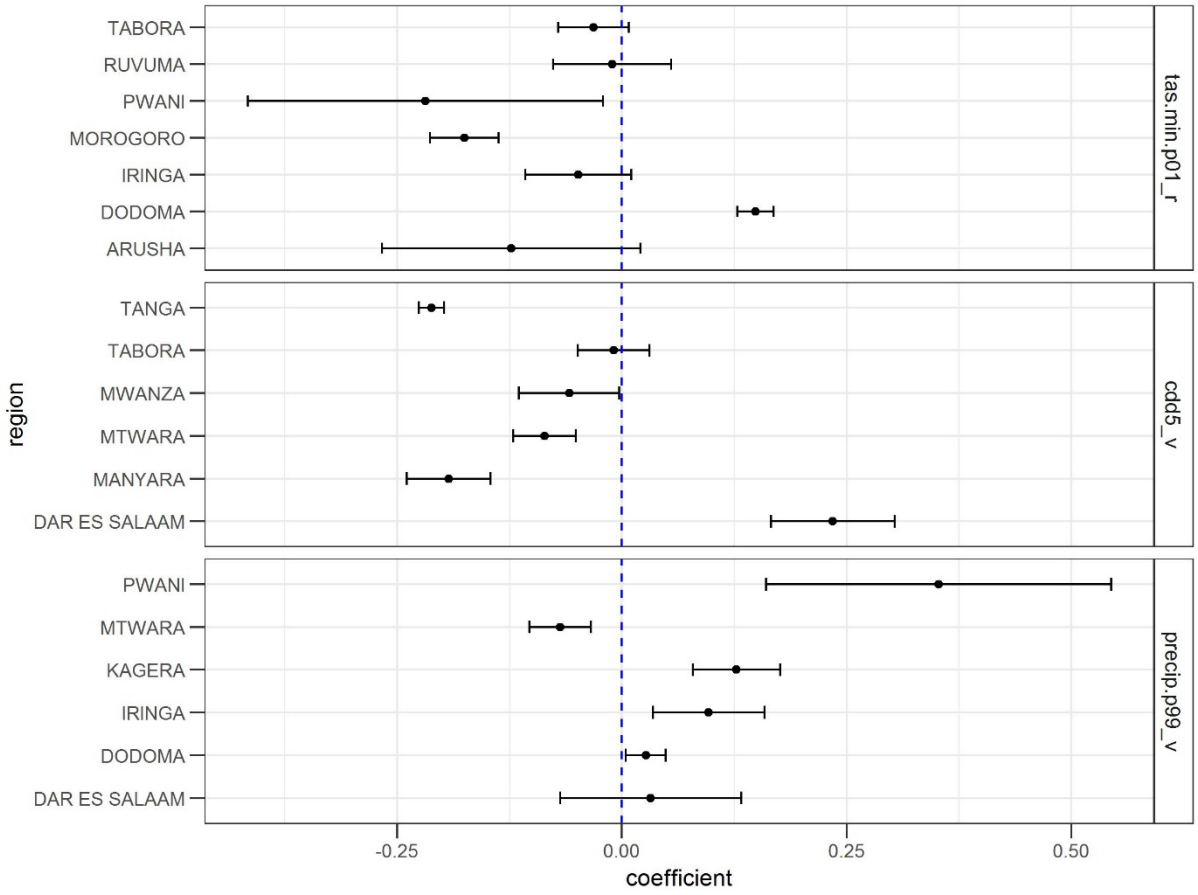

SI Fig. 1. *Estimated regression coefficients for the three most often selected weather variables for Tanzanian regions. The three most often selected variables are temperature events below the 1% minimum temperature percentile in the reproductive period (tas.min.p01_r), consecutive dry days of more than 5 days in the vegetative phase (cdd5_v) and precipitation events above the 99th precipitation percentile in the vegetative phase (precip.p99_v). Note that this analysis excludes the model coefficients with a performance lower than an NSE of 0.3 in the level 1 validation, because we assumed these models as not robust enough for further analysis. The coefficients show standardised values, i.e. they show the change in yield per standard deviation of the input variable. The horizontal bars show the 95% significance interval for the point estimator. The geographic location of the regions can be seen in SI Fig. 6.*

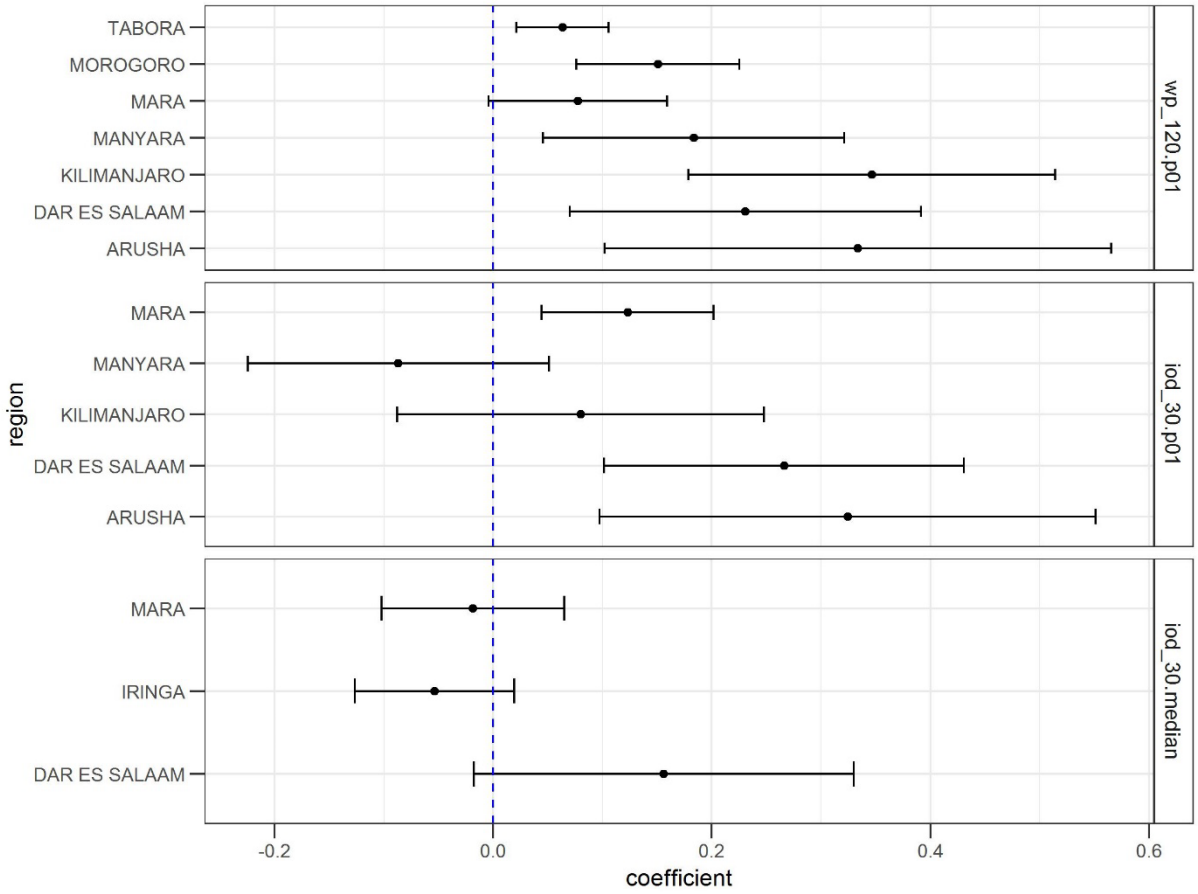

SI Fig. 2. *Estimated regression coefficients for the three most often selected sea surface temperature (SST) variables for Tanzanian regions. The three most often selected variables are the number of times the SST falls below the 1% percentile of the West Pacific considering a lead time of 120 days (wp_120.p01), the number of times the SST falls below the 1% percentile of the Indian Ocean Dipole considering a lead time of 30 days (iod_30.p01) and the median SST of the IOD considering a lead time of 30 days (iod_30.median). Note that this analysis excludes the model coefficients with a performance lower than an NSE of 0.3 in the level 1 validation, because we assumed these models as not robust enough for further analysis. The coefficients show standardised values, i.e. they show the change in yield per standard deviation of the input variable. The horizontal bars show the 95% significance interval for the point estimator. The geographic location of the regions can be seen in SI Fig. 6.*

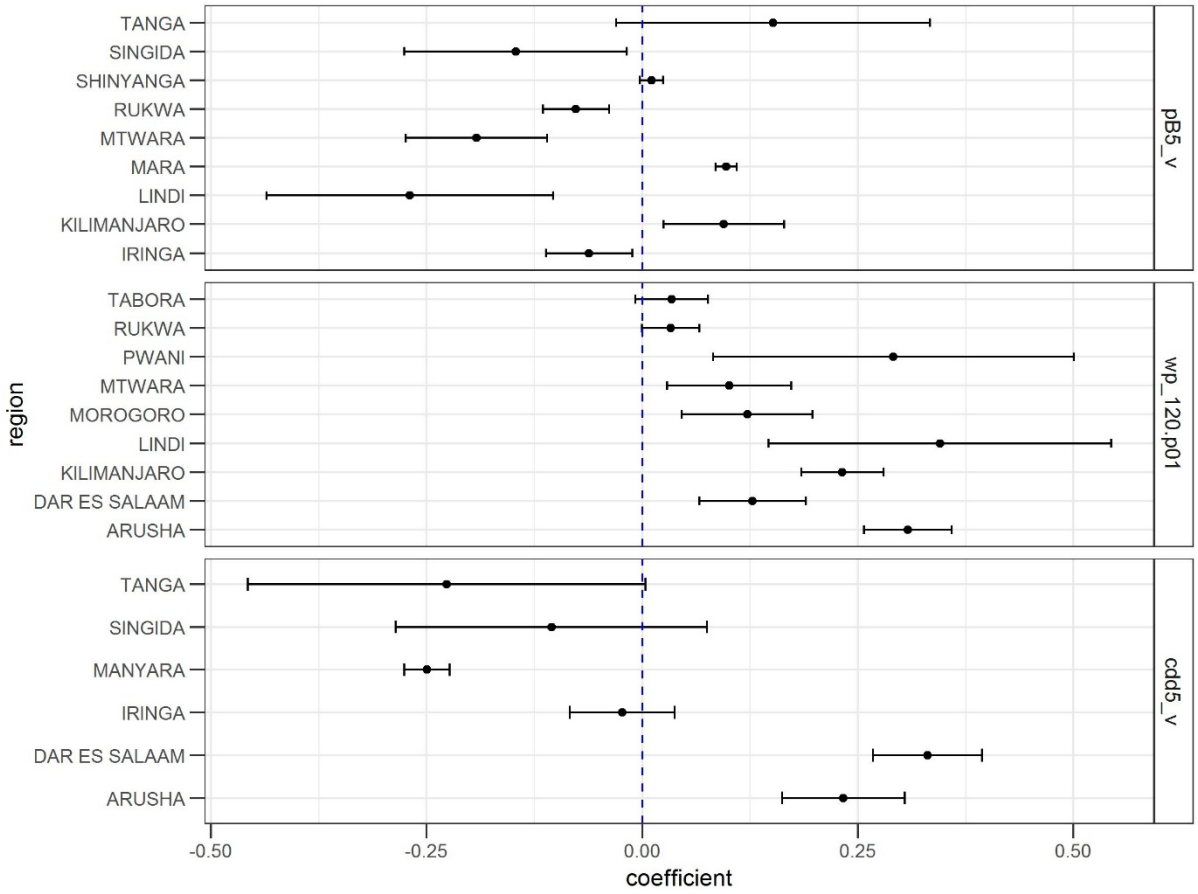

SI Fig. 3. *Estimated regression coefficients for the three most often selected variables in the forecast based on weather and sea surface temperature (SST) variables for Tanzanian regions. The three most often selected variables are precipitation events below 5 mm in the vegetative phase (pB5_v), the number of times the SST in the West Pacific falls below the 1% percentile considering a lead time of 120 days (wp_120.p01) and consecutive dry days of more than 5 days in the vegetative phase (cdd5_v). Note that this analysis excludes the model coefficients with a performance lower than an NSE of 0.3 in the level 1 validation, because we assumed these models as not robust enough for further analysis. The coefficients show standardised values, i.e. they show the change in yield per standard deviation of the input variable. The horizontal bars show the 95% significance interval for the point estimator. The geographic location of the regions can be seen in SI Fig. 6.*

3. Comparison of forecasted anomalies to a constant model

region	RMSE constant model	RMSE forecasted anomalies
Dodoma	0.28	0.08
Arusha	0.52	0.05
Kilimanjaro	0.44	0.04
Tanga	0.61	0.20
Morogoro	0.30	0.07
Pwani	0.58	0.24
Dar es Salaam	0.44	0.05
Lindi	0.30	0.11
Mtwara	0.32	0.09
Ruvuma	0.12	0.05
Iringa	0.18	0.05
Mbeya	0.13	0.01
Singida	0.24	0.10

Tabora	0.12	0.04
Rukwa	0.14	0.03
Kigoma	0.10	0.06
Shinyanga	0.16	0.01
Kagera	0.20	0.10
Mwanza	0.13	0.07
Mara	0.19	0.01
Manyara	0.31	0.03

SI Table 4. *Comparison of the performance of the forecasted yield anomalies with a lead time of ca. 6 weeks (right column) and a constant model that only takes the mean yield excluding the year that is forecasted as a predictor (middle column). The comparison is based on the root mean squared error (RMSE) between the observed yield and the modelled yield.*

4. Correlation between input variables

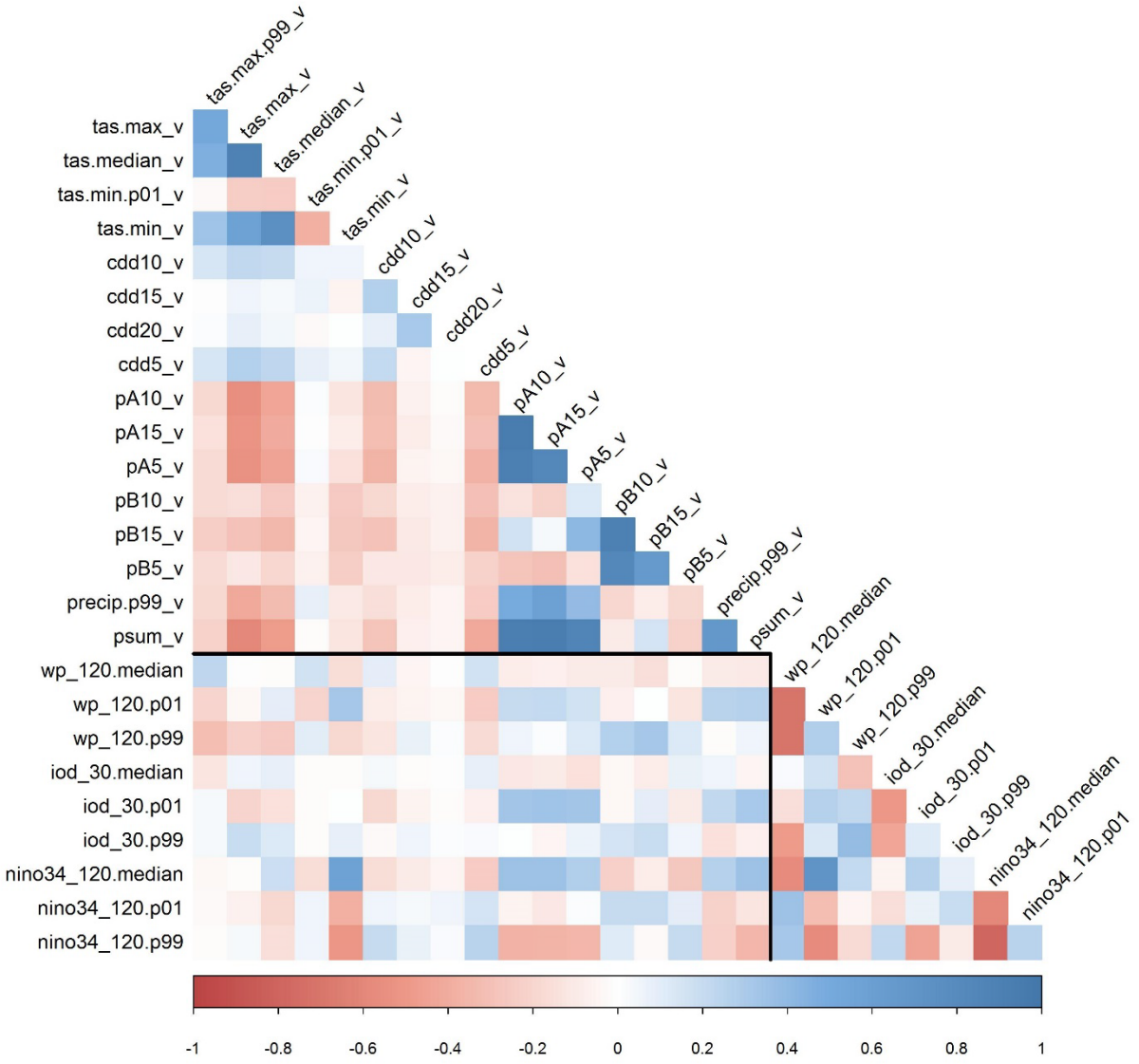

SI Fig. 4. *Correlogram of input variables in sea surface temperature (SST) and weather categories; a strong correlation (absolute value of Pearson's r coefficient > 0.5) between SST and weather variables can only be found between the minimum temperature and the median SST in the El Niño 3.4 zone with a lead time of 120 days.*

5. Performance of the forecasts derived from the model combining SST and weather inputs

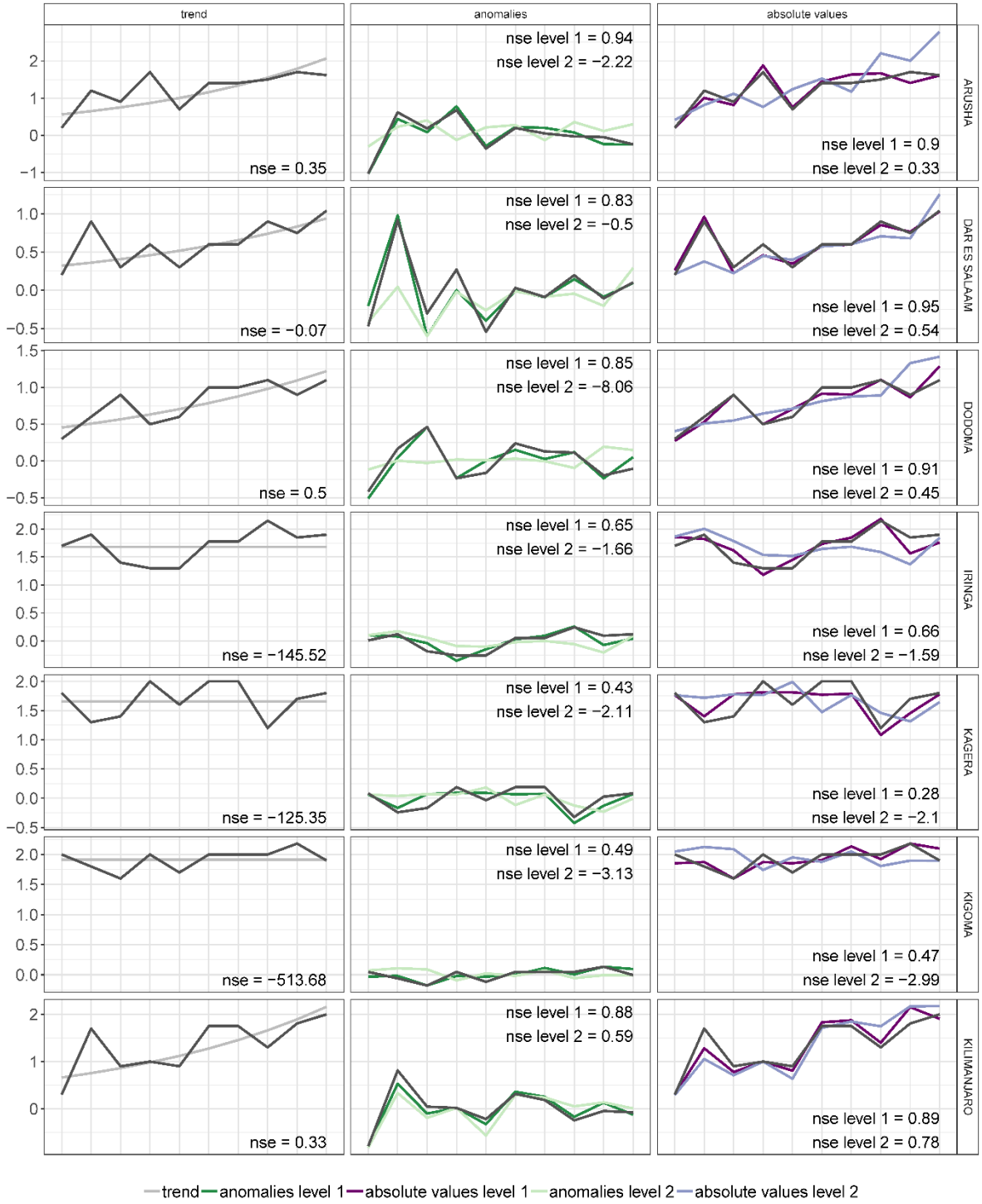

SI Fig. 5. *Regional performance of the forecasts derived from the model combining SST and weather inputs. Model assessment was done separately for the trend (left panel), the variability (middle panel) and the absolute yields, which is a combination of trend and variability (right panel). The dark colour (dark green and dark purple) shows the forecast when the level 1 validation is applied. The corresponding NSE value is shown as "nse level 1" in the upper right corner of the panels. The light colour (light green and light purple) and the "nse level 2" show the results of the level 2 validation. Because the trend was fitted based on logarithmic values, the transformation back to linear values results in a slightly curved shape.*

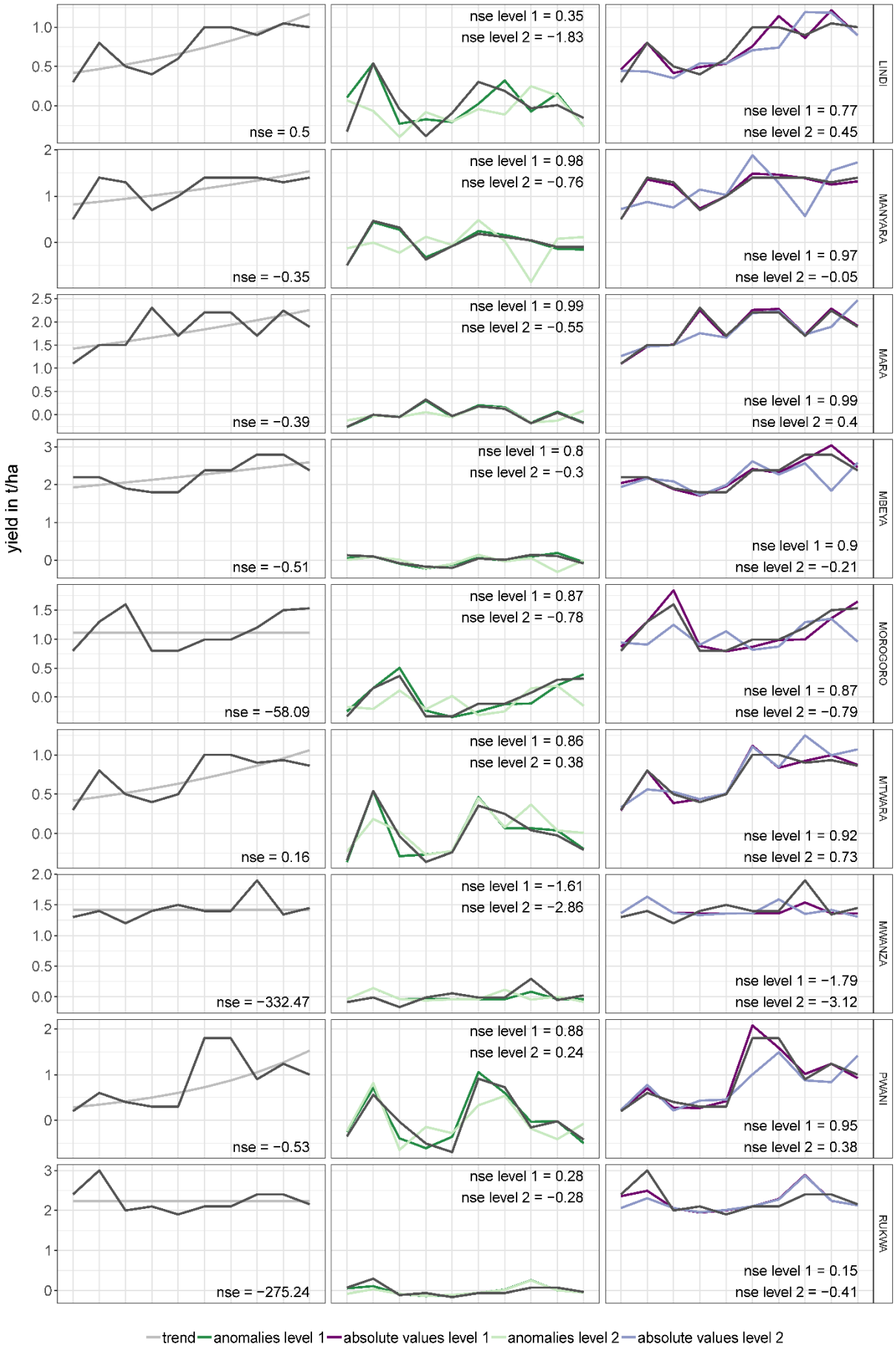

Continuation of Fig. 5

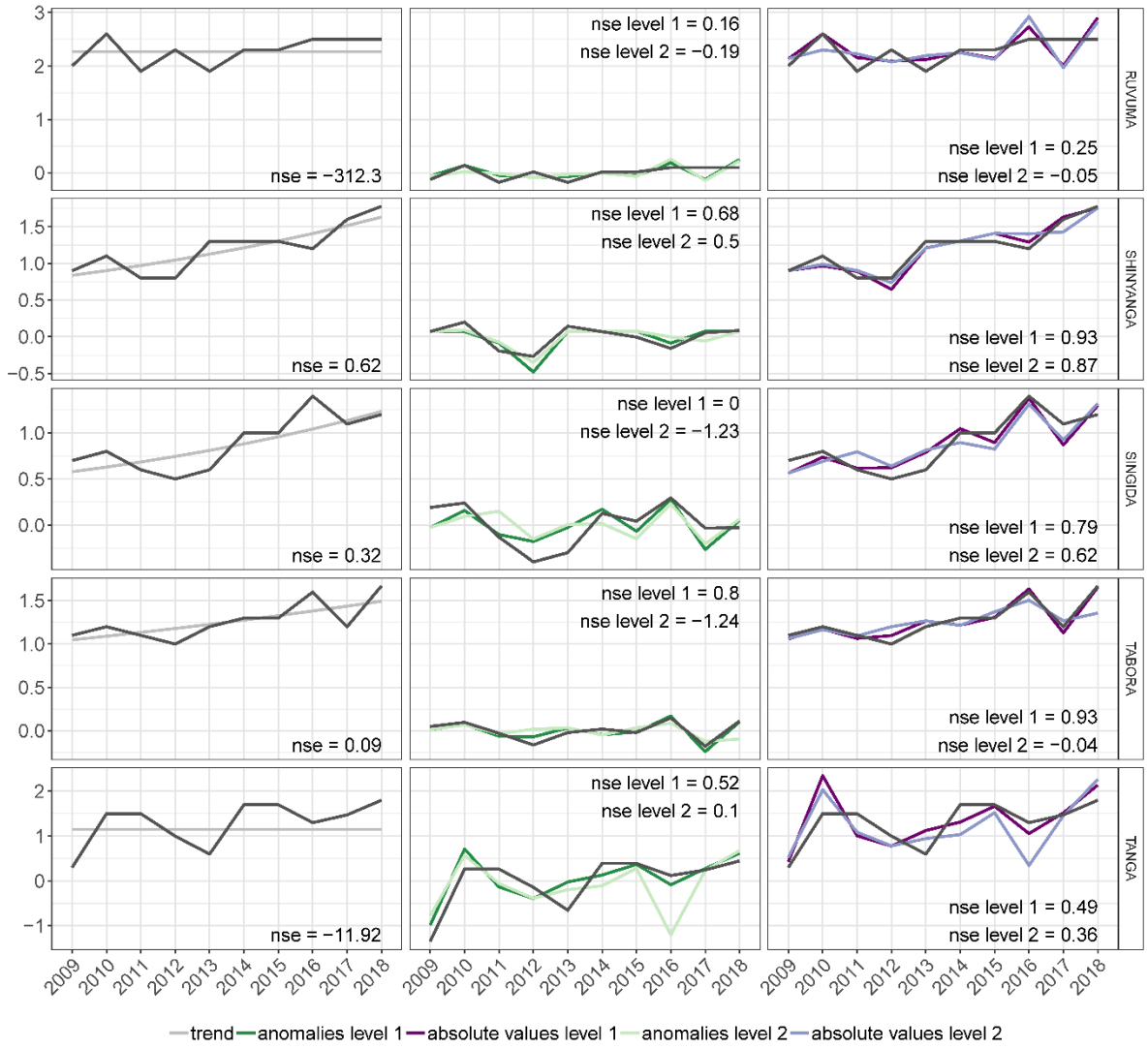

Continuation of Fig. 5

6. Strong spatiotemporal variability of maize yields in Tanzania

Maize yields in Tanzania show a high variability and are on a low average level: from 2016 to 2018 maize yields were at 1.6 t/ha on average. The regions with the highest yields (Mbeya, Ruvuma, Rukwa) show the lowest inter-annual variation. The main maize producing regions are Mbeya, Ruvuma, Iringa, Rukwa and Shinyanga).

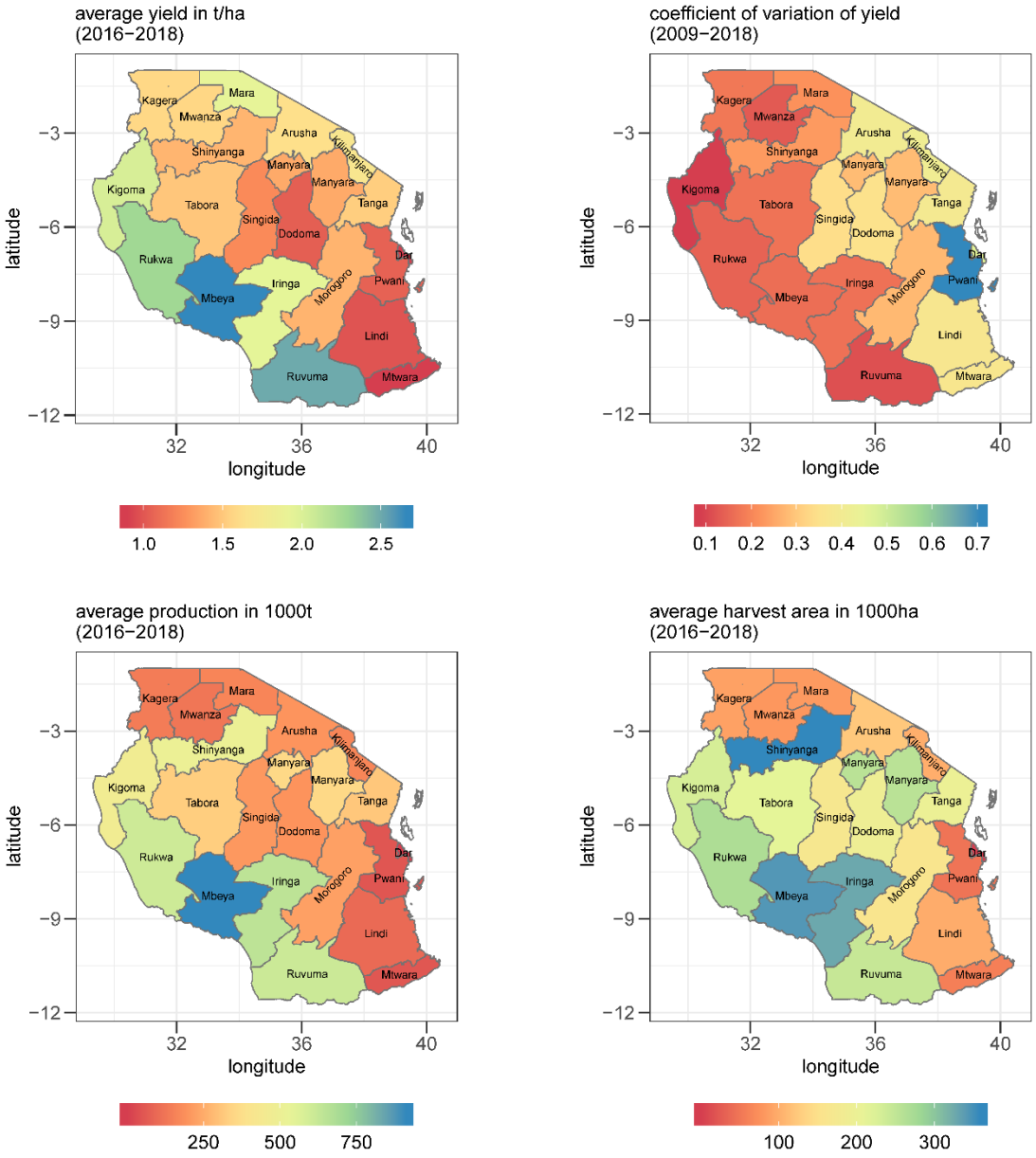

SI Fig. 6. *Average maize yields, production and harvest area from 2016 – 2018 and the coefficient of variation of yields from all available years (2009-2018).*

7. Correlation between yield and SST indices with different lead times

We assessed the influence of the following SST (sea surface temperature) indices on Tanzanian yield variability:

1) El Niño 3.4 zone (170°W – 120° W, 5°S - 5°N)
2) West Pacific Box (WP) (130°E – 160°E, 10°S – 10°N)
3) Indian Ocean Dipole (IOD), which is the non-normalised difference between the West Indian Ocean (50°E – 70°E, 10°S – 10°N) and the Eastern Indian Ocean (90°E – 110°E, 10°S - 0°N)

To account for the lag in influence of the SST on rainfall in East Africa, we tested different lag times (0, 30, 60, 90, 120, 150 and 180 days). The strongest influence of SST in the El Niño 3.4 zone on yields in Tanzania can be found at a lead time of 90 and 120 days (SI Fig. 7). There is a positive correlation between yields and the median SST in El Niño 3.4, which could be explained by higher rainfall amounts during the short rains in East Africa in relation with a higher El Niño 3.4 SST [1–3]. Extreme high and low values of the SST in El Niño 3.4 (values above the 99% and below the 1% percentiles) are related with lower maize yields in Tanzania.

Like the SST in El Niño 3.4, the IOD is also positively correlated with rainfall in East Africa during the short rains [1–3]. For most regions, the IOD shows the strongest correlations at a lead time of 30 days. At this lead time, the median IOD shows a negative correlation with Tanzanian yield variability. Values below the 1% percentile are positively correlated with yields. At other lead times, the correlation patterns show different directions and the IOD, in contrast to El Niño 3.4 and WP, has the highest region-to-region variability.

The median SST in WP is negatively correlated with maize yield variability in Tanzania. Whereas high values of the SST in WP do not show a clear direction of the correlation, yields tend to be higher in Tanzania the more often the SST falls below the 1%percentile. This can be related to the negative correlation of SST in WP with East African rainfall during the long rains [1–3]. The highest correlation can be found at a lead time of 90 and 120 days.

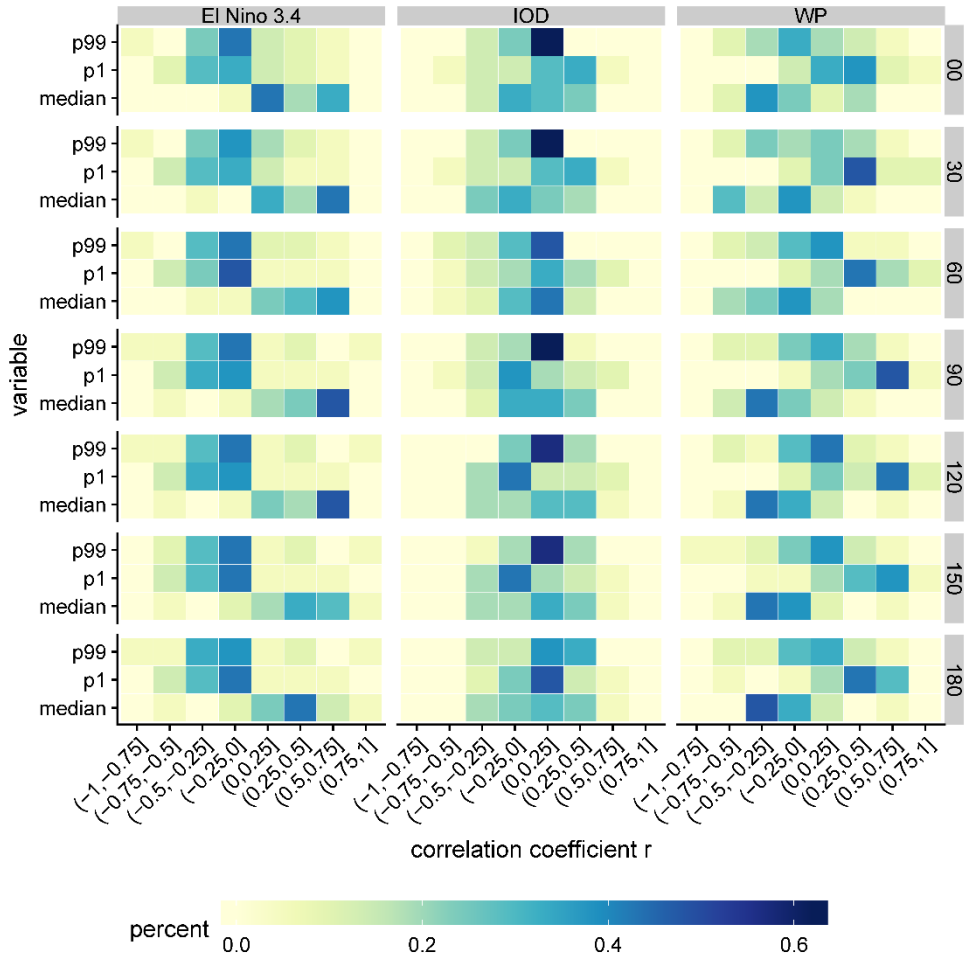

SI Fig. 7. The distribution plot shows the correlation coefficients (Pearson's r) between the demeaned and detrended yields and different standardised SST indices (median, number of times the SST is above the 99% percentile and below the 1% percentile). For a better overview, the correlation coefficients were categorized in classes of 0.25 ranges, so from -1 to -0.75, from -0.75 to -0.5 and so on. The colour indicates how many regions of 21 regions in Tanzania have a particular correlation range between yield and the SST index, e.g. dark blue indicates that 60% of regions (i.e. ca. 13 regions of 21 regions) show a correlation between yield and the SST index of e.g. between 0 and 0.25. The correlation matrix is presented separately for each SST index (horizontally) and the lead times 0, 30, 60, 90, 120, 150 and 180 days (vertically).

8. Maize growing season in Tanzania

To define the start of the growing season, we tested the several crop calendars and decided to use the approach of Dodd and Jolliffe (2001) [4] that proved to be most suitable for the purpose of our study. In the following paragraphs, we discuss advantages and disadvantages of different crop calendars for maize production in Tanzania.

8.1. FAO crop calendar

The FAO crop calendar from 2012 provides crop-specific planting and harvesting months and the growing season length on district level [5]. The calendar does not distinguish between the short and the long rains in the bimodal rainfall areas in the North and in the Coastal regions in Tanzania, even though both rainfall seasons are used for crop production [6]. Moreover, the calendar seems to have unreasonable outliers: Most parts of the Ruvuma region have a growing season from May to August, which is within the dry season. Also the district Sumbawanga Urban in Rukwa has a growing season length of 180days, in contrast to the other parts of the country that have a growing season length of 90 or 120 days.

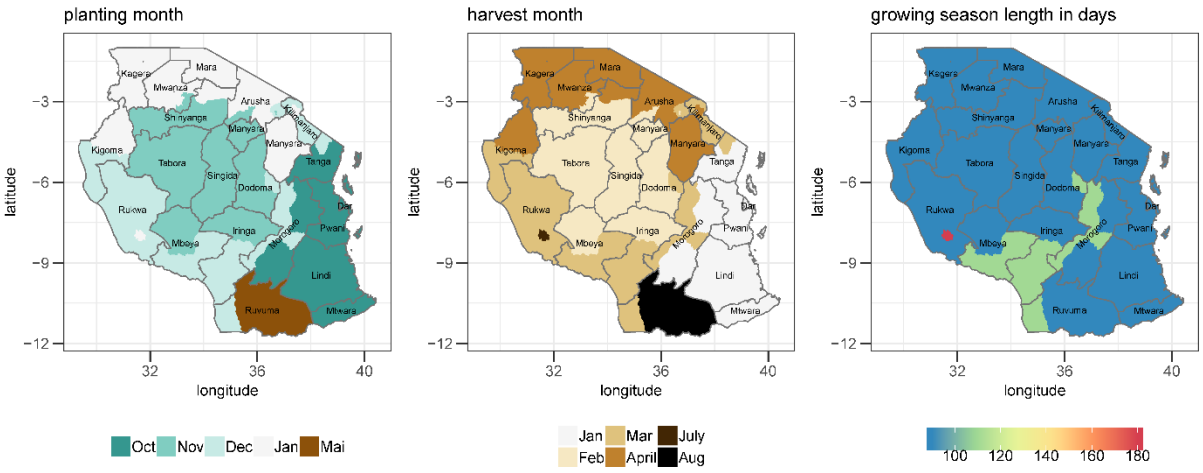

SI Fig. 8. Crop calendar for maize based on the FAO crop calendar from 2012 [5], planting is defined as the onset of planting and harvest is defined as the onset of harvest.

8.2. FEWS Net crop calendar

The Famine Early Warning Systems Network (FEWS-NET) provides a crop calendar for Tanzania [7] that distinguishes between the unimodal and bimodal rainfall regions and the calendar seems to be aligned with the onset of the rains. However, the calendar is neither crop nor region-specific and therefore does not account for the spatial heterogeneity within Tanzania.

8.3. Crop calendar based on Stern et al. (1981)

We calculated the onset of the growing season based on the approach of Stern et al. (1981) [8] that was developed for Ghana and Burkina Faso. They define the onset of the rainy season when the following three criteria are met:

1. at least 25 mm rainfall within 5 days

2. starting day and at least two other days in this 5-day period are wet (>0.1 mm)
3. no dry period of seven or more consecutive days within the next 30 days

We defined the end of the growing season as 110 days after the start. Mourice et al., (2014) determined crop specific parameters for maize cultivars in Tanzania based on field experiments and concluded that the cultivars did not differ significantly in terms of the growing season length (they ranged from 105 to 114). Therefore, we use the average growing season length over the considered cultivars, which is about 110 days.

Because of the bimodal rainfall pattern, some regions have two growing seasons. We consider the second growing season if the time between the start of the first growing season and the start of the second growing season is at least 110 days, enough time for one growth cycle.

The criteria of Stern et al. (1981) [8] were developed for Ghana and Burkina Faso. For Tanzania, the criteria seem to be too strict – leading to too late onsets of the growing season in particular in the unimodal rainfall areas. Also, in some regions no onset could be calculated for some years, e.g. in Dar es Salaam in 2008 and 2009 and in Manyara in 2009.

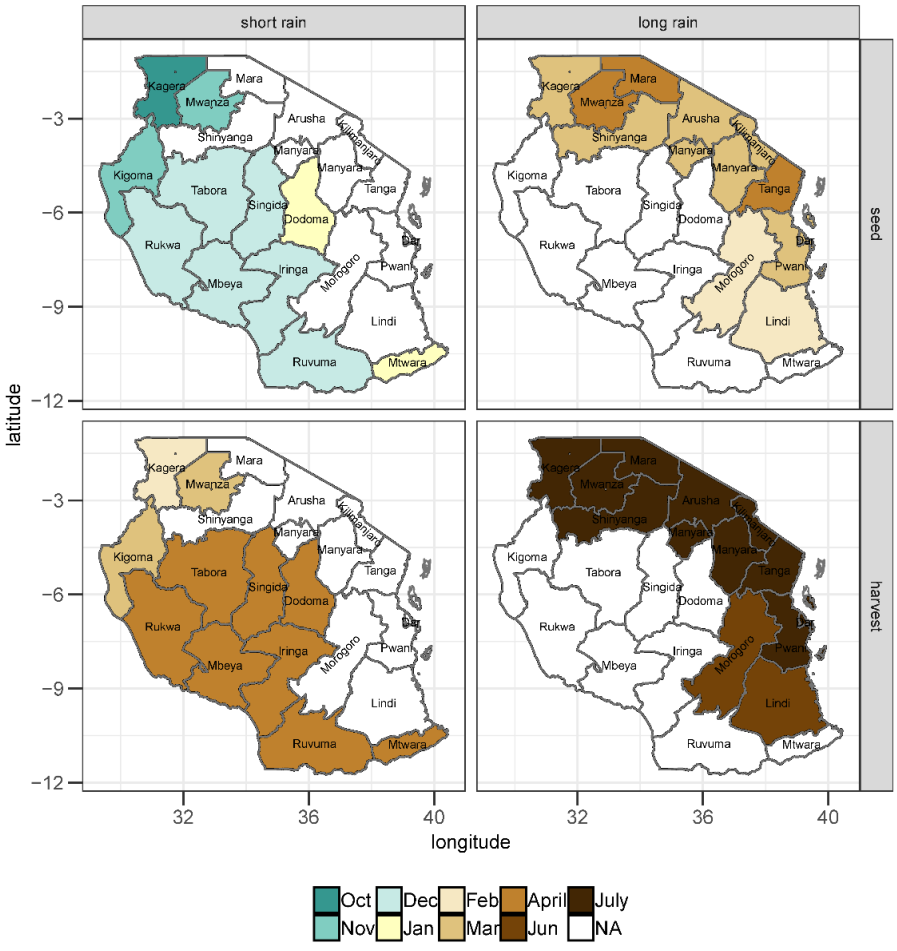

SI Fig. 9. *Crop calendar for the short (left) and long rains (right) in Tanzania; the onset of the growing season (top row) is calculated based on the approach of* Stern et al. (1981)*. The harvest dates (bottom row) represent the sowing dates plus the maize specific growing season length of 110 days according to* Mourice et al., (2014)*. The figure shows the median sowing and harvesting dates over the period from 2009 to 2018 for each region in Tanzania.*

8.4. Crop calendar based on Dodd and Jolliffe (2001)

Dodd and Jolliffe (2001) [4] further developed the approach of Stern et al. (1981) [8] to correct for too late onsets of the growing season. Their approach was tested for tropical and subtropical conditions. According to Dodd and Jolliffe (2001) [4], the onset of the growing season is defined when the following three criteria are fulfilled:

1. at least 25 mm rainfall within 6 days
2. starting day and at least two other days in this 6-day period are wet (>0.1 mm)
3. no dry period of ten or more consecutive days within next 40 days

Because of the bimodal rainfall pattern in North and North-East Tanzania, two onsets of the growing season are found for some grid points. In this case, we considered the onset of the long rains (Masika), which is the main growing season.

Following Mourice et al., (2014) [9], we consider a growing season length of 110 days, as described in section 8.3.

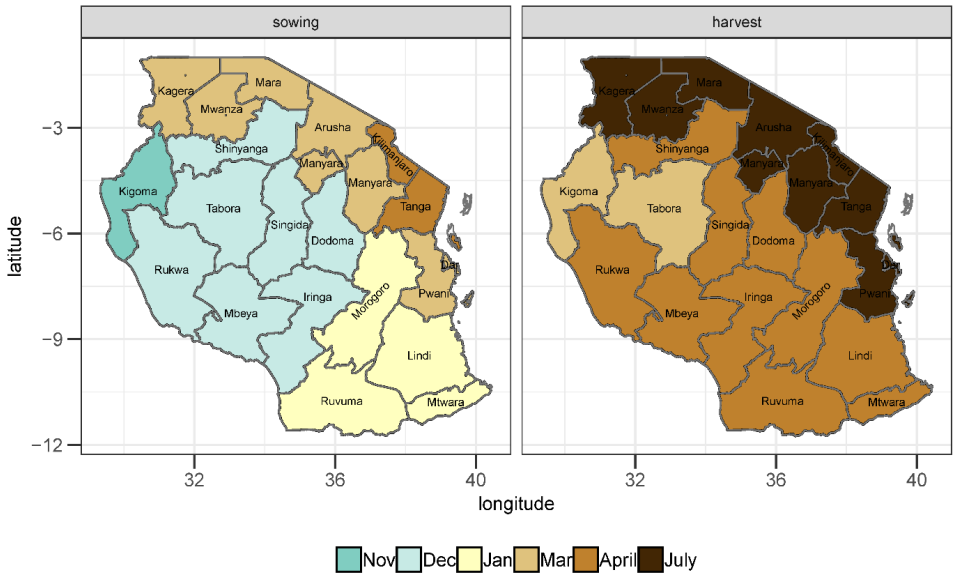

SI Fig. 10. *Sowing (left) and harvest (right) dates for Tanzania; the onset of the growing season is calculated based on the approach of Dodd and Jolliffe (2001) [4]. The harvest dates represent the sowing dates plus the maize specific growing season length of 110 days according to* Mourice et al., (2014)*. In case of two calculated rainy seasons, we considered the onset of the long rains (Masika), which is the main growing season. The figure shows the median sowing and harvesting dates over the period from 2009 to 2018 for each region in Tanzania.*

9. Equations for the calculation of GDD and percentile variables

SI Eq. 1. Calculation of percentile variables; *d* denotes the number of days within the growing season; *Days* denotes the total number of days within growing season

$$var.p99 = \sum_{d=1}^{Days} var_d^{var.p99} \qquad var_d^{var.p99} = \begin{cases} 1, & var_d > p.99 \\ 0, & otherwise \end{cases}$$

$$var.p01 = \sum_{d=1}^{Days} var_d^{var.p01} \qquad var_d^{var.01} = \begin{cases} 1, & var_d < p.01 \\ 0, & otherwise \end{cases}$$

With var as the weather or sea surface temperature (SST) variable, and $p.99$ ($p.01$) as the 99% (1%) percentile of the weather or SST variable; the percentiles were calculated over all days of the vegetative and reproductive phase of the growing season within the time period of 2009 and 2018 for each region. As a sensitivity test, we also calculated the 5% (95%) and 10% (90%) percentiles, which provided similar results.

SI Eq. 2. Calculation of growing degree days (GDD); *d* denotes the number of days within the growing season; *Days* denotes the total number of days within growing season

$$GDD = \sum_{d=1}^{Days} T_d^{GDD} \quad T_d^{GDD} = \begin{cases} 0, & T_d < T^{Base} \\ T_d - T^{Base}, & x \geq T^{Base} \leq T_d \leq T^{Opt} \\ T^{Opt} - T^{Base}, & x \geq T_d > T^{Opt} \end{cases}$$

With *T* as daily mean temperature; T^{Base} as base temperature of 10°C; T^{Opt} as optimal temperature of 30°C [10]; *d* denotes the number of days within the growing season; *Days* denotes the total number of days within growing season

10. Lead time of the yield forecast per region

region	start vegetative phase	start reproductive phase (days after sowing)	harvest	lead time of forecast in days	Performance of forecast (NSE of the level 1 - LOOCV)
Dodoma	29-Dec	22-Feb (55)	18-Apr	55	0.9
Arusha	30-Mar	19-May (50)	18-Jul	60	0.97
Kilimanjaro	03-Apr	23-May (50)	22-Jul	60	0.93
Tanga	01-Apr	22-May (51)	20-Jul	59	0.28
Morogoro	03-Jan	25-Feb (53)	23-Apr	57	0.79
Pwani	28-Mar	20-May (53)	16-Jul	57	0.63
Dar es Salaam	25-Mar	17-May (53)	13-Jul	57	0.92
Lindi	02-Jan	25-Feb (54)	22-Apr	56	0.59
Mtwara	10-Jan	05-Mar (54)	30-Apr	56	0.78
Ruvuma	02-Jan	25-Feb (54)	22-Apr	56	0.07
Iringa	29-Dec	21-Feb (54)	18-Apr	56	0.58
Mbeya	21-Dec	15-Feb (56)	10-Apr	54	0.98
Singida	26-Dec	20-Feb (56)	15-Apr	54	0.73
Tabora	07-Dec	02-Feb (57)	27-Mar	53	0.88
Rukwa	23-Dec	17-Feb (56)	12-Apr	54	0.82
Kigoma	20-Nov	16-Jan (57)	10-Mar	53	-0.39
Shinyanga	12-Dec	07-Feb (57)	01-Apr	53	0.99
Kagera	28-Mar	23-May (56)	16-Jul	54	0.25
Mwanza	26-Mar	20-May (55)	14-Jul	55	0.19
Mara	27-Mar	21-May (55)	15-Jul	55	0.99
Manyara	27-Mar	16-May (50)	15-Jul	60	0.97

SI Table 5. *Lead time in days of the yield forecast per region; the lead time of the forecast corresponds to the length of the reproductive phase; the start of the vegetative phase (2nd columns) corresponds to 0 days after sowing; the harvest date (4th columns) corresponds to 110 days after sowing; the right column shows the performance of the forecast of absolute yields measured in the NSE of the level 1 validation; unimodal rainfall regions are shaded in blue, bimodal rainfall regions are shaded in yellow*

References

1. Hoell, A. & Funk, C. Indo-Pacific sea surface temperature influences on failed consecutive rainy seasons over eastern Africa. *Climate Dynamics* **43**, 1645–1660 (2014).
2. Funk, C. *et al.* Predicting East African spring droughts using Pacific and Indian Ocean sea surface temperature indices. *Hydrology and Earth System Sciences* **18**, 4965–4978 (2014).
3. Davenport, F., Funk, C. & Galu, G. How will East African maize yields respond to climate change and can agricultural development mitigate this response? *Climatic Change* **147**, 491–506 (2018).
4. Dodd, D. E. S. & Jolliffe, I. T. Early detection of the start of the wet season in semiarid tropical climates of Western Africa. *International Journal of Climatology* **21**, 1251–1262 (2001).
5. FAO. FAOSTAT - Food and agriculutre data. http://www.fao.org/faostat/ (2019).
6. Suleiman, R. & Rosentrater, K. Current maize production, postharvest losses and the risk of Mycotoxins contamination in Tanzania. *American Society of Agricultural and Biological Engineers Annual International Meeting 2015* **4**, 3289–3414 (2015).
7. FEWS NET. East Africa - Tanzania. https://fews.net/east-africa/tanzania (2019).
8. Stern, R. D., Dennett, M. D. & Garbutt, D. J. The Start of the Rains in West Africa. *Journal of Climatology* **1**, 59–68 (1981).
9. Mourice, S. K., Rweyemamu, C. L., Tumbo, S. D. & Amuri, N. Maize Cultivar Specific Parameters for Decision Support System for Agrotechnology Transfer (DSSAT) Application in Tanzania. *American Journal of Plant Sciences* **05**, 821–833 (2014).
10. Gilmore, E. C. & Rogers, J. S. Heat Units as a Method of Measuring Maturity in Corn. *Agronomy Journal* **50**, 611–315 (1958).

6.3 Supplementary Information to: "A forecast of staple crop production in Burkina Faso to enable early warnings of shortages in domestic food availability"

Author names and affiliations:
Rahel Laudien[a*], Bernhard Schauberger[b,a], Jillian Waid[a], Christoph Gornott[a,c]

[a]Potsdam Institute for Climate Impact Research (PIK)
Member of the Leibniz Association
P.O. Box 60 12 03
D-14412 Potsdam
Germany

[b]University of Applied Sciences Weihenstephan-Triesdorf
Department of Sustainable Agriculture and Energy Systems
Am Staudengarten 1
85354 Freising
Germany

[c]Agroecosystem Analysis and Modelling
Faculty of Organic Agricultural Sciences
University of Kassel
Mönchebergstraße 19
34109 Kassel
Germany

Corresponding author:
Rahel Laudien (laudien@pik-potsdam.de, +49 331 28820771)

Co-authors:
Christoph Gornott (gornott@pik-potsdam.de)
Bernhard Schauberger (schauber@pik-potsdam.de)
Jillian Waid (waid@pik-potsdam.de)

1. Performance of yield models compared to a constant model

	Maize		Sorghum		Millet	
Province	**Yield model**	**Constant model**	**Yield model**	**Constant model**	**Yield model**	**Constant model**
Bale	127.97	359.31	74.66	174.24	153.19	232.24
Bam	201.48	315.59	126.78	213.99	123.73	196.71
Banwa	190.26	295.82	56.34	141.21	83.06	132.99
Bazega	158.17	251.70	121.19	161.23	110.71	137.42
Bougouriba	243.87	319.45	121.49	222.79	122.62	170.34
Boulgou	236.38	286.06	132.69	161.13	124.11	203.01
Boulkiemde	298.34	366.01	153.80	186.75	131.85	159.91
Comoe	217.64	268.60	117.48	208.43	97.42	214.23
Ganzourgou	193.85	339.13	115.47	160.56	113.34	167.24
Gnagna	219.55	349.28	165.70	212.43	243.78	275.28
Gourma	234.94	276.49	113.69	183.51	117.17	155.35
Houet	149.17	240.62	141.06	162.38	145.09	200.10
Ioba	188.84	240.63	86.05	166.06	95.00	151.87
Kadiogo	303.58	403.30	161.50	231.25	156.45	181.16
Kenedougou	116.43	225.14	92.48	147.00	158.15	198.41
Komandjoari	177.17	437.35	127.08	203.28	32.56	224.79
Kompienga	140.48	343.87	94.98	146.83	112.75	199.01
Kossi	192.16	295.39	131.41	158.03	76.29	129.88
Koulpelgo	89.02	184.27	106.10	145.33	93.61	183.21
Kouritenga	170.04	225.56	175.61	208.54	128.11	167.18
Kourweogo	110.92	220.49	119.95	209.40	121.01	182.00
Leraba	107.20	250.38	NA	NA	NA	NA
Loroum	130.65	389.53	146.04	227.60	80.72	238.75
Mouhoun	195.21	339.82	104.08	126.15	78.39	135.08
Nahouri	278.77	338.49	98.59	149.11	117.29	174.91
Namentenga	249.75	339.83	131.18	168.69	175.48	208.40
Nayala	152.35	284.35	104.72	176.58	108.63	168.83
Noumbiel	238.00	443.15	134.96	240.36	NA	NA
Oubritenga	174.92	291.38	128.56	182.95	67.17	130.19
Oudalan	236.91	490.12	227.39	388.39	120.37	186.64
Passore	187.42	314.66	169.86	213.45	133.60	209.52
Poni	304.77	395.60	136.84	197.02	96.88	134.01
Sanguie	333.74	430.06	96.64	151.74	98.68	141.96
Sanmatenga	231.67	345.30	164.87	208.87	154.42	192.04
Seno	163.36	334.26	173.51	230.12	119.20	199.39
Sissili	181.86	265.77	135.73	165.17	94.77	166.20
Soum	265.24	475.06	124.53	208.33	106.24	157.73
Sourou	355.13	493.75	187.56	218.80	158.66	190.15
Tapoa	304.95	364.85	122.79	191.75	147.48	224.41
Tuy	66.38	298.64	64.28	120.53	117.14	192.73
Yagha	107.47	322.41	135.44	171.12	106.58	206.18
Yatenga	187.50	322.23	145.11	166.76	141.64	205.80

Ziro	170.50	259.33	77.63	144.45	99.06	194.60
Zondoma	83.19	330.35	81.98	194.64	113.03	248.06
Zoundweogo	196.85	242.16	148.10	181.03	113.29	151.57

SI Table 1. Comparison of the model performance of yield anomalies to a constant model that only takes the mean yield excluding the year that is forecasted as a predictor for maize, sorghum and millet. The values show the root mean squared error (RMSE) in kg/ha between the observed yield and the modelled yield. A map with province names is provided in SI Fig. 2.

2. Province-specific performance of the yield model

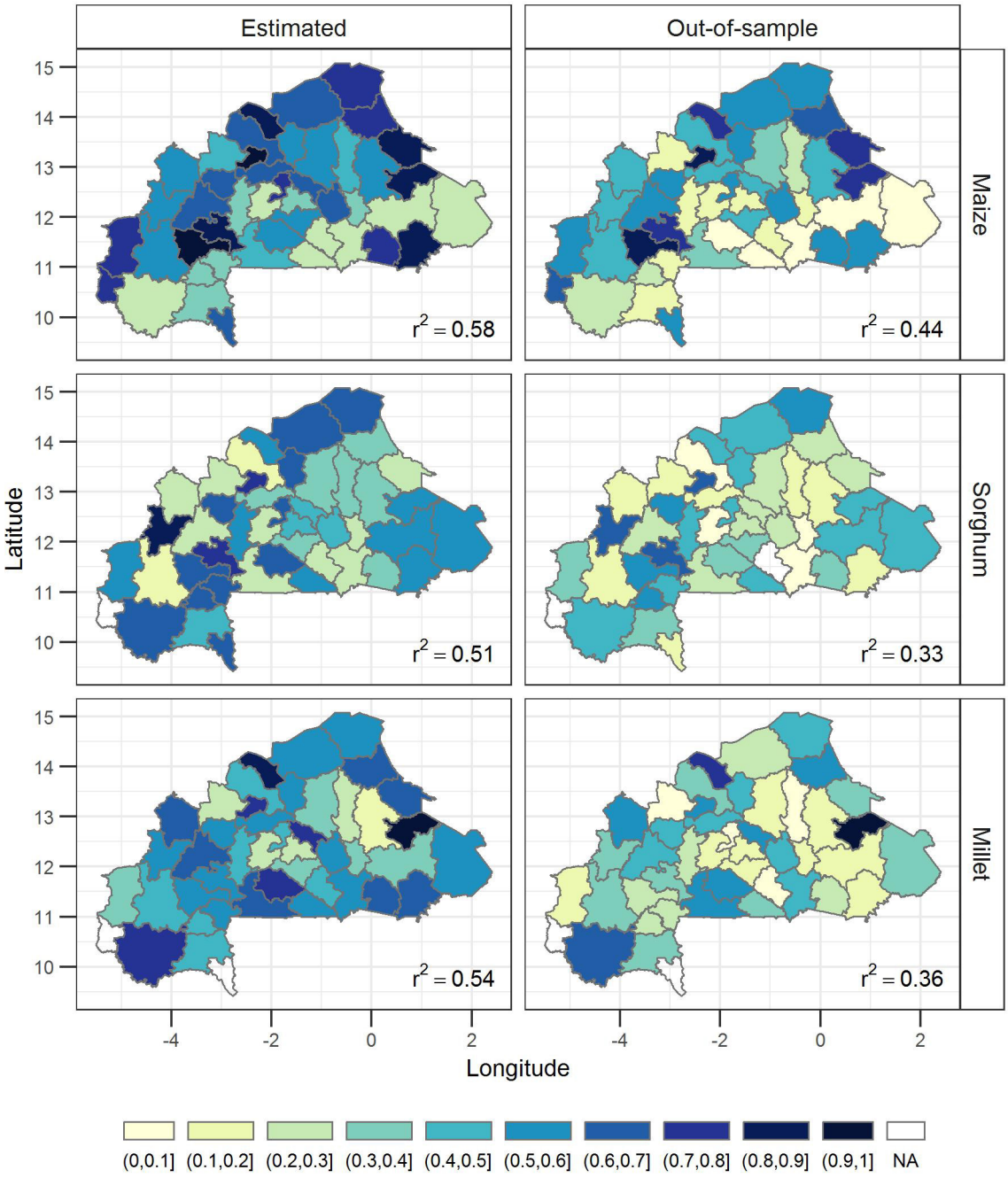

SI Fig. 1. Province-specific performance of the crop model for yield anomalies from 1984 to 2018 measured in r^2. The left panels show the estimation results (i.e. the model performance when the complete time series for each province is included).

The right hand panels show the performance for the out-of-sample validation. The median r^2 of all provinces in Burkina Faso is shown in the left corner of the panels. A map with province names is provided in SI Fig. 2.

3. Map of province names in Burkina Faso

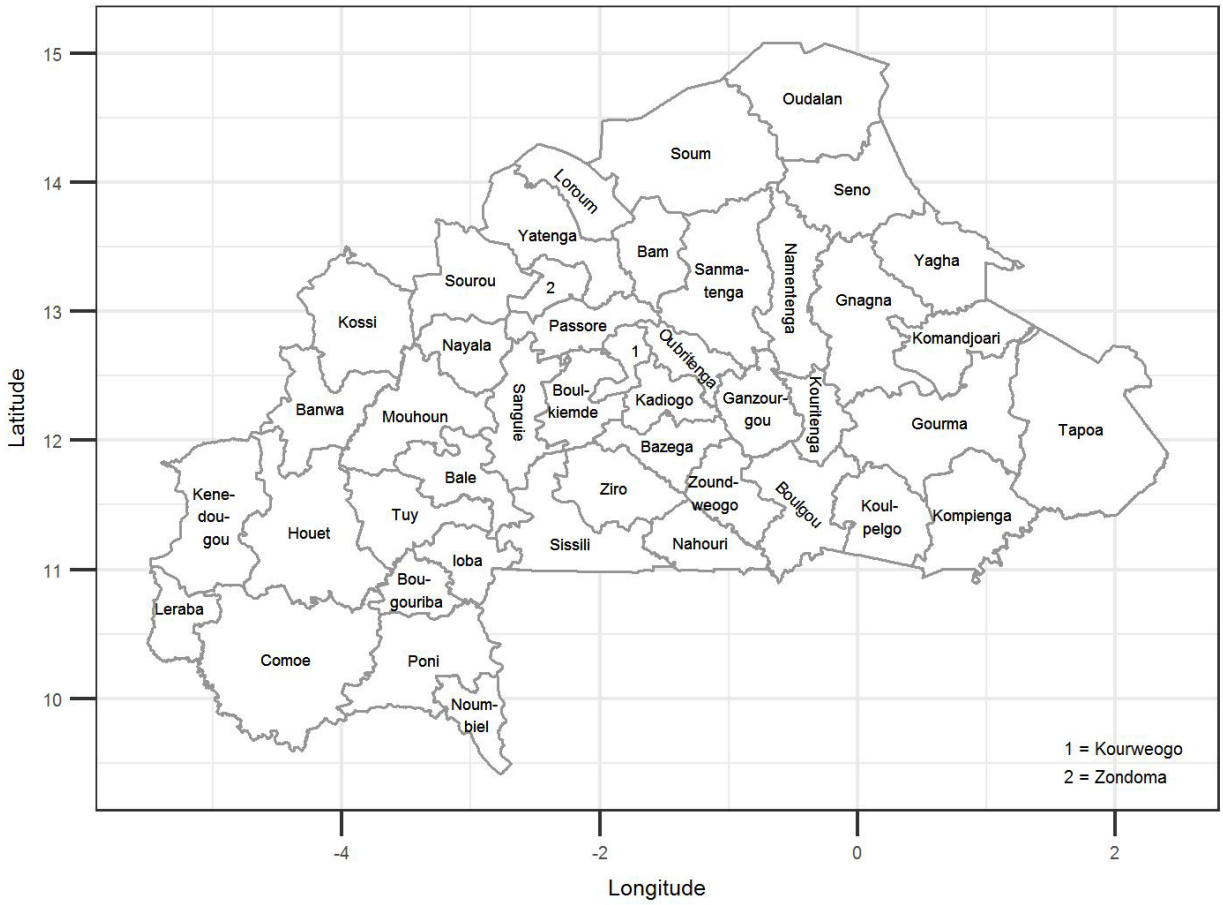

SI Fig. 2. Map of province names in Burkina Faso

4. Performance of the forecast (out-of-sample variable selection)

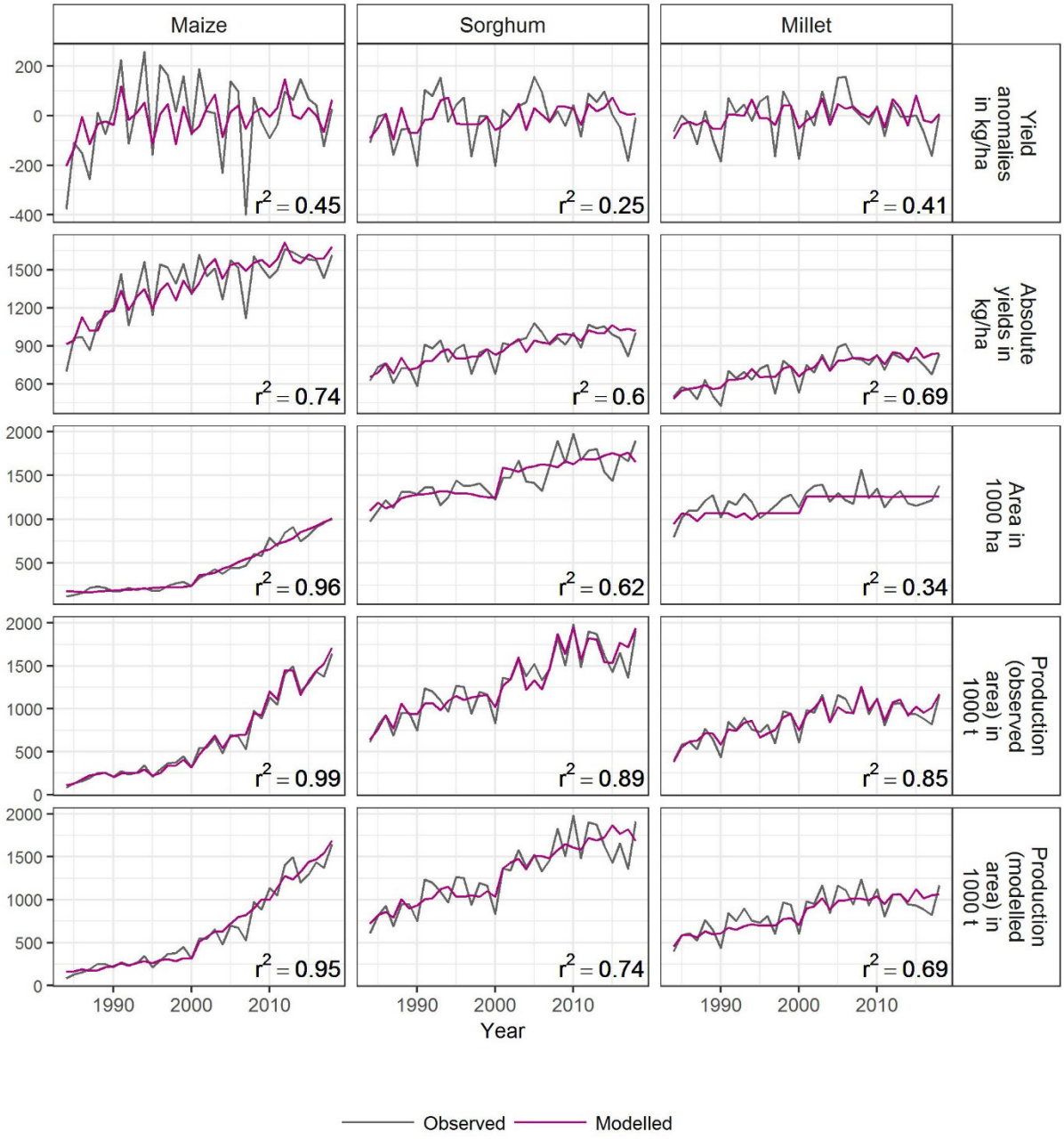

SI Fig. 3. Performance of the crop specific forecast with a lead time of one month for yield anomalies, absolute yields and harvest areas. The performance of the production forecast is shown for known harvest areas and for modelled harvest areas. The modelled yield data shows the result of the out-of-sample variable selection. The r^2 values indicate the explained variance by each model. The crop specific forecasts were the basis for the aggregated forecast of all crops together. The lead time of the forecast for all crops is one month before the sorghum and millet harvest. Please note that at this point in time, maize is already harvested so that yields could be estimated based on weather influences of the whole growing season. For practical reasons, we chose the forecast for maize also with a lead time of one month to inform early on as soon as the forecast is available.

5. Total population in Burkina Faso

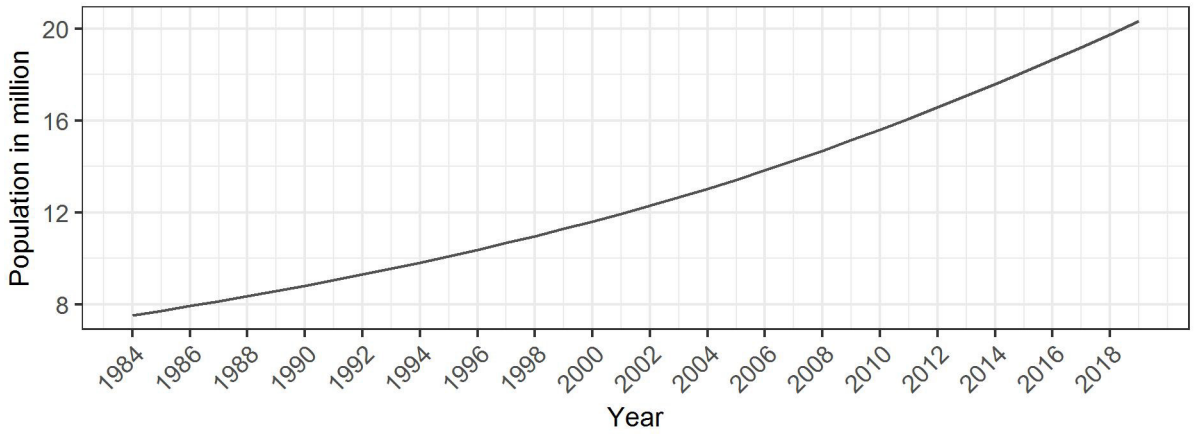

SI Fig. 4. Total population in Burkina Faso from 1984 to 2019, source: authors' illustration based on World Bank (2020)[1]

6. Trend in yield and harvest areas

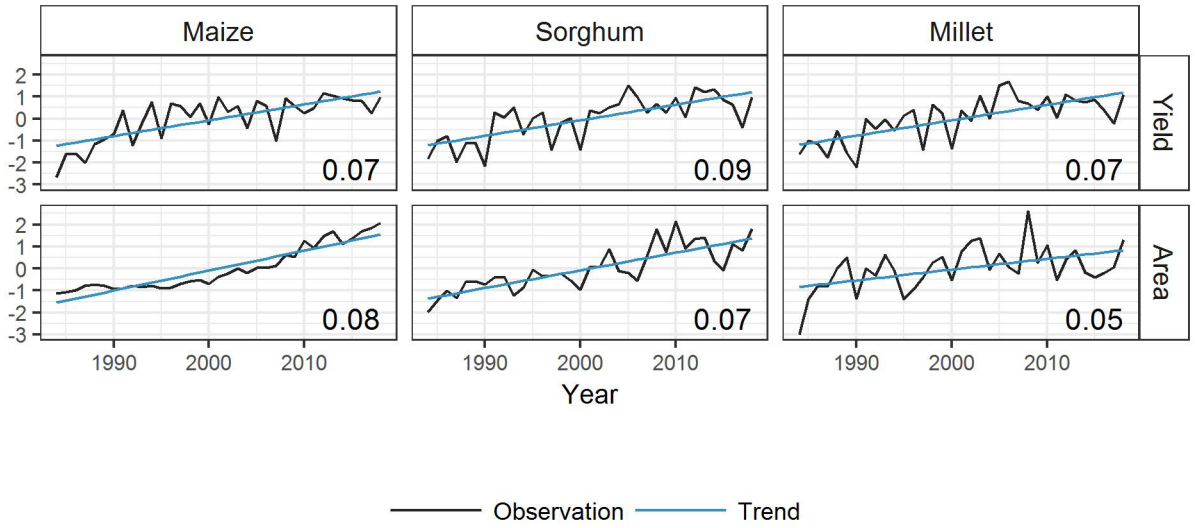

SI Fig. 5. Linear trend in yield and harvest areas for maize, sorghum and millet from 1984 to 2018; the y-axis shows standardised yields (upper panel) and harvest areas (lower panel). The slope of the trend is shown in the bottom right hand corner. A value of 0.07 means that there is a trend of 7% per year.

7. Performance of the forecast (out-of-sample validation)

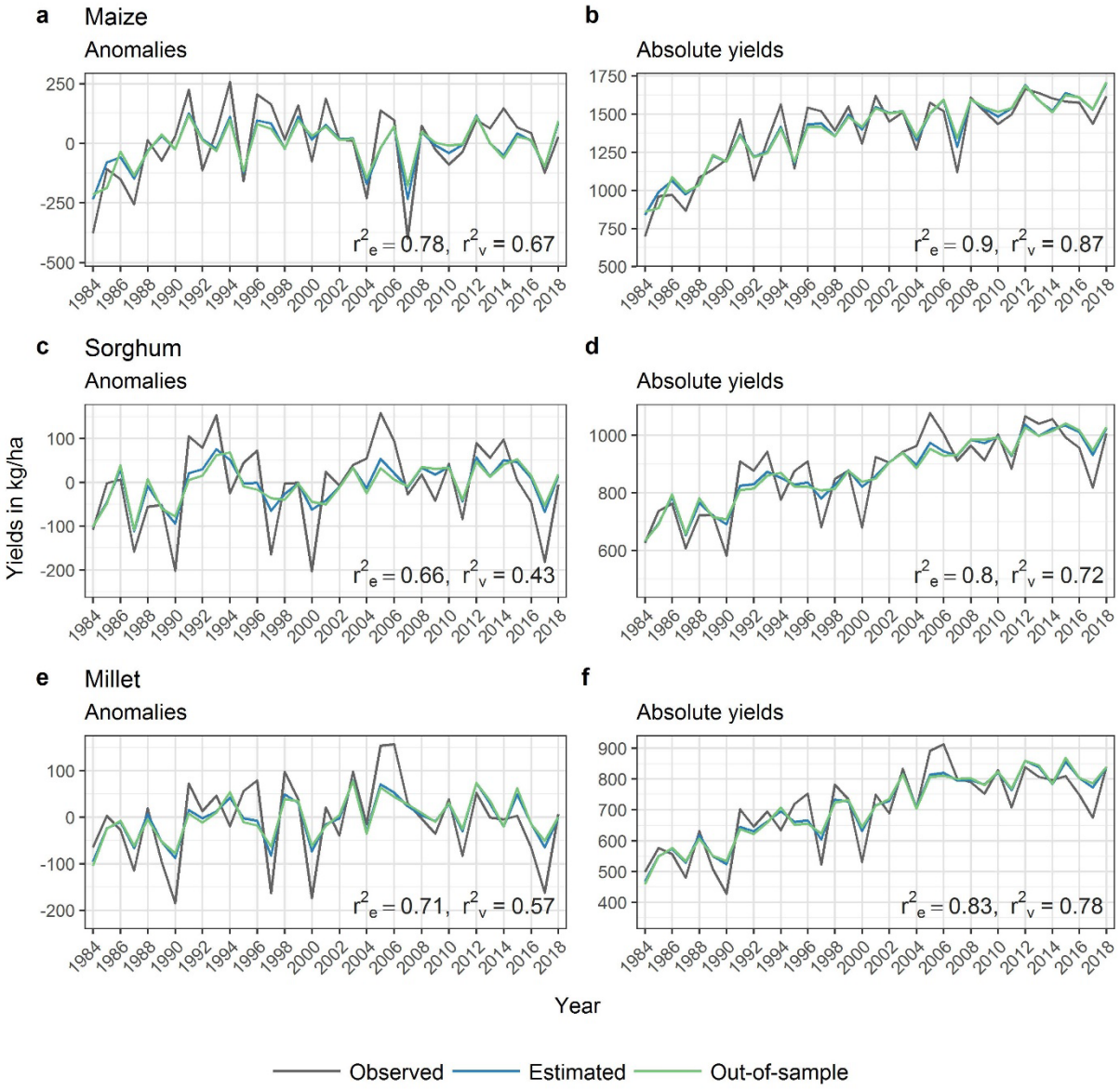

SI Fig. 6. Performance of the forecast with a lead time of one month for yield anomalies (left column) and absolute yields (right column) for maize, sorghum and millet from 1984 to 2018. The plot shows the observed yields in grey, the estimation results in blue and the out-of-sample validation results in green. The r^2_e and r^2_v values indicate the explained variance by each model, respectively.

8. Performance of a simple production model

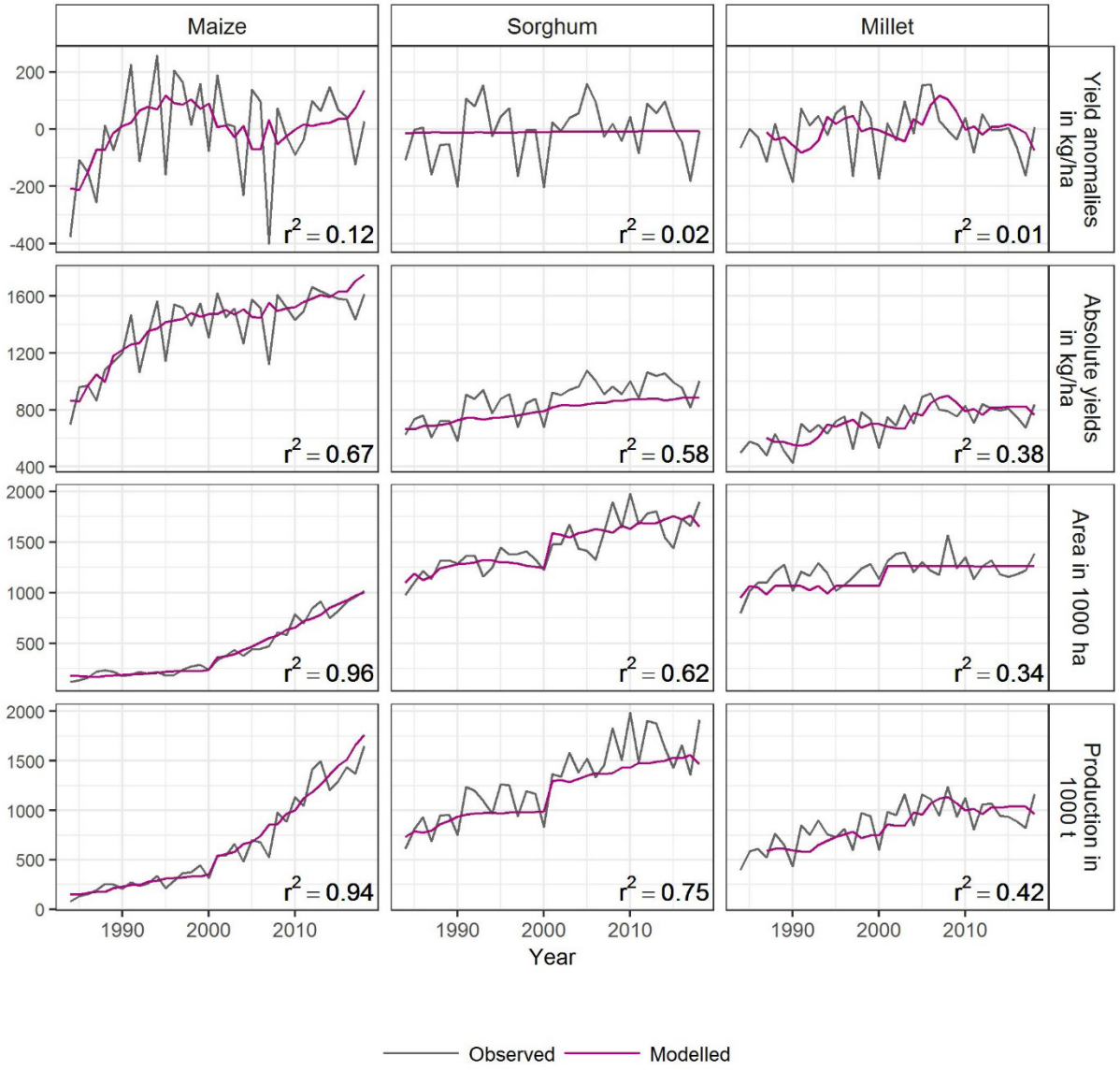

SI Fig. 7. Performance of a simple production model that is only based on yield and harvest area information from previous years. We tested the following four options: the median yield/harvest area, the median yield/harvest area of the previous three (five) years and the trend in yield/harvest areas calculated by a non-parametric LOESS function with a span of 0.9. For each crop, we chose the option that resulted in the highest correlation (Pearson's r) between the observed and the modelled data. The best option for modelling yield is the trend calculated by LOESS for maize, the median of the last 3 years for millet and the median over all years for sorghum. The best option for modelling harvest areas is the trend calculated by LOESS for maize, the median over all years for millet and the trend calculated by LOESS for sorghum. This simple production model was set up to test whether a production forecast based on a weather-driven yield model is superior to a yield model based on yield information from previous years.

9. Data cleaning of the annual production and harvest area statistics for maize, sorghum and millet on province level from 1984 to 2019

SI Text 1. We excluded observations with no harvest area or production as complete harvest losses are not likely on province level and are probably reporting errors. Yields were then calculated as production over harvest area. To guard against high outliers, yields outside the 95th percentiles (2152 kg/ha for maize, 1571 kg/ha for sorghum and 1382 kg/ha for millet) were not considered. The mean value for the 0-95% percentile (95-100% percentile) is 1120 kg/ha (2937 kg/ha) for maize, 910 kg/ha (2641 kg/ha) for sorghum and 768 kg/ha (2538 kg/ha) for millet. Lastly, data for provinces with less than 10 years (i.e. one sorghum producing province and two millet producing provinces) were omitted to allow for robust model construction and validation by preventing overfitting. In sum, after data cleaning we used 1225 out of 1313 observations for maize, 1245 out of 1575 observations for sorghum and 1232 out of 1310 observations for millet. The statistics for sorghum showed unreasonable observations for the years 2012 and 2016 (i.e. no area and no production). Therefore we aggregated the times series for white and red sorghum which became available from 2003 on and used this data from 2003 on to guarantee a continuous time series for sorghum.

Even though some yield observations could not be used to validate the yield model results because of reliability issues as described above, they were still used in the national production aggregation to not skew aggregated production levels by omission.

10. Crop specific lead time of the forecast

SI Fig. 8. Crop specific lead time of the forecast. The forecasting time is one month prior the harvest. The range in the forecasting time results from province specific sowing and harvesting dates[2] (SI Fig. 13 and SI Fig. 14).

11. Number of people affected by food insecurity and undernourishment in Burkina Faso

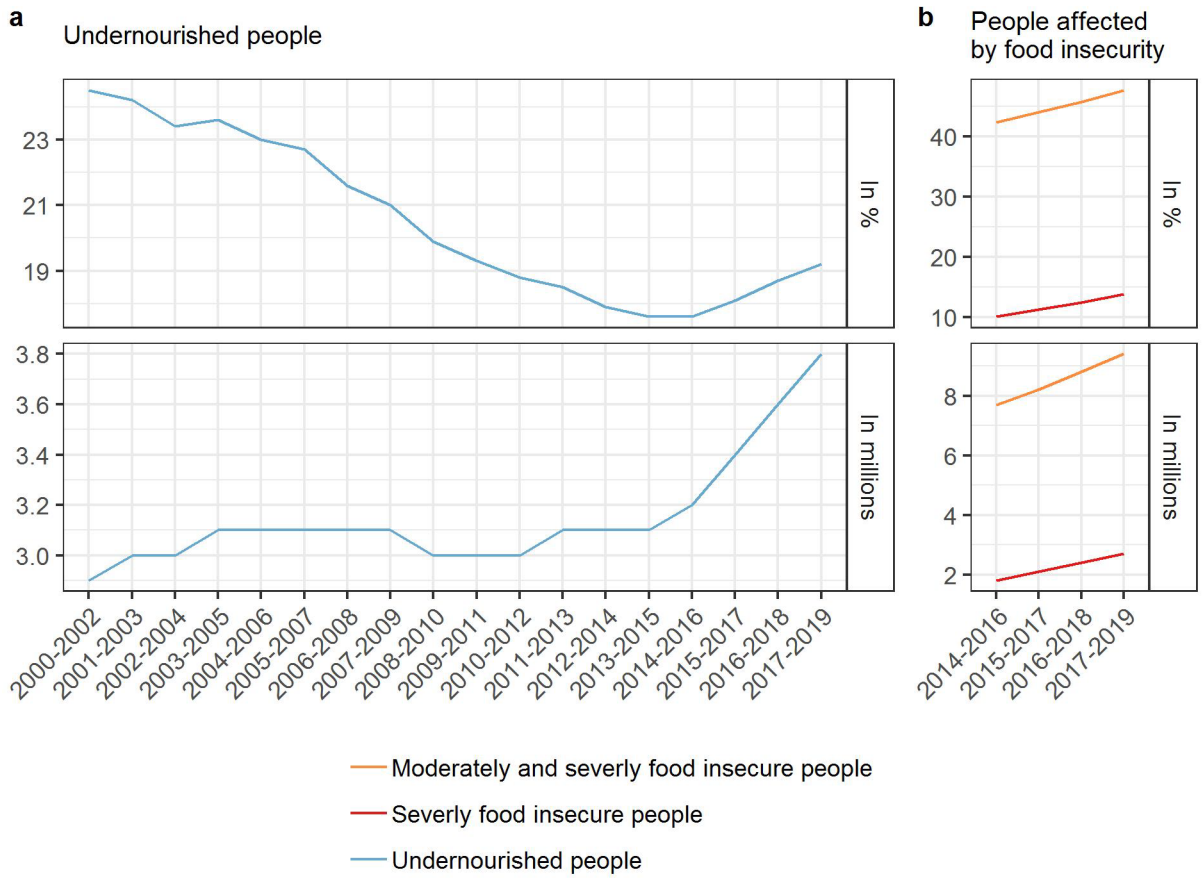

SI Fig. 9. People affected by food insecurity from 2000 to 2019 (plot a) and undernourished people from 2014 to 2019 (plot b) in Burkina Faso. The bottom panels show the absolute number of people, whereas the upper panels show the share of people in relation to the total population in Burkina Faso, source: authors' illustration based on FAO (2020)[3]

12. Consumed calories from maize, sorghum and millet compared to produced calories from these crops in Burkina Faso

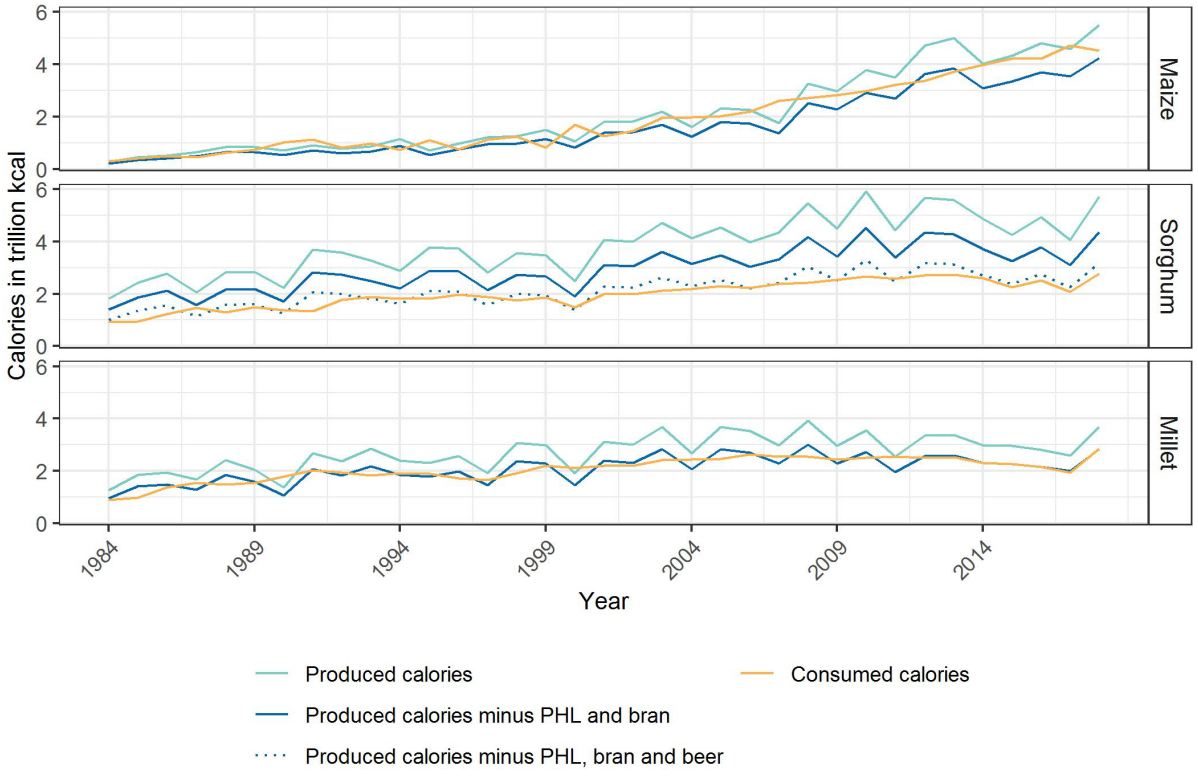

SI Fig. 10. Produced calories of maize, sorghum and millet compared to consumed calories from these crops on national level in Burkina Faso. Total produced calories[4] are shown in light blue, whereas dark blue shows the produced calories minus post-harvest losses (PHL)[5] and the bran[6]. Consumed calories were calculated by multiplying the supplied calories per person and day[7] with the number of days per year and the total population in Burkina Faso[1]. Whereas the difference between produced and consumed calories from maize and millet can mostly be explained by PHL and the share of the bran in the crops (which is used for feed in Burkina Faso), a gap remains in the case of sorghum. FAO data suggests that on average 27% of total supplied calories from sorghum originated from sorghum beer in the time from 2014 to 2018[8]. The dotted line shows the produced calories from sorghum if in addition to PHL and the bran, average calories from sorghum beer were also subtracted. Despite the high agreement between this data and the consumed calories from sorghum, we did not include sorghum beer production in our analysis as this data is only available for five years and could not be extrapolated for the whole time period.

13. Share of arable land in Burkina Faso

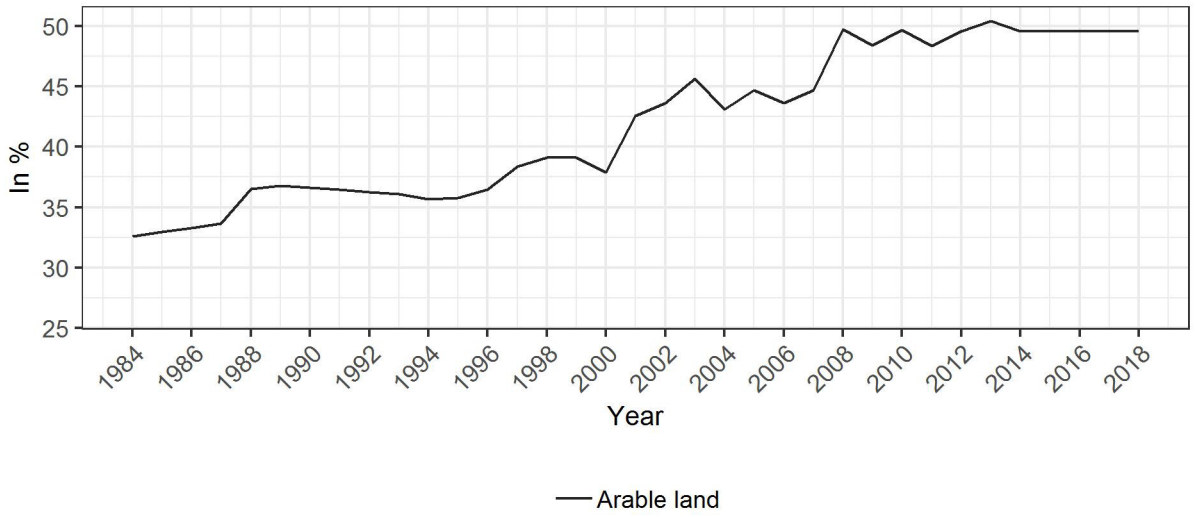

SI Fig. 11. Share of arable land in Burkina Faso from 1984 to 2018, source: authors' illustration based on FAO (2020)[9]

14. Software used in the analysis

SI Text 2. For our analysis, we used the statistical software *R* - version 4.0.5[10] with the packages *tidyr*[11] and *plyr*[12] for data pre-processing, the packages *sp*[13] and *rgdal*[14] for spatial data processing, the package *glmnet*[15] to perform LASSO regression and the package *ggplot2*[16] to generate the figures and maps.

15. Share of supplied calories from maize, sorghum and millet in the diet in Burkina Faso

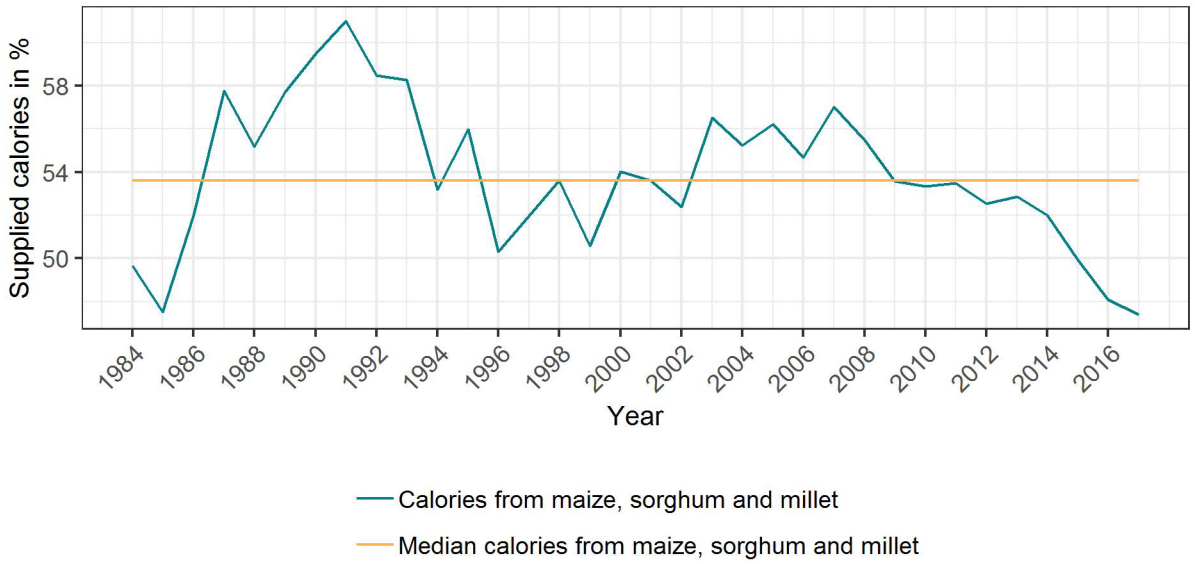

SI Fig. 12. Share of supplied calories from maize, sorghum and millet in total supplied calories per capita and day in Burkina Faso from 1984 to 2017; the yellow line shows the median value over the period 1984 to 2017, source: authors' illustration based on (FAO 2020)[7]

16. Equations for the calculation of vapour pressure deficit, growing degree days and percentile variables

SI Eq. 1. Calculation of vapour pressure deficit (VPD):

$$VPD = 6.11 * \exp\left(\frac{17.27 * Tmax}{237.2 + Tmax}\right) - \exp\left(\frac{17.27 * Tmin}{237.2 + Tmin}\right)$$

With *Tmax* as daily maximum temperature and *Tmin* as daily minimum temperature, formula according to Allen et al (1998)[17].

SI Eq. 2. Calculation of growing degree days (GDD); *d* denotes the number of days within the growing season; *Days* denotes the total number of days within growing season:

$$GDD = \sum_{d=1}^{Days} T_d^{GDD} \quad T_d^{GDD} = \begin{cases} 0, & T_d < T^{Base} \\ T_d - T^{Base}, & T^{Base} \leq T_d \leq T^{Opt} \\ T^{Opt} - T^{Base}, & T_d > T^{Opt} \end{cases}$$

With *T* as daily mean temperature; T^{Base} as base temperature of 10°C; T^{Opt} as optimal temperature of 30°C [18]; *d* denotes the day within the growing season; *Days* denotes the total number of days within growing season.

SI Eq. 3. Calculation of percentile variables:

$$var.p99 = \sum_{d=1}^{Days} var_d^{var.p99} \quad var_d^{var.p99} = \begin{cases} 1, & var_d > p.99 \\ 0, & otherwise \end{cases}$$

$$var.p01 = \sum_{d=1}^{Days} var_d^{var.p01} \qquad var_d^{var.01} = \begin{cases} 1, & var_d < p.01 \\ 0, & otherwise \end{cases}$$

With var as the weather or sea surface temperature (SST) variable, and $p.99$ ($p.01$) as the 99% (1%) percentile of the weather or SST variable; the percentiles were calculated over all days of the vegetative and reproductive phase of the growing season within the time period of 2009 and 2018 for each region. As a sensitivity test, we also calculated the 5% (95%) and 10% (90%) percentiles, which provided similar results.

17. Input variables for the yield model

input name	Definition	unit
	Variables related to precipitation	
psum	Precipitation sum	mm
pmedian	Median daily precipitation	mm
cdd5	Consecutive dry days of equal or more than 5 days	
cwd5	Consecutive wet days of equal or more than 5 days	
pB5	Number of precipitation events below 5mm per day	
pB15	Number of precipitation events below 15mm per day	
pA5	Number of precipitation events equal or above 5mm per day	
pA15	Number of precipitation events equal or above 15mm per day	
precip.p90	Number of times the daily precipitation sum exceeds the 99% percentile of the daily precipitation sum	
DWP	Number of days without precipitation	
p.cv	Coefficient of variation of the daily precipitation sum	
	Variables related to temperature	
tas.median	Median of the daily mean temperature	°C
tas.max	Median of the daily maximum temperature	°C
tas.min	Median of the daily minimum temperature	°C
tas.max.p95	Number of times the daily maximum temperature exceeds the 95% percentile of the daily maximum temperature	
tas.max.p05	Number of times the daily maximum temperature falls below the 5% percentile of the daily maximum temperature	
tas.min.p95	Number of times the daily minimum temperature exceeds the 95% percentile of the daily minmum temperature	
tas.min.p05	Number of times the daily minimum temperature falls below the 5% percentile of the daily minimum temperature	
tasmax.cv	Coefficient of variation of the daily maximum temperature	
tasmin.cv	Coefficient of variation of the daily minimum temperature	
	Variables related to vapour pressure deficit	
vpd.median	Median of the daily vapour pressure deficit	mm
vpd.p99	Number of times the daily vapour pressure deficit exceeds the 99% percentile of the daily vapour pressure deficit	
vpd.p01	Number of times the daily vapour pressure deficit falls below the 1% percentile of the daily vapour pressure deficit	
vpd.cv	Coefficient of variation of the daily vapour pressure deficit	

SI Table 2. Input variables for the yield model

SI Text 3. In addition to the median daily mean, maximum and minimum temperature over the growing season (*tas.median, tas.max, tas.min*), we included variables related to extreme temperatures. Temperatures above the optimum temperature range lead to a decline in the net photosynthesis rate because photosynthesis reduces with higher temperatures whereas respiration rates rise[19]. To account for extreme high temperatures, we included the number of days with a daily maximum temperature higher than the province-specific long term 99% percentile of the maximum temperature in the growing season (*tas.max.p99,* SI Eq. 3). Particularly low temperatures were represented by the number of times the daily minimum temperature fell below the province-specific long-term 1% percentile of the minimum temperature (*tas.min.p01*). Variations in maximum and minimum temperatures were represented by the coefficient of variation (*tasmax.cv* and *tasmin.cv*).

The overall water availability was represented by the precipitation sum (*Psum*) in the growing season. For optimal plant development, seasonal rainfall distribution and intensities are equally critical. Both excessive rain and drought stress can lead to crop failures and hinder timely planting and harvest[20]. To represent different precipitation ranges, we included the number of days with precipitation above a threshold of 5 and 15 mm (*pA5*, *pA15*, respectively) and below a threshold of 5 and 15 mm (*pB5, pB15, respectively*). We also included the number of days without precipitation (*DWP*), consecutive dry spells of more than five days (*cdd5)* and consecutive wet spells of more than five days *(cwd5)*. Extremely high precipitation events are covered by the number of times the daily precipitation sum exceeds the province-specific long-term 90% percentile of the daily precipitation sum. Variations in precipitation are covered by the median daily precipitation sum and the coefficient of variation of the precipitation sum.

Variables related to the vapour pressure deficit were included to account for water stress during plant growth. A high vapour pressure deficit leads to the closure of the stomata and therefore a reduction in carbon uptake from the atmosphere and thus crop yields[21]. As for temperature and precipitation, we included variables related to the median state (*vpd.median*), extreme low values (*vpd.p01*), high values (*vpd.p99*) and variations (*vpd.cv*).

18. Crop calendar for maize, sorghum and millet

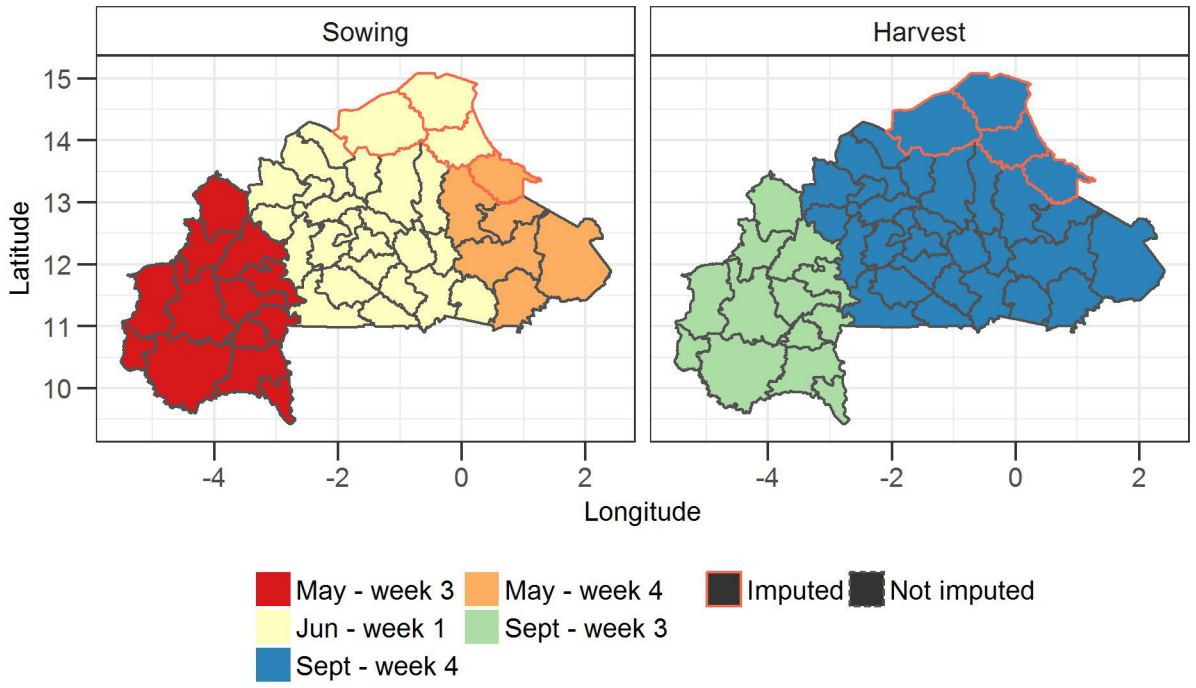

SI Fig. 13. Crop calendar for maize for Burkina Faso based on the FAO crop calendar[2]. Sowing is defined as the onset of the sowing period and harvest is defined as the end of the harvest period. The values represent the median onset of the growing season (left hand) and the median end of the growing season (left) over all available varieties (i.e. FBC 6, K.E.J. Barka, K.P.B. Wari, Espoir, SR 21, SR 22). Please note that information for the four Northern provinces Yagha, Soum, Seno and Oudalan in the Sahel zone (bordered in red lines) was not available. Therefore, we used the sowing and harvest dates of the neighbouring provinces.

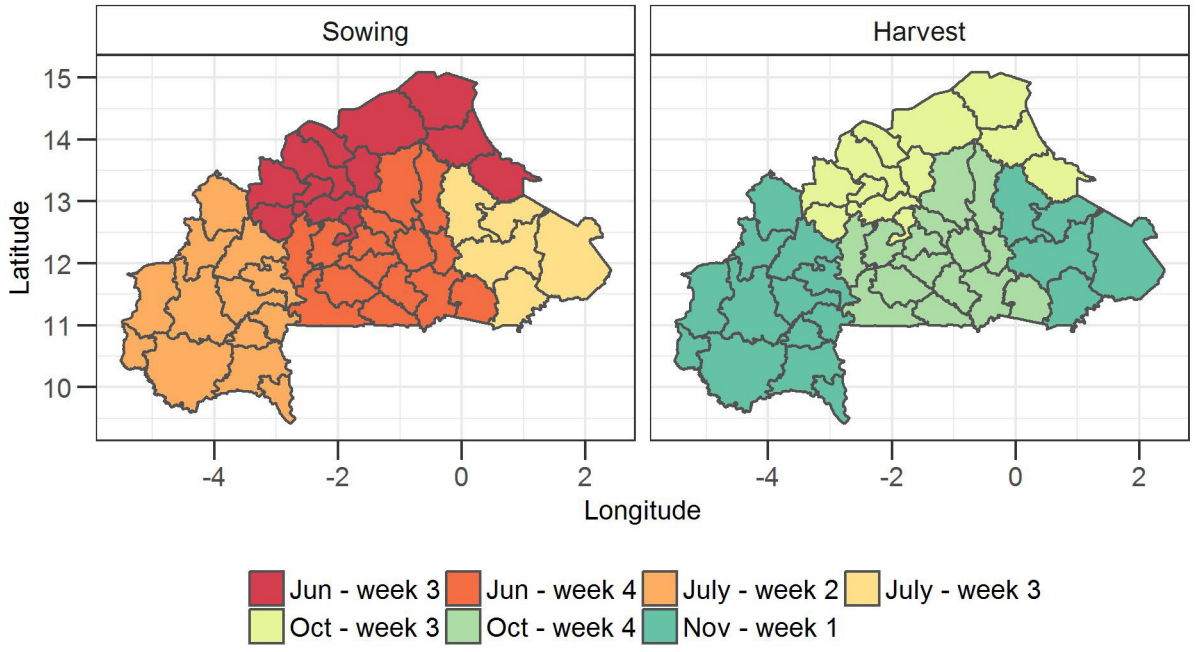

SI Fig. 14. Crop calendar for millet for Burkina Faso based on the FAO crop calendar[2]. Sowing is defined as the onset of the sowing period and harvest is defined as the end of the harvest period. The values represent the median onset of the growing season (left hand) and the median end of the growing season (left) over all available varieties of the crop calendar (i.e. IKMP1, IKMP2, IKMP3, IKMP5, IKMV 8201). This calendar was used for millet and for sorghum, because the FAO does not provide a separate calendar for sorghum and due to the similarity in sowing and harvest dates[22]

19. Production, imports and exports of maize, millet and sorghum in Burkina Faso

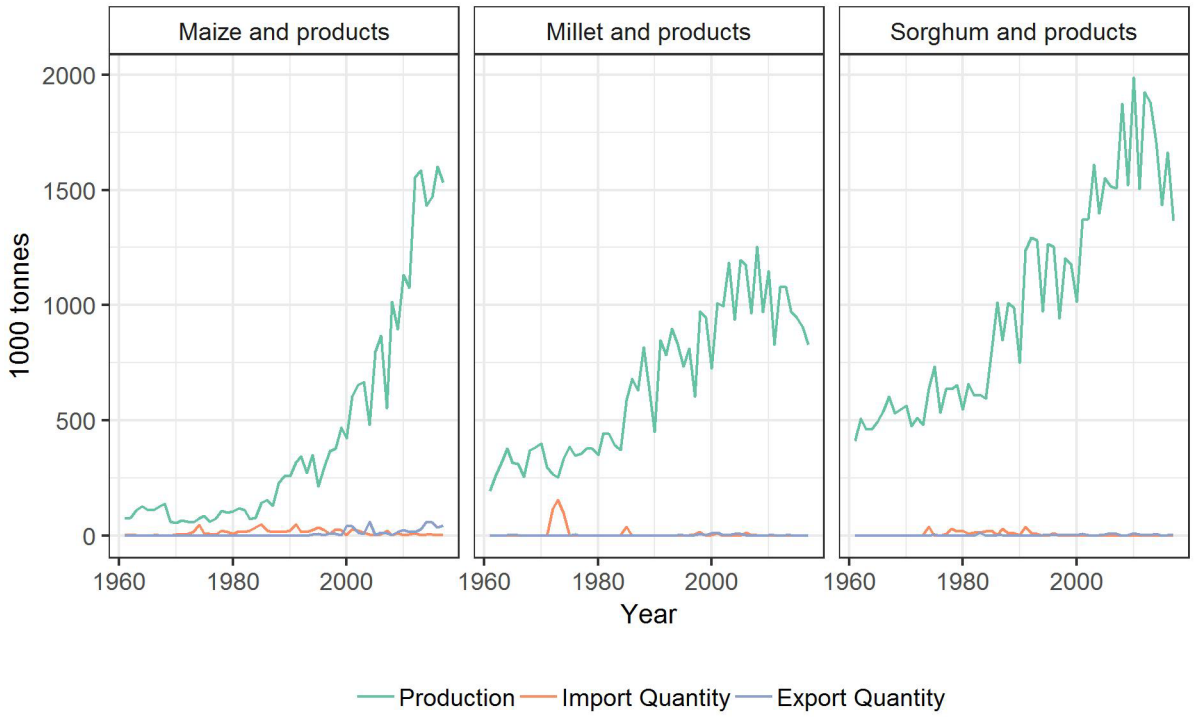

SI Fig. 15. Production, import quantity and export quantity of the crops maize, millet and sorghum in Burkina Faso from 1960 to 2017, source: authors' illustration based on FAO (2020)[23]

References

1. World Bank. Population, total. https://data.worldbank.org/indicator/SP.POP.TOTL?locations=BF (2020).

2. FAO. Crop Calendar - An Information Tool for Crop Production. https://cropcalendar.apps.fao.org/#/home (2010).

3. FAO. FAOSTAT - Suite of Food Security Indicators. http://www.fao.org/faostat/en/#data/FS (2020).

4. Ministère de l'Agriculture et des Aménagements Hydroagricoles / Direction Générale des Etudes et des Statistiques Sectorielles. *Données officielles de l'Enquête Permanente Agricole (EPA)*. (2020).

5. Aphlis. Dry weight loss: Burkina Faso - All crops - All years. https://www.aphlis.net/en/page/20/data-tables#/datatables?tab=dry_weight_losses&metric=prc&country=93&province=0 (2020).

6. FAO. *Food composition tables for international use*. (1953).

7. FAO. FAOSTAT - Food Supply - Crops Primary Equivalent. http://www.fao.org/faostat/en/#data/CC (2020).

8. FAO. FAOSTAT - Supply Utilization Accounts. http://www.fao.org/faostat/en/#data/SCL (2021).

9. FAO. FAOSTAT - Land Use Indicators. http://www.fao.org/faostat/en/#data/EL (2020).

10. R Core Team. R: A language and environment for statistical computing. http://www.r-project.org/ (2018).

11. Wickham, H. & Henry, L. tidyr: Easily Tidy Data with “spread()” and “gather()” Functions. https://cran.r-project.org/package=tidyr (2019).

12. Wickham, H. The Split-Apply-Combine Strategy for Data Analysis. *Journal of Statistical Software* vol. 40 http://www.jstatsoft.org/v40/i01/ (2011).

13. Pebesma, E. J. & Bivand, R. S. Classes and methods for spatial data in R. https://cran.r-project.org/doc/Rnews/ (2005).

14. Bivand, R., Keitt, T. & Rowlingson, B. rgdal: Bindings for the “Geospatial” Data Abstraction Library. R package version 1.3-2. https://cran.r-project.org/package=rgdal (2018).

15. Friedman, J. *et al.* Regularization Paths for Generalized Linear Models via Coordinate Descent. *J Stat Softw* **33**, 1–22 (2010).

16. Wickham, H. ggplot2: elegant graphics for data analysis. https://ggplot2-book.org/ (2009).

17. Allen, R. G., Pereira, L. S., Raes, D. & Smith, M. *Crop evapotranspiration - Guidelines for computing crop water requirements - FAO Irrigation and drainage paper 56*. (1998).

18. Gilmore, E. C. & Rogers, J. S. Heat Units as a Method of Measuring Maturity in Corn. *Agronomy Journal* **50**, 611–315 (1958).

19. Barnabás, B., Jäger, K. & Fehér, A. The effect of drought and heat stress on reproductive processes in cereals. *Plant, Cell and Environment* **31**, 11–38 (2008).

20. Rötter, R. & Van De Geijn, S. C. Climate Change Effects on Plant Growth, Crop Yield and Livestock. *Climatic Change* **43**, 651–681 (1999).

21. Yuan, W. *et al.* Increased atmospheric vapor pressure deficit reduces global vegetation growth. *Science Advances* **5**, 1–12 (2019).

22. FAO. GIEWS Country Brief Burkina Faso. *FAO* http://www.fao.org/giews/countrybrief/country/BFA/pdf_archive/BFA_Archive.pdf (2020).

23. FAO. FAOSTAT - New Food Balances. http://www.fao.org/faostat/en/#data/FBS (2020).

7 Selbstständigkeitserklärung

Erklärung:

Hiermit erkläre ich, die Dissertation selbstständig und nur unter Verwendung der angegebenen Hilfen und Hilfsmittel angefertigt zu haben. Ich habe mich anderwärts nicht um einen Doktorgrad beworben und besitze keinen entsprechenden Doktorgrad. Ich erkläre, dass ich die Dissertation oder Teile davon nicht bereits bei einer anderen wissenschaftlichen Einrichtung eingereicht habe und dass sie dort weder angenommen noch abgelehnt wurde. Ich erkläre die Kenntnisnahme der dem Verfahren zugrunde liegenden Promotionsordnung der Lebenswissenschaftlichen Fakultät der Humboldt-Universität zu Berlin vom 5. März 2015. Weiterhin erkläre ich, dass keine Zusammenarbeit mit gewerblichen Promotionsbearbeiterinnen/Promotionsberatern stattgefunden hat und dass die Grundsätze der Humboldt-Universität zu Berlin zur Sicherung guter wissenschaftlicher Praxis eingehalten wurden.

Declaration:

I hereby declare that I completed the doctoral thesis independently based on the stated resources and aids. I have not applied for a doctoral degree elsewhere and do not have a corresponding doctoral degree. I have not submitted the doctoral thesis, or parts of it, to another academic institution and the thesis has not been accepted or rejected. I declare that I have acknowledged the Doctoral Degree Regulations which underlie the procedure of the Faculty of Life Sciences of Humboldt-Universität zu Berlin, as amended on 5th March 2015. Furthermore, I declare that no collaboration with commercial doctoral degree supervisors took place, and that the principles of Humboldt-Universität zu Berlin for ensuring good academic practice were abided by.

.....

Datum/Date, Unterschrift der Kandidatin/signature of the candidate